Guidelines for Design & Construction of Geosynthetic-Reinforced Soil Structures in New Zealand

Transfund New Zealand Research Report No. 239

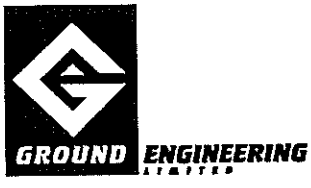

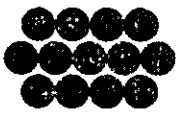

The Reinforced Earth Company

Groupe TAI

Guidelines for Design & Construction of Geosynthetic-Reinforced Soil Structures in New Zealand

A.K. Murashev
Beca Carter Hollings & Ferner Ltd
Wellington, New Zealand

Transfund New Zealand Research Report No. 239

ISBN 0-478-25099-1
ISSN 1174-0574

© 2003, Transfund New Zealand
PO Box 2331, Lambton Quay, Wellington, New Zealand
Telephone 64-4-473 0220; Facsimile 64-4-499 0733

Murashev, A.K.* 2003. Guidelines for design and construction of geosynthetic-reinforced soil structures in New Zealand. *Transfund New Zealand Research Report No.239.* 216 pp.

*Beca Carter Hollings & Ferner Ltd, PO Box 3942, Wellington

Keywords: construction, design, earthquakes, failure, geosynthetics, guidelines, loading, New Zealand, reinforcement, roads, run-off, stability, strength, structures

An Important Note for the Reader

The research detailed in this report was commissioned by Transfund New Zealand. Transfund New Zealand is a Crown entity established under the Transit New Zealand Act 1989. Its principal objective is to allocate resources to achieve a safe and efficient roading system. Each year Transfund New Zealand invests a portion of its funds on research that contributes to this objective.

While this report is believed to be correct at the time of its preparation, Transfund New Zealand and its employees and agents involved in its preparation and publication cannot accept any liability for its contents or for any consequences arising from its use. People using the contents of the document, whether directly or indirectly, should apply and rely upon their own skill and judgement. They should not rely on its contents in isolation from other sources of advice and information. If necessary, they should seek appropriate legal or other expert advice in relation to their own circumstances to the use of this report.

The material contained in this report is the output of research and should not be construed in any way as policy adopted by Transfund New Zealand but may form the basis of future policy.

Acknowledgments

The funding for the project was provided by Transfund New Zealand, Anchor Wall Systems Ltd (US & Australia), Firth Industries Ltd (New Zealand), Geotech Systems Ltd (New Zealand), Ground Engineering Ltd (New Zealand), and The Reinforced Earth Company (Australia & New Zealand).

Dr John Wood of Phillips & Wood Ltd (New Zealand) and Mr Geoffrey Farquhar of Meritec Ltd (New Zealand) are thanked for their detailed review of the original manuscript. Also the efforts of Messrs Mike Dobie of Tensar International (SE Asia & Australia), Garry Power of The Reinforced Earth Company (Australia), Malcolm Boyd consultant to The Reinforced Earth Company and Freyssinet International Groups (Australia), Don Asbey-Palmer of The Reinforced Earth Company (New Zealand), John Schramm of Anchor Wall Systems Ltd (US), Craig Cottle of Firth Ltd (New Zealand) and Graeme Jamieson of Bloxam Burnett & Oliver Limited (New Zealand) are acknowledged for their comments which substantially improved the original manuscript.

Contents

Executive Summary

Introduction

Geosynthetic-reinforced soils (GRS) have been found to be cost-effective compared to traditionally used retaining structures in specific situations. As a consequence the application of GRS to structures carrying roads and/or pedestrian traffic is rapidly increasing. Possible applications of GRS structures on highways include:

- Reinforced embankments in place of viaducts;
- Reinforced embankments supporting highways;
- Repair of slope failures;
- Bridge abutments.

In addition to their low cost compared with conventional structures, evidence from the 1995 Kobe Earthquake (Japan) indicates that GRS structures are less prone to damage under seismic loads than conventional type structures.

GRS is a comparatively new technique. For example, in Japan the first project involving GRS was undertaken in 1988 and the use of GRS on a wider scale started only in 1992. Therefore the design methods for GRS are not well established, and New Zealand geotechnical engineers currently use several different overseas standards and design guidelines to design GRS structures, and to different standards.

Aims of Research Project

Research was undertaken to prepare guidelines for design and construction of GRS structures in New Zealand. Stage 1 of the project was undertaken in 1997-1998, and results were published as a Review & Discussion paper in 1998.

This report presents results of Stages 2 and 3, undertaken in 1999-2002, as comprehensive guidelines for design and construction of GRS structures, both walls and slopes, in New Zealand. The guidelines have been developed for use by New Zealand consultants, contractors, and Road Controlling Authorities.

Design procedures for GRS structures address a number of important aspects such as design tensile strength and durability of geosynthetic reinforcement, load combinations, properties of backfill materials, interaction between backfill and geosynthetic reinforcement, methods to assess stress–strain state and stability of GRS structures, as well as uncertainties associated with the design procedures, etc.

The adequacy of GRS design procedures is normally assessed based on large-scale testing of GRS structures, and on information about satisfactory long-term post-construction behaviour of a large number of GRS structures designed using these procedures. Most of the existing design procedures for GRS structures are empirical design methods based on simplified models of GRS behaviour and GRS case studies rather than on pure theoretical analysis.

General Information concerning GRS Structures

The following information about GRS structures is provided:

- Limitations,
- Lateral displacement,
- Minimum embedment depth for walls,
- Seismic design,
- Tolerance of facing to differential and internal settlement,
- Design life,
- Site investigations, for both feasibility assessments and detailed investigations,
- Properties of foundation and reinforced-backfill soils,
- Design philosophy,
- Load combinations (and the load factors to be applied),
- The Serviceability Limit State.

Design of GRS Walls

GRS walls: incorporate planar geosynthetic reinforcement in earth structures having faces that are less than 30° inclination from the vertical.

Guidelines for the design of GRS walls for external stability under static conditions are separated into the main failure modes likely to occur:

- Forward sliding,
- Overturning,
- Bearing capacity failure,
- Deep-seated failure.

Guidelines for the design of GRS walls for external stability under seismic conditions are based first on an assessment of seismicity of the site, together with a determination of accepted probability of occurrence and the design-basis earthquake. Then procedures for analysing the external stability of GRS walls under seismic conditions are presented.

Guidelines for the design of GRS walls for internal stability under static and seismic conditions are given under the following failure modes:

- Reinforcement rupture,
- Pullout,
- Internal sliding.

Guidelines for local stability analysis of GRS walls consider the following:

- Structural strength of facing elements,
- Durability of facing elements,
- Resistance to bulging,
- Strength of connections between facing elements and geosynthetic reinforcement,
- Local overturning,
- Stability of unreinforced facing section above the highest reinforcement layer.

Design of GRS Slopes

GRS slopes: incorporate planar geosynthetic reinforcement in earth structures having faces that are more than 30° inclination from the vertical.

Guidelines for the design of GRS slopes for external stability under static and seismic conditions are separated into the main failure modes likely to occur:

- Forward sliding,
- Deep-seated failure,
- Bearing capacity failure,
- Local bearing capacity failure,
- Excessive settlement.

Guidelines for the design of GRS slopes for internal stability under static conditions summarise the analysis methods adopted, as follows:

- Maximum size of the zone to be reinforced,
- Geosynthetic reinforcement tension,
- Chart design procedures,
- Distribution of reinforcement,
- Length of reinforcement required,
- Trial layout of reinforcement

Guidelines for the design of GRS slopes for internal stability under seismic conditions recommend use of the pseudo-static stability analysis method.

The need for intermediate reinforcement layers in GRS slopes is an additional check that is to be undertaken.

Subsurface & Surface Water in GRS Structures

Measures to control subsurface and surface water run-off are discussed.

Contracting Procedures

The *Method and Material Specification* approach includes the development of a detailed set of GRS structure drawings and material specifications. An example of this specification is given in Appendix F1.

The *Performance or Design Build Specification* approach is to purchase design, materials and construction from a single source, an example of which is given in Appendix F2.

Both approaches have advantages and disadvantages, and these are discussed.

Computer Programs for Design of GRS Structures

Eleven computer programs for the design of GRS structures that have been developed by suppliers and researchers are listed.

Appendices

The appendices include reprints from standard works and methods, specifications, and other material necessary as guidelines.

A. Design tensile strength and soil–reinforcement interaction

B. Environmental conditions and durability of geosynthetic reinforcement (reprinted from an FHWA research report).

C. Information about geosynthetic reinforcement to be supplied by the manufacturer/supplier.

D. Deformation analysis method, being a reprint of Cai & Bathurst (1996) Seismic-induced permanent displacement of geosynthetic-reinforced segmental retaining walls. *Canadian Geotechnical Journal 33:* 937-955.

E. Local stability of GRS walls with segmental precast concrete unit facings.

F. Specifications for GRS Structures: Method and material specification; Performance specification.

G. Worked Examples for GRS Walls.

H. Design Charts and Worked Examples for GRS Slopes, being a reprint of Jewell (1991) Application of revised design charts for steep reinforced slopes. *Geotextiles and Geomembranes 10 (1991)*: 203-233.

Abstract

Geosynthetic-reinforced soils (GRS) have been found to be cost-effective compared to traditionally used retaining structures in specific situations. As a consequence the application of GRS to structures carrying roads and/or pedestrian traffic is rapidly increasing. Also GRS structures are less prone to damage under seismic loads than conventional type structures.

GRS is a comparatively new technique and the design methods for GRS are not well established. As a result, New Zealand geotechnical engineers currently use several different overseas standards and design guidelines to design GRS structures.

Therefore research was undertaken to prepare guidelines for design and construction of GRS structures in New Zealand. Stage 1, undertaken in 1997-1998, was published as a Review & Discussion paper in 1998. The results of Stages 2 and 3, undertaken in 1999-2002, are these comprehensive guidelines for design and construction of GRS structures, both walls and slopes, in New Zealand. They have been developed for use by New Zealand consultants, contractors, and Road Controlling Authorities.

1. Introduction

Geosynthetic-reinforced soils (GRS) have been found to be cost-effective compared to traditionally used retaining structures in specific situations. As a consequence the application of GRS to structures carrying roads and/or pedestrian traffic is rapidly increasing. Possible applications of GRS structures on highways are shown on Figures 1.1 and 1.2. These applications include:

- Reinforced embankments in place of viaducts;
- Reinforced embankments supporting highways;
- Repair of slope failures;
- Bridge abutments.

Very often GRS structures can provide substantial cost savings compared with conventional type structures such as reinforced-concrete retaining walls. Like steel-reinforced mechanically stabilised embankments (e.g. Reinforced Earth walls and slopes), GRS structures may replace conventional structures in many applications.

In addition to their low cost compared with conventional structures, evidence from the 1995 Kobe Earthquake (Japan) indicates that GRS structures are less prone to damage under seismic loads than conventional type structures. Also GRS and Reinforced Earth structures located in strongly shaken areas of Kobe City survived with insignificant or no damage and only minor permanent displacements, but the conventional type reinforced concrete structures were severely damaged and many of them collapsed. On the basis of this factual data, many of the severely damaged conventional type structures in Kobe City have been reconstructed using GRS techniques, and the use of GRS structures has been expanded for many important roading projects in Japan, in place of conventional reinforced concrete structures.

GRS is a comparatively new technique. For example, in Japan the first project involving GRS was undertaken in 1988 and the use of GRS on a wider scale started only in 1992. Therefore the design methods for GRS are not well established. New Zealand geotechnical engineers currently use several different overseas standards and design guidelines to design GRS structures.

Although static behaviour of GRS structures is comparatively well understood and design practice is well established, there are still variations between sizes of GRS block and amounts of reinforcement predicted by different design methods. Also, there does not appear to be any widely held consensus on seismic design procedures for GRS structures.

Most of the design methods given in overseas standards do not include procedures to allow seismic loads to be taken into account. Moreover, there is disagreement between different researchers' points of view and different standards on how to take into account seismic loads in GRS design.

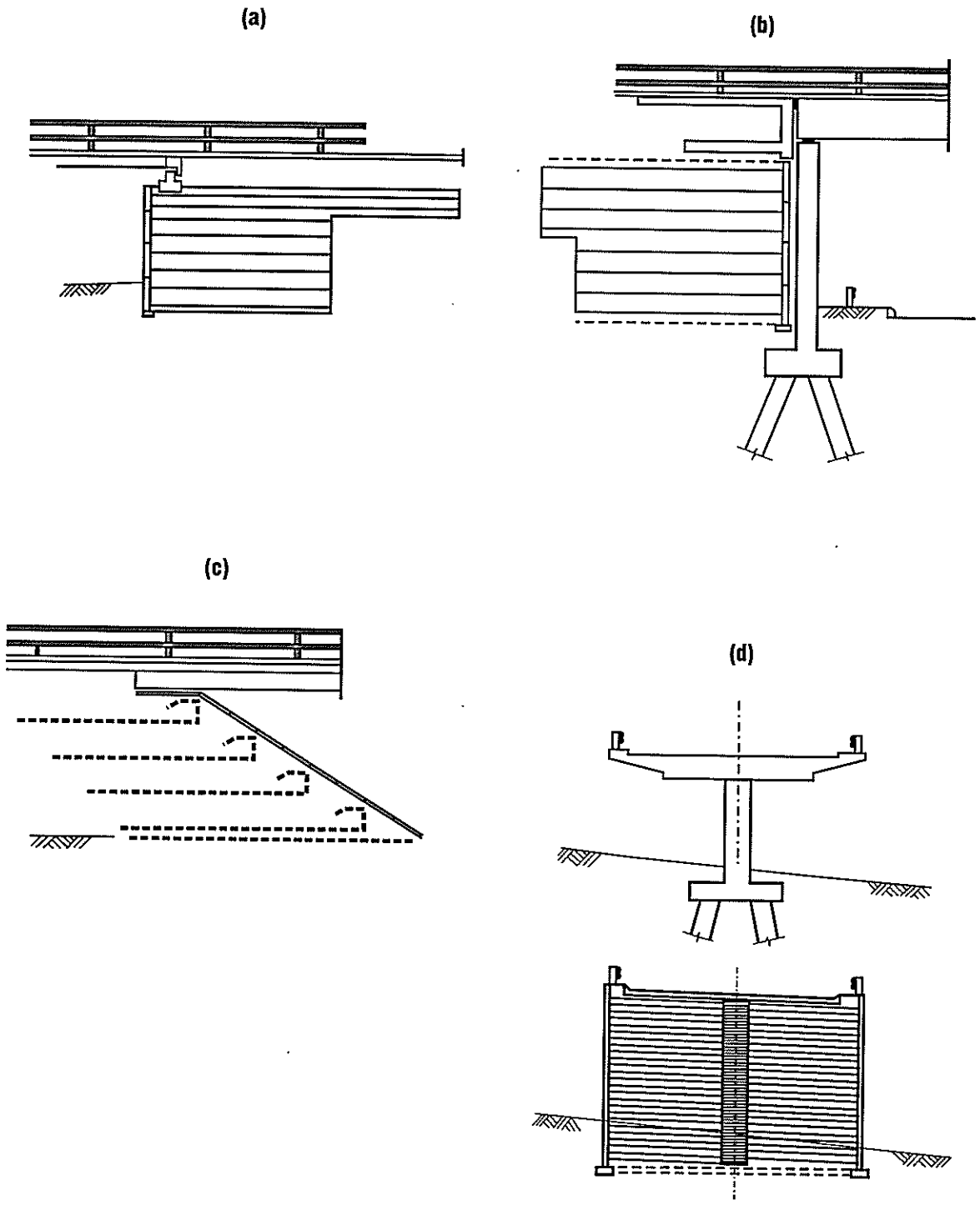

Figure 1.1 Applications of GRS: (a), (b), (c) Bridge abutments; (d) Reinforced embankment in place of viaduct.

20/4/98
CAD FILE 3401650SK10.CDR AM/LG

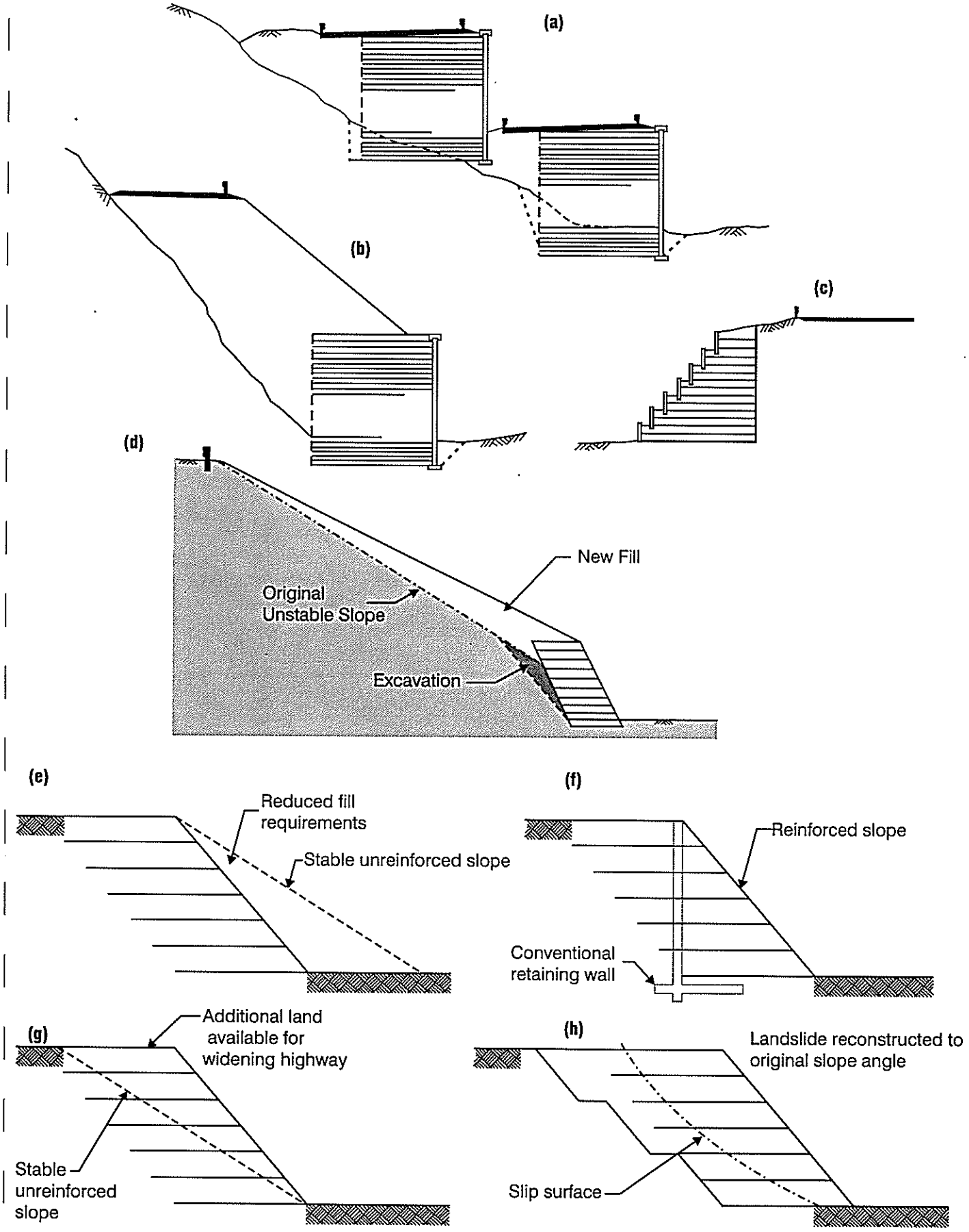

Figure 1.2 Applications of GRS: (a), (b), (c) reinforced embankments supporting highways; (d) repair of unstable slope; (e) construction of new embankments with reduced fill requirements; (f) alternative to conventional retaining walls; (g) widening existing embankments without encroachment beyond designation boundary; (h) repair of landslides.

13/12/00
CAD FILE 3401650SK11.CDR AM/LG/MT

The amount of laboratory and field testing specified and types of soil strength parameters used by different overseas standards and design guidelines also differ. Reports have also been published of failures of GRS structures under static loads. On the other hand manufacturers of geosynthetic materials every year produce a number of booklets and design manuals introducing new reinforcing materials and design methods (including the software products they sell). All this results in GRS structures in New Zealand being designed to different standards and, therefore, with different levels of static and seismic resistance, and different risks of failure under seismic loads.

Because of these uncertainties, some New Zealand consultants still prefer to use conventional reinforced-concrete structures rather than GRS structures. Alternatively, consultants use performance-type specifications making a contractor carry all responsibility for design, preparation of detailed specifications and drawings, and erection of GRS structures. Very often in the latter case potential contractors are forced into a situation where they do not have sufficient information on ground conditions or enough time to undertake the additional geotechnical investigations required to develop cost-effective preliminary GRS designs during the tender period. This normally results in higher cost of GRS structures to Road Controlling Authorities (RCA).

Given that the use of GRS structures in New Zealand is increasing, the establishment of the design and construction guidelines for GRS structures in New Zealand is obviously far behind their practical application. Therefore, this research project was undertaken to prepare guidelines for design and construction of GRS structures in New Zealand.

Stage 1 of the project was undertaken in 1997-1998, and results were published as a Review & Discussion paper in 1998 (Murashev 1998). A large number of existing standards, guidelines and recommendations for design and construction of GRS structures, as well as more than 200 New Zealand and overseas GRS case histories, were reviewed as part of Stage 1 of the project.

This report presents the results of Stages 2 and 3 of the research project, as comprehensive guidelines for design and construction of GRS structures in New Zealand. The guidelines have been developed for use by New Zealand consultants, contractors, and Road Controlling Authorities. Both GRS walls and GRS slopes are covered. Although the design procedures adopted in the guidelines are based on the results of the GRS research review (Murashev 1998) and a draft of the guidelines (Murashev 2001), this report is to be read as a stand-alone document.

2. General Information concerning GRS Structures

2.1 Background

Design procedures for GRS structures address a number of important aspects such as design tensile strength and durability of geosynthetic reinforcement, load combinations, properties of backfill materials, interaction between backfill and geosynthetic reinforcement, methods to assess stress–strain state and stability of GRS structures, uncertainties associated with the design procedures, etc. The adequacy of GRS design procedures is normally assessed based on large scale testing of GRS structures and on information about satisfactory long-term post-construction behaviour of a large number of GRS structures designed using these procedures. Most of the existing design procedures for GRS structures are empirical design methods based on simplified models of GRS behaviour and GRS case studies rather than on pure theoretical analysis.

Design methods for GRS used in current engineering practice differ from country to country. Also there does not appear to be any widely held consensus on seismic design procedures for GRS. Very often, available GRS design methods are not capable of accurately describing some aspects of static or seismic behaviour of GRS structures but, if based on extensive research and a large number of case studies, normally result in reliable design solutions.

The design guidelines in this report cover the most important GRS design aspects, and are primarily based on the existing design methods that have been used extensively in New Zealand and overseas, and on sound research data (Christopher et al. 1990b; Berg 1993; Elias 1997; Elias & Christopher 1997; Holtz et al. 1995; NCMA 1997, 1998b; BSI 1995 (BS 8006); SA 1996 (AS DR 96405)). The research review, undertaken between 1997 and 1998 and published as Transfund New Zealand Research Report No.123 (Murashev 1998), indicated that these methods in most cases provide safe design solutions.

Most New Zealand material codes are, or are about to be, expressed in the limit state design format using a load and resistance factored design approach. In the last six years (1994-2000) the limit state design approach has been actively promoted by the New Zealand Geotechnical Society (NZGS) (Pender & Matushka 1994; Pender 2000). Therefore, these guidelines have been written in the limit state design format using a load and resistance factored design approach.

This report is intended to serve as guidelines only. Other design methods (e.g. those developed by material suppliers or included in GRS standards or guidelines published elsewhere) can be used but in each case their use should have a sound justification, should consistently cover all aspects of the design (i.e. design methods, material and load factors, and test methods should be compatible), and should be supported by extensive research data and information about satisfactory post-construction behaviour of GRS structures designed by these methods.

Some of the recommendations given in these guidelines may need to be modified as required by engineering judgement and experience, based upon project-specific design and performance criteria. GRS technology is an area of ongoing research and refinement and, therefore, some amendments to these guidelines may be required as new research data becomes available.

2.2 Terminology

2.2.1 General

The following terms will be used throughout these guidelines:

Geosynthetics – a generic term that encompasses flexible polymeric materials used in geotechnical engineering, such as geotextiles and geogrids.

Geotextile – a permeable geosynthetic comprised solely of textiles.

Geogrid – a geosynthetic used for reinforcement which is formed by a regular network of tensile elements with apertures of sufficient size to allow strike-through of surrounding soil, rock or other geotechnical material. Geogrids comprise a regular network of integrally connected elements, which may be linked by extrusion, bonding or interlacing.

Mechanically Stabilised Earth (MSE) – a generic term that includes *reinforced soil.*

Reinforced Soil – a term used when multiple man-made elements are incorporated in the soil to improve its behaviour. The elements act as reinforcement in soils placed as fill.

Geosynthetic-reinforced Soil (GRS) – soil reinforced with geosynthetics.

Geosynthetic-reinforced Soil (GRS) Walls – a form of mechanically stabilised earth (MSE) that incorporates planar geosynthetic reinforcement in constructed earth structures having face inclinations from the vertical of less than 30 degrees.

Geosynthetic-reinforced Soil (GRS) Slopes – a form of mechanically stabilised earth that incorporates planar geosynthetic reinforcement in constructed earth structures having face inclinations from the vertical of 30 degrees or more.

Retained Backfill – the fill material between the reinforced soil block and the natural soil.

Reinforced Backfill – the fill material in which the reinforcements are placed.

Facing – a component of the reinforced soil system used to prevent the soil from ravelling out between the layers of reinforcement. The facing also plays a minor structural role in the stability of the structure.

Only GRS structures with geogrid and geotextile reinforcement are discussed in these design guidelines.

2.2.3 Facing Systems

The most common facing types for GRS structures are:

Rap-Around Facing – this type includes various types of geosynthetics that are looped around at the facing to form the exposed face of GRS structures.

Post-Construction Facing – for wrap-around walls, this type can be attached after construction of the wall and can comprise shotcreting, cast-in-place concrete, panels made of concrete, wood, etc.

Gabion Facing (rock-filled wire baskets) – can be used as facing with reinforcing elements consisting of geogrids and geotextiles. A geotextile filter is typically used between the back face of the gabion baskets and the reinforced backfill to prevent the soil from piping throughout the gabion stones.

Proprietary Segmental Precast Concrete Units – are relatively small concrete units, solid or with cores, with mass of 20 to 50 kg, that have been specially designed and manufactured for retaining wall applications. Unit heights typically range from 100 mm to 200 mm.

Units are normally dry stacked (i.e. without mortar). Vertically adjacent units may be connected with shear pins, lips or keys. These facing elements are also known as segmental retaining wall (SRW) units, modular concrete units or modular block wall units.

Segmental Precast Concrete Panels – are similar to the panels used to face metallic MSE systems. Stiff polyethylene geogrids are exclusively used for precast concrete panel faces, where tabs of the geogrid are cast into the concrete and are connected to the soil-reinforcing geogrid layers in the field. Flexible polyester geogrids are not used because casting them into wet concrete would expose the geogrids to a high alkaline environment.

Full Height Precast Concrete Panels – are used where aesthetics of full height panels are specifically desired. Similar to segmental precast concrete panels, stiff polyethylene geogrids are exclusively used for precast concrete panel faces where the tabs are cast into the panel.

Erosion Control Mats or Vegetation – are used for GRS slopes with face angles flatter than 1V:1H, and with reinforcements at close spacings.

2.3 Limitations

GRS structures should not be used under the following conditions :

- When utilities other than highway drainage must be constructed within the reinforced zone, and where future access for repair would require the reinforcement layers to be cut.

- When flood-plain erosion may undermine the reinforced fill zone, or where the depth to scour cannot be reliably determined.

GRS walls should be limited to 15 m in height. A minimum reinforcement length of 0.7 H is recommended for GRS walls where H is the height of the wall.

GRS slopes should be limited to 30 m in height. GRS slopes taller than 30 m have been constructed successfully, but long-term performance data is not available.

2.4 Lateral Displacement

Lateral displacement of the GRS structure face occurs primarily during construction, although some displacement also can occur because of post-construction static surcharge loads or seismic loads. Post-construction deflections can also occur because of structure settlement. Currently, no standard method is available for evaluating the overall lateral displacement of reinforced soil structures. However, several empirical methods to assess lateral displacement of GRS walls have been developed.

The major factors influencing lateral displacements during construction include compaction intensity, reinforcement stiffness to soil stiffness ratio, reinforcement length, slack in reinforcement connections at the wall face, and deformability of the facing system. An empirical relationship for estimating relative lateral displacements of GRS walls with granular backfills during construction is given in Figure 2.1.

Lateral displacement of GRS walls resulting from seismic loads can be estimated as described in Section 3.2 and Appendix D (Cai & Bathurst 1996) of these guidelines.

In any case provisions should be made to accommodate the calculated displacement without encroaching on required clearances.

Lateral displacement of GRS slopes is probably of the same order as that for GRS walls of similar size and with no surcharge, but there are no commonly accepted empirical methods to assess this displacement. Some references to these methods are given in Section 4 of these guidelines.

2.5 Minimum Embedment

The following minimum embedment depth is recommended at the front of GRS walls (Holtz et al. 1995).

Table 2.1 Minimum embedment depth for GRS walls.

Slope in Front of Wall	Minimum Embedment
Horizontal	H/10
3H : 1V	H/10
2H : 1V	H/7
3H : 2V	H/5

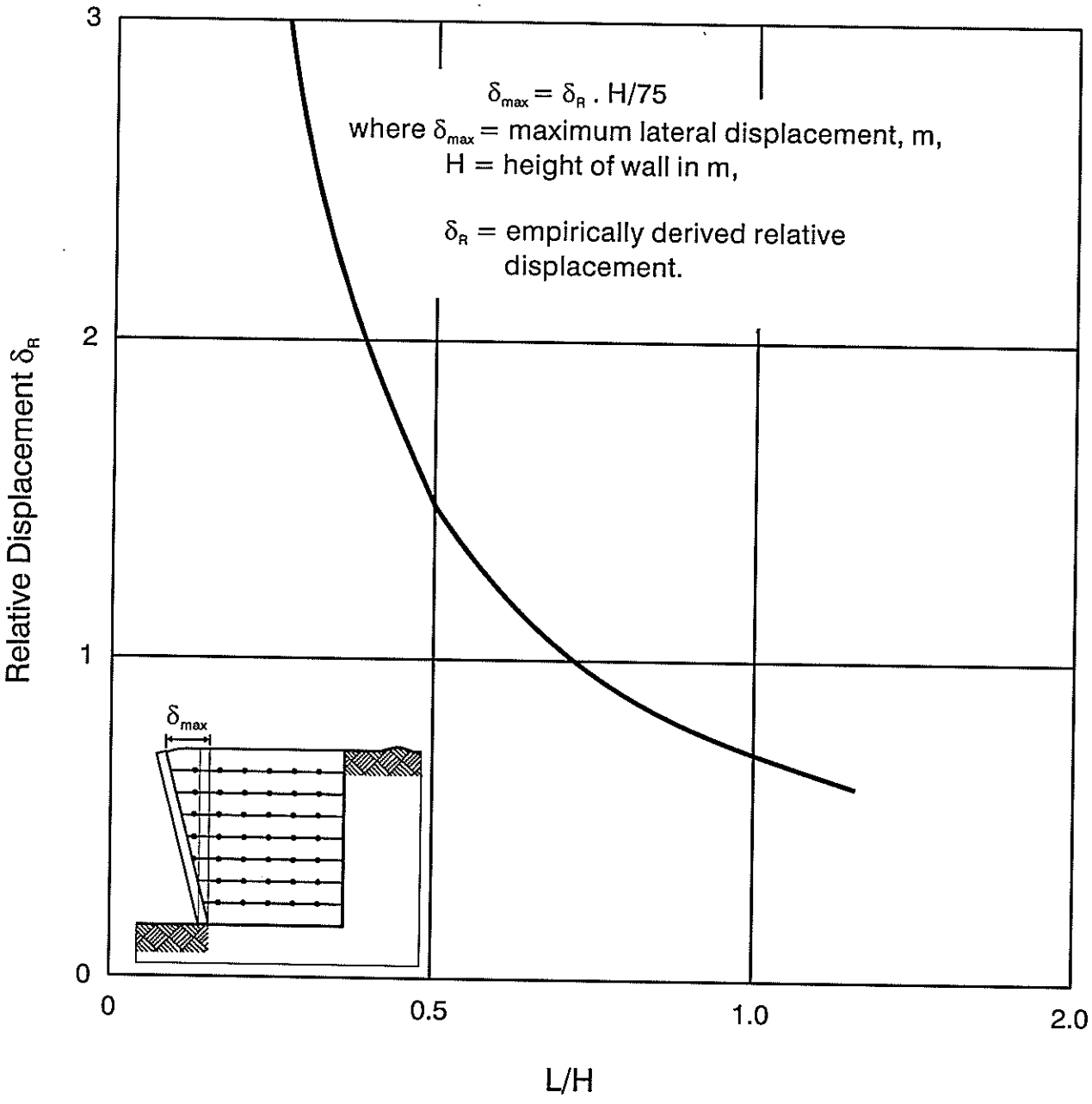

Based on 6m high walls, relative displacement increases approximately 25% for every 20 kPa of surcharge. For higher walls, the surcharge effects may be greater. Actual displacements will also depend on soil characteristics,compaction effort and contractor workmanship.

Figure 2.1 Lateral displacement of GRS walls during construction (after Elias & Christopher 1997).

27/11/00
CAD FILE 3401650SK15.CDR MT

Larger values may be required depending on the site ground conditions, shrinkage and swelling of foundation soils, overall stability of the GRS wall, seismic activity, etc. In any case minimum embedment of 0.5 m is recommended, except for structures founded on rock at the surface where no embedment may be required.

A horizontal bench that has a minimum width of 1.2 m shall be provided in front of GRS walls founded on slopes.

For walls constructed alongside rivers and streams for which the depth of scour has been reliably determined, a minimum embedment of 0.6 m below this depth is recommended.

Embedment is not required for GRS slopes unless dictated by stability requirements.

2.6 Seismic Design

Because of their flexibility, GRS structures are quite resistant to dynamic forces developed during a seismic event, as confirmed by their satisfactory performance in several recent earthquakes. The peak horizontal ground acceleration coefficient (PGA) should be assessed for each site on the basis of a site-specific assessment of seismicity or (in the absence of such assessment) can be taken as

$$PGA = 0.42\ Z\ R$$

where:

Z is the zone factor from Figure 5.3 of the Transit New Zealand Bridge Manual (1994),
R is the risk factor from Table 5.8 of that Manual.

A risk factor of R = 1 corresponds to a 450-year return period event. An earthquake of this return period has a 10% probability of exceedance in a 50-year design life. For walls with a design life longer than 50 years an R greater than 1.0 should be used. A relationship between the Risk Factor and earthquake return period suitable for wall design is given in Figure 5.5 of the Bridge Manual.

For sites where the acceleration coefficient is greater than 0.3, significant total lateral structure movements may occur. Therefore a detailed consideration should be given to the stability and potential seismic deformation of the GRS structure.

All sites should be checked for seismic stability including liquefaction, pore pressure build-up and associated bearing capacity problems, seismic settlement, stability of slopes under seismic conditions, lateral spreading, etc.

Where it is not practical or economically justifiable to eliminate risk of GRS structure failure caused by a strong earthquake, a detailed assessment of the manner, extent and impact of such failure should be undertaken.

2.7 Tolerance of Facing to Settlement

2.7.1 Differential Settlement

Conventional settlement analyses should be undertaken to ensure that settlement of a GRS structure during and after construction is less than the performance requirements for a GRS structure, and for roads or structures supported by the GRS structure.

GRS structures have significant deformation tolerance, both longitudinally along a structure and perpendicularly to the front face. However, where large differential settlements are expected, the tolerance of facing to the differential settlements should be carefully considered.

Facing systems comprising precast concrete panels and segmental precast concrete units are sensitive to differential settlement. If significant differential settlement is anticipated, sufficient joint width and/or slip joints must be provided. Discrete facing panels generally adapt better to larger differential settlements than full height concrete panels or segmental precast concrete units.

The following indicative minimum joint widths are recommended for discrete precast facing panels depending on the expected magnitude of differential settlements (Elias & Christopher 1997).

Table 2.2 Recommended joint width for segmental precast facing panels.

Joint Width (mm)	Differential Settlement
20	1/100
13	1/200
6	1/300

Full-height precast concrete panel facings should not be used if the expected differential settlement is higher than 1/500.

Segmental precast concrete unit facings should not be used if the expected differential settlement is higher than 1/200.

Discrete concrete facing panels with joint widths greater than 1% of their maximum dimension may be used where differential settlements up to 1/100 are expected.

Where large differential static or seismic settlements are expected, ground improvement works may be required to limit the settlements of GRS structures.

2.7.2 Internal Settlement

Facing systems should also accommodate internal settlement within the reinforced soil block. The internal settlement is highly dependent on the nature of reinforced backfill, compaction quality and vertical pressures within the fill.

The following minimum vertical movement capacities are recommended in BS 8006 (BSI 1995):

- for discrete panels – joint closure of 1/150 relative to panel height;
- for full height panels – vertical movement capacity of connections 1/150 relative to panel height;
- for wrap-around facing – no specific limit except for serviceability considerations.

2.8 Design Life

The intended period of time over which a GRS structure is required to fulfil its function is referred to as its 'design life' and should be considered in the design process.

In GRS structures the life of reinforcement, facing system and connections shall have compatible durability requirements with the remainder of the structure, and with the design life of the roads and/or structures which are supported by those GRS structures. Table 2.3 lists the design lives that are normally recommended:

Table 2.3 Recommended design life for GRS structures.

	Typical Application	Recommended Design Life (years)
A	Temporary site works	3
B	GRS structures for permanent applications (except for C)	50-90
C	Structures on state highways	100

2.9 Site Investigation Requirements

2.9.1 General

Comprehensive site investigations should be undertaken before designing GRS structures to assess existing topography; subsurface conditions; site stability; foundation-bearing capacity; settlement potential; ground-water regime and chemical composition; need for drainage; availability, properties and characteristics of the proposed fill, etc.

Investigations should be undertaken not only in the area of the construction but also in adjacent areas which may affect the stability of the proposed GRS structure during or after construction.

The extent and complexity of the site investigations should be related to the size, complexity and form of the proposed GRS structure.

2.9.2 Feasibility Assessment

Available information on subsurface site conditions should be collected from previous investigations and geological maps, and analysed. A site visit by a Geotechnical Engineer should be undertaken to:

- Assess relevance of the collected available information;
- Observe and record evident geological features;
- Identify areas of potential instability (soft or organic soils, liquefiable materials, unstable slopes, etc.);
- Obtain data on potential of the site for flooding, erosion, surface drainage patterns and seepage;
- Identify potential borrow areas and sources of reinforced and retained fill material;
- Scope the required investigation work.

2.9.3 Detailed Investigations

Detailed investigations must be sufficient to assess the geologic and subsurface profiles in the area of construction, and to design the GRS structure. Detailed investigations should include a consideration of the following:

- Site topography;
- Founding conditions including soil type, compressibility and strength parameters;
- Existing ground-water levels;
- Location of existing or proposed adjacent structures that may be affected by the proposed GRS structure;
- Availability, nature and properties of reinforced and retained fill materials (including size, grading, strength parameters, chemical properties, compaction characteristics, etc.);
- Subsurface drainage and seepage;
- Seismic stability as described in Section 2.6 of these guidelines.

The minimum scope of field investigations should be as follows, unless a reduced scope of investigations can be justified on the basis of preliminary assessment:

- Boreholes (and in some cases Cone Penetration tests) at 20-30 m centres along the proposed GRS structure, extending at least to a depth equal to twice the height of the proposed GRS structure (or to a shallower depth if this can be justified), with associated sampling and Standard Penetration Tests (SPT);
- Soil samples should be extracted from boreholes for visual identification and laboratory testing;
- Measurement of ground-water levels in boreholes;
- Bulk samples of the proposed reinforced and retained fill materials should be obtained from identified borrow areas;
- Test pits to obtain more information on ground conditions and extract bulk samples of fill materials from the proposed borrow areas;

- Description of soil samples by a Geotechnical Engineer and logging the samples in accordance with the NZGS Guidelines for the Field Description of Soils and Rocks in Engineering Use (NZGS 1988);
- Identification of the potential for hydrostatic pressures or seepage forces on or within proposed GRS structures;
- Identification of existing or future hazardous materials, unnatural chemicals, or microbiological activity at the site.

Minimum scope of laboratory testing should include:

- Grading, Atterberg limits, natural moisture content, bulk unit weight, dry unit weight and other appropriate tests on soil samples, extracted from boreholes and test pits to allow the soils to be classified in accordance with NZGS Guidelines for the Field Description of Soils and Rocks in Engineering Use (NZGS 1988);
- Consolidation tests (for sites with soft compressible materials);
- Appropriate tests (such as triaxial tests, direct shear tests or unconfined compression tests) to obtain strength parameters of soils. Where extensive information on local soils and reliable correlations between physical properties of soils and their strength parameters are available, tests can be omitted;
- Grading tests and Atterberg limits tests on candidate reinforced and retained fill materials;
- Soil pH testing on all candidate reinforced and retained fill materials (if a potential for chemical degradation is suspect).

2.10 Properties of Foundation & Reinforced Backfill Soils

The soil materials within and adjacent to a GRS structure have the greatest influence on the final design of the structure.

Properties of foundation soils established as part of the detailed geotechnical investigations (Section 2.9 of these guidelines) should be used to assess seismic stability of the site, seismic and static bearing capacity, seismic and static settlements of the soils supporting a GRS structure. Properties of reinforced backfill material should be used to assess long-term performance of a GRS structure during its design life, construction phase stability, and the degradation environment for geosynthetic reinforcement.

The soil friction angle ϕ, the soil cohesion c, unit weight γ, and ground-water level are normally required for the design. Peak shear strength parameters should be used. The friction angle of soils should be consistent with its unit weight.

The soil friction angle ϕ and the soil cohesion c shall be obtained by one of the following methods:

- Laboratory testing;
- Field testing;

- Analysis of historical geotechnical data;
- Knowledge of geotechnical conditions and engineering judgement.

Most of the case studies and experience with GRS structures to date relate to structures with granular reinforced backfills. Therefore, where possible granular materials should be used as reinforced backfill.

Properties of reinforced backfill material can influence the stress–strain state of the GRS structure during its construction and design life, pullout resistance of reinforcement, the shape of potential failure surface, degradation mechanisms affecting geosynthetic reinforcement, etc. Therefore, selection of reinforced backfill should be based on the consideration of the degradation environment created for geosynthetic reinforcement, compactability of backfill, and the post-construction behaviour of the GRS structure.

Some of the material suppliers have developed reinforcement-specific or structure-specific acceptance criteria for reinforced backfill. These criteria should be used where appropriate and subject to other considerations.

If suppliers' acceptance criteria are not available, the following acceptance criteria should be used (Holtz et al. 1995):

- Reinforced backfill should be free from organic or other deleterious materials with the following grading:

For GRS walls:

Sieve Size	**Percent Passing**
20 mm	100%
4.75 mm	20-100%
0.425 mm	0-60%
0.075 mm	0-15%

(The maximum particle size can be increased up to 100 mm on the condition that appropriate testing is undertaken to evaluate the reduction factor for installation damage.)

For GRS slopes:

Sieve Size	**Percent Passing**
100 mm	75-100%
4.75 mm	20-100%
0.425 mm	0-60%
0.075 mm	0-50%

- Plasticity index of reinforced backfill should be less than 12 for GRS walls, and less than 20 for GRS slopes.
- Chemical properties of reinforced backfill and their effect on durability of geosynthetic reinforcement should be assessed (refer to Appendix B).

- Reinforced backfill should be compacted to 95% of maximum dry density determined by the Standard Compaction Test (NZS 4402:1986, test 4.1.1, SANZ 1986).

Reinforced backfill material outside the above gradings and plasticity index requirements have been used successfully, but long-term (>15 years) performance field data is not available. For clay or silt backfills, laboratory shear and pullout tests should be performed under all circumstances.

2.11 Design Philosophy

The design methods for GRS structures described in these guidelines are based on the limit state design approach. Ultimate limit state (collapse or major damage) and serviceability limit state (movement or damage in excess of specified design limits) are considered to ensure that GRS structures will comply with the performance requirements.

The following ultimate limit state design approach is used in these guidelines:

$$F^* = \sum \alpha_i F_i \leq T^* = \Phi T \qquad (1)$$

where:

F^* is the design load;
α_i are load factors;
F_i are the applied loads;
$\sum \alpha_i F_i$ is the design load equal to the sum of all factored loads;
T^* is the design resistance;
T is the ideal resistance;
Φ is the factor covering one or a combination of possible decreases in the resistance related to various factors, unknowns, uncertainties and consequences of failure.

An exception has been made for the internal stability design of GRS slopes where a traditional total factor of safety approach is used. This approach makes the GRS slope design guidelines consistent with most of the GRS slope analysis computer programs that are currently available.

2.12 Load Combinations

The most adverse loads likely to be applied to the GRS structure should be considered. Load factors should be applied to each component of load for different load combinations as set out in Table 2.4. These load combinations are based on those recommended in BS 8006 (BSI 1995).

In addition to load combinations given in Table 2.4, all other possible load combinations should be checked to ensure that the critical condition has been found and considered.

Table 2.4 Load factors for GRS wall structures.

Effects	Load Factors for the following load combinations			
	A	B	C	D
Mass of the reinforced soil block	1.5	1.0	1.0	1.0
Mass of the backfill and other dead loads:				
– on top of the reinforced block	1.5	1.0	1.0	1.0
– behind the reinforced block	1.5	1.5	1.0	1.0
Soil active pressure:				
– from retained backfill behind the reinforced block	1.5	1.5	1.0	1.0
– from reinforced backfill within the reinforced block (for internal stability calculations)	1.5	1.5	1.0	1.0
Earthquake inertia forces	–	–	–	1.0
Traffic load and other live loads:				
– on reinforced soil block	1.5	0	0	0.3
– behind reinforced soil block	1.5	1.5	0	0.3

Load combinations A, B and C usually identify the worst static combination for the various criteria but are for guidance only. All load combinations should be checked for each layer of reinforcement within each GRS structure to ensure that the most critical condition has been found and considered.

Only the dead load portion of any uniformly distributed and/or concentrated surcharge loads should be considered to calculate stabilising forces or moments in the analysis of external and internal stability. Live loads are considered to contribute to de-stabilising forces only.

Combination A
Considers the maximum values of all loads and therefore normally generates the maximum reinforcement tension and the maximum foundation bearing pressure; may also determine the reinforcement requirement to satisfy pull-out resistance.

Combination B
Considers the maximum overturning loads together with minimum self mass of structure and superimposed traffic load; normally dictates the reinforcement requirement for pullout resistance and is normally the worse case for sliding along the base.

Combination C
Considers dead loads only without load factors; used to determine foundation settlements and reinforcement tensions for checking the serviceability limit state.

Combination D
Considers loads under seismic conditions.

2.13 Serviceability Limit State

Movement of a GRS structure should not result in local damage to the structure (which could shorten the structure's intended design life) or in the need for extensive maintenance works. Adverse effect of a GRS structure's movement on roads or structures supported by the GRS structure should be also considered. Deformations of GRS structures are affected by both the construction procedures and design.

Post-construction deformations of GRS structures may be caused by (but not limited to) one or a combination of the following:

- external ground movement;
- settlement of foundation soils;
- creep extension of geosynthetic reinforcement;
- creep movement of soil reinforcement interface;
- consolidation of poorly compacted reinforced backfills;
- deterioration of geosynthetic reinforcement.

Possible deformation modes of GRS structures include:

- rotation of reinforced soil mass about the toe of the structure resulting in lateral displacement of the facing, with largest displacement being at the crest of the structure (typical for GRS walls);
- bulging of reinforced soil block, resulting in bulging of the facing;
- settlement of GRS structure;
- translation (uniform lateral displacement) of the reinforced soil block.

Because of the complex stress–strain state of the reinforced soil mass (including facing, reinforced backfill and geosynthetic reinforcement), currently no commonly accepted methods to design GRS structures for serviceability limit state are available.

Conventional settlement analyses should be undertaken to ensure that settlement of a GRS structure during and after construction are less than performance requirements for a GRS structure, and for roads or structures supported by the GRS structure. If total or differential settlement of foundation soils exceeds project requirements, ground improvement works should be undertaken to reduce the predicted settlement.

Lateral displacement of GRS structures should be assessed. A number of empirical methods to estimate lateral displacement of GRS structures are available, and these methods are described in Sections 2.4, 3.2, 4.1.2 of these guidelines.

Internal strain criteria may be used to assess predicted performance of a GRS structure. However, most of the existing design guidelines do not include any requirements with respect to serviceability limits on internal strain. Adequate ultimate limit state design (based on the geosynthetic design tensile strength defined in terms of creep deformation) and construction procedures normally result in

satisfactory post-construction behaviour of GRS structures in terms of internal strain (also refer to Appendix A1.3).

BS 8006 (BSI 1995) recommends the following serviceability limits on post-construction internal horizontal strains:

For GRS walls:
- bridge abutments 0.5%
- retaining walls 1.0%

For GRS slopes:
- usually strains are not critical;
- strains of the order of 5% may be acceptable but consideration should be given to the impact of the GRS block deformation on the roads or structures supported by the slope.

The total internal strain in a GRS structure is difficult to assess as it is the sum of the reinforcement strain during construction, loading and subsequent creep of reinforcement and soil-reinforcement interface during its design life.

According to BS 8006, the strain related to creep extension of geosynthetic reinforcement between the end of construction and the end of design life can be estimated from the isochronous strain curves for these two times. An average tensile load along the total length of each reinforcement layer should be assessed, and the strain at the end of the design life should be determined from the isochronous strain curves and compared with the recommended limits.

3. Design of GRS Walls

3.1 Design for External Stability under Static Conditions

3.1.1 General

The following potential failure modes should be checked in the external stability analysis:

- Forward sliding;
- Overturning;
- Bearing capacity failure;
- Deep-seated failure.

These failure modes are shown on Figure 3.1. Stability analysis for GRS walls is made by assuming that the reinforced block acts as a rigid body. The influence of passive earth pressures in front of the wall on the stability of GRS walls should be ignored.

Where the external stability analysis indicates that, where one or more failure mechanisms are possible, the following options to improve the stability should be considered:

- increase the size of the GRS block;
- reduce backfill slope;
- use retained backfill with higher strength parameters;
- undertake ground improvement works;
- stage the loading;
- use drainage to reduce pore pressures.

The coefficient of active soil pressure (K_{af}) is calculated as follows:

- For walls with a face inclination to the vertical θ of less than 10°, and a horizontal backfill slope ($\beta = 0$):

$$K_{af} = \tan^2(45 - \phi/2) \qquad (2)$$

- For walls with a face inclination to the vertical θ of less than 10°, and a backfill slope ($\beta > 0$):

$$K_{af} = \cos\beta \left[\frac{\cos\beta - \sqrt{\cos^2\beta - \cos^2\phi}}{\cos\beta + \sqrt{\cos^2\beta - \cos^2\phi}} \right] \qquad (3)$$

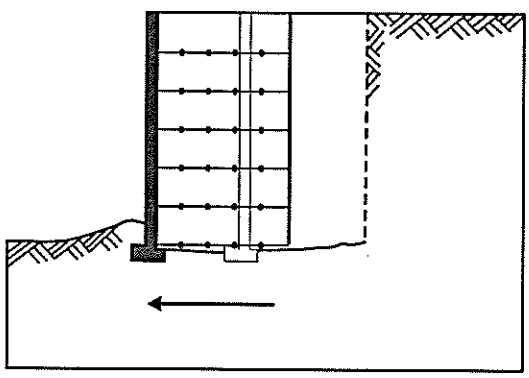

(a) Sliding

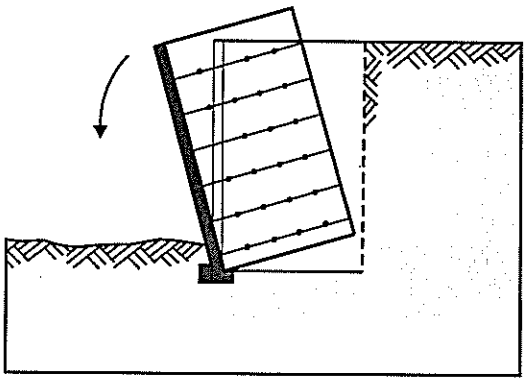

(b) Overturning

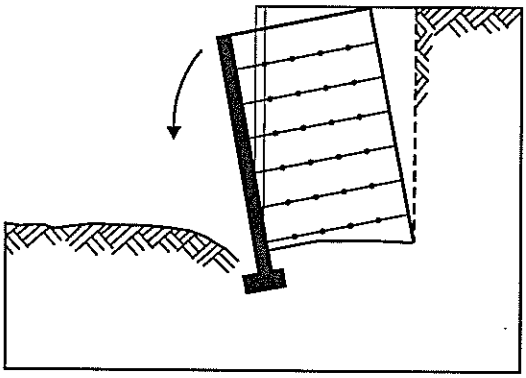

(c) Bearing Capacity

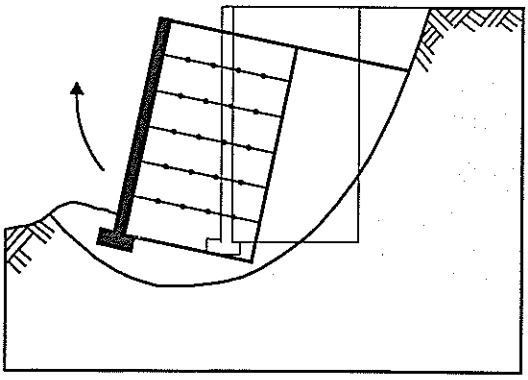

(d) Deep-Seated Failure

Figure 3.1 External failure modes.

- For walls with front face inclination angle to the vertical θ greater than 10°, and a backfill slope (β>0):

$$K_{af} = \frac{\sin^2(\theta+\phi)}{\sin^2\theta \sin(\theta-\delta)\left[1+\sqrt{\frac{\sin(\phi+\delta)\sin(\phi-\beta)}{\sin(\theta-\delta)\sin(\theta+\beta)}}\right]^2} \quad (4)$$

where:

K_{af} is the coefficient of active soil pressure;

β is the backfill slope angle;

δ is the angle of friction between the wall and the retained backfill:
(δ = β can be used assuming Rankine pressure distribution);

θ is the inclination of the wall face from the horizontal (positive in a clockwise direction from the horizontal);

ϕ is the angle of internal friction for retained backfill ($\phi = \phi_f$).

For GRS walls with broken backfill slopes, the angle I should be substituted for the equivalent infinite backfill slope angle β, and the angle I should be defined as shown on Figure 3.2.

An example of the distribution of soil pressures acting at the back of the reinforced zone is shown on Figure 3.3. The soil pressures generated by the retained fill zone are considered to act at the back of the reinforced zone over a height h.

The force F_A due to retained active soil thrust is calculated as follows:

$$F_A = 0.5 K_{af} \gamma_f h^2 \quad (5)$$

where:

F_A is the total active soil force;

K_{af} is the coefficient of active soil pressure for retained backfill;

γ_f is the unit weight of retained backfill;

h is the height over which the active soil pressures are considered to act (Figure 3.3).

The earth force due to a uniformly distributed surcharge *q* acting over the retained soil surface is given by:

$$F_q = q\, K_{af}\, h \quad (6)$$

where:

q is the uniformly distributed surcharge.

If concentrated vertical and horizontal loads are applied at the top of the wall, distribution of stresses from these loads should be considered in the external and internal stability calculations as shown on Figures 3.4 and 3.5, and lateral forces resulting from the loads should be taken into account.

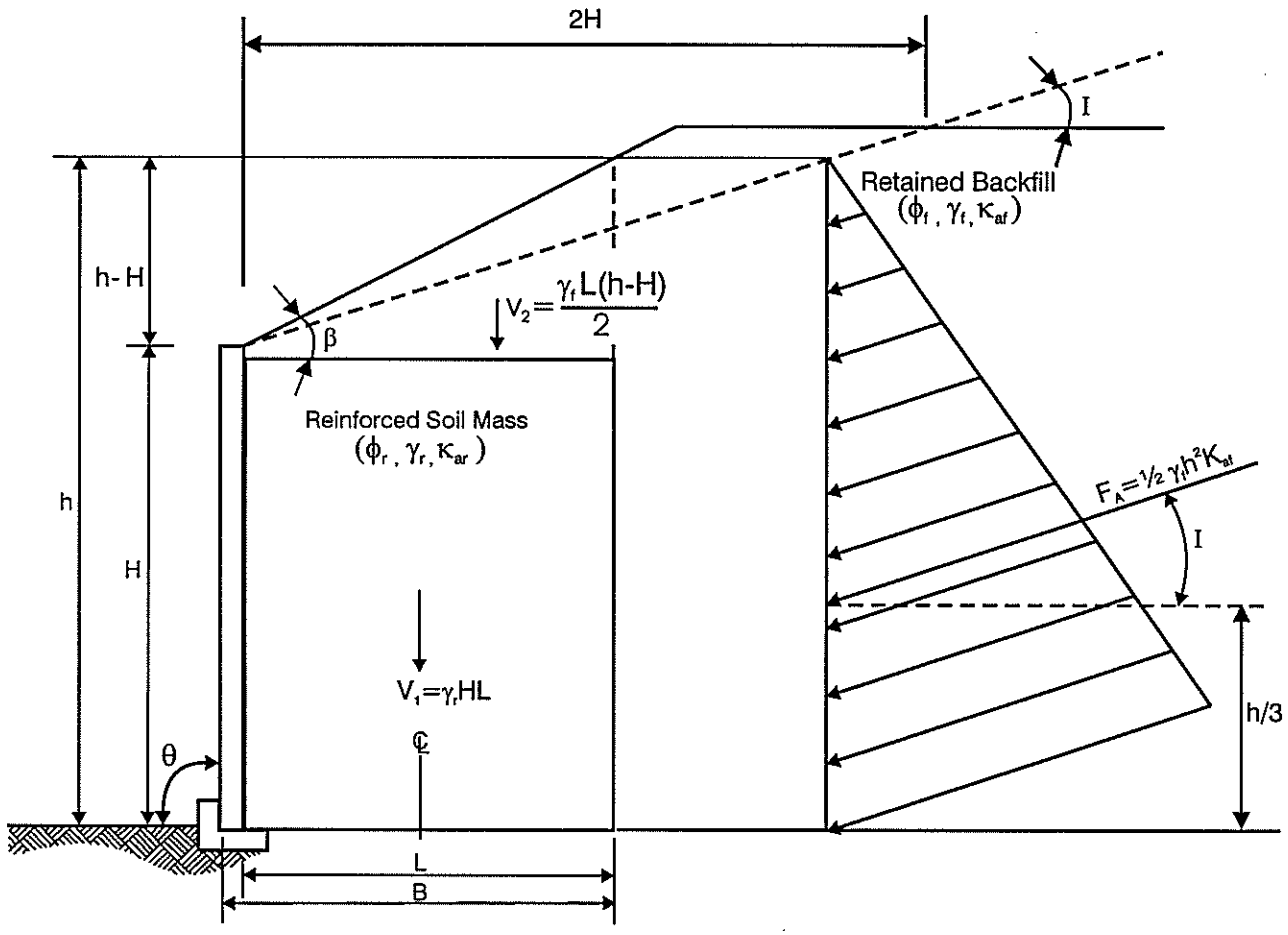

For Infinite Slope I = β

Figure 3.2 Broken backslope case.

15/11/00
CAD FILE 3401650SK4.CDR MT

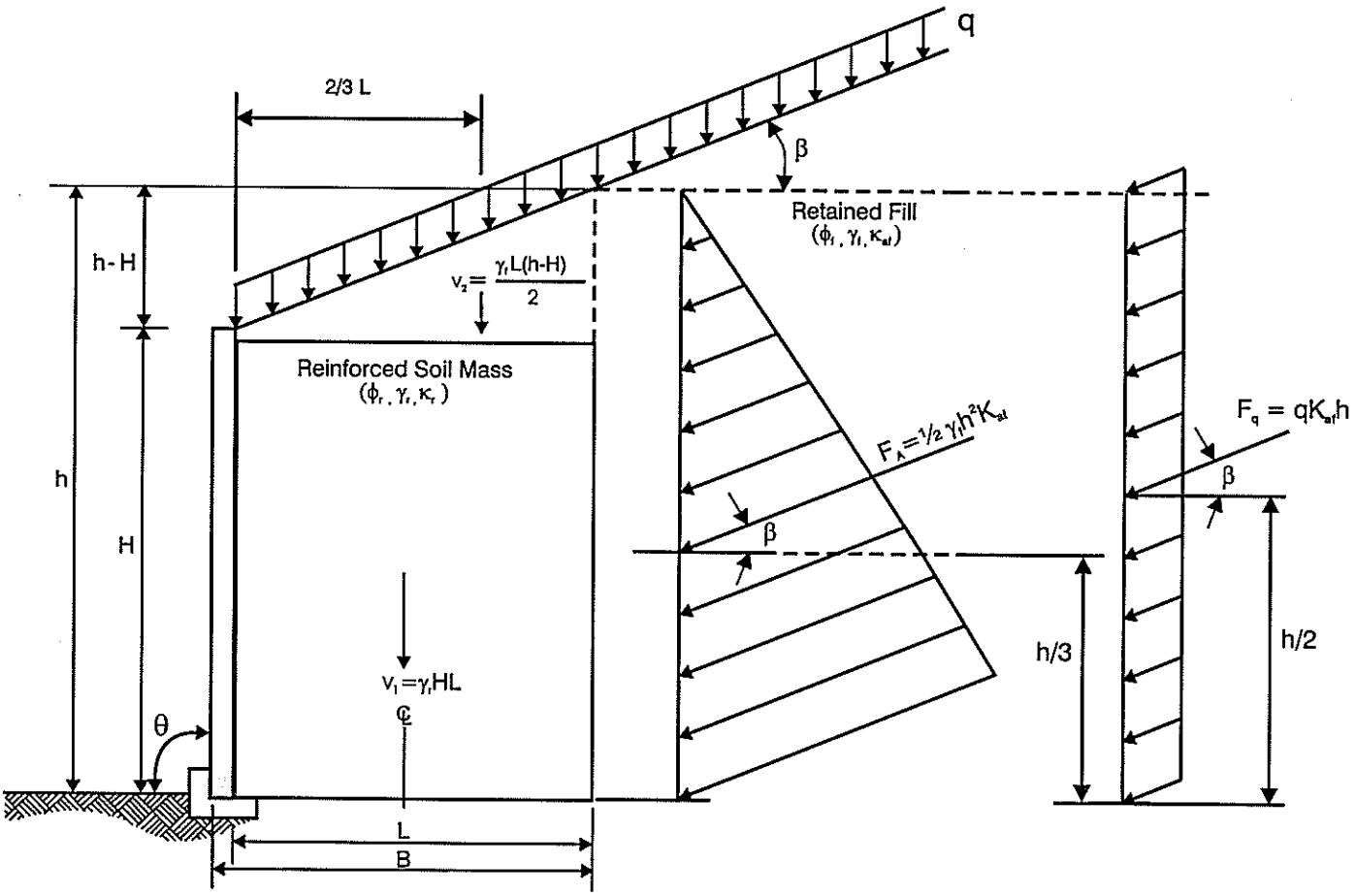

Figure 3.3 Forces and geometry for external stability calculations.

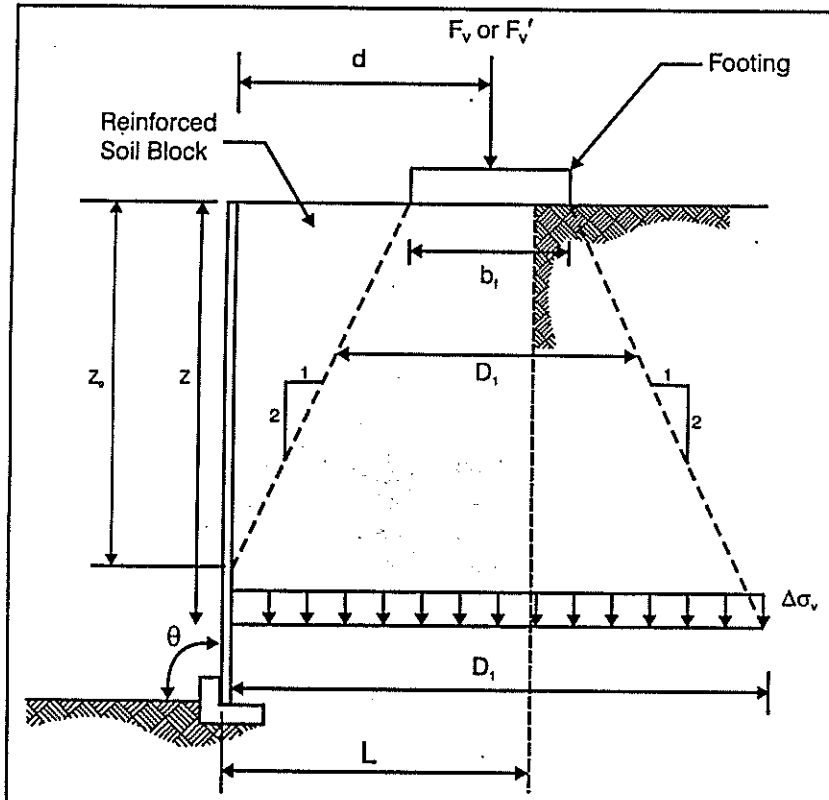

a) Distribution of Stress for Internal Stability Calculations.

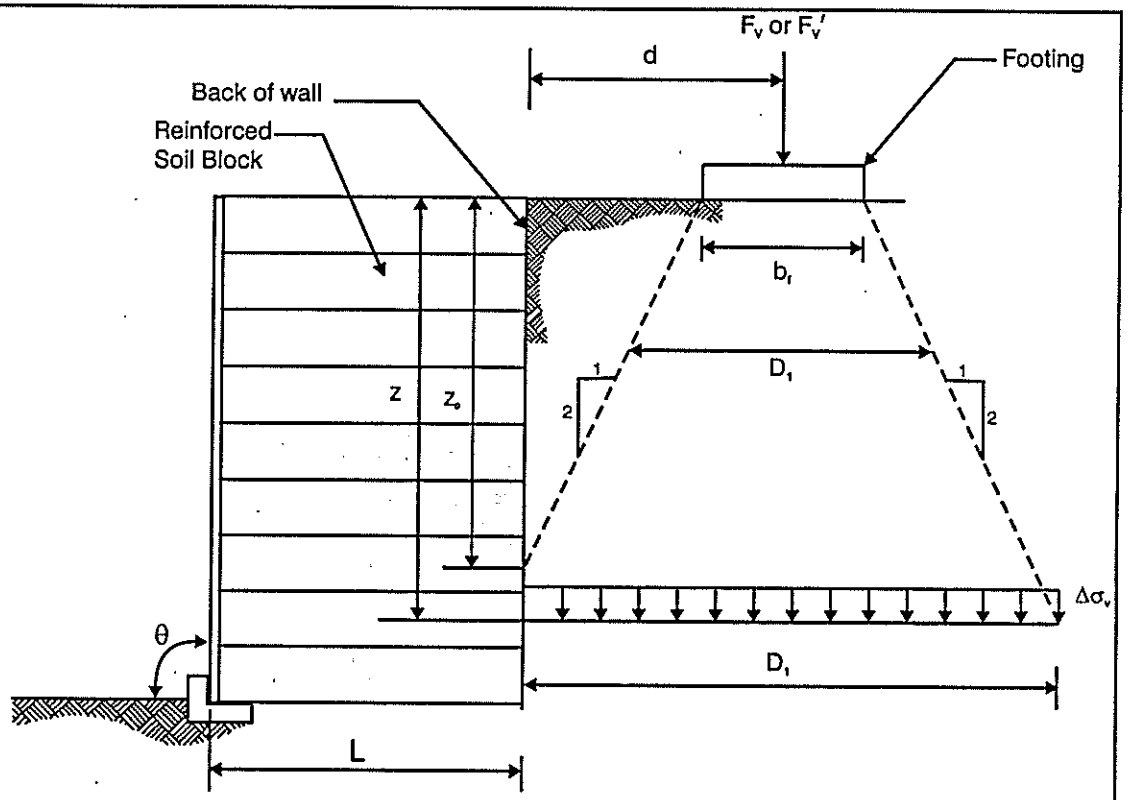

b) Distribution of Stress for External Stability Calculations.

For $Z \le Z_o$

$D_1 = b_f + Z_1$

For $Z \ge Z_o$

$$D_1 = \frac{b_f + Z_o}{2} + d$$

For Strip load:

$$\Delta\sigma_v = \frac{F_v}{D_1}$$

For Isolated footing load:

$$\Delta\sigma_v = \frac{F_v'}{D_1(L_o+Z)}$$

For point load:

$$\Delta\sigma_v = \frac{F_v'}{D_1^2} \quad \text{with } b_f = 0$$

Where: $\Delta\sigma_v$ = increment of vertical pressure at any depth z due to concentrated vertical load.

D_1 = effective width of applied load at any depth z.

b_f = width of applied load. For footings which are eccentrically loaded (e.g., bridge abutment footings), set b equal to the equivalent footing width by reducing it by 2e. where e is the eccentricity of the footing load (i.e., b_f - 2e).

L_o = length of footing

F_v = load per linear meter of strip footing

F_v' = load on isolated rectangular footing or point load

z_o = depth where effective width intersects back of wall face.

Assume the increased vertical stress due to the surrounding surcharge load has no influence on stresses used to evaluate internal stability if the surcharge load is located behind the reinforced soil block. For external stability, assume the surcharge has no influence if it is located outside the active zone behind the wall. Horizontal pressures at any depth $z \ge z_o$ for internal and external stability calculations can be assessed as $\Delta\sigma_h = K_a \Delta\sigma_v$

24/11/00

CAD FILE 3401650SK9.CDR MT

Figure 3.4 Distribution of stress from concentrated vertical load for internal and external stability calculations.

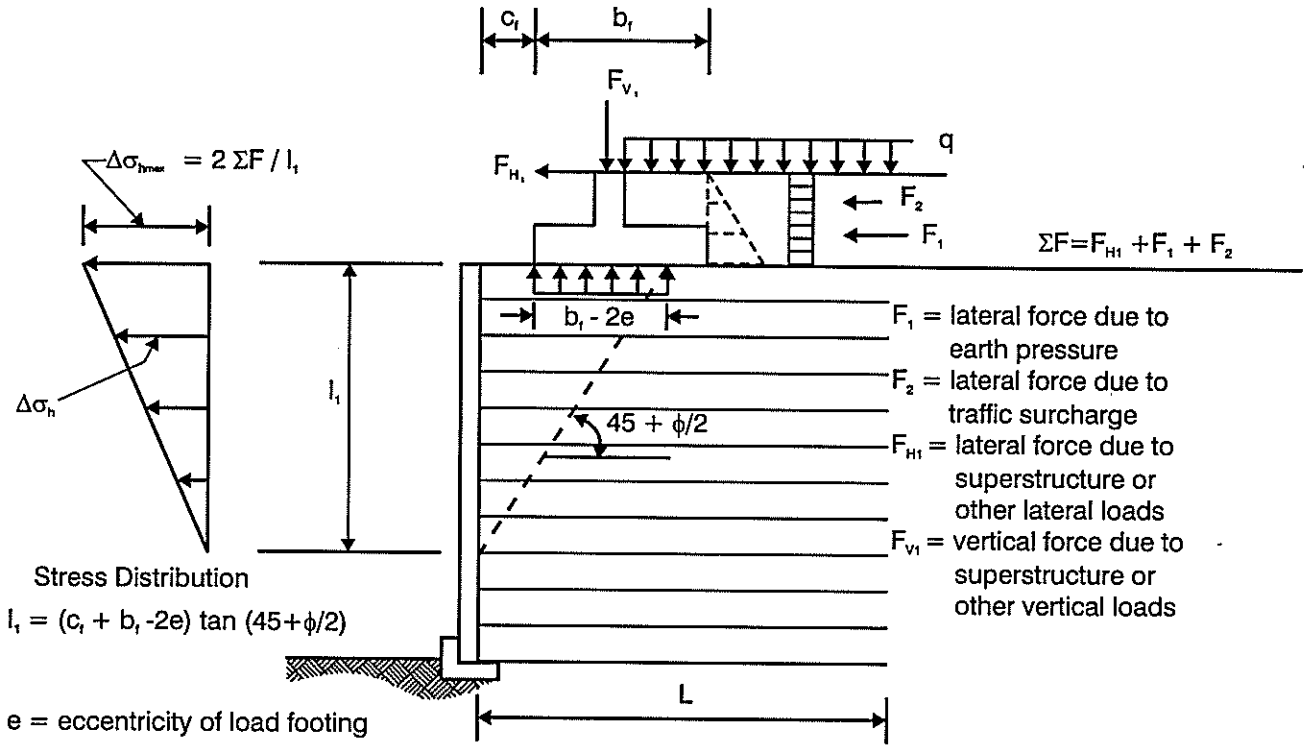

a) Distribution of Stress for Internal Stability Calculations.

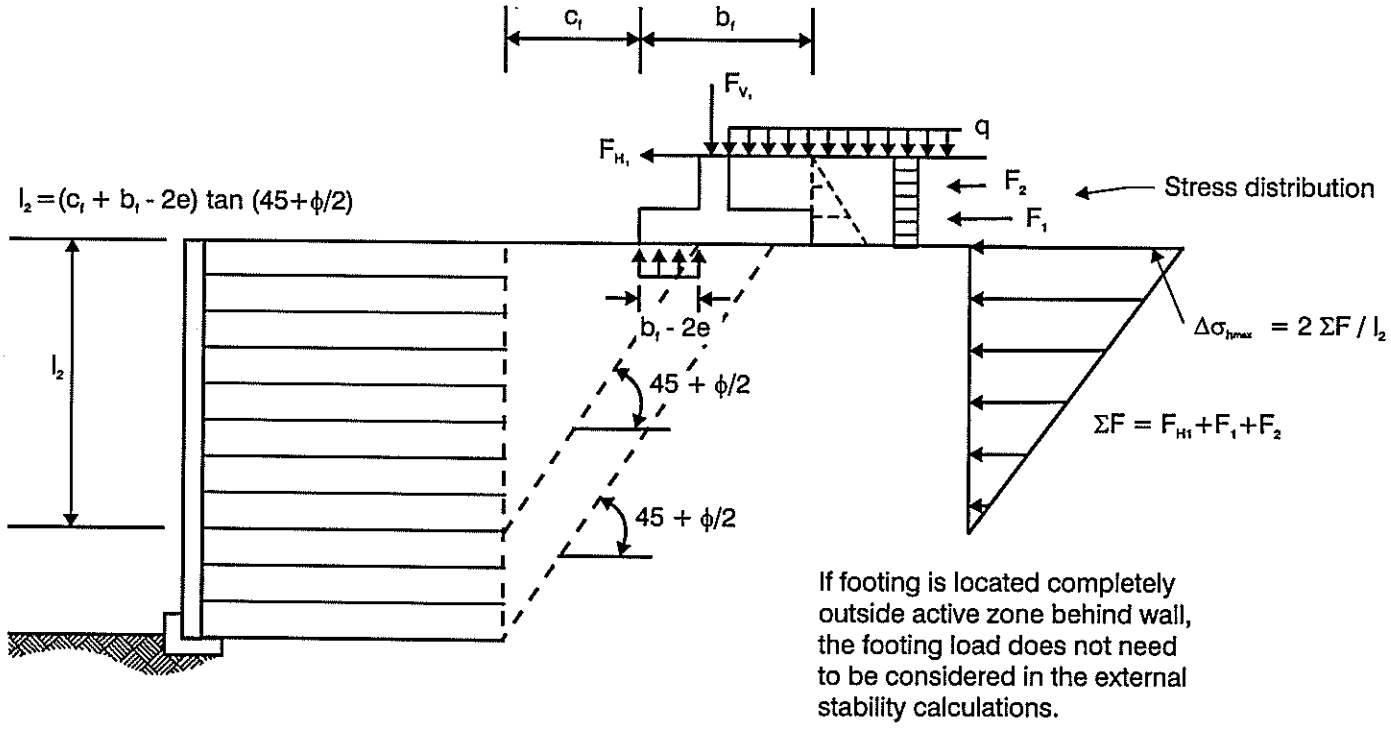

b) Distribution of Stress for External Stability Calculations.

Figure 3.5 Distribution of stresses from concentrated horizontal loads.

21/11/00

CAD FILE 3401650SK7.CDR MT

3.1.2 Forward Sliding

The magnitude of the base sliding resistance is controlled by the shear strength of the weakest soil, or friction between soil and reinforcement at the base of the GRS structure. Forward sliding is illustrated in Figure 3.1(a).

Therefore, the following cases should be considered:

A. Sliding along the foundation soil;

B. Sliding along the reinforced backfill;

C. Sliding along the weaker of the upper and lower soil-reinforcement interfaces.

The horizontal stability of GRS structures should be checked as follows:

$$F^*_h \leq \Phi F^*_v \tan \phi \quad \text{(for cases A and B)} \tag{7}$$

$$F^*_h \leq T^*_{di,2} \quad \text{(for case C)} \tag{8}$$

For cohesive foundation soils, short-term stability should also be checked:

$$F^*_h \leq \Phi c_u L \tag{9}$$

where:

- F^*_h is the horizontal component of the resultant of all factored horizontal disturbing forces (refer to Table 2.4 for load factors);
- F^*_v is the resultant of all factored vertical forces (refer to Table 2.4 for load factors);
- ϕ is the smallest of the friction angles for foundation soil and reinforced backfill;
- c_u is the undrained shear strength of foundation soil;
- L is the reinforcement length of the base of the GRS walls;
- $T^*_{di,2}$ is the design soil reinforcement interaction strength for direct shear (refer to Appendices A4, A4.2, A4.3);
- Φ is the reduction factor for sliding: $\Phi = 1.0$.

3.1.3 Bearing Capacity Failure

In the bearing capacity analysis, the reinforced block is assumed to act as a continuous strip footing. Potential failure from this mode is illustrated in Figure 3.1(c).

The typical bearing pressure imposed by a GRS structure along the base of a wall is shown on Figure 3.6. For bearing capacity analysis, a bearing pressure based upon a Meyerhof distribution may be assumed:

$$\sigma^*_v = F^*_v / (L - 2e) \tag{10}$$

where:

- σ^*_v is the design bearing pressure acting on the base of the wall;
- F^*_v is the resultant of all factored vertical load components (refer to Table 2.4 for load factors);
- L is the reinforcement length of the base of the wall;
- e is the eccentricity of resultant load F^*_v about the centre line of the reinforced soil block.

The bearing pressure σ^*_v should be compared with the factored ultimate bearing capacity of the foundation soil as follows:

$$\sigma^*_v \leq \Phi\, q_u \qquad (11)$$

where:

q_u is the ultimate bearing capacity of the foundation soil assessed by methods of classical soil mechanics;

Φ is the reduction factor for ultimate bearing capacity: $\Phi = 0.6$.

3.1.4 Overturning

The requirement with respect to the minimum width of GRS walls and their flexibility makes it unlikely that GRS walls would actually overturn. This failure mode is illustrated in Figure 3.1(b). However, the overturning criteria should be checked and, if justified, should limit excessive outward tilting and distortion:

$$M^*_d \leq \Phi\, M^*_r \qquad (12)$$

where:

M^*_d is the resultant of all driving moments of factored forces about the toe of the wall (load factors are given in Table 2.4);

M^*_r is the resultant of all retaining moments of factored forces about the toe of the wall (load factors are given in Table 2.4);

Φ is the reduction factor for overturning: $\Phi = 0.75$.

3.1.5 Deep-Seated Failure

The general mass movement of a GRS structure and adjacent soil mass is called a deep-seated (or global stability) failure (Figure 3.1(d)).

Analysis of the stability of soil masses comprising the GRS wall and adjacent soil should be undertaken, using rotational and wedge type analyses. These can be performed using classical slope stability analysis methods. Some of the available computer programs for these analyses are listed in Section 7 of these guidelines. More detailed recommendations on the deep-seated failure analysis for GRS slopes are given in Section 4.1.3 of these Guidelines. These recommendations are also applicable to GRS walls.

For simple GRS walls with rectangular geometry, uniform reinforcement spacings and near-vertical faces, compound failure surfaces (i.e. passing through both un-reinforced and reinforced zones) will not generally be critical. For more complex conditions (e.g. walls with changes in reinforced backfill properties or length of geosynthetic reinforcement, high surcharge loads, walls with sloping faces, stacked walls, etc.), compound failure surfaces may be critical. Therefore, in such cases GRS walls should not be considered as a rigid body for the global stability analysis. Computer programs that model the reinforced fill and geosynthetic reinforcements should be used.

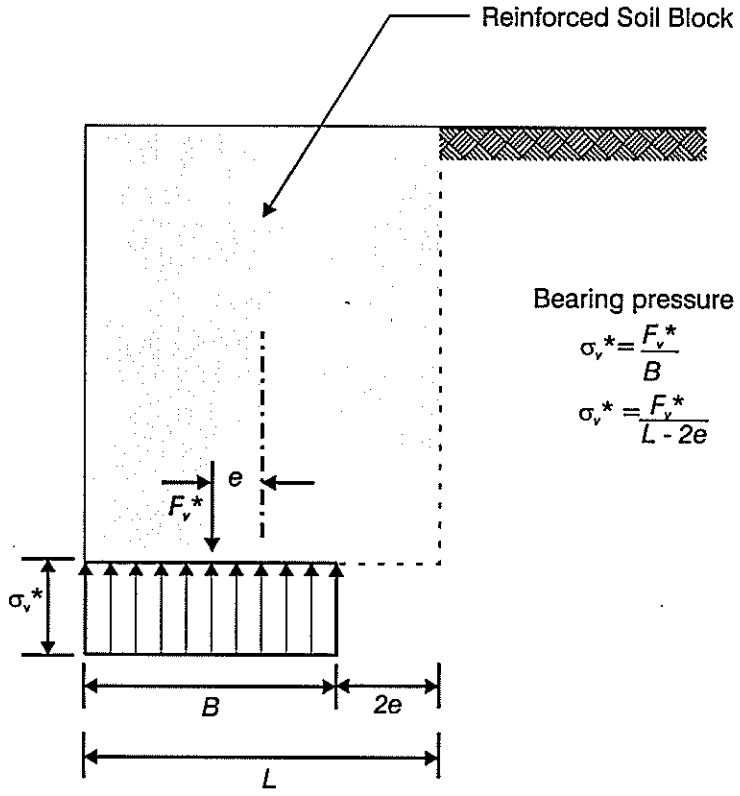

Figure 3.6 Pressure distribution along base of wall.

20/11/00

CAD FILE 3401650SK6.CDR MT

3.2 Seismic Loading

Ideally, the peak ground acceleration coefficient (PGA) for the design of GRS structures should be based on an assessment of seismicity at the particular site together with determination of the accepted probability of occurrence. GRS structures are normally designed for accelerations corresponding to the design basis earthquake, or the maximum credible earthquake.

The design basis earthquake is based on the recurrence interval that would be typical of the design life of the GRS structure. In the absence of site-specific assessment of seismicity, the PGA can be taken as:

$$PGA = 0.42\ Z\ R$$

where:

Z is the zone factor from Figure 5.3 of the Bridge Manual (TNZ 1994), and
R is the risk factor from Table 5.8 of the same Manual.

The maximum credible earthquake is defined as the ground acceleration likely to occur at a long recurrence interval of typically 10 000 years.

GRS structures should be designed for acceleration corresponding to the design basis earthquake unless a higher level of seismic resistance can be justified.

Currently, there is no any widely held consensus on seismic design procedures for GRS structures. The seismic design procedures given in these Guidelines are based on American GRS design methods (Christopher et al. 1990b; Elias & Christopher 1997; NCMA 1998b) with minor adjustments to reflect New Zealand experience and research data.

For the design of GRS structures, the vertical seismic coefficient a_v is commonly assumed to equal zero. However, Cai & Bathurst (1995) suggested that significant vertical accelerations may occur at sites located at short epicentral distances and, therefore, engineering judgement must be exercised in the selection of vertical and horizontal seismic coefficients for the design of GRS structures.

The choice of horizontal seismic coefficient a_h for design of GRS structures is related to a site PGA and the ability of structures to tolerate lateral movements.

An approximate order of magnitude of the permanent lateral movement expected for GRS structures can be assessed as follows:

$$\text{Lateral movement} = 254\ PGA\ (mm) \qquad (13)$$

Reduced seismic coefficients can be used for the GRS structures which have unrestrained base (i.e. are not founded on piles or similar), and can tolerate lateral movement resulting from sliding of the structure. For the analysis of external stability and internal sliding stability of unrestrained GRS structures, the horizontal seismic coefficient is taken as the horizontal peak ground acceleration reduced by 40% as follows:

$$a_h = a_{h,ext} = 0.6 \text{ PGA} \quad (14)$$

For the analysis of internal stability of GRS walls (except for internal sliding stability analysis where $a_{h,ext}$ should be used), the horizontal seismic coefficient is assessed as follows:

$$a_h = a_{h,int} = (1.3 - \text{PGA}) \text{ PGA} \quad (15)$$

Recommendations on $a_{h,int}$ for GRS slopes are given in Section 4.3 of these Guidelines.

Limit equilibrium pseudo-static methods are commonly used for design of GRS structures. However, for some combinations of soil friction angle, backfill slope angles and ground acceleration values, solutions using the Mononobe–Okabe method are either not possible or result in a very conservative design. In these cases a deformation analysis of GRS structures using a Newmark-type displacement method should be carried out. The displacement analysis is also recommended for sites with a design peak horizontal ground acceleration higher than 0.42g The deformation analysis method suggested by Cai & Bathurst (1996; paper reproduced in Appendix D of these Guidelines) can be used for this purpose as well as similar methods proposed by others (Ling at al. 1997).

The Mononobe–Okabe earth pressure theory is adopted to calculate dynamic active soil pressure. The dynamic active soil force F_{AE} is calculated as follows (Elias & Christopher 1997; NCMA 1998b):

$$F_{AE} = 0.5 \, (1 \pm a_v) \, K_{AE} \, \gamma h^2 \quad (16)$$

where:

- a_v is a vertical seismic coefficient;
- γ is the unit weight of backfill material
  - $\gamma = \gamma_f$ for the external stability calculations:
  - $\gamma = \gamma_r$ for the internal stability calculations;
- h is the height over which the force F_{AE} acts;
- K_{AE} is the Mononobe–Okabe earth pressure coefficient.

$$K_{AE} = \frac{\cos^2(\phi - \xi - 90 + \theta)}{\cos\xi \cos^2(90 - \theta)\cos(I + 90 - \theta + \xi)\left[1 + \sqrt{\dfrac{\sin(\phi + I)\sin(\phi - \xi - I)}{\cos(I + 90 - \theta + \xi)\cos(I - 90 + \theta)}}\right]^2} \quad (17)$$

where:

- I is the backfill slope angle (Figure 3.2):
  - for continuous backfill slopes, I=β,
  - for broken backfill slopes, angle I should be calculated as shown on Figure 3.2;

$$\xi = \tan^{-1} \frac{a_h}{1 \pm a_v} \quad (18)$$

- ϕ is the soil angle of friction;
- θ is the slope angle of the wall face (Figure 3.7).

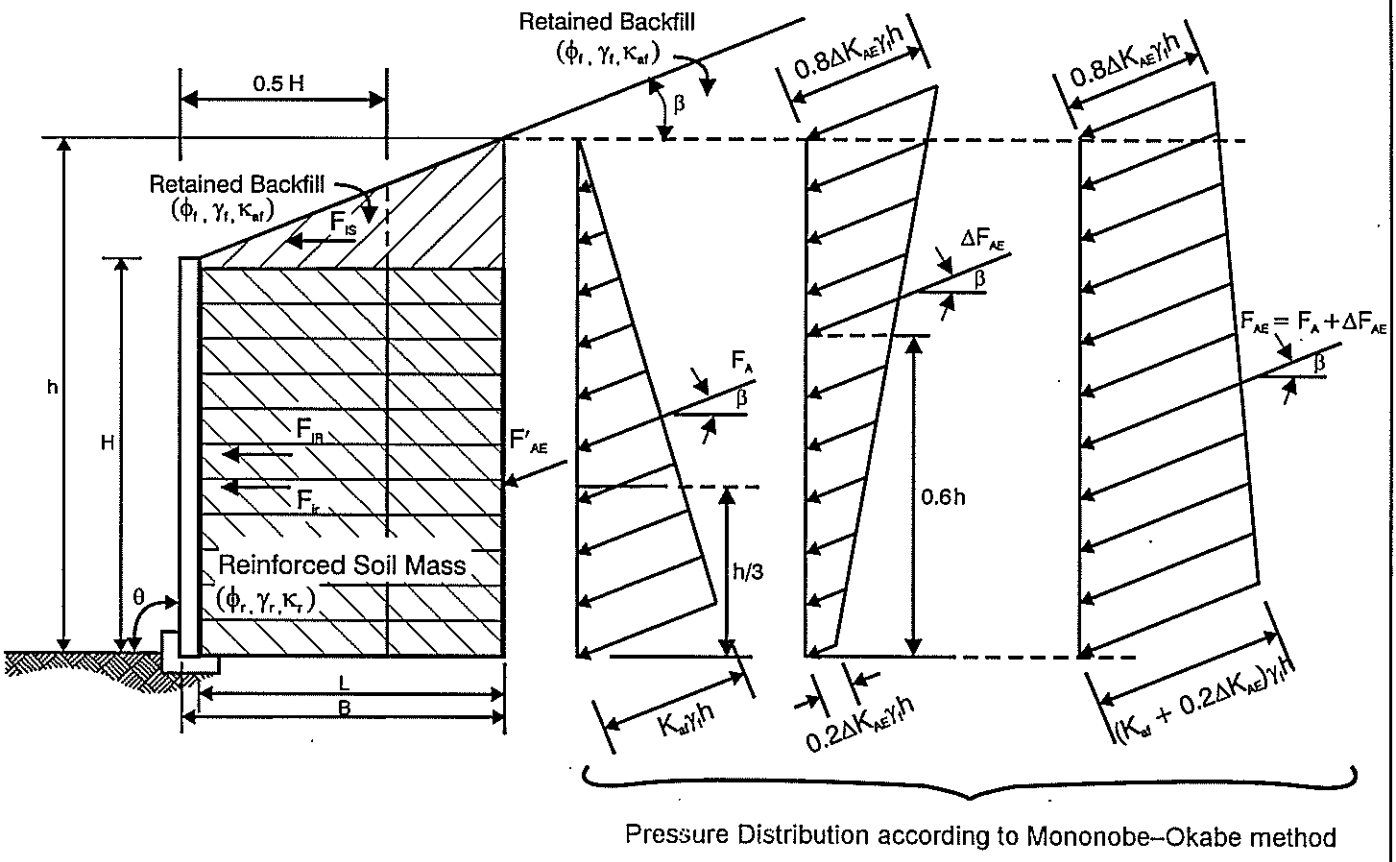

Figure 3.7 Dynamic soil pressure distribution under seismic loading.

For convenience the total dynamic active soil force F_{AE} can be broken down into two components, representing the static active soil force F_A and the incremental seismic soil force ΔF_{AE} (Figure 3.7):

$$F_{AE} = F_A + \Delta F_{AE} \quad (19)$$

where:

F_A is given by Equation 5 (Section 3.1.1);

ΔF_{AE} is the increment of the seismic soil force:

$$\Delta F_{AE} = 0.5 \Delta K_{AE} \gamma h^2 \quad (20)$$

ΔK_{AE} is the increment of the seismic soil pressure coefficient:

$$\Delta K_{AE} = (1 \pm a_v) K_{AE} - K_A \quad (21)$$

$K_A =$ K_{af} for retained backfill, and

$=$ K_{ar} for reinforced backfill.

3.3 Design for External Stability under Seismic Conditions

The dynamic soil pressure distribution shown on Figure 3.7 is used to analyse external stability of GRS walls[1].

Equation 14 (Section 3.2) is used to assess the magnitude of the horizontal seismic coefficient in all external stability calculations.

For large backfill slope angles β, solutions by the Mononobe–Okabe method are either not possible or result in a very conservative design. High peak ground accelerations may also result in a conservative design. Therefore, the recommendation is that, in these cases, the reinforced zone width should be initially restricted to 1.0-1.2 times the height (H) of the GRS wall:

$$L \leq 1.0\text{-}1.2\ H \quad (22)$$

and the external stability of the GRS wall in this case should then be analysed using the deformation analysis method (Appendix D, Cai & Bathurst 1996), and the reinforced width increased if required.

Where the problem can be solved by applying the Mononobe–Okabe method, and the peak ground accelerations are moderate, the horizontal inertia forces (shown on Figure 3.7), are calculated as follows:

[1] The pressure distribution shown in Figure 3.7 for the earthquake loading increment is the traditionally accepted form taken from NCMA 1998b. This pressure distribution is used for external, internal and facing stability analysis (Figures 3.7, 3.10, 3.11 and E4). Recent research (Bathurst & Hatamai 1998) has shown that the earthquake pressure distributions may be significantly different from the traditionally accepted form, with the earthquake pressure increment increasing with depth rather than decreasing. The shape and magnitude of the earthquake pressure increment has also been shown to be sensitive to the flexibility of the reinforcement layers. In most design applications the traditional shape, with higher pressures at the top, is likely to be more conservative than more correct pressure distributions. Many existing structures designed to the traditional pressure shape have performed satisfactorily under gravity and earthquake loads.

Total inertia force F_{IR} acting at the combined centroid of forces F_{ir} and F_{is}:

$$F_{IR} = F_{ir} + F_{is} \quad (23)$$

- Inertia force for the reinforced soil block F_{ir}:

$$F_{ir} = 0.5\, a_{h,\,ext}\, \gamma_r\, H^2 \quad (24)$$

- Inertia force for the soil surcharge above reinforced backfill F_{is}:

$$F_{is} = 0.125\, a_{h,\,ext}\, \gamma_f\, H^2 \tan\beta \quad (25)$$

Equations 24 and 25 are based on the assumption that horizontal inertial forces induced in the reinforced block and the retained fill will not reach peak values at the same time during an earthquake. Therefore, only a portion of the reinforced block extending to a distance 0.5 H beyond the wall face is used to calculate inertia forces acting on the reinforced block and the soil surcharge above the block (Elias & Christopher 1997). If the unit weight of the wall-facing system is substantially different from that of the reinforced backfill, in addition to F_{ir} the inertia force due to the weight of facing should be also considered.

For walls of moderate height and firm soils, the out-of-phase effects might be less than indicated by Equations 24 and 25. However, the equations have been adopted as other effects such as outward deformation and high damping in the soil can also reduce the earthquake forces on the wall.

In the analyses of external stability and internal sliding stability, the dynamic soil force increment ΔF_{AE} should be reduced by 50% and a reduced resultant force F'_{AE} should be considered instead of the total dynamic active soil force F_{AE} (NCMA 1998b):

$$F'_{AE} = F_A + 0.5\, \Delta F_{AE} \quad (26)$$

The reduced dynamic force given in Equation 26 has been adopted from NCMA (1998b). However, the reason for the reduction in the dynamic force increment is not clearly stated in the NCMA manual. Since the adopted earthquake pressure distribution is believed to be conservative for the upper wall sections the reduction to the dynamic active soil force is considered to result in designs with satisfactory resistance to sliding. Walls designed to the recommended earthquake forces will be unlikely to slide in the upper sections, and some sliding movement in the lower third of the wall would not be likely to impair the overall stability.

The sliding resistance of the GRS wall should be checked, as described in Section 3.1.2 of these Guidelines, by inserting load factors given in Table 2.4 (for the seismic conditions) and the reduction factor for sliding of $\Phi = 0.9$ in Equations 7 and 9.

The bearing capacity analysis should be undertaken as described in Section 3.1.3 of these Guidelines by inserting load factors given in Table 2.4 (for seismic conditions) and a reduction factor for ultimate bearing capacity of $\Phi = 0.7$ in Equation 11.

The overturning check should be undertaken as described in Section 3.1.4 using load factors given in Table 2.4 (for seismic conditions) and a reduction factor of $\Phi = 0.9$ in Equation 12.

3.4 Design for Internal Stability under Static Conditions

3.4.1 General

Internal stability is concerned with the integrity of the reinforced soil block. The following failure modes, shown on Figure 3.8, should be checked in the internal stability analysis:

- Pullout;
- Reinforcement rupture;
- Internal sliding.

The most critical slip surface in a GRS wall is assumed to coincide with the maximum tensile forces line (i.e. the locus of the maximum tensile forces in each layer of reinforcement).

The maximum tensile force surface is assumed to be linear and to pass through the toe of the GRS wall (Figure 3.9).

For GRS walls with vertical faces, the maximum tensile force surface is inclined at an angle $\psi = 45° + \phi_r/2$ to the horizontal.

For GRS walls with front face angles of greater than 10° to the vertical, angle ψ should be calculated using the equation given on Figure 3.9 (Elias & Christopher 1997).

Lateral soil pressures caused by reinforced backfill, and imposed surcharge loads, are assumed for the purposes of internal stability analysis, to be distributed linearly with depth, based on the following lateral soil pressure coefficients:

- for walls with face inclination of less than 10° to the vertical:
  $K_{ar} = \tan^2 (45° - \phi_r/2)$ (27)

- for walls with face slopes in excess of 10° from the vertical:
  $$K_{ar} = \frac{\sin^2(\theta + \phi_r)}{\sin^3\theta\left[1 + \frac{\sin\phi_r}{\sin\theta}\right]^2} \quad (28)$$

where:

ϕ_r is the angle of internal friction for reinforced backfill;
θ is the inclination of the back of the wall facing as measured from the horizontal.

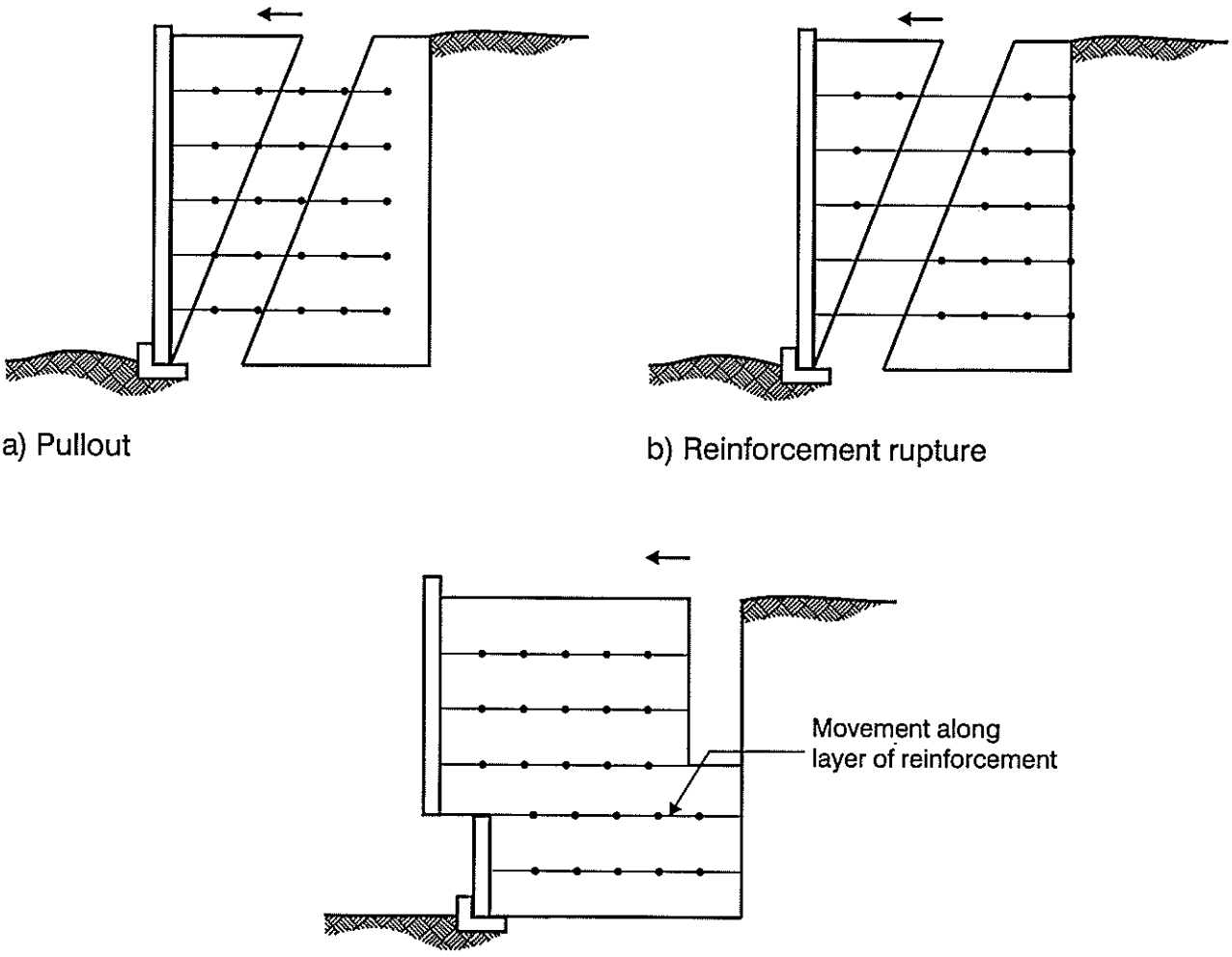

Figure 3.8 Modes of internal failure.

23/11/00
CAD FILE 3401650SK8.CDR MT

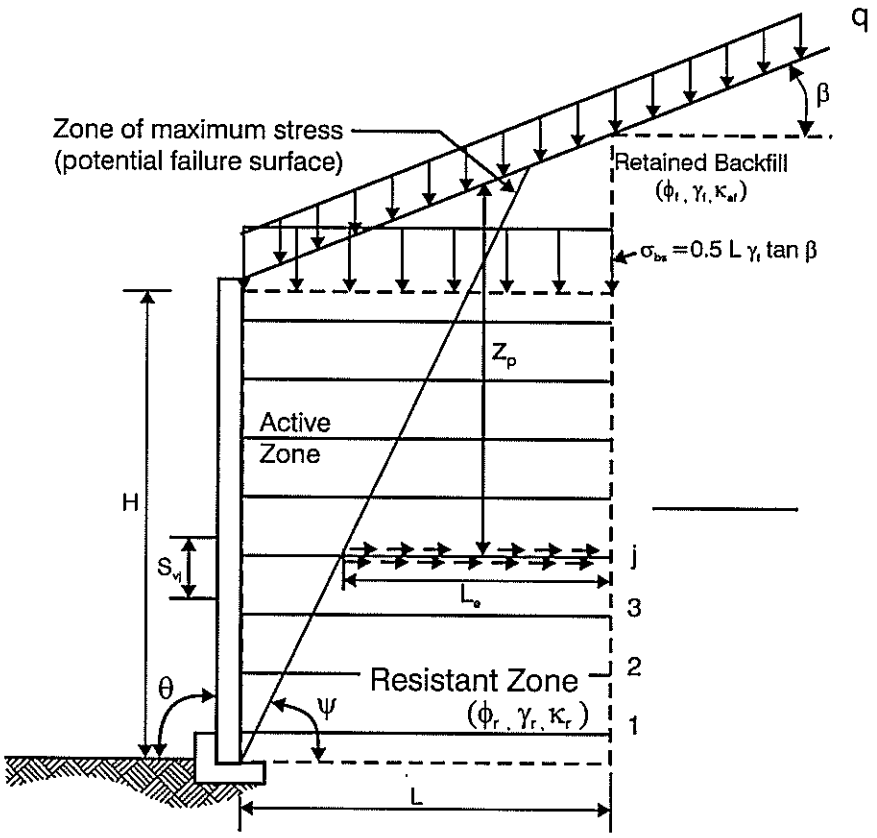

For vertical walls with horizontal backslope: $\psi = 45 + \phi/2$

For walls with vertical and inclined face batters and sloping backfill:

$$\tan(\psi - \phi) = \frac{-\tan(\phi-\beta) + \sqrt{\tan(\phi-\beta)[\tan(\phi-\beta)+\cot(\phi+\theta-90)][1+\tan(\delta+90-\theta)\cot(\phi+\theta-90)]}}{1+\tan(\delta+90-\theta)[\tan(\phi-\beta)+\cot(\phi+\theta-90)]}$$

where $\delta=\beta$, $\phi = \phi_r$

Figure 3.9 Location of potential failure surface for internal stability calculations.

The above equations for K_{ar} are for the horizontal backfill slope ($\beta = 0$). These lateral soil pressure coefficients can also be used for GRS walls with backfill slopes $\beta>0$, but a uniformly distributed load σ_{bs} should be applied at the top of the reinforced soil block as shown on Figure 3.9 to account for sloping backfill condition.

Horizontal design soil pressure σ^*_{hj} at the elevation $z = z_j$ of the j-th layer of geosynthetic reinforcement should be calculated as follows:

$$\sigma^*_{hj} = \sigma^*_{h,A} + K_{ar}(\sigma^*_{bs} + q^* + \Delta\sigma^*_v) + \Delta\sigma^*_h \quad (29)$$

where:

$\sigma^*_{h,A}$ is the factored horizontal stress due to active thrust (unfactored component of this stress for static conditions is shown on Figure 3.10);

σ^*_{bs} is the factored uniformly distributed surcharge to account for sloping backfill condition;

q^* is the factored uniformly distributed surcharge load;

$\Delta\sigma^*_v$ is the factored increment of vertical stress due to vertical concentrated loads (unfactored component of this stress is shown on Figure 3.4);

$\Delta\sigma^*_h$ is the factored increment of horizontal stress due to horizontal concentrated loads (unfactored component of this stress is shown on Figure 3.5).

Load factors are given in Table 2.4.

3.4.2 Maximum Tensile Force

The maximum design tensile force in each reinforcement layer per unit width of the wall can be calculated as follows:

$$F^*_j = \sigma^*_{hj} S_{vj} \quad (30)$$

where:

F^*_j is the maximum design tensile force in the j-th layer of reinforcement;

S_{vj} is the contributory area of the j-th layer of geosynthetic reinforcement (Figure 3.10).

3.4.3 Tensile Strength

The maximum tensile force carried by the j-th layer of reinforcement should be checked as follows:

$$F^*_j \leq T^*_d \quad (31)$$

where:

F^*_j is the maximum design tensile force in the j-th layer of reinforcement (Equation 30);

T^*_d is the design tensile strength of geosynthetic reinforcement (Appendix A1).

3.4.4 Pullout

The maximum tensile force carried by the j-th layer of reinforcement shall not exceed the design anchorage capacity of geosynthetic reinforcement. Therefore, stability of GRS walls with respect to pullout failure should be checked for each layer of reinforcement as follows:

$$F^*_j \leq T^*_{di,1} \quad (32)$$

where:

F^*_j is the maximum design tensile force in the j-th layer of reinforcement (Equation 30);

$T^*_{di,1}$ is the design soil–reinforcement interaction strength for pullout (Equation A5, Appendix A4).

In the calculations of the resultant of all factored vertical stresses σ^*_v at the soil–reinforcement interface (Equation A7, Appendix A4.1), the following stresses should be considered:

- Vertical stress due to the reinforced backfill self weight. An average depth z_p of soil overburden acting over the anchorage length L_e of the j-th reinforcement layer should be used to calculate this stress (Figure 3.9);
- Vertical stress due to sloping backfill;
- Vertical stress due to uniformly distributed surcharge;
- Vertical stress due to concentrated vertical loads.

Only dead load components of the uniformly distributed surcharges and concentrated vertical loads should be taken into account in the calculations of the vertical stress σ^*_v.

3.4.5 Internal Sliding Failure

The potential for an internal sliding failure along the surface of a reinforcement layer must be examined for each reinforcement elevation. Destabilising forces will be resisted by the shear resistance between the retained backfill and geosynthetic reinforcement. The failure plane generated on the retained backfill–geosynthetic layer interface will have to propagate through the wall facing. Therefore, additional shear resistance provided by the wall facing should be considered if appropriate.

The internal sliding stability of GRS walls should be checked as follows :

$$F^*_{h,z} \leq T^*_{di,2} + T^*_{fr} \quad (33)$$

where:

$F^*_{h,z}$ is the resultant of factored horizontal components of destabilising forces acting on a portion of the GRS wall above the reinforcement layer under consideration (refer to Table 2.4 for load factors);

$T^*_{di,2}$ is the design soil–reinforcement interaction strength for direct shear (Equation A6, Appendix A4);

T^*_{fr} is the design shear resistance provided by the wall facing (where appropriate); recommendations on shear resistance of segmental control unit facing are given in Appendix E.

Disturbing forces should be calculated in a manner similar to that for the analysis of external stability (Figure 3.3), but only over the portion of the GRS wall that is above the sliding failure surface (reinforcement layer) under consideration. The resultant

σ^*_v of all factored stresses at the soil–reinforcement interface (Equation A8, Appendix A4.2) should be calculated as described in Section 3.4.4.

Only dead load components of uniformly distributed surcharges and vertical loads should be taken into account in the calculations of the vertical stress σ^*_v.

3.5 Design for Internal Stability under Seismic Conditions

3.5.1 Tensile Forces

The soil pressure distribution for internal stability analysis for a simplified case assuming horizontal ground surface behind the wall, no superstructure or surcharge loads, is shown on Figure 3.10. In this case, design tensile force is the j-th layer of reinforcement calculated as the factored soil pressure integrated over the contributory area of that layer:

$$F^*_j = (\sigma^*_{hj} + \Delta\sigma^*_{hj,\,AE} + \sigma^*_{hj,\,q})\, S_{vj} \qquad (34)$$

where:

F^*_j is the design tensile force in the j-th layer of reinforcement;

σ^*_{hj} is the horizontal component of factored soil pressure from static loads (Equation 29) calculated at the elevation $z = z_j$;

$\Delta\sigma^*_{hj,\,AE}$ is the horizontal component of the factored seismic soil pressure increment (refer to Table 2.4 for load factors);

$\sigma^*_{hi,\,q}$ is the factored horizontal pressure resulting from seismic lateral forces applied at the top of the wall (e.g. inertia forces affecting structures or road embankments supported by the GRS wall).

The horizontal component of the unfactored seismic soil pressure increment $\Delta\sigma_{hj,AE}$ should be calculated as follows (NCMA 1998b):

$$\Delta\sigma_{hj,AE} = (0.8 - 0.6\frac{z_j}{H})\Delta K_{AE}\gamma_r H\cos\beta \qquad (35)$$

where:

z_j is the depth of the j-th reinforcement layer measured from the crest of the wall;

H is the height of the wall;

γ_r is the unit weight of reinforced backfill;

ΔK_{AE} is the seismic soil pressure coefficient increment (Equation 21) calculated for reinforced backfill ($a_h = a_{h,im}$).

For heavy facing, the design tensile force F^*_j should be further increased by adding the factored inertia force due to the weight of a facing element A (Figure 3.10) with the height S_{vj}.

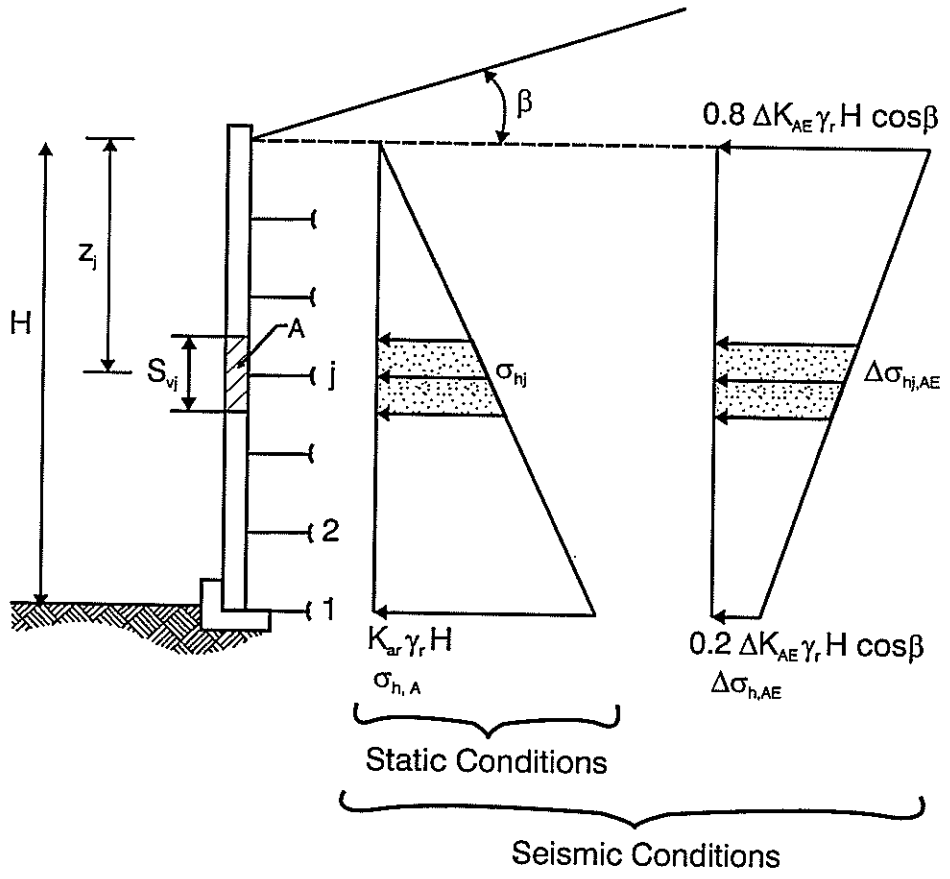

Figure 3.10 **Pressure distribution for internal stability analysis.**

25/11/00
CAD FILE 3401650SK13.CDR MT

3.5.2 Tensile Strength

Stability of GRS walls with respect to breakage of the geosynthetic reinforcement should be checked as follows:

$$F^*_j \leq T^*_d \quad (36)$$

where:

F^*_j is the maximum design tensile force in the j-th layer of reinforcement for seismic conditions (Equation 34);

T^*_d is the design tensile strength of geosynthetic (Equation A5, Appendix A1) calculated assuming the reduction factor for creep deformation $\Phi_{rc} = 1.0$.

3.5.3 Pullout

The maximum tensile force carried by the j-th layer of reinforcement, under seismic conditions, shall not exceed the design anchorage capacity of geosynthetic reinforcement. Therefore seismic stability of GRS walls with respect to pullout failure should be checked for each layer of reinforcement as follows:

$$F^*_j \leq T^*_{di,1} \quad (37)$$

where:

F^*_j is the design tensile force, in the j-th layer of reinforcement for seismic conditions (Equation 34);

$T^*_{di,1}$ is the design soil–reinforcement interaction strength for pullout (Appendix A4).

Only dead load components of the uniformly distributed surcharges and vertical loads should be taken into account in the calculations of the vertical stress σ^*_v in Equation A7, Appendix A4.

3.5.4 Internal Sliding Failure

A simplified pressure distribution for the analysis of internal sliding (assuming no superstructure or surcharge loads) is shown on Figure 3.11. In general cases, the internal sliding stability of GRS walls should be checked as described in Section 3.4.5 of these Guidelines. Disturbing forces should be calculated in a manner similar to that for the external stability analysis (Section 3.3) but only over that portion of the GRS wall that is above the sliding failure surface under consideration.

As stated in Sections 3.2 and 3.3 of these Guidelines, the horizontal seismic coefficient a_h in the calculations of inertia forces F_{is} and F_{ir} should be taken as for the external stability analysis: $a_h = a_{h,\ ext}$. Similar to the external sliding stability calculations (Section 3.3), only 50% of the external seismic thrust increment $\Delta F_{AE}(Z)$, acting over the height h_{zi}, should be considered for the internal sliding stability calculation.

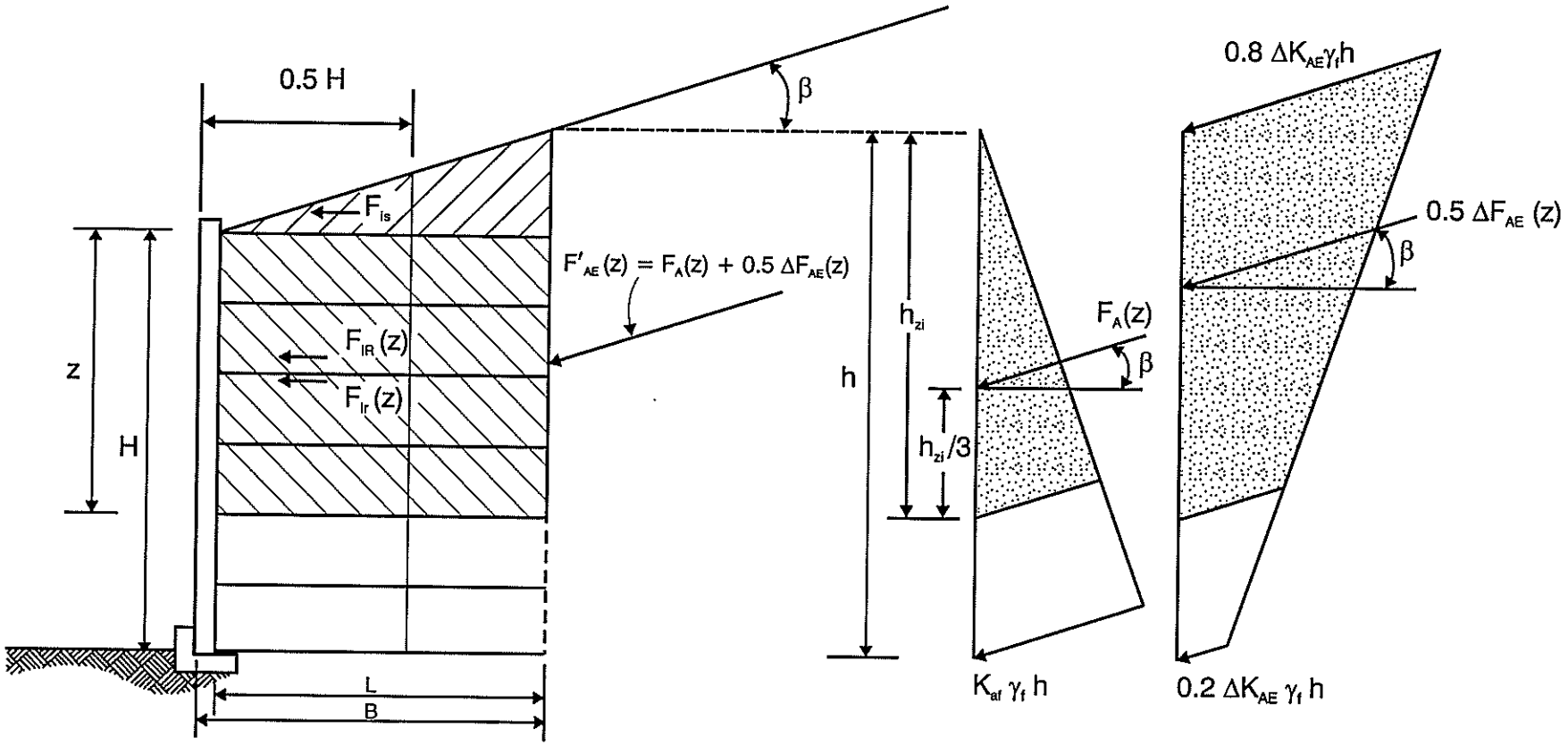

Figure 3.11 **Pressure distribution for analysis for internal sliding stability.**

27/11/00
CAD FILE 3401650SK14.CDR MT

3.6 Local Stability

The local stability analysis should be undertaken to ensure that a facing system is stable, has adequate strength and durability at all elevations above the toe of the wall. The following should be considered:

- structural strength of facing elements (for concrete, steel or timber facing);
- durability of facing elements;
- resistance to bulging (for flexible facing systems);
- strength of the connection between facing elements and geosynthetic reinforcement;
- local overturning (for facing systems where such failure is possible);
- stability of the unreinforced facing section above the highest reinforcement layer.

Structural facing elements of GRS walls (such as concrete, steel or timber facing) should be designed to resist the horizontal forces (horizontal stresses) discussed in Sections 3.4.1 and 3.5.1.

Geosynthetic facing elements should not be exposed to sunlight for permanent walls. A protective facing (e.g. concrete, shotcrete, etc.) should be constructed if required. For structures where geosynthetic facing elements are exposed to sunlight, only geosynthetics stabilised against ultraviolet radiation shall be used. Product-specific test data should be obtained and extrapolated to the intended design life to prove that the material is capable of performing in an exposed environment.

Flexible facings (e.g. segmental concrete unit or steel mesh facings) should be designed to prevent excessive bulging.

Connection strength is specific to each facing–reinforcement combination and must be developed uniquely by test for each combination.

Geogrid reinforcement may be structurally connected to precast panels by casting a tab of the geogrid into the panel and connecting it to the full length of geogrid with a bodkin joint. Polyester geogrids and geotextiles should not be cast into concrete for connections because they have potential for chemical degradation (Appendix B).

The anchorage resistance and tensile strength of the geogrid tab, as well as its connection (bodkin or similar) to the reinforcement layer should be sufficient to resist the maximum design tensile force in the reinforcement. As stated in Appendix A1.9, in some cases connection strength may limit and therefore control the design tensile strength of geosynthetic reinforcement.

In GRS walls with proprietary segmental precast unit facings, segmental units are connected either by structural connection (pins, lips, etc.), or by friction between the segmental units (including friction developed in the granular material filling the core of the units), or by a combination of both. The connection strength for walls with segmental unit facings should be determined by testing.

To provide an example, a more detailed consideration of the local stability for GRS walls with segmental precast concrete unit facing is given in Appendix E.

4. Design of GRS Slopes

4.1 Design for External Stability under Static & Seismic Conditions

4.1.1 General

The following potential failure modes should be checked in the external stability analysis:

- Forward sliding;
- Deep-seated failure;
- Bearing capacity failure;
- Local bearing capacity failure (lateral squeeze);
- Excessive settlement.

These failure modes are shown on Figure 4.1. Where the external stability analyses indicate that one or more failure mechanisms are possible, the following options to improve the stability should be considered:

- reduce the slope angle;
- increase the width of the reinforced soil block;
- undertake ground improvement works;
- stage the loading;
- use a berm (counterweight);
- use drainage to reduce pore pressures (sand drains or wick drains).

4.1.2 Forward Sliding

The following forces should be considered in the forward sliding stability analysis:

- active thrust (static or seismic) applied at the back of the reinforced block;
- surcharge loads applied at the top of the reinforced block;
- weight of the reinforced soil block;
- friction resistance at the bottom of the reinforced soil block calculated using the total weight of the reinforced soil block;
- inertia force applied to the reinforced soil block (for seismic conditions). Only 60% of the inertia force acting on the active zone should be taken into account. The forward sliding check should be undertaken in a manner similar to that for GRS walls, described in Sections 3.1.2 (for static conditions) and 3.3 (for seismic conditions) of these Guidelines.

While seismic and static active thrusts acting at the back of the reinforced soil block can be calculated in a manner similar to that for GRS walls, the inertia force applied to the reinforced soil block is different from that used in the GRS wall seismic analysis. The inertia force for GRS slopes can be assessed from the model proposed by Christopher et al. (1990a).

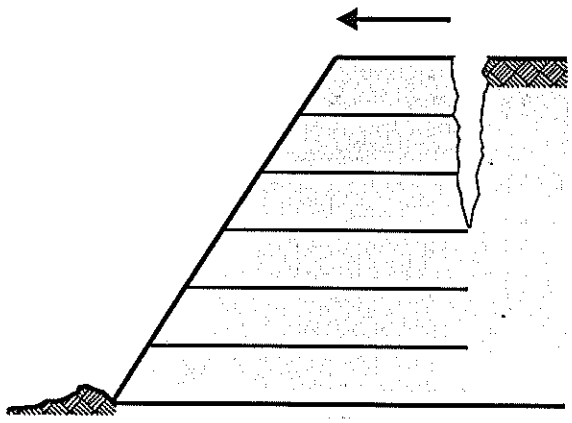

a) Forward Sliding

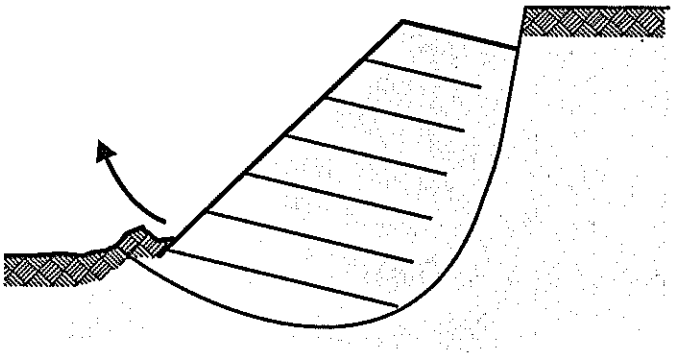

d) Deep-Seated Failure

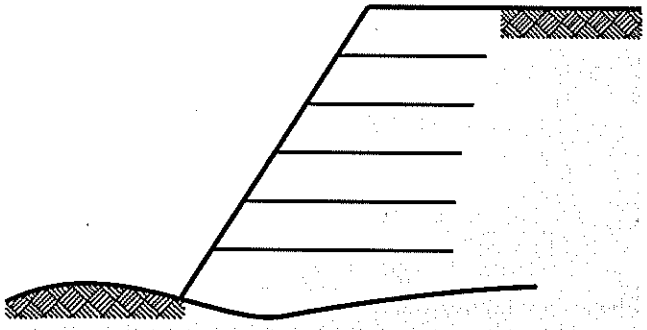

c) Bearing Capacity Failure

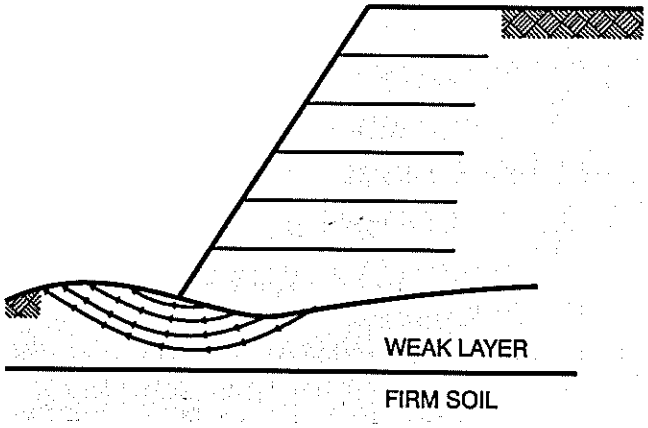

d) Local Bearing Capacity (Lateral Squeeze) Failure

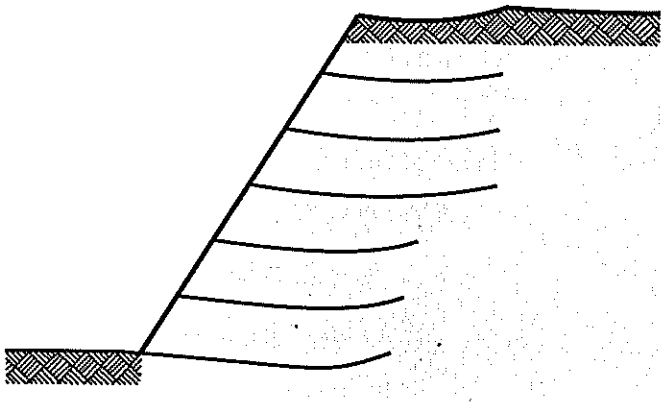

e) Excessive Settlement

Figure 4.1 External failure modes for GRS slopes.

According to Christopher's model (Figure 4.2 in these Guidelines), only 60% of the inertia force F_I acting on the active zone of the reinforced soil block should be taken into account in the sliding stability analysis. This is to allow for out-of-phase effect and reduction of earthquake forces on the slope caused by outward deformation and high damping in the soil. Also the total dynamic active soil force $F_{AE} = F_A + \Delta F_{AE}$ (rather than the reduced force $F'_{AE} = F_A + 0.5\ \Delta F_{AE}$) should be used. The reduction factors for sliding should be taken as for GRS walls (Sections 3.4.2 and 3.3 of these Guidelines).

For sites with high peak ground accelerations, the sliding stability analysis (using lateral seismic thrust assessed by the Mononobe–Okabe method) may result in a very conservative design. Therefore, the recommendation is that, in these cases, the deformation analysis method should be used. The deformation method proposed for GRS walls (Appendix D, Cai & Bathurst 1996) can be used to assess permanent displacement but amendments should be made to the inertia force acting on the reinforced block (Figure 4.2).

4.1.3 Deep-Seated Failure

Potential deep-seated failure surfaces behind the reinforced soil mass and extending below the toe of the GRS slope should be analysed. Both circular arc (simplified Bishop) and sliding wedge (simplified Janbu) methods should be used.

A number of slope stability analysis computer programs are available (Section 7), most of which use unfactored loads and soil parameters. Therefore, the recommendation is to use unfactored loads and soil parameters for the deep-seated failure analysis.

The following target factors of safety against deep-seated failure are recommended:

- for static conditions: $f_s = 1.5$
- for seismic conditions: $f_d = 1.1$

The factors of safety for the unreinforced slope are calculated as follows:

$$f_s = \frac{\text{resisting moment}}{\text{driving moment}} = \frac{\int_0^L \tau_f R\ dL}{Wx + Qd} \tag{38}$$

$$f_d = \frac{\text{resisting moment}}{\text{driving moment}} = \frac{\int_0^L \tau_f R\ dL}{Wx + a_{h,ext} Wy + Qd} \tag{39}$$

where:

W is the weight of the sliding soil mass (Figure 4.4);

Q is the surcharge;

τ_f is the shear strength of soil;

x,d,y are the moment arms for W, Q, and $a_{h,ext}$W respectively;

L is the length of failure surface;

$a_{h,ext}$ is the horizontal seismic coefficient for the analysis of external stability (as for GRS walls, Section 3.2);

R is the radius of circular failure surface.

Under static conditions (including live load surcharge where appropriate), a minimum calculated factor of safety against deep-seated failure should be f_s =1.5 unless specific justification is given for a lower value.

Where lower values are used, a detailed geotechnical engineering design report should be prepared for the GRS slope and suitable monitoring installed to check the slope during and after construction. The designer should develop acceptable limits for monitoring measurements. During construction, lower factors of safety may be accepted but the value should generally exceed 1.2.

In some cases, slope stability analysis for seismic conditions (using circular arc and sliding wedge methods) may indicate that the target factor of safety cannot be achieved without either substantially increasing the size of the reinforced block, or costly and complex ground improvement works.

In these cases Newmark sliding block-type methods of analysis for predicting permanent displacements of slopes subjected to earthquake shaking should be used, and the predicted performance of the slope (in terms of deep-seated failure) should be assessed from the calculated permanent displacement (for example, Ambraseys & Menu 1988).

4.1.4 Bearing Capacity Failure

The bearing capacity analysis for steep slopes should be based on the procedures adopted for GRS walls (Section 3). The soil properties and loads shown on Figures 3.3, 3.4, 3.5 and 3.7 should be taken into account when assessing bearing capacity of the foundation soils.

For shallow slopes, bearing capacity should be analysed using slip circle techniques, and vertical stress caused by the weight of a GRS slope can be treated as an average stress over the entire width of the reinforced soil block.

4.1.5 Lateral Squeeze

Consideration should be given to the local bearing capacity failure of foundation soils at the toe of the GRS slope if a confined soft layer with a total thickness less than the height of the GRS slope is present beneath the reinforced block.

The weight of the GRS slope can cause substantial lateral stresses in the confined soft layer and cause a lateral squeeze-type failure. The following conditions should be satisfied to prevent lateral squeeze-type failure (Silvestri 1983):

$$2C_u \geq \gamma_r^* d \tan(180 - \theta) \qquad (40)$$

where:

- C_u is the undrained shear strength of soft soil beneath the GRS slope;
- γ_r^* is the factored unit weight of reinforced fill (refer to Table 2.4 for load factors);
- d is the thickness of soft soil beneath the base of the GRS slope;
- θ is the inclination of the slope face from the horizontal (positive in a clockwise direction from the horizontal).

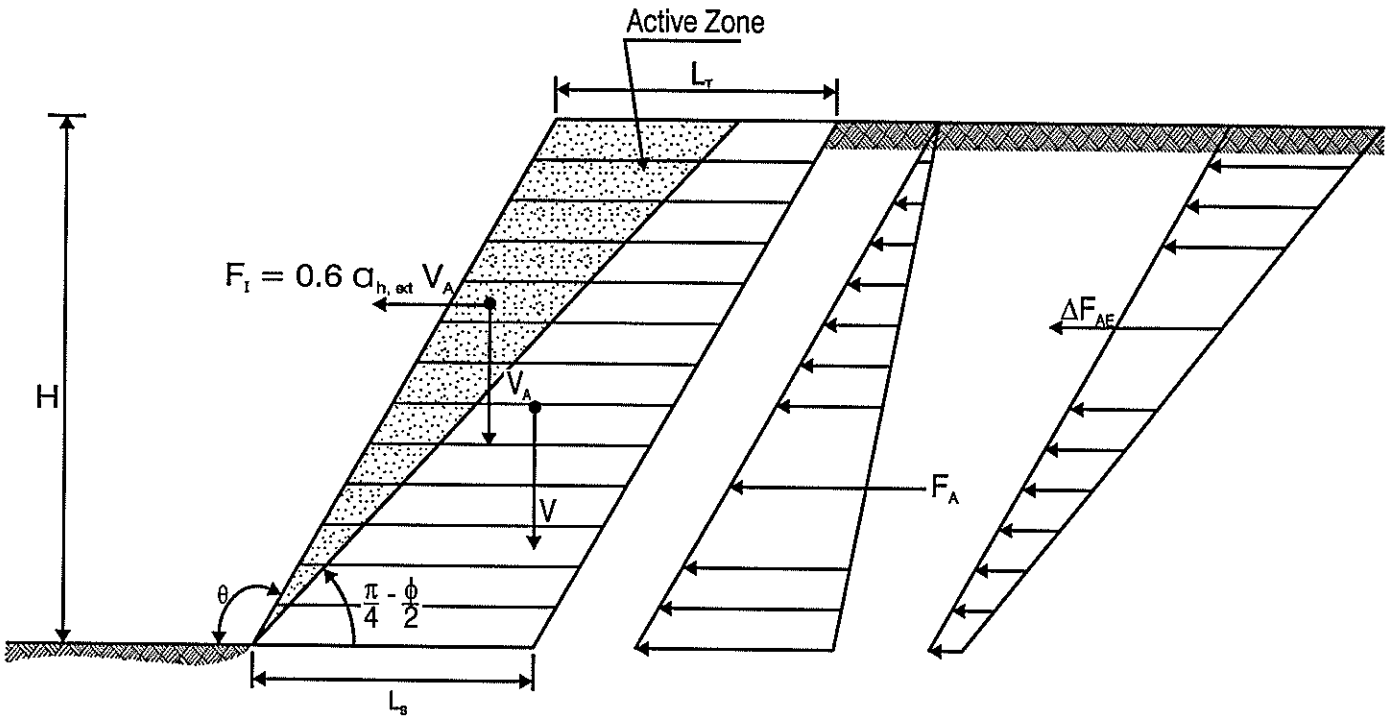

Figure 4.2 Forces for sliding stability analysis of GRS slopes (from Christopher et al. 1990)

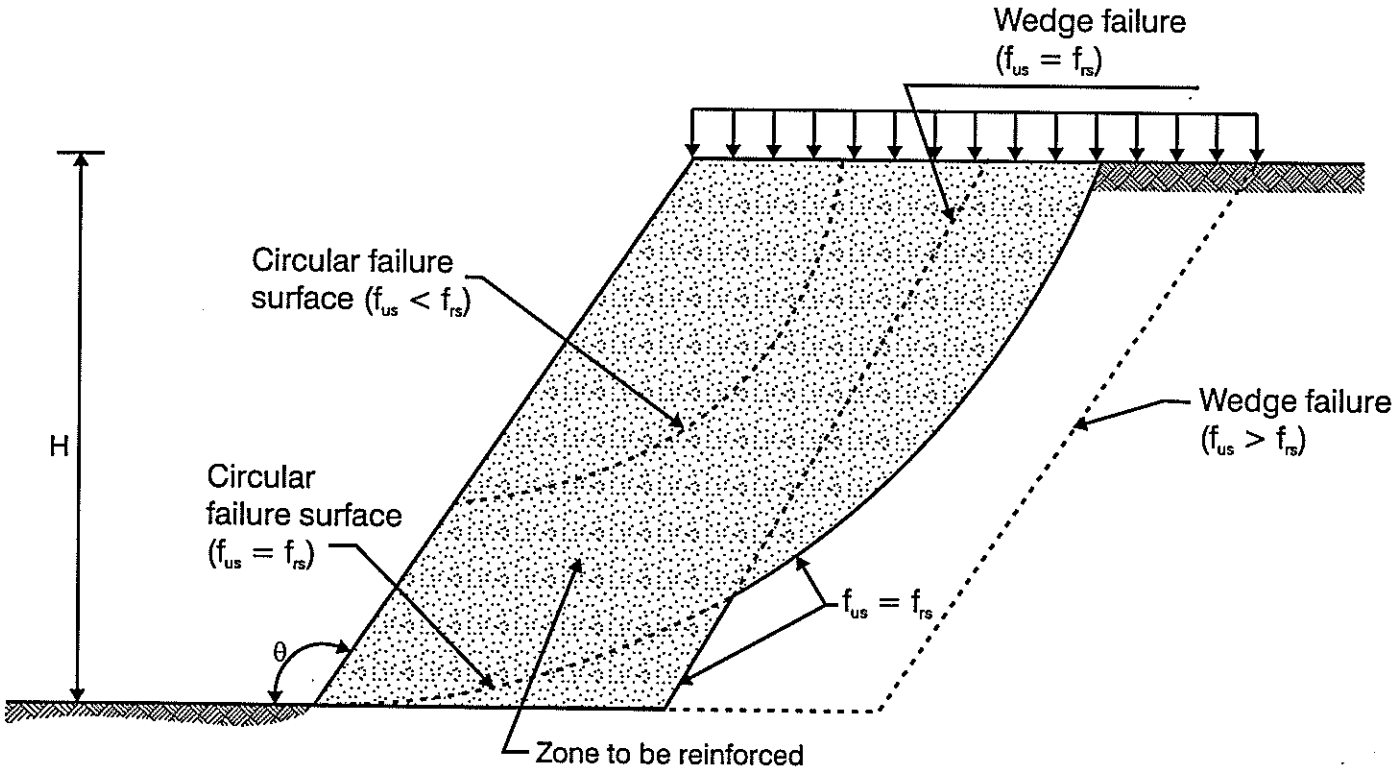

Figure 4.3 Approximate extent of the zone to be reinforced.

4.1.6 Settlement

The settlement of foundation soils should be assessed using methods of classical soil mechanics. If the assessed total and differential settlement exceeds project requirements, ground improvement works should be undertaken to reduce the predicted settlement.

4.2 Design for Internal Stability under Static Conditions

4.2.1 General

A number of methods to design GRS slopes for internal stability are available. Several available design methods are summarised in Transfund NZ Research Report No. 123 (Murashev 1998). A simplified design procedure, proposed by Christopher et al. (1990b), and developed further by Holtz et al. (1995) and Marr & Werden (1997), is recommended. This design procedure is summarised in the following Sections 4.2.2–4.2.7.

4.2.2 Maximum Size of Zone to be Reinforced

The proposed slope should be analysed without reinforcement, to determine the approximate maximum size of the zone to be reinforced using conventional stability methods. The analysis is undertaken using unfactored loads and unfactored soil parameters. Both circular arc (simplified Bishop method) and sliding wedge (simplified Janbu method) failure surfaces exiting through the toe, through the slope face (at several elevations), and below the toe (deep-seated) should be analysed. A number of slope stability analysis computer programs are available for this analysis (Section 7).

The approximate size of the zone to be reinforced (this zone is also referred to as the critical zone) should be determined as follows:

- Examine all failure surfaces with "unreinforced" factors of safety (f_{us}) less or equal to the required factor of safety (f_{rs}) for the reinforced slope. (A minimum factor of safety of $f_{rs} = 1.5$ is recommended.) Plot all these failure surfaces on the cross-section of the slope.
- The surfaces that just meet the required factor of safety f_{rs} indicate the approximate extent of the zone to be reinforced.

The procedure is illustrated in Figure 4.3. The bottom width of the reinforced soil block, in some cases, may be controlled by the forward sliding stability requirements (Section 4.1.2).

4.2.3 Geosynthetic Reinforcement Tension

Analyse each potential circular surface located inside the zone to be reinforced (Figure 4.4) and calculate the total reinforcement tension force T_t required to achieve the recommended factor of safety f_{rs} (for each failure surface analysed) as follows:

$$T_t = (f_{rs} - f_{us})\frac{M_d}{R} \tag{41}$$

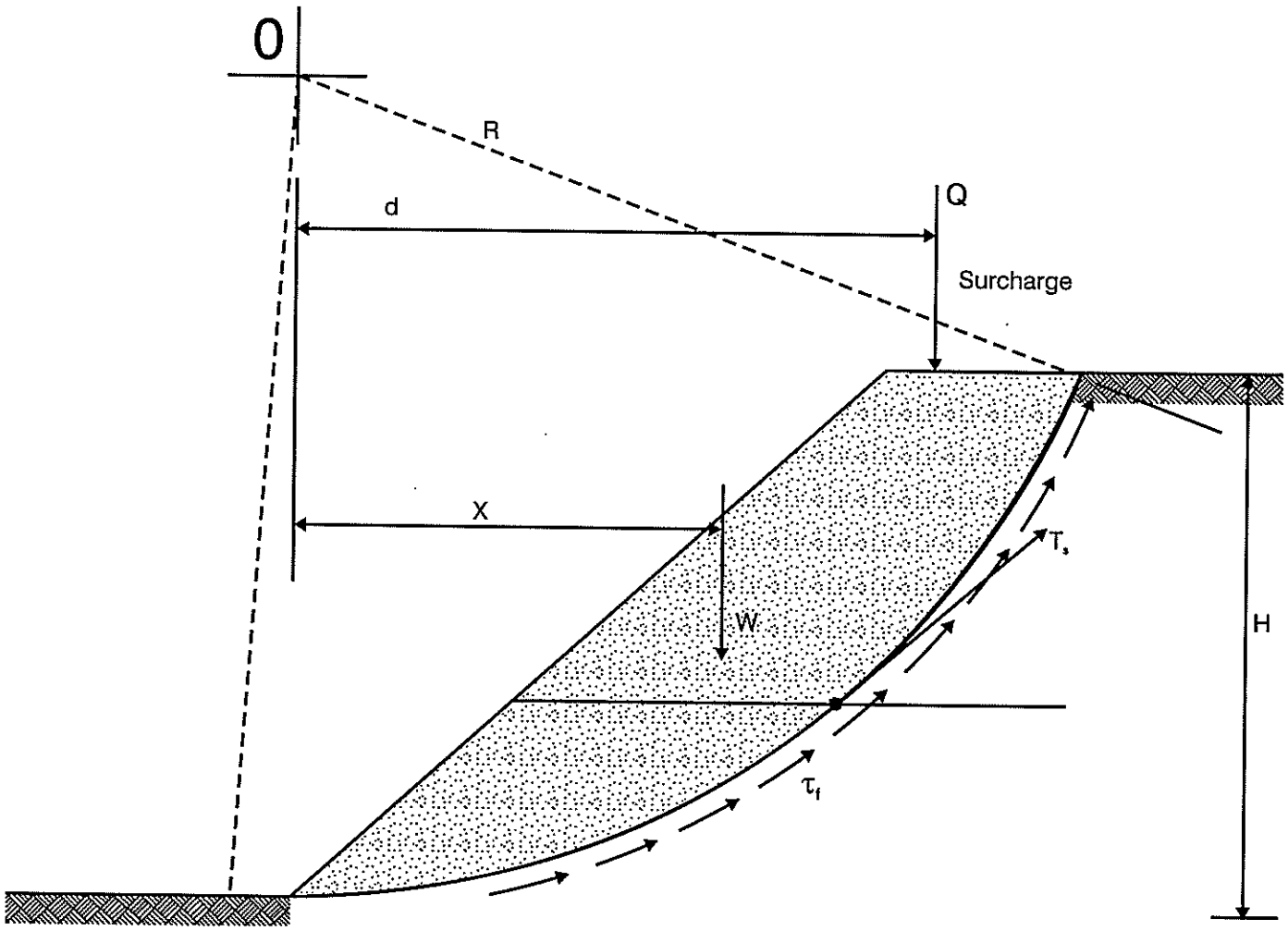

Note: T_s is assumed to act tangentially to the failure surface.

Figure 4.4 Analysis of total tension force in reinforcement.

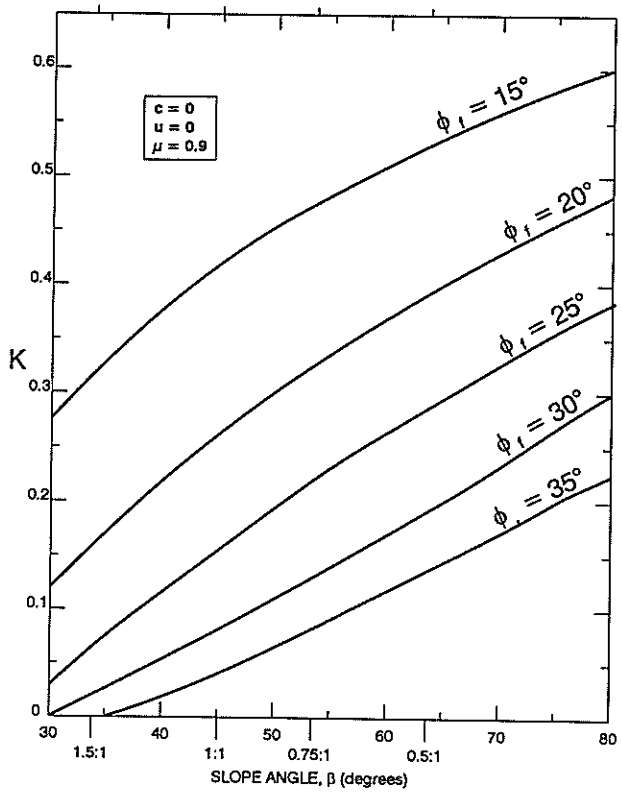

a) Reinforcement Force Coefficient.

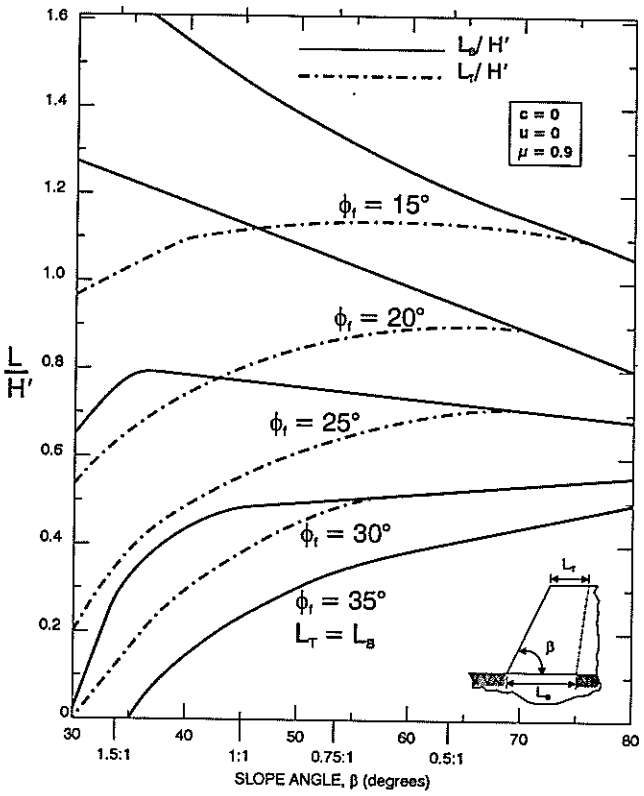

b) Reinforcement Length Ratio

CHART PROCEDURE:

1. Determine force coefficient K from figure A above where: $\phi_f = \tan^{-1}\left(\frac{\tan \phi_r}{f_{rs}}\right)$

   where: ϕ_r = friction angle of reinforced backfill

2. Determine:

$$T_{t,max} = 0.5\, K\, \gamma_r H'^2$$

   where: $H' = H + q/\gamma_r$

   q = a uniform surcharge

3. Determine the required reinforcement length at the top L_T and bottom L_B of the slope from figure B.

Limiting Assumptions:

- Slopes constructed with uniform, cohesionless soil (c=0).
- No pore pressures within slope.
- Competent, level foundation soils.
- No seismic forces.
- Uniform surcharge no greater than $0.2\gamma_r H$.
- Relatively high soil/ reinforcement interface friction angle of $0.9\,\phi_r$, i.e. $\mu = 0.9$ (may not be appropriate for some geosynthetic reinforcements); μ is the coefficient of interaction equal to the ratio of the soil-reinforcement shear strength to the internal soil shear strength.

Figure 4.5 Chart solution for determining the reinforcement strength requirements (after Schmertmann et al. 1987).

18/12/00

CAD FILE 3401650SK24.CDR MT

where:

- T_t is the total reinforcement tension force (i.e. the sum of the tensile forces in all reinforcement layers intersecting the failure surface) needed to achieve the required factor of safety f_{rs} for the considered failure surface;
- M_d is the driving moment about the centre of the failure circle;
- R is the radius of the failure surface;
- f_{us} is the "unreinforced" factor of safety for the circular failure surface considered (i.e. assuming unreinforced slope);
- f_{rs} is the required minimum factor of safety for both the reinforced and unreinforced soils.

The most critical failure surface with the largest T_t that is required to achieve the specified factor of safety f_{rs} should be identified. The most critical failure surface with $T_t = T_{t,max}$ is usually different from the failure surface with the lowest f_{us} obtained from unreinforced slope stability analysis.

4.2.4 Chart Design Procedures

Schmertmann Method

Figure 4.5 provides a chart design procedure that can be used to check the computer-generated results (Schmertmann et al. 1987). The charts are based on a simplified analysis of two-part and one-part wedge-type failure surfaces, and are limited by the assumptions noted on the figure. The required maximum tension force $T_{t,max}$ should be determined from Figure 4.5 and compared with $T_{t,max}$ from Section 4.2.3. If the discrepancy between the two values is within 30%, the highest value should be used in further analysis. If the discrepancy is more than 30%, additional analysis using other methods should be undertaken.

Jewell Method

Chart design procedures can be also utilised to design slopes without computer programs. A comprehensive chart design procedure was developed and published by Jewell (1990, 1991; refer to Appendix H). While Jewell uses a partial factor of safety approach different from the limit state design approach used in these Guidelines, Jewell's method produces reliable designs and has been successfully used for years.

Other design charts are also available (Werner & Resl 1986; Ruegger 1986; Leschinsky & Boedeker 1989).

4.2.5 Distribution of Reinforcement

The required distribution of reinforcement of slopes is determined in two steps.

Step 1

The following assumptions are made with respect to the distribution of geosynthetic reinforcement:

- For GRS slopes with a total height H≤6 m, a uniform reinforcement distribution is assumed and the force $T_{t,\ max}$ is used to determine tension forces F_j for each reinforcement layer.

- For GRS slopes with a total height H>6 m, the reinforced block should be divided into two (top and bottom) or three (top, middle and bottom) zones with equal height and uniform reinforcement distribution. The total tensile forces in reinforcement for each zone should be determined as follows:

  If two zones are assumed:
  - for the top zone $T_{t1} = 0.25\ T_{t,\,max}$
  - for the bottom zone $T_{t2} = 0.75\ T_{t,\,max}$

  If three zones are assumed:
  - for the top zone $T_{t1} = 0.167\ T_{t,\,max}$
  - for the middle zone $T_{t2} = 0.333\ T_{t,\,max}$
  - for the bottom zone $T_{t3} = 0.500\ T_{t,\,max}$

If the tensile reinforcement strength is known and constant through each zone, the vertical spacings between reinforcement layers can be determined for each zone as follows:

$$S_{vj} \leq \frac{H_j\ T^*_d}{T_{tj}} \qquad (42)$$

where:

S_{vj} is the reinforcement spacing in zone j;

H_j is the total height of zone j;

T_{tj} is the total reinforcement tensile force for zone j;

T^*_d is the design tensile strength of geosynthetic reinforcement (see Appendix A);

j is the zone index, in which

j = 1 for slopes with H ≤6 m;

j = 1, 2 or 1, 2, 3 for slopes with H >6 m.

If the reinforcement spacing S_{vj} is known for each zone, the required reinforcement tensile strength can be calculated as follows:

$$T^*_d \leq F_j = \frac{T_{tj}\ S_{vj}}{H_j} = \frac{T_{tj}}{N_j} \qquad (43)$$

where:

T^*_d, T_{tj}, S_{vj}, H_j are defined in Equation 42;

N_j is the number of reinforcement layers in zone j;

F_j is the tensile force in any particular reinforcement layer of zone j.

Step 2

To ensure that the reinforcement distribution determined in Step 1 is adequate, additional stability analysis of potential circular failure surface, exiting just above each layer of primary reinforcement, should be undertaken. The failure surfaces are analysed in groups. Each group comprises a "bunch" of failure surfaces exiting just above a particular layer of primary reinforcement.

The maximum total reinforcement tensile force T_t required to achieve the specified factor of safety f_{rs} is determined for the most critical local failure surface in each group of circular failure surfaces.

The maximum total reinforcement tensile force T_t for each group of failure surfaces should be determined in a manner similar to that described in Section 4.2.3 using Equation 41.

The available tensile strength of reinforcement layers (intersecting the critical failure surface for the group analysed) is then compared with the maximum total tensile force T_t for the same group and, if found insufficient, additional layers are added or reinforcement layers with higher tensile strength are used.

4.2.6 Length of Reinforcement

The required length of reinforcement for slopes should be determined as shown in Figure 4.6.

The embedment length L_e of each reinforcement layer beyond the most critical circular failure surface (i.e. the failure surface with $T_t=T_{t,\,max}$) should be sufficient to satisfy the following condition:

$$F_j \leq \Phi\, T^*_{di,l} \qquad (44)$$

where:

F_j is the tensile force in a reinforcement layer considered;

$T^*_{di,l}$ is the design soil–reinforcement interaction strength for pullout (Equation A5, Appendix A);

Φ is the reduction factor for pullout $\Phi = 0.7$.

For layers of reinforcement with calculated embedment lengths less than 1 m, a minimum value of L_e = 1 m should be adopted.

Lower layers of reinforcement should extend at least to the approximate limits of the the zone to be reinforced (also called the critical zone, see Section 4.2.2) as shown on Figure 4.6. The length required for sliding stability will generally control the length of lower reinforcement layers.

Upper levels of reinforcement may not need to be extended to the critical zone boundary if sufficient reinforcement exists in the lower levels to provide the specified factor of safety (f_{rs}) for all circular failure surfaces within the critical zone.

Note that reinforcement layers should also extend a distance Le (but not less than 1 m) beyond the local critical failure surface, exiting above each primary reinforcement layer, as identified in Section 4.2.5, Step 2.

An additional check of wedge-type sliding failure potential, using the simplified Janbu method for wedges with horizontal sliding planes exiting at the bottom of the middle third and the bottom of the top third of the slope, should be undertaken.

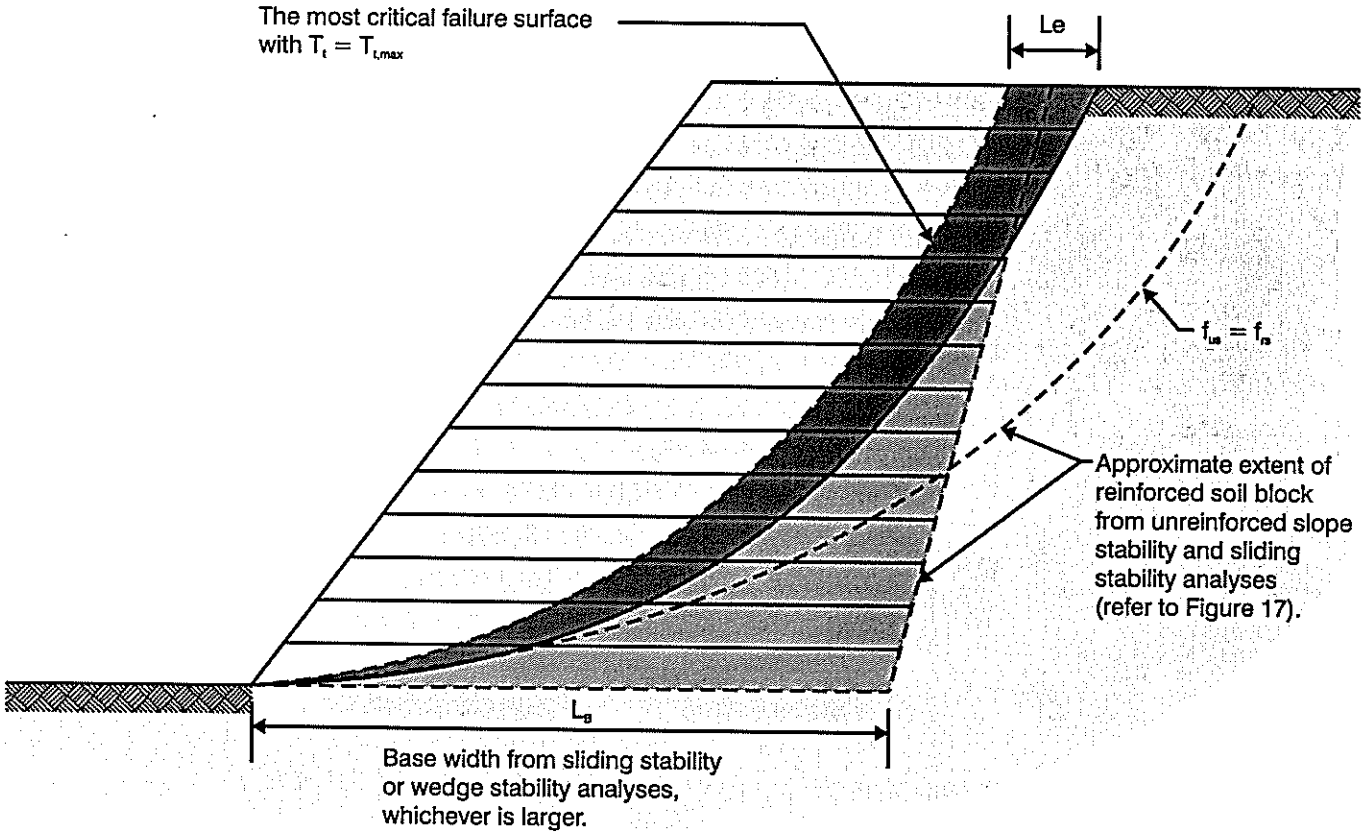

Note: Shaded area represents minimum reinforcement length requirements

Figure 4.6 Length of reinforcement for slopes.

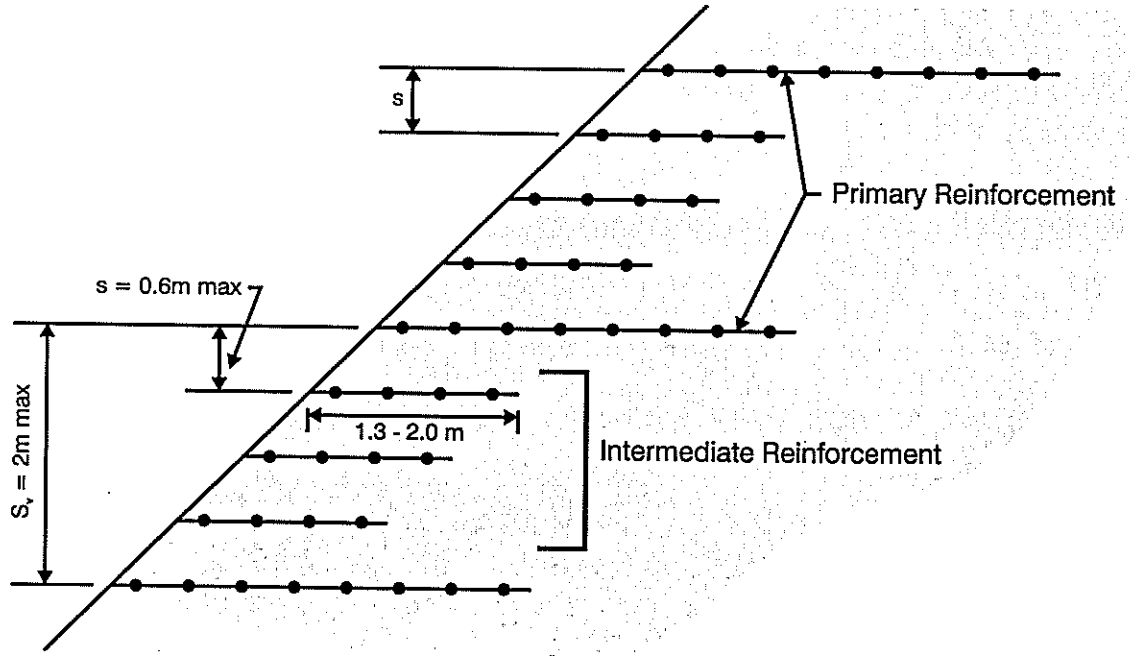

Figure 4.7 Primary and intermediate reinforcement layout.

If wedges with factors of safety lower than f_{rs} are found, the reinforcement should be extended to the active portion of the wedge's sliding plane.

The reinforcement layout can then be simplified by lengthening some reinforcement layers to create two or three zones of equal reinforcement length.

4.2.7 Analysis of Trial Layout of Reinforcement

An alternative to reinforcement design procedures described in Sections 4.2.3-4.2.6 is to develop a trial layout of reinforcement, and analyse the GRS slope using an appropriate reinforced slope-stability computer program. A trial layout should include number, length, design tensile strength, and vertical distribution of geosynthetic reinforcement. The charts given in Figure 4.5 can be used to develop a trial reinforcement layout.

The GRS slope with the trial reinforcement layout should then be analysed using an appropriate computer program. The calculations are done by generating numerous trial circular- and wedge-type failure surfaces, and calculating a factor of safety for each trial failure surface. Tensile forces in reinforcement are taken as the design tensile strength or design soil–reinforcement interaction strength whichever is lesser.

The GRS slope factor of safety is assumed to be equal to the lowest factor of safety value determined for all trial failure surfaces.

4.3 Design for Internal Stability under Seismic Conditions

The pseudo-static stability analysis method is recommended, i.e. the seismic stability of a GRS slope should be checked for all potential circular failure surfaces with horizontal and/or vertical inertia forces applied at the centroid of each slice as follows.

For the design of GRS slopes, the vertical seismic coefficient is commonly assumed to equal zero.

The horizontal seismic inertia force is equal to the horizontal seismic coefficient a_h multiplied by the weight of the sliding mass. It is common to assume that only the driving moment will be affected (i.e. the inertia force has no influence on the normal force and resisting moment).

The horizontal seismic coefficient $a_{h,int}$ for the internal stability analysis is assessed as follows:

$$a_{h,int} = 0.5 \text{ PGA} \tag{45}$$

where:

PGA is the peak ground acceleration coefficient.

The horizontal seismic coefficient $a_{h,int}$ for GRS slopes given by Equation 45 is lower than that for GRS walls (Equation 15) as GRS slopes can tolerate greater outward movements than most GRS walls.

The design tensile strength T^*_d for seismic conditions should be calculated assuming the reduction factor for creep deformation $\Phi_{rc} = 1.0$ (Equation A1, Appendix A1).

The design procedure is similar to that for static conditions, with additional moment due to the inertia forces added to the disturbing moment in the calculations of the factor of safety for seismic conditions. The recommended factor of safety for seismic conditions is $f_{rs,d} = 1.1$.

The designer needs to ensure that the most critical loading case has been analysed. Because increased design tensile reinforcement strength is required for seismic conditions, static stability is very often more critical than seismic stability.

4.4 Intermediate Reinforcement Layers

Additional checks should be undertaken to determine the need for intermediate layers. Intermediate layers are used to maintain face stability and compaction quality.

Intermediate reinforcement layers should be introduced if the vertical spacing between primary reinforcement layers exceeds 0.6 m (Figure 4.7). For slopes flatter than 1V:1H, closer spaced reinforcement layers ($S_v \leq 0.4$ m) preclude having to wrap the face.

Wrapped faces are required to prevent sloughing for slopes where significant seepage from the slope through the face is anticipated, and for slopes steeper than 1V:1H. Intermediate reinforcement should be placed in continuous layers but need not be as strong as the primary reinforcement. Short lengths (1.3-2.0 m) of intermediate reinforcement are recommended to maintain a maximum vertical spacing of 0.6 m or less for face stability and compaction quality.

5. Subsurface & Surface Water in GRS Structures

5.1 Subsurface Water Control

Uncontrolled subsurface water seepage can decrease stability and ultimately result in GRS structure failure. For example, hydrostatic forces on the rear of the reinforced mass and uncontrolled seepage into the reinforced mass will decrease stability. Seepage through the mass can reduce pullout capacity of the geosynthetic and create erosion at the face (especially for wrap-around facings).

The water source and the permeability of the natural and fill soils through which water must flow should be considered when designing subsurface water drainage features. Therefore, flow rates, filtration, placement and outlet details should be addressed. Drains are typically placed at the rear of the reinforced mass, while the lateral spacing of outlets is dictated by site geometry and expected flow. Outlet design should include long-term performance and maintenance requirements. Geocomposite drainage systems or conventional granular blanket and trench drains can be used.

Where drainage is critical for maintaining stability of a GRS structure, special emphasis is recommended on the design and construction of subsurface drainage features. Redundancy in the drainage system is also recommended in these cases.

5.2 Surface Water Run-off

Stability of GRS structures with wrap-around facing can be threatened by erosion caused by surface water run-off. Erosion rills and gullies can lead to surface sloughing and possibly deep-seated failure surfaces. Erosion control and revegetation measures must, therefore, be an integral part of wrap-around GRS system designs and specifications.

Surface water run-off should be collected above the GRS structure and channelled or piped below the base of the GRS structure.

If not otherwise protected, GRS slopes and GRS walls with wrap-around facing slopes should be vegetated after construction to prevent or minimise erosion caused by rainfall and run-off on the face. The steepness of the slope affects the amount of water absorbed by the soil before run-off occurs. Once vegetation is established on the slope face, it should be maintained to ensure its long-term survival, and a synthetic (permanent) erosion control mat with seeding may be required in some cases.

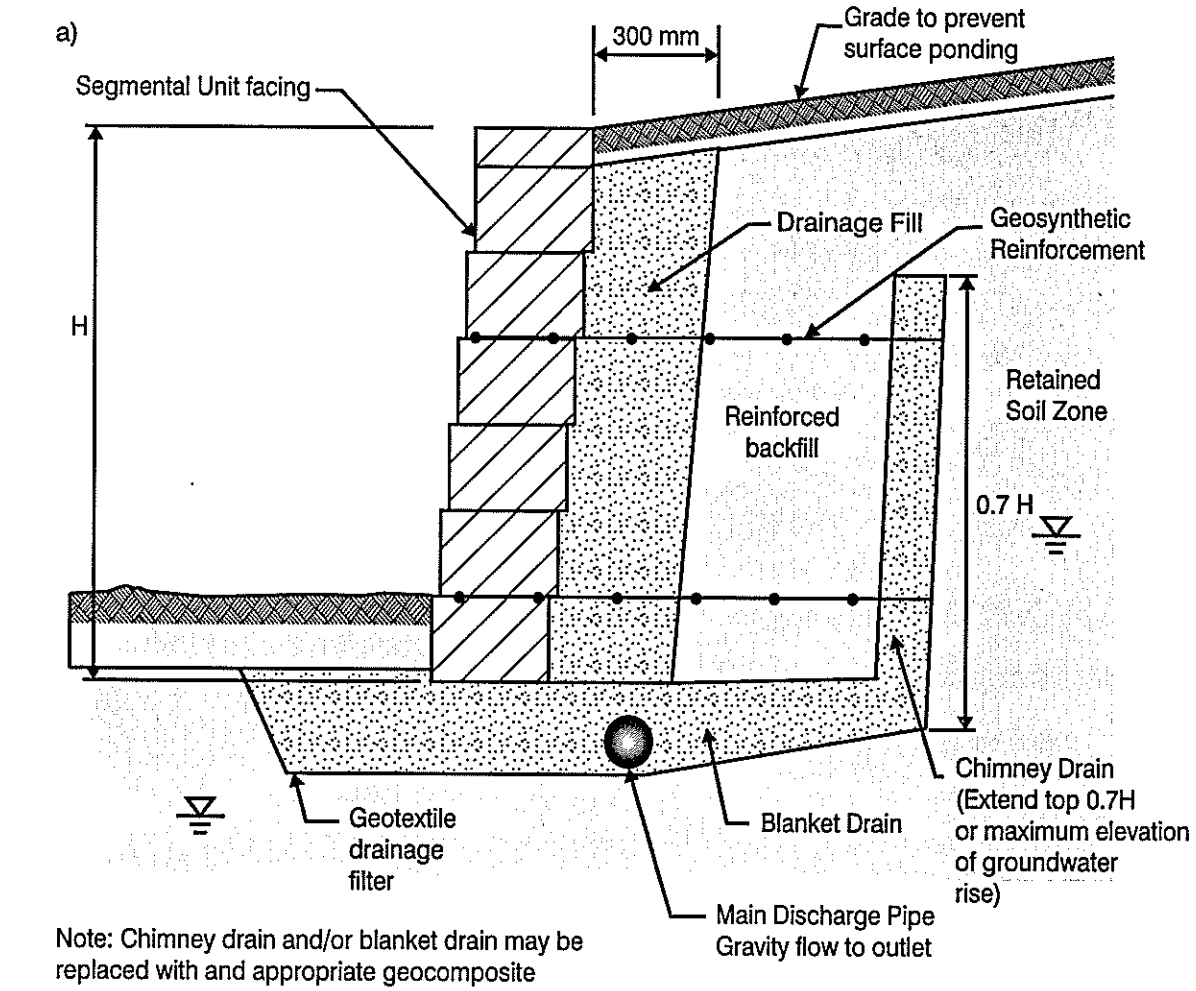

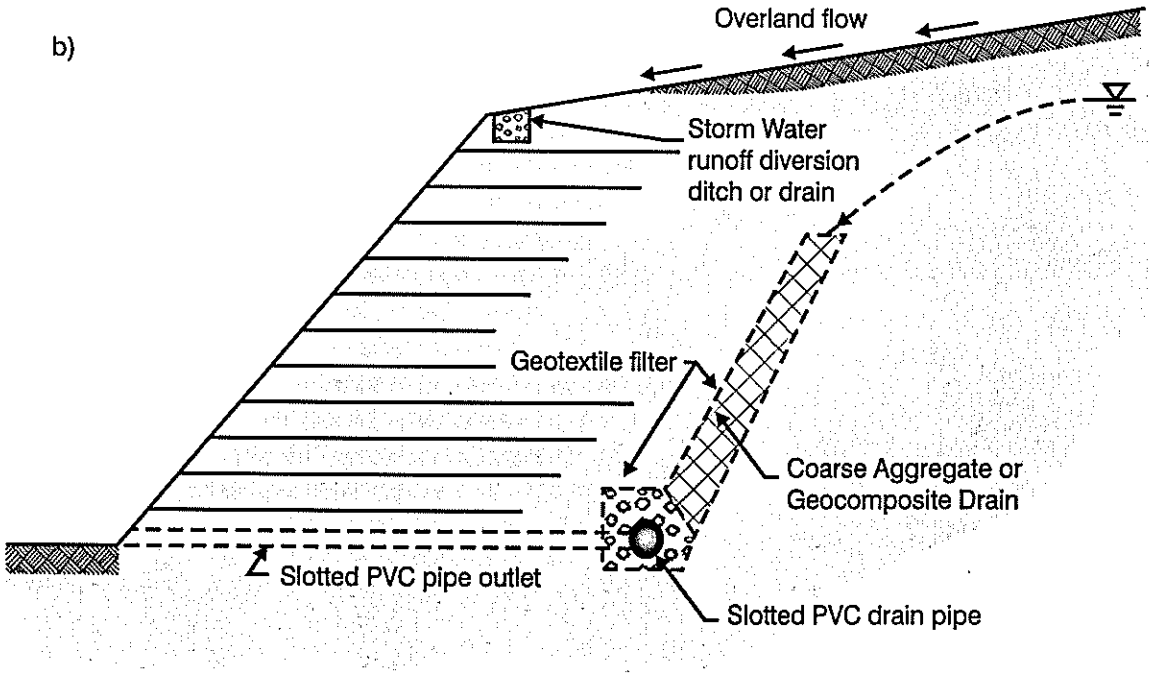

Figure 5.1 Examples of surface and subsurface water control measures for (a) GRS walls and (b) GRS slopes.

19/12/00

CAD FILE 3401650SK25.CDR MT

The erosion control mat serves three functions:

- to protect the bare soil face against erosion until vegetation is established,
- to reduce run-off velocity for increased water absorption by the soil, thereby promoting long-term survival of the vegetation cover,
- to reinforce the root system of the vegetation cover (maintenance of vegetation will still be required).

A permanent synthetic mat may not be required for flat slopes (flatter than 1V:1H), low height slopes, and/or where run-off is moderate. In these cases, a temporary (degradable) erosion blanket may be specified to protect the slope face and promote growth until vegetation cover is firmly established.

Examples of subsurface and surface water control measures are given in Figure 5.1.

6. Contracting Procedures

The recent availability of many new GRS systems and geosynthetic reinforcement materials requires Engineers to consider many alternatives before preparing contract bid documents so that a proven, cost-effective system and/or material can be chosen. GRS structures can be constructed using two different approaches (NCMA 1997).

6.1 Approach A – Method and Material Specification

This contracting approach (Appendix F1) includes the development of a detailed set of GRS structure drawings and material specifications in the bidding documents. Traditional method and material specifications are prepared with reinforcement material properties, installation requirements and other details explicitly specified in the contract documents. All available alternative systems/materials should be considered and generic specifications for reinforcement and other system elements should be prepared. In other words, design should be such that specified system/element properties can be met by a number of suppliers.

6.2 Approach B – Performance or Design Build Specification

The goal in use of this specification (Appendix F2) is to purchase design, materials and construction from a single source. Performance-type material specifications for components of systems and drawings of the geometric requirements for a GRS structure are prepared. All feasible, cost-effective system alternatives should be considered. Contract documents should be such that specified requirements can be met by a number of contractors and system suppliers.

With this approach the Contractor takes responsibility for all internal and all external failure modes (including bearing capacity and deep-seated failure). The Engineer would assume responsibility for the global stability assessment of the existing and final combinations of loads (based on consideration of ground conditions, groundwater and strata profiles). The Engineer would also be responsible for providing the Contractor with the factual results of all geotechnical investigations undertaken, and the parameters used for the Engineer's global stability assessment (including existing and final loads, ground conditions, ground water, and strata profiles and soil parameters). The Contractor would then be responsible for the review of all these parameters, the identification of any changes from these parameters (which he and his professional advisors believe to be appropriate), agreement of any such changes with the Engineer, and additional global stability assessments as may be appropriate for a particular type of GRS structure used and the construction sequence and programme proposed for the completion of the works.

An alternative approach where the Contractor takes responsibility for all internal and external failure modes (excluding bearing capacity and deep-seated failure) can also be used. With this alternative approach, the Engineer would assume design responsibility for checking external stability (including bearing capacity and deep-seated failure) and total and differential settlement. The Contractor or Supplier would assume responsibility for both external stability (including forward sliding, overturning, compound failures), internal and local stability.

Performance specifications for GRS structures should clearly state which approach has been adopted and should list the Engineer's and the Contractor's responsibilities with respect to design parameters and analysis of various failure modes. Therefore Clause 2.3 of the guideline specification included in Appendix F2 should be expanded to reflect project-specific requirements of the adopted approach.

6.3 Advantages & Disadvantages of Approaches A & B

Both approaches are acceptable if properly implemented, and each approach has advantages and disadvantages.

The advantage of Approach A is that the complete design, details and material specifications can be developed and reviewed over a much longer design period. This approach allows the Engineer to examine more options during design but requires engineering staff to be trained in MSE and GRS technology.

The disadvantage is that, for alternative bids, additional sets of design documentation must be developed but only one will be implemented. A further disadvantage is that newer and potentially less expensive systems or components may not be considered during the design stage.

Approach B offers several benefits. The advantage is that one source, experienced in the design and construction of a particular system, will be responsible for the structure which will be built economically because of competition. Also system components have been successfully and routinely used together, which may not be the case for Approach A with generic specifications for components. With Approach B some of the project design costs are transferred to construction.

The disadvantage is that the Engineer may not fully understand a proposed GRS technology at first and therefore may not be fully qualified to review and approve construction modifications. Newer and potentially less expensive systems may not be considered because the Engineer lacks confidence to review and accept these systems. In addition, some geotechnical issues and special details may not be fully considered until after the contract has been awarded.

This disadvantage can be addressed by requiring the Contractor to assume responsibility for both design and design review, enabling him to utilise professional advisors with suitable skills and experience with the proposed GRS technology. The Engineer's role is then less demanding technically, giving the Contractor increased scope for innovation.

Any GRS system component or a complete GRS system should be approved (for Approach A) or reviewed and accepted (for Approach B) by the Engineer.
A complete GRS system includes:

- design calculations and construction drawings;
- geosynthetic reinforcement material;
- facing details;
- erosion measures;
- drainage details;
- construction site assistance.

The approximate extent of information on a GRS system or components to be supplied by Contractor/Supplier for review/approval is given in Appendix C.

A successful GRS project will require well prepared specifications to communicate project requirements as well as construction guidance to the Contractor. Examples of "method and material" and "performance" guideline specifications for a wrap-around GRS structure are given in Appendix F. These examples are based on specifications published by Berg (1993) and on specifications used on recent GRS projects in New Zealand.

7. Computer Programs for Design of GRS Structures

A number of computer programs for design of GRS structures have been developed by various material/system suppliers and researchers. Some of the commercially available software products are listed below.

Given the many possible combinations of input information for GRS problems and the complex nature of computer codes, most computer program developers find it impossible to guarantee the complete accuracy of the final software. Therefore, computer analysis results should be used as only one part of an overall effort to analyse the stability of a GRS structure of a given design.

The ultimate responsibility for the accuracy of each solution and the safety of a particular GRS design should rest with the designer. It is, therefore, imperative that the designer understands potential limitations on the accuracy of the results obtained using a particular software product, endeavour to cross-check those results with other methods, and to test the reasonableness of those results with the wisdom of his engineering knowledge and experience.

Computer Program	Developer	Use for GRS
WinWall	Tensar International, London, UK	Design of GRS walls reinforced with TENSAR geogrids
WinSlope	Tensar International, London, UK	Design of GRS slopes reinforced with TENSAR geogrids
ReSlope	Department of Civil Engineering of Delaware, Newark, USA	Design of GRS slopes (including steep slopes)
TENAX Software – Tnxslope	TENAX SPA, Geosynthetic Division, Vigano, Italy	Design of steep GRS slopes reinforced with TENAX geogrids
TENAX Software – TnxWall	TENAX SPA, Geosynthetic Division, Vigano, Italy	Design of GRS walls reinforced with TENAX geogrids
Anchor wall	Jarret & Associates Inc., Kingston, Ontario, Canada	Design of segmental GRS walls
RSS (Reinforced Slope Stability), based on modified version of STABL	GEOCOMP Corporation, Acton, USA	Design of GRS slopes
MSEW (Mechanically Stabilised Earth Walls)	ADAMA Engineering Inc. Newark, USA	Design of GRS walls
GEO-SLOPE Office – SLOPE/W	GEO-SLOPE International Ltd, Calgary, Alberta, Canada	Stability analysis for GRS slopes
TALREN	TERRASOIL, Montreal, France	Stability analysis for GRS slopes
Slope	Geosolve, London, UK	Stability analysis for GRS slopes

Note: Some of the computer programs listed have several functions.
Only their use relating to GRS structures is outlined in this table.

8. References

AASHTO. 1990a. *Standard specifications for Geotextiles – M288, Standard specifications for transportation materials and methods of sampling and testing:* 689-692. American Association of State Highway and Transportation Officials (AASHTO), Washington DC.

AASHTO. 1990b. Design guidelines for use of extensible reinforcements (Geosynthetic) for mechanically stabilised earth walls in permanent applications. *Task Force 27 Report, In Situ Soil Improvement Techniques*. AASHTO, Washington DC.

AASHTO. 1992. *Standard specification for highway bridges.* 15th edition, AASHTO, Washington DC. Amended 1993, 1994, 1995.

Ambraseys, N.N., Menu, J.M. 1988. Earthquake-induced ground displacements. *Earthquake Engineering and Structural Dynamics 16:* 985-1006.

ASTM. 1990. Obtaining hydrostatic design basis for thermoplastic pipe materials. *ASTM D2837.* American Society for Testing and Materials (ASTM), Philadelphia, Pennsylvania.

ASTM. 1994. Tensile properties of geotextiles by the wide-width strip method. *ASTM D4595.* ASTM, Philadelphia, Pennsylvania.

ASTM. 1996. Standard practice for determining the specification conformance of geosynthetics. *ASTM D4759.* ASTM, Philadelphia, Pennsylvania.

ASTM. 2000. *Annual book of ASTM Standards for soil and rock, dimension stone and geosynthetics.* ASTM, Philadelphia, Pennsylvania.

Bathurst, R.J., Benjamin, D.J., Jarrett, P.M. 1988. Laboratory study of geogrid reinforced soil walls. R.D. Holtz (Ed.): *Geogrid Reinforced Soil Walls*. Royal Military College of Canada, Kingston, Ontario. *Proceedings of the Symposium on Geosynthetics for Soil Improvement,* American Society of Civil Engineers (ASCE) National Convention, Nashville, Tennessee. *ASCE Geotechnical Special Publication N° 18:* 178-192.

Bathurst, R.J., Koerner, R.M. 1988. Results of Class A predictions for the RMC reinforced soil wall trials. P.M. Jarrett & A. McGown (Eds): *The application of polymeric reinforcement in soil retaining structures:* 127-171.

Bathurst, R.J., Wawrychuk, W.F., Jarrett, P.M. 1988. Laboratory investigation of two large-scale geogrid reinforced soil walls. P.M. Jarrett & A. McGown (Eds): *The application of polymeric reinforcement in soil retaining structures:* 71-125.

Bathurst, R.J., Jarrett, P.M. 1990. Grid-reinforced retaining wall model tests. Den Hoedt (Ed.): *Geotextiles, Geomembranes and Related Products:* 119.

Bathurst, R.J., Hatamai K. 1998. Seismic response analysis of a geosynthetic-reinforced soil retaining wall. *Geosynthetics International.5 (1-2):* 127-166.

Berg, R.R. 1993. *Geosynthetic mechanically stabilized earth slopes on firm foundations:* 1-43. Federal Highway Administration, USA.

Bonaparte, R., Schmertmann, G.R., Williams, N.D. 1986. Seismic design of slopes reinforced with geogrids and geotextiles. Pp. 273-278 in *Foundations and Reinforced Embankments. Proceedings of Third International Conference on Geotextiles*, Vienna, Austria.

British Standards Institution (BSI). 1995. Reinforced soils. Code of practice: Strengthened/reinforced soils and other fills. *BS 8006:1995:* 160.

Cai, Z., Bathurst, R.J. 1995. Seismic response analysis of geosynthetic reinforced soil segmental retaining walls by finite element method. *Computers & Geotechnics 17(4):* 523-546.

Cai. Z., Bathurst, R.J. 1996. Seismic-induced permanent displacement of geosynthetic-reinforced segmental retaining walls. *Canadian Geotechnical Journal 33:* 937-955.

Christopher, B.R., Gill, S.A., Giroud, J.P., Juran, I., Mitchell, J.K., Schtosser, F., Dunnicliff, J. 1989. *Reinforced soil structures. Summary of research and systems information 2:* 1-158. US Department of Commerce National Technical Information Service.

Christopher, B.R., Holtz, R.D., Allen, T.M. 1990a. Instrumentation for a 12.6 m high geotextile-reinforced wall. *Performance of Reinforced Soil Structures, British Geotechnical Society:* 73-78.

Christopher, B.R., Safdar, A.G., Giroud, J., Juran, I., Mitchell, J.K., Schlosser, F., Dunnicliff, J. 1990b. *Reinforced soil structures. Design and construction guidelines 1:* 1-301. Federal Highway Administration (FHWA), McLean, Virginia.

Christopher, B.R., Berg, R.R. 1990. Pullout evaluation of geosynthetic in cohesive soils. *Proceedings of the 4th International Conference on Geotextiles, Geomembranes and Related Products:* 731-736. The Hague, Netherlands.

Elias, V. 1990. *Durability/corrosion of soil reinforced structures.* 173 pp. Federal Highway Administration (FHWA), McLean, Virginia.

Elias, V. 1997. Corrosion/degradation of soil reinforcements for mechanically stabilized earth walls and reinforced soil slopes. *Demonstration Project 82, Reinforced Soil:* 1-105. *Report FHWA-SA-96-072.* US Department of Transportation, FHWA, Washington DC.

Elias, V., Christopher, B.R. 1997. *Mechanically stabilized earth walls and reinforced soil slopes design and construction guidelines.* 371 pp. US Department of Transportation Federal Highway Administration (FHWA), Washington DC.

European Committee for Standardisation (ECS). 1996. Geotetxtiles – wide-width tensile test. *EN ISO 10319*, European Committee for Standardisation, Brussels.

European Committee for Standardisation (ECS). 1998. Geotextiles and geotextile-related products – Determination of tensile creep and creep rupture behaviour. Final draft. *EN ISO 13431.* European Committee for Standardisation, Brussels.

Geosynthetic Research Institute (GRI). 1988a. *GRI Test Method GG1: Geogrid rib tensile strength.* Geosynthetic Research Institute, Drexel University, Philadelphia.

Geosynthetic Research Institute (GRI). 1988b. *GRI Test Method GG2: Geogrid junction strength.* Geosynthetic Research Institute, Drexel University, Philadelphia.

Geosynthetic Research Institute (GRI). 1988c. *GRI Test Method GG3a: Tension creep testing of stiff geogrids.* Geosynthetic Research Institute, Drexel University, Philadelphia.

Geosynthetic Research Institute (GRI). 1990. *GRI Standard of Practice GG4a: Determination of the long-term design strength of stiff geogrids.* Geosynthetic Research Institute, Drexel University, Philadelphia.

Geosynthetic Research Institute (GRI). 1991a. *GRI Test Method GG3b: Tension creep testing of flexible geogrids.* Geosynthetic Research Institute, Drexel University, Philadelphia.

Geosynthetic Research Institute (GRI). 1991b. *GRI Standard of Practice GG4b: Determination of the long-term design strength of flexible geogrids.* Geosynthetic Research Institute, Drexel University, Philadelphia.

Geosynthetic Research Institute (GRI). 1991c. *GRI Test Method GG5: Test method for geogrid pullout.* Geosynthetic Research Institute, Drexel University, Philadelphia.

Geosynthetic Research Institute (GRI). 1991d. *GRI Test Method GS6: Interface friction determination by direct shear testing.* Geosynthetic Research Institute, Drexel University, Philadelphia.

Geosynthetic Research Institute (GRI). 1992a. *GRI Test Method GT5: Tension creep testing of geotextiles.* Geosynthetic Research Institute, Drexel University, Philadelphia.

Geosynthetic Research Institute (GRI). 1992b. *GRI Test Method GT6: Geotextile pullout.* Geosynthetic Research Institute, Drexel University, Philadelphia.

Geosynthetic Research Institute (GRI). 1992c. *GRI Standard of Practice GT7: Determination of long-term design strength of geotextiles.* Geosynthetic Research Institute, Drexel University, Philadelphia.

Holtz, R.D., Christopher, B.R., Berg, R.R. 1995. Geosynthetic design and construction guidelines. *NHI Course N° 13213 – Participant Notebook:* 225-324.

Jewell, R.A. 1990. *Revised design charts for steep reinforced slopes, reinforced embankment: theory and practice in the British Isles.* Thomas Telford, London, UK.

Jewell, R.A. 1991. Application of revised design charts for steep reinforced slopes. *Geotextiles and Geomembranes* 10 (1991): 203-233.

Leshchinsky, D. 1995. Design procedure for geosynthetic reinforced steep slopes. *Technical Report REMR-GT-120* (temporary number), US Army Engineer Waterways Experiment Station, Vicksburg, MS.

Leshchinsky, E., Boedeker, R.H. 1989. Geosynthetic reinforced soil structures. *Journal of Geotechnical Engineering, ASCE 115(10):* 1459-1478.

Ling, H.I., Leshchinsky, D., Perry, E.B. 1997. Seismic design and performance of geosynthetic-reinforced soil structures. *Géotechnique 47(5):* 933-952.

Marr, A., Werden, S. 1997. *Reinforced slope stability, a microcomputer program.* 92 pp. US Department of Transportation, FHWA, Washington DC.

Murashev, A.K. 1998. Design and construction of geosynthetic reinforced soil structures in New Zealand: Review and discussion paper. *Transfund New Zealand Research Report No. 123.* 110 pp.

Murashev, A.K. 2001. Guidelines for design & construction of geosynthetic-reinforced soil structures in New Zealand: draft for comment. *Transfund New Zealand Research Report No. 194.* 156 pp.

NCHRP. 1991. *Manuals for the design of bridge foundations: 308 pp.* National Cooperative Highway Research Program (NCHRP) Report No. 343, Washington D.C.

NCMA. 1997. *Design manual for segmental retaining walls.* 1st ed. National Concrete Association, Virginia, USA. 289 pp.

NCMA. 1998a. *Concrete masonry standards.* National Concrete Masonry Association, Virginia, USA. 179 pp.

NCMA. 1998b. *Segmental retaining walls – Seismic Design Manual.* 2nd ed. National Concrete Association, Virginia, USA. 118 pp.

NZ Department of Transport Highways and Traffic. Revised 1987. Reinforced and anchored earth retaining walls and bridge abutments for embankments. *Technical Memorandum BE 3/78:* 1-49.

NZ Geomechanics Society (NZGS). 1988. *Guidelines for the field description of soils and rocks in engineering use.* New Zealand Geomechanics Society. 42 pp.

Pender, M.J., Matushka. T. 1994. *Geotechnical limit state design seminar notes.* New Zealand Geotechnical Society. 45 pp.

Pender, M.J. 2000. Ultimate limit state design of foundations. *NZ Geotechnical Society Short Course:* 147-197.

Ruegger, R. 1986. Geotextile reinforced soil structures on which vegetation can be established. *Proceedings of 3rd International Conference on Geotextiles*, Vienna, Austria, *Vol.II:* 453-458.

Schmertmann, G.R., Chouery-Curtis, V.E., Johnson, R., Bonaparte, R. 1987. *Design charts for geogrid reinforced soil slopes.* Session 1B: 108-120. *Proceedings of Slopes and Walls Geosynthetic Conference*, New Orleans, USA.

Silvestri, V. 1983. The bearing capacity of dikes and fills founded on soft soils of limited thickness. *Canadian Geotechnical Journal 20(3).*

Standards Association of NZ (SANZ). 1986. Soil compaction tests. Test 4.1.1 NZ standard compaction test. *NZS 4402:1986.* 6 pp.

Standards Australia (SA). 1996. Earth retaining structures (including reinforced soils) – Draft Australian Standard for comment. *AS DR 96405.* 96 pp. Standards Australia, Canberra.

Tensar Corporation. 1997. *The design of reinforced soil structures using Tensar geogrids.* 45 pp.

Transit New Zealand. 1994. *Bridge Manual.* Transit NZ, Wellington, New Zealand.

Werner, G., Resl, S. 1986. Stability mechanisms in geotextile reinforced earth-structures. *Proceedings of 3rd International Conference on Geotextiles*, Vienna, Austria, *Vol.II:* 465-470.

Wood, J.H., Elms, D.G. 1990. Seismic design of bridge abutments and retaining walls. *National Roads Board (NRB) Road Research Unit (RRU) Bulletin 84(2):* 1-90. NRB RRU, Wellington, New Zealand.

Appendix A

Design Tensile Strength & Soil–Reinforcement Interaction

Appendix A Design Tensile Strength & Soil–Reinforcement Interaction

A1. Design Tensile Strength

The design tensile strength of soil reinforcement shall be determined using partial material strength reduction factors (i.e. factors that cover the effect of identified causes of decrease in strength and are drawn from test data) and uncertainty factors (i.e. factors that cover unknowns and uncertainties) as follows:

$$T^*_d = T_{ult}\ \Phi_m \Phi_{rc}\ \Phi_e \Phi_i\ \Phi_{rch}\ \Phi_{rb}\ \Phi_d\ \Phi_j\ \Phi_n \qquad (A1)$$

where:

T^*_d is the design tensile strength of geosynthetic, kN/m;

T_{ult} is the ultimate geosynthetic tensile strength, kN/m;

Φ_m is the uncertainty factor (manufacturing), dimensionless;

Φ_{rc} is the reduction factor for creep deformation (ratio of creep limiting strength to T_{ult}), dimensionless;

Φ_e is the uncertainty factor (extrapolation), dimensionless;

Φ_i is the reduction factor (installation damage), dimensionless;

Φ_{rch} is the reduction factor (chemical degradation), dimensionless;

Φ_{rb} is the reduction factor (biological degradation), dimensionless;

Φ_d is the uncertainty factor (overall degradation), dimensionless;

Φ_j is the reduction factor (joints, seams and connections), dimensionless;

Φ_n is the reduction factor associated with ramification of failure, dimensionless.

Note that the connection geosynthetic strength to facing elements may limit and therefore control the design tensile strength.

The following methods can be used to define the strength reduction factors (these methods are listed in the order of preference):

- Direct adequate testing (as described in Sections A1.2–A1.9);
- Individual default values (note that the default reduction factors recommended in Sections A1.2–A1.9 were developed for use when one or two reduction factors are undefined, along with other defined reduction factors);
- Overall default values (as described in Section A3).

A1.1 Ultimate Strength (T_{ult})

Ultimate strength values shall be based upon minimum average roll values (MARV) determined in accordance with ASTM D4759 (in ASTM 2000). Ultimate strength for agency quality insurance purposes may be determined according to ASTM D4595 Tensile Properties of Geotextiles by the Wide-Width Strip Method (ASTM 1994) or GRI Test method GG1: Geogrid Rib Tensile Strength (GRI 1988a).

Alternatively EN ISO 10319 (ECS 1996) can be used for both geotextiles and geogrids.

The test procedure used to determine ultimate strength must be the same as that used to define Φ_{rc}.

A1.2 Manufacturing (Φ_m)

The uncertainty factor Φ_m deals with the consistency of manufacture and how variations in this may affect strength. This factor should take into account whether or not a standard for specification, manufacture and central testing of the reinforcement exists. For geosynthetic reinforcement, quality should be specified on the basis of either characteristic or mean base strength (the characteristic being the 95th percentile value). If appropriate, audited quality control and assurance procedures are employed (e.g. BS/EN ISO 9002), and the following values can be used as a guide:

- If a characteristic base strength is specified:
  $\Phi_m = 1.0$;
- If a mean base strength is specified:
  $\Phi_m = 1/(1 + 1.64\sigma/(\mu - 1.64\sigma))$ (A2)

where:

μ is the mean reinforcement base strength;

σ is the standard deviation of the reinforcement.

A1.3 Creep (Φ_{rc})

Long-term tension-strain-time geosynthetic reinforcement behaviour shall be determined from results of controlled laboratory creep tests, that are conducted for a minimum duration of 10 000 hours for a range of load levels on samples of the finished product, according to the ASTM D5262 Test Methods for Unconfined Tension Creep Behaviour of Geosynthetics (in ASTM 2000). Alternatively EN ISO 13431 (ECS 1998) can be used.

The requirement for a 10 000 hour minimum creep test period for geogrids and geotextiles may be waived for a new reinforcement product if the product can be demonstrated to be sufficiently similar to a proven 10 000 hour creep-tested product of similar nature. Product similarity must consider base resin, resin additives, product manufacturing process, product geometry, and creep response. When these conditions are met, creep testing shall be conducted for a minimum of 1000 hours. The 1000 hour creep curves shall pattern very closely the 1 000 hour portion of the 10,000 hour creep curves of the similar product.

Creep test data at a given temperature may be directly extrapolated over time, up to one order of magnitude, in accordance with standard polymeric practices. Accelerated testing is required to extrapolate 10 000-hour creep test data to a

minimum 75-year design life. Procedures for test acceleration are discussed in GRI: GG4a & GG4b test methods (1990, 1991b) and GRI:GT7 (1992c) Standards of Practice.

Formulation of the ratio of ultimate strength to creep–limiting strength is defined in GRI:GG3a & GG3b (1998c, 1991a) and GRI:GT5 (1992a). Φ_{rc} can be calculated as the reciprocal of that ratio.

The creep ultimate load criterion can be defined in terms of creep deformation or rupture.

If a criterion based on creep deformation is adopted (in other words, a strain-limited geosynthetic tensile strength is used), the internal strain check for the GRS structure is not required. However, the long-term strain criterion should be pre-selected before testing to ensure that lateral deformations of the GRS structure remain within tolerable limits. The strain level of 10% is known to be consistent with documented performance of GRS structures and empirical experience (NCMA 1997; Berg 1993). Lower values of performance limit strain may be selected for deformation-sensitive or critical structures to minimise lateral movements and increase the overall lateral stiffness of GRS structures.

If a rupture criterion is used, internal horizontal strains of geosynthetic reinforcement should be checked, as described in Section 2.13 of these guidelines, to assess post-construction performance of the GRS structure.

A default reduction factor for creep is not permitted for detailed and final design. However, creep-reduction factors, given in Table A1 (from AS DR 96405, SA 1996), may be used for preliminary design. These factors are appropriate if the creep behaviour is defined in terms of rupture.

Table A1 Reduction factor (Creep), Φ_{rc} (from AS DR 96405, SA 1966).

Material	**Time (years)**	Φ_{rc}
Polyester	30	0.63
	100	0.60
Polyethylene	30	0.33
	100	0.30
Polypropylene	30	0.20
	100	0.17

A1.4 Extrapolation

The uncertainty factor Φ_e is given by:

$$\Phi_e = \Phi_{e1} \times \Phi_{e2} \qquad \text{(A3)}$$

where:

Φ_{e1} is an uncertainty factor that reflects a measure of confidence in the available data which is to be subsequently extrapolated. This factor should be derived from statistical study of quantity, quality, relevance and duration of available data.

Φ_{e1} can be taken as 1 where the body of test data accrues from creep tests carried out at a test temperature equal to the maximum operational temperature, and a large amount of directly relevant data is available. In other cases a value of Φ_{e1} less than unity is necessary.

Φ_{e2} is an uncertainty factor that relates to confidence in extrapolation of data beyond the duration of test data to the selected design life of the reinforcements. The uncertainty factor Φ_{e2} should be estimated on the basis of Table A2 (AS DR 96405, SA 1996).

Table A2 Uncertainty factor (Extrapolation), Φ_{e2} (from AS DR 96405, SA 1966).

Material	Time (years)	Φ_{e2} Log Cycles of Extrapolation		
		0	1	2
Polyester	30	1.00	0.97	0.93
	100	1.00	0.95	0.90
Polyethylene	30	1.00	0.90	0.80
	100	1.00	0.80	0.60
Polypropylene	30	1.00	0.75	0.55
	100	1.00	0.70	0.50

A1.5 Installation Damage (Φ_i)

The effect of installation damage on geosynthetic reinforcement shall be determined from the results of full scale construction damage tests. Values must be substantiated by construction damage tests for the selected geosynthetic material conducted with similar or more severe backfills and similar, or more severe placement and compaction techniques as described in GRI:GG4a & 4b (1990, 1991b) and GRI:GT7 (1992c) Standards of Practice. Alternatively recommendations given in Annex D of BS 8006 (BSI 1995) can be used.

Table A3 Reduction factor (Installation Damage), Φ_I (from Elias & Christopher 1997).

Geosynthetic	For backfill with max. size:	
	102 mm, D_{50} about 30 mm	20 mm, D_{50} about 0.7 mm
HDPE uniaxial geogrid	0.70	0.83
PP biaxial geogrid	0.70	0.83
PVC coated PET geogrid	0.54	0.77
Acrylic coated PET geogrid	0.49	0.71
Woven geotextiles (PP & PET)[(1)]	0.45	0.71
Non-woven geotextiles (PP & PET)[(1)]	0.40	0.71
Slit film woven PP geotextile[(1)]	0.33	0.5

[(1)] Minimum weight 270 g/m^2

If handling and storage of geosynthetic materials on site does not comply with the manufacturer's requirements, an appropriate reduction factor for storage and handling shall be introduced.

A1.6 Chemical Degradation (Φ_{rch})

The detrimental effects of chemical exposure on the reinforcement is dependent on material composition, including resin type, resin grade, additives, manufacturing process and physical structure of final product. Those effects include any action or reaction which can raise the operational temperature above the maximum value assumed in design or, more commonly, the effect of chemicals. Detailed description of possible degradation mechanisms is given in Appendix B.

Soil pH testing should be conducted in all candidate reinforced and retained fill materials comprising soils that are of potential concern, listed in Appendix B, for GRS structures with reinforcement made of polymer as these may be adversely affected by these fill materials. Where there is a probability of aggressive chemicals coming into contact with the reinforcements, this should be taken into account or prevented by the incorporation of suitable drainage or sealing.

In the absence of specific test data and if no detrimental affect from chemical exposure is expected (refer to Appendix B), a default chemical degradation factor of $\Phi_{rch} = 0.5$ should be used. For polyester products more detailed recommendations on default factors are available and given in Table A4 (from Elias & Christopher 1997).

Table A4 Chemical degradation reduction factors for polyester, Φ_{rch} (from Elias & Christopher 1997).

N°	Product*	Reduction Factor, Φ_{rch}	
		5≤pH≤8	3≤pH≤5 8≤pH≤9
1	Geotextiles Molecular Weight <20 000 40< Carboxyl End Group Number <50	0.63	0.5
2	Coated geogrids Molecular Weight >25 000 Carboxyl End Group Number <30	0.87	0.77

*Use of materials outside the indicated pH or molecular property range requires specific product testing.

The following is recommended for soil fill pH (NCMA 1997):

- 3≤ pH ≤9 - acceptable
- pH <3 or pH ≥12 - should not be used
- pH >9 - should only be used with supporting test data for the specific product

A1.7 Biological Degradation (Φ_{rb})

Polymers used for geosynthetics are generally not susceptible to biological degradation by micro-organisms such as fungi and bacteria. If biological degradation potential is suspect, geosynthetic resistance to biological effects should be measured as described in Appendix B. In the absence of specific information on biological degradation of a geosynthetic material, a reduction factor $\Phi_{rb} = 0.8$ should be used.

A1.8 Overall Degradation (Φ_d)

Methods to predict strength loss due to degradation of geosynthetics are not yet well developed and are the subject of current research and development studies. Therefore the recommendation is to use the following uncertainty factors :

- tested geosynthetics: $\Phi_d = 0.95$
- untested geosynthetics: $\Phi_d = 0.80$

A1.9 Joints, Seams and Connections (Φ_j)

The effect of the joint strength must be factored into design strength when separate lengths of geosynthetics are connected together or overlapped in the direction of primary force development. The value Φ_j should be taken as the ratio of the jointed specimen strength to the unjointed specimen strength.

Testing should be conducted in accordance with ASTM D4595 (1994) for mechanically connected joints, and GRI:GG5 (1991c) or GRI:GT6 (1992b) for overlap joints. Sustained tension tests of 1,000-hour minimum duration should also be conducted on mechanically connected joints, according to GRI:GG4a& 4b (1990, 1991b), and GRI:GT7 (1992c). A load level equal to the design strength, T^*_d is suggested for long-term testing. Limits on number and location of joints and seams in a slope or wall structure should be addressed in the project specifications.

The connection geosynthetic strength to the wall facing element may limit strength and therefore control the design tensile strength. Connection strength must be addressed in wall designs.

A1.10 Ramification of Failure (Φ_n)

The reduction factor Φ_n should be applied to take account of the ramifications of failure of the structure. The factor should be assigned values given in Table A5 dependent upon the class of risk for a particular structure.

Table A5 Reduction factor for ramification of failure.

Structure Category	Description	Φ_n
1	Retaining walls and slopes less than 1.5 m in retained height where failure would result in minimal damage and loss of access	1.0
2	Retaining walls and slopes where failure would result in moderate damage and loss of access	1.0
3	Structures directly supporting highways, trunk and principal roads or railways or inhabited buildings, etc.	0.9

A2. Implementation

The determination of the factors for creep, extrapolation, chemical and biological durability require extensive testing, and is product-specific. Testing standards for determination of these reduction factors are not fully developed; and as a result test procedures and interpretation of test data can vary. Therefore, evaluation of supplier submittals is not an easy process for many consulting engineers.

Detailed lists of items to be supplied by potential geosynthetic reinforcement material suppliers and GRS system suppliers, are presented in Appendix C.

Implementation of GRS slope and GRS wall technologies has been significantly hampered by the review required to assess geosynthetic long-term allowable strength. Many consulting engineers find the procedure too laborious and time-consuming for post-bid evaluation of materials or are not able to implement a complete review process for a variety of reasons (e.g. the lack of in-house expertise to complete an evaluation).

Implementation of well-documented, cost-effective geosynthetic-reinforced slope and wall technologies is costly, and sometimes an easier and/or quicker procedure for implementing and determining long-term allowable strength quantification and geosynthetic product acceptance is needed. Therefore, an alternative procedure for determining long-term allowable strength has been proposed by Holtz et al. (1995). This alternative procedure is to be used in conjunction with, and to complement, the detailed procedure presented in Sections A1.1-A1.9.

A3. Alternative Procedure for Determining Long-Term Allowable Strength

The goal of providing an alternative method is to foster widespread use of geosynthetic reinforced slopes and walls in transportation facilities. Specific objectives include providing:

- an easy-to-use method for determining design strengths;

- design engineers with a method to generically specify geosynthetic reinforcement with a defined default design strength that suppliers will be required to use, unless detailed testing and evaluation of their specific products has been completed;
- design tensile strengths that are conservative;
- design tensile strengths that are sufficiently conservative so that thorough testing and evaluation of geosynthetic materials by manufacturers and suppliers is still promoted;
- a method for use with conservative soil environment parameters.

These objectives and goals can be achieved by using a single overall default reduction factor (Φ_{do}) on ultimate tensile strength, to account for consistency of manufacture, creep, extrapolation, installation damage, chemical degradation, biological degradation and connections. The default reduction factor Φ_{do} should be based on engineering judgement. Testing shall be conducted to define the ultimate geosynthetic tensile strength. The default design tensile strength should be defined with the default reduction factor Φ_{do} and the reduction failure associated with ramification of failure Φ_n.

At first glance, the product of the default reduction factors recommended in Sections A1.2 – A1.9 could possibly be used. However, the product of the default reduction factors is too low and therefore it does not meet the objective of providing a reasonable and economical value. The reduction factors recommended in Sections A1.2 – A1.9 were developed for use when one or two reduction factors are undefined, along with other defined, reduction factors.

The default reduction factor Φ_{do} should be limited to projects where the soil environment meets the following requirements:

- granular soils (sands, gravels);
- $5 \leq pH \leq 9$;
- biologically inactive environments;
- maximum backfill particle size of 20 mm.

Other qualifiers on application of this default reduction factor is limiting use to projects where:

- maximum retaining walls height is 10 m;
- face element shall be a non-agressive environment for the geosynthetic;
- maximum reinforced slope height is 15 m;
- geotextile reinforcement meets AASHTO M288 (1990a) specification strength requirements for High Survivability Level, for separation applications;
- the manufacturer certifies that the supplied geosynthetic is intended for and fit to use as long-term soil reinforcement.

Use of this alternative allowable strength procedure for structurally faced GRS retaining walls does not eliminate the requirement of connection strength testing. Testing shall be conducted to define the ultimate, short-term connection strength.

The default long-term design connection strength should be defined with an appropriate reduction factor based on engineering judgement.

The design tensile strength is defined by the lower of the default design tensile strength and the default long-term design connection strength.

There does not appear to be any widely held consensus on the default reduction factors. Holtz et al. (1995) recommend the blanket default reduction factor $\Phi_{do} = 0.1$ on the ultimate geosynthetic tensile strength for all geosynthetic materials, and the default reduction factor of 0.17 on the short-term connection strength for all connection types. Other researchers believe that Holtz's reduction factors are inappropriate, not conservative enough, or too conservative and that the default factors should be related to material type, connection type, and loading conditions (i.e. static or seismic).

Blanket long-term use of a default reduction factor will penalise many current suppliers and limit economic benefit of geosynthetic-reinforced structures. Those manufacturers and suppliers who have conducted the extensive testing to document reduction factors should be allowed to use those factors. Exclusive use of a blanket default value will also severely impede further evolution of this technology.

A4. Soil–Reinforcement Interaction

A4.1 Introduction

The design soil–reinforcement interaction strength of the soil reinforcements shall be determined using the following equations:

$$T^*_{di,1} = T_{i,1}\,\Phi\,\Phi_n \qquad \text{(A5)}$$

$$T^*_{di,2} = T_{i,2}\,\Phi\,\Phi_n \qquad \text{(A6)}$$

where:

$T^*_{di,1}$ $T^*_{di,2}$ are design soil–reinforcement interaction strengths for pullout and direct shear respectively;

$T_{i,1}$ $T_{i,2}$ are ultimate soil–reinforcement interaction strengths for pullout and direct shear respectively;

Φ is uncertainty factor for soil–reinforcement interaction; it should be assessed by designer; appropriate range of values is given in Table A6 (AS DR 96405, SA 1996);

Φ_n is reduction factor associated with ramification of failure (see Table A5).

Table A6 Uncertainty factors for soil–reinforcement interaction (from SA 1996).

Failure Mode	Soil Conditions	Strength and Stability Load Cases	Serviceability Load Case
Pull out	Engineered fills	0.8	1
Sliding across reinforcement surface (direct shear)	Engineered fills	0.8	1
	Natural or in-situ soils	0.75	1

Two types of soil–reinforcement interaction coefficients or interface shear strengths must be determined for design: pullout coefficient and direct shear coefficient. Pullout coefficients are used in stability analyses to compute mobilised tensile force at the front and tail of each reinforcement layer in slopes and at the tail in walls. Direct shear coefficients are used to check factors of safety against outward sliding of the entire reinforced mass.

A4.2 Pullout Resistance

Design of GRS structures requires evaluation of the long-term pullout performance with respect to three basic criteria:

- Pullout capacity (the pullout resistance of each reinforcement should be adequate to resist the design working tensile force);
- Allowable displacement (the relative soil-to-reinforcement displacement required to mobilise the design tensile force should be smaller than the allowable displacement);
- Long-term displacement (the pullout load should be smaller than the critical creep load).

The pullout resistance of the reinforcement is mobilised through one or a combination of two basic soil-reinforcement intersection mechanisms. The two mechanisms by which load may be transferred between soil and geosynthetic are interface friction and passive soil resistance: geotextile pullout resistance is developed with an interface friction mechanism; and geogrid pullout resistance may be developed by both interface friction and passive soil resistance against transverse elements.

The load transfer mechanisms mobilised by a specific geogrid depends primarily on its structural geometry (composite reinforcement versus linear or planar elements, thickness of in-plane or out-of-plane transverse elements, and aperture dimension to grain-size ratio). The soil-to-reinforcement relative movement required to mobilise the design tensile force depends mainly upon the load transfer mechanism, the extensibility of the reinforcement material, and the soil type.

The long-term pullout performance (i.e. displacement under constant design load) is predominantly controlled by the soil's creep characteristics and the reinforcement material. Soil reinforcement systems will generally not be used with cohesive soils susceptible to creep. Therefore, creep is primarily an issue of the reinforcement type.

The basic aspects of pullout performance in terms of the major load transfer mechanism, relative soil-to-reinforcement displacement in granular (and low-cohesive) soils for generic extensible reinforcement types, are presented in Table A7 (from Christopher et al. 1989).

Table A7 Basic aspects of reinforcement pullout performance in granular and low cohesive soils for GRS structures (from Christopher et al. 1989).

Reinforcement Type	Major Load Transfer Mechanism	Displacement to Pullout	Long-Term Performance
Geogrids	Frictional + passive HD	Dependent on reinforcement extensibility (25 to 50 mm)	Dependent on reinforcement structure and polymer creep
Geotextiles	Frictional (interlocking) LD	Dependent on reinforcement extensibility (25 to 100 mm)	Dependent on reinforcement structure and polymer creep

Note: LD – low dilatancy effect, HD – high dilatancy effect

Pullout resistance of geosynthetic reinforcement is defined by the lower value of:

- the ultimate tensile load required to generate outward sliding of the reinforcement through the soil mass; or
- the tensile load which produces a 38 mm displacement.

Several approaches and design equations have been developed and are currently being used to estimate pullout resistance by considering frictional resistance, passive resistance, or a combination of both. The design equations use different interaction parameters, and therefore it is difficult to compare the pullout performance of different reinforcements for a specific application.

The ultimate pullout resistance $T_{i,l}$ of the reinforcement per unit width of reinforcement is given by:

$$T_{i,l} = F^* \alpha \sigma^*_v L_e C \qquad (A7)$$

where:

$L_e C$ is the total surface area (m^2) per unit width of the reinforcement in the resistant zone behind the failure surface;

L_e is the embedment or adherence length (m) in the resistant zone behind the failure surface (Figure 3.9 in these guidelines);

C is the reinforcement effective unit perimeter; C=2 for geogrids and geotextiles (dimensionless);

F* is the pullout resistance (or friction-bearing-interaction) factor (dimensionless) obtained from testing or by empirical methods (Appendix A4.3);

α is a scale effect correction factor to account for a non-linear stress reduction over the embedded length of highly extensible reinforcements, based on laboratory data (generally 0.6 to 1.0 for geosynthetic reinforcements);

σ^*_v is the resultant of all factored effective vertical stresses at the soil–reinforcement interface, including those due to the reinforced backfill self weight, sloping backfill, uniformly distributed concentrated surcharge loads (kN/m^2) (refer to Table 2.4 in these guidelines for load factors).

The pullout resistance factor F* can be most accurately obtained from pullout tests performed on the specific, or representative backfill to be used on the project. Refer to GRI Test Method GG5: Geogrid Pullout (1991c) and GRI Test Method GT6: Geotextile Pullout (1992b), as applicable, for pullout test procedures. Note that this test method produces pullout interaction coefficients that are classified as either short-term or long-term. Design of GRS structures for permanent applications requires use of long-term interaction coefficients. For pullout under seismic conditions, F* should be reduced to 80% of the static value.

Alternatively, F* can be derived from empirical or theoretical relationships developed for each soil–reinforcement interaction mechanism or provided from the reinforcement supplier. For any reinforcement, F* can be estimated using the general equation (Christopher et al. 1989), as follows:

F^* = Passive Resistance + Frictional Resistance

or

$F^* = F_q \ \alpha_\beta + K \ \mu^* \ \alpha_f$

where:

- F_q is the embedment (or surcharge) bearing capacity factor;
- α_β is a structural geometric factor for passive resistance;
- K is a ratio of the actual normal stress to the effective vertical stress; it is influenced by the reinforcement's geometry;
- μ^* is an apparent friction coefficient for the specific reinforcement;
- α_f is a structural geometric factor for frictional resistance.

Passive resistance is applicable only to geogrids, and not to geotextiles. The passive resistance portion of the above equation assumes long-term junction strength between the transverse and longitudinal ribs to ensure stress transfer. Long-term stress transfer is assured if the geogrid is creep-tested with the through-the-junction method per GRI:GG3a (1988c).

Long-term pullout interaction coefficients should be quantified for geogrids with one of the following:

1. quick, effective stress pullout tests and through-the-junction creep-testing of the geogrid per GRI:GG3a test method (1988c);
2. quick, effective stress pullout tests of the geogrid with severed transverse ribs;
3. quick, effective stress pullout tests of the entire geogrid structure if summation of shear strengths of the joints occurring in a 12-inch (304.8 mm) length of grid sample is equal to or greater than the ultimate strength of the grid element to which they are attached (AASHTO 1990b); or
4. long-term effective stress pullout tests of the entire geogrid structure.

Long-term pullout interaction coefficients should be quantified for geotextiles with:

5. quick, effective stress pullout tests.

Test Method (a) Controlled Strain Rate Method for Short-Term Testing, as in GRI:GG5 (1991c) and GRI:GT6 (1992b), is recommended for testing under conditions (1), (2), (3) and (5) above. Test method (d) Constant Stress (Creep) Method for Long-Term Testing as in GRI:GG5 (1991c) is recommended for condition (4) above.

Joint shear strength shall be measured in accordance with GRI:GG2 (1988b) and ultimate strength shall be measured with either GRI:GG1 (1998a) or ASTM D4595 (1994) for condition (3) above.

Long-term testing may also be required if cohesive soils are utilised, to define long-term effective stress (drained) pullout resistance. Procedures and results for long-term testing in cohesive soils have been presented by Christopher & Berg (1990). Their method is a combination of GRI:GG5 (1991c) and GRI:GT6 (1992b) methods, (c) Incremental Stress Method for Short-Term Testing and (d) Constant Stress (Creep) Method for Long-Term Testing.

A4.3 Direct Shear Resistance

The ultimate soil-geosynthetic interaction strength for direct shear per unit width of wall base is given by:

$$T_{i,2} = (\tan \rho)\ \alpha\ \sigma^*_v\ L_e \qquad \text{(A8)}$$

where:

α; σ^*_v; L_e are defined in Section A4.2;

ρ is soil–reinforcement interface friction angle mobilised along reinforcement.

Soil–geosynthetic ultimate direct shear resistance $T_{i,2}$ should be determined using test results obtained in accordance with GRI Test Method GS6: Interface Friction Determination by Direct Shear Testing (1991d). The test method requires project-specific soils to be placed at field densities above and below samples of the candidate geosynthetic, and then sheared along the plane of geosynthetic. The value of ρ can be expected to vary with normal stress and, therefore, the test should be carried out over a range of confining pressures expected for reinforcement layers in the proposed GRS structure.

A4.4 Empirical Methods for Soil-Reinforcement Interaction

Most speciality system suppliers have developed recommended pullout parameters for their products, when used in conjunction with the select backfill for GRS structures. The semi-empirical relationships summarised below are consistent with results obtained from laboratory and field pullout testing at a 95% confidence limit, and generally consistent with suppliers developed data (Elias 1997). Some additional economy can be obtained from site- or product-specific testing, where the source of the backfill in the reinforced volume has been identified during design.

In the absence of site-specific pullout testing data, it is reasonable to use these semi-empirical relationships in conjunction with the standard specifications for backfill to provide a conservative evaluation of pullout resistance.

For geosynthetic sheet reinforcement, the friction factor F* is commonly taken as:

$$F^* = (2/3) \tan \phi \qquad \text{(A9)}$$

For geogrid reinforcement, the friction factor is commonly taken as:

$$F^* = 0.8 \tan \phi \qquad \text{(A10)}$$

Where used in the above relationships, ϕ is the peak friction angle of the soil which, for GRS walls using select granular backfill, is taken as 34° degrees unless project-specific test data substantiates higher values. For GRS slopes, the ϕ angle of the reinforced backfill is normally established by test, as a reasonably wide range of backfills can be used. A lower bound value of 28° is often used.

The soil–geosynthetic interface friction angle for the assessment of the direct shear resistance should preferably be measured by means of interface direct shear tests. In the absence of direct shear test data, the interface friction factor (tan ρ) may be assumed on the basis of F* values for pullout resistance as given above.

Appendix B

Environmental Conditions & Durability of Geosynthetic Reinforcement

(extracts from FHWA-SA-96-072, Elias 1997)

Appendix B Environmental Conditions & Durability of Geosynthetic Reinforcement

(extracts from FHWA-SA-96-072 (Elias 1997))

B1. Degradation Mechanisms

Polymers consist of long chains of principally carbon atoms, with various branches and side groups. Under certain environmental conditions this structure can be attacked by oxidation promoted thermally, catalytically, or by ultraviolet light, by other forms of chemical attack including hydrolysis, by the combined effect of chemicals and mechanical load, or by micro-organisms. Most polymers used in geosynthetics contain additives and stabilisers that improve the resistance of the basic polymer. However, these additives themselves can be susceptible to leaching or to biological attack, ultimately leaving the polymer unprotected. In addition, the structure can be damaged during compaction or by subsequent abrasion. The principal results of these degradative mechanisms are loss of mechanical strength and changes in elongation properties. The potential degradation mechanisms and the available testing methods to quantify tensile strength losses and the role of additives/antioxidants in enhancing long-term, in-ground durability are briefly described below, based on research data by Elias (1990).

B1.1 Oxidation of Polyolefins: Polypropylene (PP) and High Density Polyethylene (HDPE)

The predominant degradation mechanism for most polymeric materials is chain scission, which is a polymeric reaction that breaks a bond on the backbone of a polymer chain, reducing the chain length and thereby reducing molecular weight. This in turn significantly changes the polymeric structure and material strength and elongation properties.

The oxidation process is initiated by heat, light (UV radiation), mechanical stress, catalyst residue from manufacturing remaining in the geosynthetic, or by reaction with impurities.

Geosynthetics intended for long-term use should be produced with antioxidants. Antioxidants are additives that interrupt the degradation process in different ways, depending on their structure. The two major classifications are:

- chain terminating primary antioxidants and
- hydroperoxide decomposing secondary antioxidants.

Primary antioxidants are often sterically hindered phenols. They react rapidly to terminate chain scission and protect the polymer chain. Secondary antioxidants are most effective at elevated temperatures, as during manufacture processing, and effectively protect both the polymer and the primary antioxidant. They would include

but not be limited to phosphite/phosphonite compounds. A new class of UV stabilisers, called sterically hindered amine light stabilisers (HALS), are very effective in imparting stability at the lower temperatures consistent with in-ground use.

Often, the protection obtained against oxidation by using a mixture of primary and secondary antioxidants in certain proportions is stronger than the sum of the protection effects obtained with individual compounds used separately. These synergistic mixtures are known as "master batch" and are proprietary to each producer. They can be varied to satisfy the intended usage and use regime.

For long-term protection against oxidation induced strength losses, the geosynthetic should be produced with primary antioxidants that are not consumed during manufacturing process.

B1.2 Hydrolysis of Polyester

Hydrolysis is the reverse reaction of the mixing (synthesis) of terephthalic acid and ethylene glycol, which forms polyethylene terephthalate (PET) and water. Since this is an equilibrium reaction, it is reversible. Therefore, it is possible for the PET to react with water and to revert to acid and glycol, which is a non-reversible process. In neutral environments (pH = 7), the reaction is initiated by the carboxyl end group (CEG) of the macro-molecule of PET and is relatively slow. In alkaline environments, the reaction is more rapid due to the more reactive OH-ion present compared to the water molecules as reagents in neutral (pH = 7) reactions. The effect of these reactions is to decrease the molecular weight (Mn) with a corresponding decrease in strength.

The rate of hydrolysis is primarily effected by:

- Carboxyl End Group (CEG) Concentration: these end groups are situated at the end of the molecular chains. The amount of CEGs in a particular PET product is dependent on the polymerisation process used. Typically, the high tenacity fibre produced for geogrid and high strength woven products have lower CEG numbers compared to fibre produced for non-woven geotextiles. Recent research has indicated that the hydrolysis rate of PET with higher CEG numbers proceeds faster under equivalent conditions.
- Molecular Weight: molecular weight directly affects the CEG concentration under the same polymerisation conditions. Therefore PET polymers with a higher molecular weight contain less CEG than those with lower molecular weight and are less susceptible to hydrolysis under equivalent conditions.
- Temperature: as with oxidation, hydrolysis proceeds at a faster rate with increasing temperature.
- pH Level: high levels of environmental alkalinity will cause fibre dissolution in addition to hydrolytic reactions.
- Relative Humidity: the rate of hydrolysis increases as relative humidity increases.

For long-term usage, PET products of high molecular weight (Mn) and low CEG will be least susceptible to strength losses due to hydrolysis. PET should not be used in highly alkaline environments characterised by pH greater than 9 without significant test data to document suitability.

B1.3 Stress Cracking

Semi-crystalline polymers such as high density polyethylene (HDPE) have a potential for stress cracking, which is a material failure caused by tensile stresses less than the short-term mechanical strength. The failure is characteristically brittle, with no elongation adjacent to the failure. This phenomenon has two phases: crack initiation and crack growth.

Environmental stress cracking (ESC) is the rupture of a polymer in a stressed state when exposed to a chemical environment. ESC tests are, therefore, differentiated from chemical resistance tests, in general, by the fact that the test specimens are exposed to a chemical environment while under stress.

Experience in the plastic pipe industry has shown that certain grades of polyethylene (PE) can experience stress cracking under certain conditions, and recent data has suggested a potentially similar behaviour for some grades of PE used in geomembranes. It follows, therefore, that a possibility of stress cracking in geogrids fabricated of PE exists. This issue is currently under study.

Under 'low' stresses at ambient temperatures, PE could fracture by slow crack growth given sufficient time. This mode of failure may limit the lifetime of and/or stress levels on PE used for reinforcement applications.

Because of the viscoelastic character of polyethylene, failure of this material is time-dependent and can be traced to either stress (creep) rupture or slow crack growth.

The maximum stress level under either mode of failure determines an allowable stress basis.

B1.4 UV Degradation

UV degradation occurs when geosynthetics are exposed to the influence of sunlight, rain, temperature, and oxygen. This type of degradation is caused primarily by the UV content of sunlight, which initiates the photo-oxidation process. The rate of degradation depends on the intensity of the relevant wave length and such additional factors as temperature, the presence of water and of certain atmospheric components such as ozone, nitrous oxides, hydrocarbons, etc. Other factors are the material structure and the rate at which degraded layers are removed by rain and wind and new surfaces are exposed to UV radiation.

For polyolefin geosynthetics, significant resistance to UV radiation is obtained with the addition of antioxidants such as phenolics, hindered-amine light stabilisers (HALS), and carbon black. These act as a screen to harmful portions of the light spectra. Once the geosynthetic is buried, the UV light-induced degradative process ceases because exposure to the UV source is terminated. Polyester is less affected by UV radiation because of the resistance of ester bonds to breakage.

Recent research has shown that the outdoor degradation process is a synergistic one in which both photo-oxidation caused by UV radiation and oxidation caused by elevated temperatures have an effect on the rate of degradation. The data indicated that the major effect is photo-oxidation, and therefore consideration of annual average energy incidence alone at a site may be sufficient to evaluate the effects of UV exposure.

The resistance to UV degradation is measured in the laboratory by ASTM D4355 for duration of up to 500 hours, or outdoors under ASTM D1435 (in ASTM 2000).

B1.5 Biological Degradation

Micro-organisms causing deterioration are found in a wide range of environmental conditions. These micro-organisms require a source of carbon for growth and obtain it from reactions degrading organic-based materials such as some of the polymers and additives that can be used in geosynthetics. Environmental factors controlling biodeterioration are temperature, humidity, pH, etc. In general, elevated temperatures, high humidity, and the absence of UV light are the required conditions.

Micro-organisms of importance in biodeterioration are bacteria, fungi, actinomycetes, algae and yeast. To grow, micro-organisms excrete enzymes into the surrounding medium. The enzymes degrade the host material by breaking down its large molecular units into much smaller units which serve as food for the micro-organisms. The net effect is a reduction in molecular weight, with ensuing deterioration of physical properties such as weight, strength and elongation.

High-molecular-weight, high-density polymers used for geosynthetics do not appear to be susceptible to direct enzymatic degradation by micro-organisms such as fungi and bacteria. Several biodegradability studies have shown little loss in strength of any typical polymers used in geosynthetics when exposed to biologically active environments (e.g. mildew) for periods of one year or more. Some indication is that very low molecular weight polymers can be consumed, especially in the presence of nutrient fillers such as starch.

No completely relevant test to measure the resistance of geosynthetics to biological effects in unstressed states is presently available. ASTM 3083 (in ASTM 2000) has been used and can be adopted on an interim basis. Statistically significant strength losses measured from this test should disqualify a candidate geosynthetic for long-term in-ground applications.

B1.6 General Chemical Dissolution

Exposure of polymeric materials to extremely aggressive chemicals may accelerate the oxidation/hydrolysis processes in conjunction with a process of dissolution which is a separation into component molecules by solution. Such regimes are not likely to be found in natural soils, but may be encountered in hazardous waste sites.

With regard to specific chemicals that may affect polymers, numerous chemical compatibility tables have been published by geosynthetic manufacturers. Several considerations are needed if using such tables. Test conditions, including the exposure time (always short, less than one year), temperature, chemical concentration (usually very high), and strength evaluation methods, vary between the tables. For any specific polymer, the plastic formulations may vary considerably, especially between industries. Also, the form of the material evaluated (e.g. strap, fibre, block) and the material additives will have affects. Therefore, these tables of compatibility are only useful in identifying specific regimes that are aggressive and therefore incompatible with specific geosynthetics.

The resistance of geosynthetics to chemical effects in unstressed states can be measured in accordance with:

- ASTM D5322 *Practice for Immersion Procedures for Evaluating the Chemical Resistance of Geosynthetics to Liquids*. This is a relatively short-term test (120 days) that should be modified for longer durations. A minimum of 9 months is recommended. The selection of immersion liquids is not specified.
- EPA 9090 *Compatibility Tests for Wastes and Membrane Liners* is a similar test at higher than ambient temperatures (50°C), conducted with specific chemicals considered to be present at the investigated site.

Statistically significant strength losses measured from these short-term tests should disqualify a candidate geosynthetic for long-term, in-ground applications where the chemical condition is anticipated. Neither test however provides a sound basis for determining a reduction factor for strength.

B2. Summary of Degradation Mechanisms

The principal mechanisms of polymeric degradation outlined in Section B1 decrease tensile strength and change elongation characteristics of geosynthetics. Geosynthetics are seldom degraded by a single environmental condition or mechanism, but often by a combination of synergistic actions or events. Table B1 presents a list of commonly identifiable degradation mechanisms, their source, effect and test procedures to identify and quantify by short-term laboratory tests their consequence on long-term strength.

A general approach to quantifying geosynthetic durability and making lifetime predictions requires that the following objectives be achieved:

- Identify the nature of potential degradation mechanisms within a particular site and functional use, by examining the mechanisms and sources listed in Table B1.
- Identify the nature of the physical and chemical effects that these mechanisms have on candidate geosynthetics and their properties.
- Identify the type of test data necessary.
- Evaluate the degradation from available test data.

Table B1 Commonly identifiable degradation mechanisms.

Mechanism	Source	Effect	Variables	Test Procedures
PHYSICAL				
Stress/pressure	Installation/ in use	Rupture, creep, stress cracking	Stress level, Backfill grain size	ASTM D5262 Stress Rupture Tests ASTM D5818
Water	Installation/ in use	Leaching of additives and plasticisers, hydrolysis	Temperature, pH	ASTM D5496 Immersion Testing
Solvents/ hydrocarbons	Installation: diesel, mineral oils. In use: contaminated sites	Leaching of additives, swelling and embrittlement, plasticisation	Temperature, Chemical concentration	EPA 9090 and Leaching tests
Biological	Installation/ in use: birds, animals, insects	Localised damage	Soil type and density	Not available
CHEMICAL				
Heat (+ oxygen)	In use: ambient environment temperature	Chain scission and oxidation; loss in tensile properties	Temperature, Oxygen content, Transition metals	Oven Ageing Tests at multiple temperatures
Light (+ oxygen)	Installation: UV exposure	Chain scission and oxidation; loss in tensile properties	Radiation Intensity, Temperature, Humidity	ASTM D4355
Water (pH)	In use: hydrolysis in acid, neutral & alkaline soils	Chain scission; loss in tensile properties	Temperature, pH concentration, Acid & alkali exposure	Hydrolysis testing at multiple temperatures
General chemicals	In use: exposure to natural soils & waste deposits	Degradation of polymer structure via oxidative/hydrolytic chain scission	Temperature, Concentration	Immersion tests EPA 9090, ASTM D5322
Micro-organisms	In use: bacterial & fungal attack in soils	Polymer chain degradation; loss in tensile properties	Temperature, pH soil type, Organism type	ASTM D3083

See ASTM (2000) for the ASTM standards.

This process can be illustrated in the following example of a permanent geosynthetic-reinforced retaining wall. The wall is to be built along a stream bank with a wrapped facing using local gravel as backfill. The soil is determined to have a pH value of 8.5. Based on this information, the probable ageing mechanisms can be identified as oxidation, hydrolysis, stress-cracking, UV degradation, and installation damage. Therefore, the design engineer should require the following geosynthetics to be considered for use:

- Polypropylene and polyethylene materials that contain an antioxidant package to inhibit oxidation.
- Polyester materials that have suitably high molecular weight and low CEG numbers to inhibit hydrolysis.
- Polyethylene materials manufactured from stress-crack resistance grade polymer.
- The material is UV-stabilised and is handled in a manner which minimises exposure to sunlight on the project site. Further, a UV-resistant coating, such as bitumen or shotcrete, should be applied to the wall face. Alternatively, a wood or concrete panel facing can be constructed.

Installation damage testing should be available for each candidate material that is consistent with the available gravel fill.

B3. Soil Environments which Accelerate Degradation

The soil environments that could accelerate degradation can be identified by their geological origins and composition. The physical regime (temperature and ground water) can accelerate the degradation.

Since not all polymers are subject to accelerated degradation in the same environments, it follows that an appropriate geosynthetic (polymer type) material can be chosen.

Soil contains both inorganic and organic chemicals with the inorganic material derived largely from the weathering of rocks and minerals, and the organic materials from plants, animals, and micro-organisms. In most soils, inorganic substances constitute the bulk of the soil material. In addition, the inorganic fraction contains acids and alkalis. Organic matter normally varies from less than 1% to 10% in soils that may be considered as highway construction fills. (However in separation or stabilisation applications, the geosynthetic may be placed directly over highly organic soils that may contain as much as 95% organic matter.)

The bulk of most soils is made up of inorganic matter that ranges from 60% to 99% of the total weight, averaging 95%. About 47% is oxygen, the most abundant element, with oxides being the most prevalent form.

The physical soil environment, which includes such factors as temperature and moisture, ranges widely.

Highway fills where reinforcement may be used are generally compacted near optimum moisture, which for many of the soils used would mean saturation percentages in excess of 65% and often near 95%. In the lower parts of GRS structures geosynthetics may be below the piezometric water levels and therefore under fully saturated conditions.

Inorganic chemicals that are believed to affect buried geosynthetics comprise mineral acids, alkalis, salts, certain bivalent metals, gases and water. The organic compounds in soils affecting durability of geosynthetics are believed to be organic acids and solvents.

Certain natural soil environments can contain significant amounts of chemical substances which are degradable. The following natural processes have been identified as sources of chemicals, with water, oxygen and water, or heat being the catalyst:

- *Sulphur Transformation* – producing sulphuric acid, sulphur dioxide, hydrogen sulphide and water.
- *Ammonification* – producing ammonia in gaseous and aqueous state, ammonia bearing salts.
- *Nitrification* and *denitrification* – producing nitrates, nitric acid, nitrogen dioxide and nitrous oxide.
- *Ferralitisation* – producing hydroxides/oxides and ionised forms of iron and aluminium.
- *Phosphorus Transformation* – producing phosphate and phosphoric acid.

These and other processes form aggressive soils such as acid-sulphate soils, organic soils, saline-alkali soils and calcareous soils. Other chemically reactive soils are ferruginous soils, which are high in iron content, and soils containing metals of manganese, copper, cobalt, and chromium (transition metals), as well as modified soils that may contain cement, lime, or de-icing salts. Cinders or slags may contain significant amounts of iron or other metals and sulphur.

As chemical durability of geosynthetics is mainly affected by pH of the surrounding environment, the following pHs are normally recommended for soil fill:

- $3 \leq pH \leq 9$ – acceptable;
- $pH \leq 3$ or $pH \geq 12$ – should not be used;
- $pH > 9$ – should only be used with supporting test data for a specific product.

The composition of some of the major natural soil groups identified as being potentially aggressive follows.

- **Salt-affected Soils**

Salt-affected soils are generally found in regions where precipitation is low and evaporation and transpiration rates are high. Sodic soils, a sub-group of salt-affected soils, are characterised by low permeability and thus restricted water flow. The pH of these soils is high, usually higher than 9 to 9.5, and the clay and organic fractions are dispersed because of the high levels of monovalent sodium and hydroxyl (OH) ions.

- **Acid-sulphate Soils**

Acid-sulphate soils are extremely acidic with pHs of less than 3.5 and even lower. Such low pH levels are indicative of the presence of strong acids in the soils and thus hydrogen is the main acidic culprit. The origin of these strong acids is often the oxidation of pyrite (iron sulphide), which is oxidised to sulphuric acid.

Generally, rock containing pyritic sulphur in excess of 0.5%, and containing little or no alkaline minerals, will produce pH of less than 4.5 which has considerable potential to produce sulphuric acid. These soils or rock are identified by the presence of noticeable yellow mottles attributable to pyrite oxidation.

Typically, acid-sulphate soils contain soluble levels or iron, manganese, copper, zinc, aluminium, and chlorides, although levels vary greatly. When excavated and in the presence of ground water, these soils produce sulphuric acid in significant quantity.

- **Calcareous Soils**

Calcareous soils are those that contain large quantities of carbonate such as calcite (calcium carbonate), dolomite (calcium-magnesium carbonate), and sodium carbonates and sulphates such as gypsum. These soils are characterised by alkaline pHs but are not saline. Under certain conditions, they are characterised by pH in the range of 9 to 10.

- **Organic Soils**

Most organic soils are water-saturated for most of the year unless they are drained. The major organic components are fulvic, humic, and humin materials. Organic acids are generally negligible. Biological degradation of geosynthetics in these environments is possible because of the presence of nutrients for bacteria and micro-organisms.

- **Soils Containing Transition Metals**

The literature has indicated adverse effects on polyolefin oxidation rates when transition metals such as copper, iron, chromium, manganese and cobalt are present. These metals are generally not found in the free state but rather as sulphides and oxides. Iron, the most abundant metal in the earth's crust, is not generally found in a free state but rather as sulphides such as pyrite (FeS_2) or ferrous silicates $(MgFe)_2SiO_4$, or from weathering in the form of oxides such as ferric oxide, hydrous oxide, ferrous carbonate and ferrous-ferric oxide, which characterise the "red earth" ferruginous soils.

The rest of these metals are rarely found in nature other than in spoil areas developed from mining operations or in fills constructed from these spoils. Their presence, therefore, would indicate the potential for accelerated degradation by oxidation of any polyolefin geosynthetic (PP, HDPE).

- **Modified Soils**

Modified soils such as cement- or lime-treated fills can be quite alkaline depending on the soil type and the quantity of additive. Sandy soils of low plasticity treated with cement are often characterised by a pH greater than 10. Lime modification (1-2% lime) of sodic soils is also likely to increase the pH to 10 or more. Lime stabilisation (5-10% lime) will always raise any soil pH above 12.

Table B2 gives an indication of anticipated resistance of various polymers to specific soil environments, and indicates that certain polymers should not be considered without site-specific testing for their long-term durability, or without specific knowledge of their additives or molecular structure.

It should be noted that polymers identified in Table B2 as "questionable use, exposure tests required" may perform satisfactorily if manufactured with specific antioxidants or additives to prevent degradation in that specific environment.

Table B2 Anticipated resistance of polymers to specific soil environments.

Soil Environment	Polymer Type		
	PET	HDPE	PP
Acid Sulphate Soils	NE	?	?
Organic Soils	NE	NE	NE
Saline Soils pH<9	NE	NE	NE
Calcareous Soils	?	NE	NE
Modified Soils (Lime-, cement-treated)	?	NE	NE
Sodic Soils, pH>9	?	NE	NE
Soils with Transition Metals	NE	?	?
NE = No effect ? = Questionable use, exposure tests required			

Appendix C

Information about GRS System or Component to be supplied by Manufacturer/Supplier

Appendix C Information to be Supplied by Manufacturer/ Supplier

The manufacturer/supplier must submit a package which satisfactorily addresses the following items.

For GRS systems and their components (including geosynthetic reinforcement):

1. GRS system or component development and the year it was commercialised.
2. GRS system or component supplier organisational structure, engineering and construction support staff.
3. Limitations and disadvantages of system or component.
4. Current capability to supply.
5. Representative list of previous and current projects/users including names, addresses and telephone numbers.
6. Sample material and control specifications showing material type, quality, certification, test data, acceptance and rejection criteria and placement procedures.
7. A documented field construction manual.
8. Design calculations and drawings (for performance type approach) or design recommendations in conformance with current engineering practice (for method type approach).
9. Unit cost.

For geosynthetic reinforcement the following additional information is required:

1. Polymer and additive composition of geosynthetic material, including polymer and additive composition of any coating materials.
2. Past practical applications of geosynthetic material use with descriptions and photos.
3. Limitations and disadvantages of geosynthetic material.
4. Sample long-term design strength and interaction values, and index property specifications.
5. Laboratory test results documenting creep performance over a range of load levels, for minimum duration of 10,000 hours.
6. Laboratory test results, along with comprehensive literature review, documenting extrapolation of creep data to a 75-year design life.
7. Field and laboratory test results, along with literature review, documenting reduction factors for installation damage.
8. Laboratory test results and extrapolation techniques, along with comprehensive literature review, documenting chemical resistance of all material components of the geosynthetic and reduction factors for chemical degradation.

9. For projects where a potential for biological degradation exists, laboratory test results, extrapolation techniques, along with comprehensive literature review, documenting biological resistance of all material components of the geosynthetic and reduction factors for biological degradation.
10. Laboratory test results documenting method and value of short-term strength, T_{ult}.
11. Laboratory test results documenting joint (seams and connection) strength and values for reduction factor for joints and seams.
12. Laboratory tests documenting long-term pullout interaction coefficients for various soil types or project site-specific soils.
13. Laboratory tests documenting direct sliding coefficients for various soil types or project site-specific soils.
14. Manufacturing quality control programme and data indicating minimum test requirements, test methods, test frequency, etc. Minimum conformance requirements shall be indicated.

Data shall be from a qualified registered laboratory. An in-house manufacturer or independent laboratory may be acceptable.

Geosynthetic materials can be submitted for consideration with reduction factors as recommended by the manufacturer/supplier (based on product-specific testing) or a combination of manufacturer/supplier recommended values and default values (refer to Appendix A) in regards to the design tensile strength.

Appendix D

Deformation Analysis Method
(reprint Cai & Bathurst 1996)

Seismic-induced permanent displacement of geosynthetic-reinforced segmental retaining walls

Z. Cai and R.J. Bathurst

Abstract: This paper describes the application of conventional displacement methods to estimate seismic-induced permanent displacements of geosynthetic-reinforced segmental retaining walls constructed on firm foundations. Permanent displacements associated with three sliding mechanisms are investigated: (1) external sliding along the base of the total wall structure; (2) internal sliding along a reinforcement layer and through the facing column; and (3) block interface shear between facing column units. A pseudostatic method based on the Mononobe-Okabe earth pressure theory is used to determine the value of critical acceleration associated with each potential failure mechanism. Newmark's sliding block displacement method and a number of empirical methods are briefly summarized and can be used to estimate the permanent displacements of segmental retaining walls. An example is given to illustrate the application of the methods presented.

Key words: segmental retaining walls, geosynthetics, seismic, Newmark, sliding block, displacement methods.

Résumé : Cet article décrit l'application des méthodes conventionnelles de déplacement pour estimer les déplacements permanents induits par des séismes dans les murs de soutènements segmentaires armés de géosynthétiques construits sur fondations compactes. Des déplacements permanents associés à trois mécanismes de glissement sont étudiés : (1) un glissement vers l'extérieur le long de la base de l'ensemble de la structure du mur; (2) un glissement interne le long d'une couche d'armature et à travers le parement; et (3) un cisaillement à l'interface de bloc entre les unités du parement juxtaposées. Une méthode pseudo-statique basée sur la théorie de pression des terres de Mononobe-Obabe est utilisée pour déterminer la valeur de l'accélération critique associée avec chaque mécanisme de rupture potentielle. La méthode de déplacement de blocs glissants de Newmark et un nombre de méthodes empiriques sont résumées brièvement et peuvent être utilisées pour estimer les déplacements permanents des murs de soutènement segmentaires. Un exemple est donné pour illustrer l'application des méthodes présentées.

Mots clés : murs de soutènement segmentaires, géosynthétique, séismique, Newmark, bloc glissant, méthodes de déplacement.

[Traduit par la rédaction]

Introduction

The term segmental retaining wall (SRW) has been recently adopted by the National Concrete Masonry Association (NCMA) in North America to identify soil retaining wall structures built with a hard facing comprising a column of dry-stacked masonry or wet cast modular concrete units (Simac et al. 1993; Bathurst et al. 1993*a*). These walls are often reinforced with geosynthetic layers to achieve greater heights. An example structure is illustrated in Fig. 1.

The dry-stacked (mortarless) concrete blocks are discrete units that transmit shear through interface friction, concrete keys, mechanical connectors, or a combination of these methods. The interfaces between the dry-stacked facing units result in potential failure planes through the facing column, and this requires that stability calculations be carried out to estimate interface shear forces and to compare these forces with available shear capacity. In addition, the connection between the reinforcement layers and the facing column is typically formed by extending the reinforcing layers along the interface between facing units to the front of the wall. The connection detail must also be evaluated for satisfactory design capacity (Bathurst and Simac 1993). A summary of the state of practice in North America with respect to geosynthetic-reinforced soil segmental retaining walls has been given by Bathurst and Simac (1994).

A large number of geosynthetic-reinforced segmental retaining wall structures have been built in seismically active areas on the west coast of North America. Despite concerns regarding the stability of the dry-stacked facing column during a seismic event (e.g., Allen 1993), these structures have performed well during earthquakes in recent years (Eliahu and Watt 1991; Collin et al. 1992; Sandri 1994; Bathurst and Cai 1995). Nevertheless, the guidelines published by the NCMA are restricted to routine structures in which seismic loading is not a concern. In an earlier paper (Bathurst and Cai 1995), the authors have extended the analysis and design methodologies published by the

Received April 15, 1996. Accepted August 13, 1996.

Z. Cai and R.J. Bathurst.[1] Department of Civil Engineering, Royal Military College of Canada, Kingston, ON K7K 5L0, Canada.

[1] Author to whom all correspondence should be addressed.

Fig. 1. Example geosynthetic-reinforced soil segmental retaining wall cross section (after Simac et al. 1991).

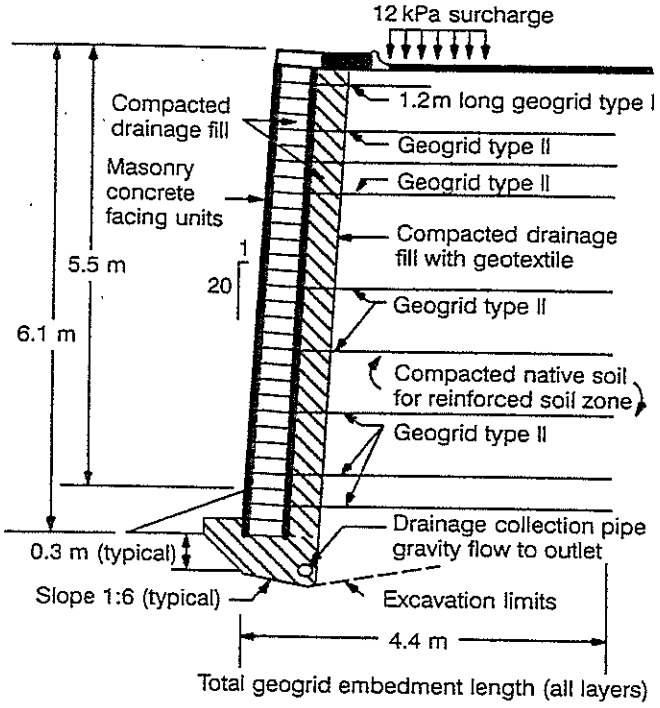

Fig. 2. Modes of failure: (*a–c*) external; (*d–f*) internal; (*g–i*) facing (adapted from Simac et al. 1993).

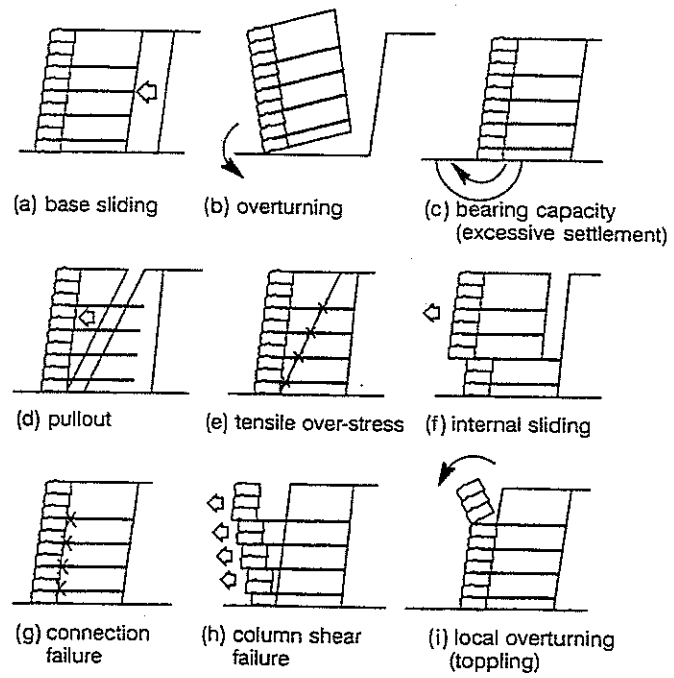

NCMA to include a limit-equilibrium, pseudostatic approach for the stability analyses of these structures under seismic loading. The approach uses Mononobe-Okabe (M-O) earth pressure theory. The authors have demonstrated that a consistent application of M-O theory may result in the requirement to increase the number and length of the reinforcement

Fig. 3. Interface shear-capacity envelopes for segmental wall units with and without geosynthetic inclusions (peak load criteria).

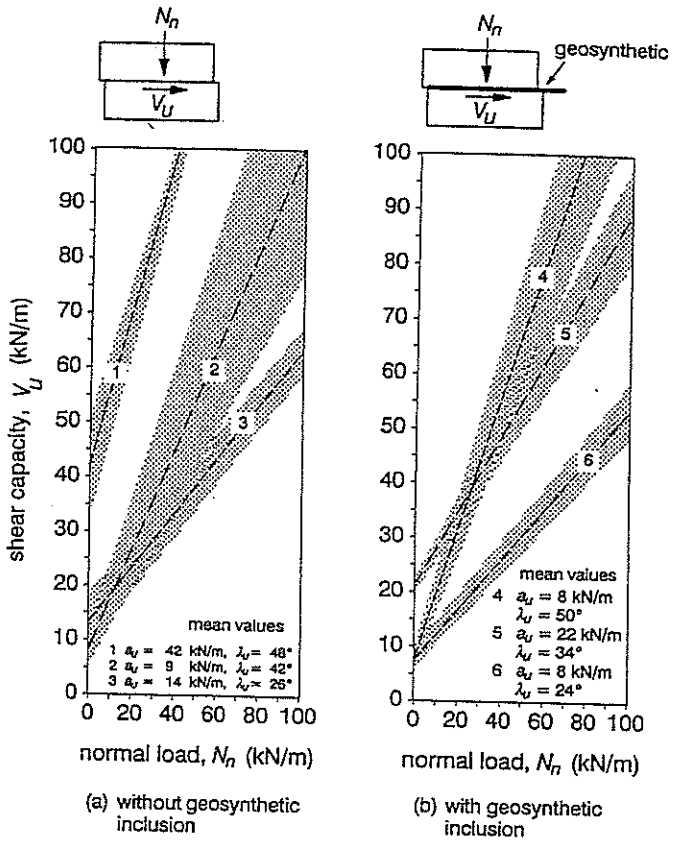

layers close to the wall crest to ensure satisfactory performance during an earthquake (i.e., compared with values based on static analyses). However, as with all limit-equilibrium methods of analyses, the pseudostatic approach cannot explicitly include wall deformations. This is an important shortcoming, since failure of these soil retaining wall systems may be manifested as unacceptable movement without structural collapse.

Displacement methods have been proposed in the literature to predict the permanent horizontal displacements that may accumulate at the base of conventional gravity retaining structures during a seismic event (e.g., Richards and Elms 1979; Whitman 1990). Geosynthetic-reinforced soil *segmental* retaining walls can be considered to be a special class of gravity wall structures. The current paper proposes a methodology for the stability analysis of three potential failure modes for geosynthetic-reinforced soil segmental retaining walls within the framework of conventional displacement (sliding block) methods and demonstrates the approach by an example.

Potential sliding failure modes

General

Potential failure modes for geosynthetic-reinforced soil segmental retaining walls are summarized in Fig. 2. Sliding-block methods can be applied to those failure

mechanisms associated with horizontal sliding. Hence in this paper the following failure mechanisms are considered: (1) external sliding along the base of the total structure, which includes the reinforced soil mass and the facing column (Fig. 2*a*); (2) internal sliding along a reinforcement layer and through the facing (Fig. 2*f*); and (3) block interface shear between facing column units (Fig. 2*h*).

Interface shear capacity

Resistance to internal sliding and block interface shear will be influenced by the magnitude of interface shear capacity available between the segmental block units. The interface shear capacity (with and without a geosynthetic inclusion) can only be established by full-scale direct shear testing. A large-scale test apparatus to quantify interface shear capacity under varying normal load has been described by Bathurst and Simac (1994) and a test protocol based on this apparatus has been adopted by the NCMA (Simac et al. 1993) to obtain shear-capacity data for design. The interface shear capacity for a segmental facing unit system can be conveniently described using a Mohr-Coulomb-type law:

$$[1] \qquad V_u = a_u + N_n \tan \lambda_u$$

where V_u is the interface shear capacity (kN/m), a_u is the minimum available shear capacity (kN/m), N_n is the normal load (kN/m), and λ_u is the equivalent interface friction angle (degrees). Shear-capacity envelopes for design are based on peak shear-capacity values and (or) shear-capacity values recorded after a relative displacement criterion of 2% of the height of the unit, according to recommendations by the NCMA. The 2% displacement criterion is used in the design of critical structures to ensure that the cumulative displacement at the wall crest will not exceed 2% of the height of the wall. Results of shear testing have shown that the presence of a geosynthetic inclusion within the shear interface may reduce available interface shear capacity (Bathurst and Simac 1994).

Shear-capacity envelopes for a wide range of segmental retaining wall systems on the market today are shown in Fig. 3 and are taken from the results of tests carried out by the authors on 20 different combinations of segmental blocks and geogrid reinforcement materials. Fig. 3*a* shows ranges of peak shear-capacity envelopes for block to block interfaces without geosynthetic inclusions and, Fig. 3*b* shows ranges for tests carried out with typical reinforcing geogrids located within the block to block interface. The three groups of data in each figure have been established based on similar trends in the regressed Mohr-Coulomb failure envelopes described by eq. 1.

Dynamic active earth pressure and its distribution

To calculate the critical acceleration associated with any potential mode of horizontal displacement, the dynamic active earth force and its distribution acting on the translating body are required.

Calculation of dynamic earth forces

The Mononobe-Okabe (M-O) earth pressure theory (Okabe 1926) is adopted to calculate dynamic active earth forces. The soil is assumed to be homogeneous, unsaturated, and cohesionless. The dynamic active earth force P_{AE} imparted by the soil mass acting at the back of a planar retaining wall structure is calculated by (Seed and Whitman 1970)

$$[2] \qquad P_{AE} = \frac{1}{2}(1 \pm k_v)K_{AE}\gamma H^2$$

where k_v is a vertical seismic coefficient, γ is the unit weight of the retained soil, and H is the height of the inclined surface against which P_{AE} acts. The parameter K_{AE} in eq. 2 is the M-O active dynamic earth pressure coefficient and can be calculated by

$$[3] \qquad K_{AE} = \frac{\cos^2(\phi + \psi - \theta)}{\cos(\theta)\cos^2(\psi)\cos(\delta - \psi + \theta)\left[1 + \sqrt{\dfrac{\sin(\phi + \delta)\sin(\phi - \beta - \theta)}{\cos(\delta - \psi + \theta)\cos(\psi + \beta)}}\right]^2}$$

where ϕ is the angle of internal friction of the retained soil, ψ is the wall inclination angle from vertical (typically 3–15° for segmental retaining walls), δ is the mobilized friction angle at the interface between the retaining structure and the retained soil, β is the backslope angle (from horizontal), and θ is the seismic inertial angle, given by

$$[4] \qquad \theta = \tan^{-1}\frac{k_h}{1 \pm k_v}$$

where parameters k_h and k_v are horizontal and vertical seismic acceleration coefficients, respectively, expressed as fractions of the gravitational constant, g.

The choice of positive or negative values of the vertical acceleration coefficient k_v will influence the magnitude of dynamic earth forces calculated using eqs. 2–4. In addition, the resistance terms in factor of safety expressions introduced later in the paper will be influenced by the choice of sign for k_v. An implicit assumption in many papers on pseudostatic design of conventional gravity wall structures is that the vertical component of seismic (inertial) body force acts upward (i.e., $-k_v$). This case has been shown to produce the most critical factors of safety for horizontal sliding mechanisms of failure for typical reinforced segmental retaining walls subjected to seismic loading (Bathurst and Cai 1995). Thus, in the analyses to follow, the vertical seismic force is assumed to act upward when $k_v \neq 0$.

For the purpose of parametric analyses reported later in the paper, the peak value of vertical ground acceleration is assumed to vary linearly with the peak value of horizontal

Fig. 4. Calculation of dynamic (total) earth pressure distribution under seismic loading (after Bathurst and Cai 1995).

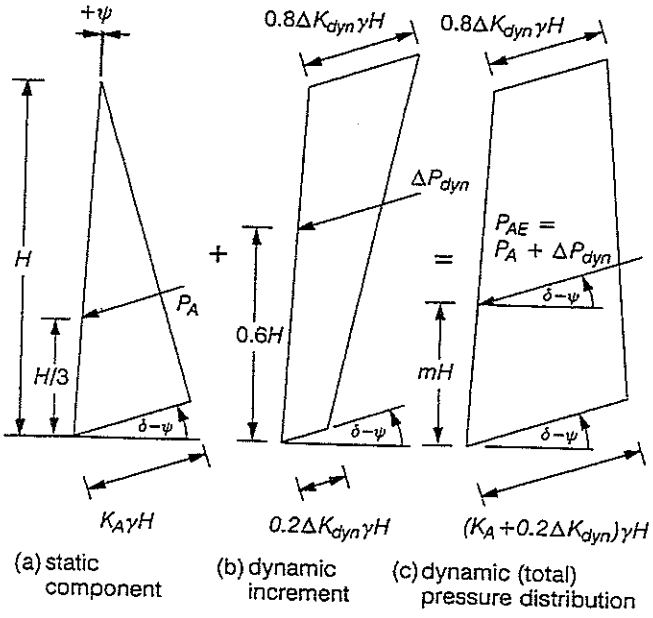

Fig. 5. Free body diagram of composite gravity mass comprising facing column and reinforced soil zone for base-sliding analysis.

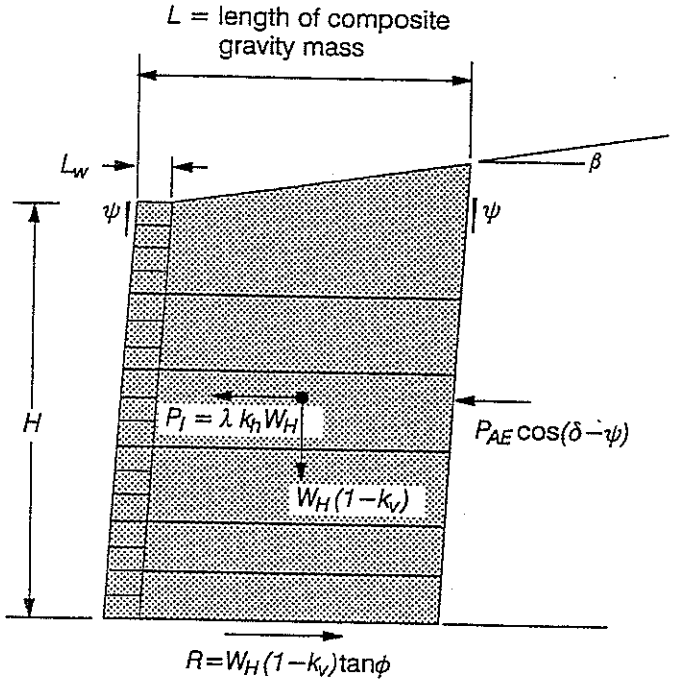

ground acceleration. A conservative estimate (i.e., conservative for design) is $k_v = -2k_h/3$ based on seismic data recorded in the Los Angeles area (Stewart et al. 1994). The ratio of the peak ground acceleration components is assumed to persist through the composite soil mass and retained soil. This condition is likely an extreme case. In fact, a review of the literature by Bathurst and Cai (1995) reveals that common practice in North America is to assume that $k_v = 0$ for the design of conventional earth retaining structures. Finally, both horizontal and vertical accelerations are assumed to be uniform at all locations within the retained soil mass, reinforced soil mass, and the facing column.

Equations 2–4 are an analytical solution to the classical Coulomb wedge problem that is modified to include the inertial forces acting on the failure wedge. The admissible range of interface friction angle is $0 \leq \delta \leq \phi$ in the Coulomb wedge analysis. The reader is referred to the paper by Bathurst and Cai (1995) for a discussion on the selection of δ values for external, internal, and facing column stability modes of failure.

The total active earth force P_{AE} calculated according to eqs. 2 and 3 can be decomposed into two components representing the static earth force P_A and the incremental (dynamic) earth force ΔP_{dyn} due to seismic effects. Hence,

$$[5] \qquad P_{AE} = P_A + \Delta P_{dyn}$$

or

$$[6] \qquad (1 - k_v)K_{AE} = K_A + \Delta K_{dyn}$$

where K_A is the static active earth pressure coefficient calculated using the Coulomb earth pressure theory, and ΔK_{dyn} is the incremental dynamic active earth pressure coefficient. The dynamic earth force P_{AE} acts outward and is inclined at an angle of $(\delta - \psi)$ from the horizontal.

Only the horizontal component of P_{AE}, i.e., $P_{AE}\cos(\delta - \psi)$, is used in the analyses to follow in order to simplify stability calculations and to be consistent with the convention adopted in the NCMA guidelines (Simac et al. 1993). This assumption results in a conservative estimate (for design) of the dynamic factors of safety and critical accelerations for the three translational modes of failure investigated in the paper.

Based on a review of the literature reported by Bathurst and Cai (1995) that is focused on conventional gravity structures, the distributions for static and dynamic increment of active earth pressures are assumed to be those illustrated in Fig. 4. The normalized point of application of the total earth pressure is a function of the magnitude of dynamic increment and varies over the range $1/3 \leq m \leq 0.6$, where m is the ratio of moment arm of dynamic active earth force to wall height. Steedman and Zeng (1990) used a pseudo-dynamic approach to show that the resultant total earth pressure against cantilever retaining walls with a fixed base acts above $H/3$. The assumed pressure distributions adopted in the current study are identical to those recommended for the design of flexible anchored sheet pile walls under seismic loads (Ebling and Morrison 1993).

It should be noted that possible amplification of horizontal accelerations through the height of the structure is not directly considered in the approach used here. The results of finite element modelling of reinforced soil walls by Segrestin and Bastick (1988) and Cai and Bathurst (1995) and some limited half-scale experimental work (Chida et al. 1982) have shown that the average acceleration of the composite soil mass may be equal to or greater than peak (site) horizontal acceleration (a_m) depending on a

number of factors such as magnitude of peak ground acceleration, predominant modal frequency of ground motion, duration of motion, height of wall, and stiffness of the composite mass. Based on their pseudodynamic model, Steedman and Zeng (1990) have shown that the effect of horizontal amplification with height above the base of conventional gravity wall structures results in an increase in total earth pressure that is qualitatively similar to an increase in k_h applied uniformly through the depth of retained soil. It can also be argued that the dynamic earth pressure increment distribution illustrated in Fig. 4 may indirectly account for amplification of horizontal ground accelerations, since the centre of gravity of this distribution is above one-third of the wall height as described earlier.

A detailed discussion on strategies to select an appropriate value of peak ground acceleration based on ground acceleration records is beyond the scope of this paper. Bathurst and Cai (1995) have concluded that there is no consensus view on how to select a design value for k_h in pseudostatic earth pressure calculations. For example, Whitman (1990) reports that values of k_h from 0.05 to 0.15 are typical for the design of conventional gravity wall structures and these values correspond to one-third to one-half of the peak acceleration of the design earthquake. Bonaparte et al. (1986) used $k_h = 0.85\ a_m/g$ to generate design charts for geosynthetic-reinforced slopes under seismic loading using the M-O method of analysis. Current Federal Highway Administration (FHWA) guidelines (Christopher et al. 1989) use an equation proposed by Segrestin and Bastick (1988) that relates k_h to a_m according to $k_h = (1.45 - a_m/g) \times a_m/g$ and results in $k_h > a_m/g$ for $a_m < 0.45g$. It appears that, in practice, the selection of k_h for design is based on engineering judgement, experience, and, in some instances, local regulations.

Determination of critical accelerations for SRW structures

Permanent displacements are assumed to accumulate each time the critical acceleration, a_c ($a_c = k_c g$, where k_c is the critical horizontal seismic coefficient), associated with each of the three displacement mechanisms described earlier is exceeded by the horizontal input (ground) acceleration $a(t)$. This section of the paper describes the analytical procedures used to determine critical acceleration values.

Critical acceleration against external sliding

A free body diagram of the composite monolithic gravity mass consisting of the facing column and the reinforced soil zone is shown in Fig. 5. Horizontal sliding of the entire mass is assumed to occur through the soil along the base of the gravity mass. The destabilizing forces are the dynamic active earth force (P_{AE}) acting at the back of the reinforced soil zone and the seismic inertial force (P_I) acting at the centre of gravity of the composite mass. The resisting force is the frictional resistance (R) mobilized along the sliding boundary at the base of the composite mass. The dynamic factor of safety against base sliding of the mass is calculated by

$$[7a] \qquad FS_{dyn} = \frac{R}{P_{AE}\cos(\delta - \psi) + P_I} = \frac{\left(\frac{L - L_w}{H}a_2 + \frac{L_w}{H}\right)(1 - k_v)\tan\phi}{\frac{1}{2}K_{AE}(1 - k_v)a_1^2\cos(\delta - \psi) + k_h\lambda\left(\frac{L - L_w}{H}a_2 + \frac{L_w}{H}\right)}$$

where

$$[7b] \qquad a_1 = 1 + \frac{L - L_w}{H}\tan\beta$$

$$[7c] \qquad a_2 = 1 + \frac{L - L_w}{2H}\tan\beta$$

and where L is the width of the composite mass from the front face of the wall to the back of the reinforced soil zone, L_w is the width (toe to heel) of the facing column, λ is the inertial force reduction factor for gravity mass, and a_1 and a_2 are geometric constants that account for the effect of the backslope angle (β) on the height and weight of the reinforced soil zone. The dimension L is taken as the minimum length of the primary reinforcement layers and does not include any additional length for those uppermost reinforcement layers that may be extended to prevent pullout of these layers close to the top of the wall. In other words, the reinforced gravity mass is assumed to be essentially a trapezoid with parallel front and back surfaces. To simplify eq. 7*a*, the unit weight of the facing blocks is assumed to be identical to that of the soil. Negligible error is introduced by this assumption, since for typical walls $L_w << L$.

Parameter λ in eq. 7*a* is an empirical value that is used to reduce the magnitude of the horizontal inertial force $k_h W_H$, where W_H is the total weight of composite mass. Parameter λ is taken to be less than unity in order to account for the short duration of the peak ground motion and the expectation that the inertial forces induced in the sliding mass and the retained soil zone are not likely to reach peak values simultaneously during a seismic event. A value of $\lambda = 0.6$ is adopted in the analyses to follow and is the same value recommended by the FHWA for geosynthetic-reinforced soil walls (Christopher et al. 1989) and for reinforced earth walls that use steel reinforcement strips (RECO 1991; Segrestin and Bastick 1988).

Solutions to eq. 7*a* are presented in Fig. 6 using two sets of input parameters. The critical horizontal acceleration coefficient (k_c) for any given set of input parameters corresponds to the value of k_h that gives $FS_{dyn} = 1.0$.

Example solutions for the critical acceleration coefficient (k_c) for a range of soil friction angles are shown in Fig. 7. The data in Fig. 7 indicate that the value of k_c for base sliding increases rapidly with an increase in the magnitude of friction angle (ϕ) of the soil and is reduced with increasing

Fig. 6. Influence of horizontal acceleration coefficient k_h, soil friction angle ϕ, and backslope angle β on factor of safety against base sliding of composite gravity mass.

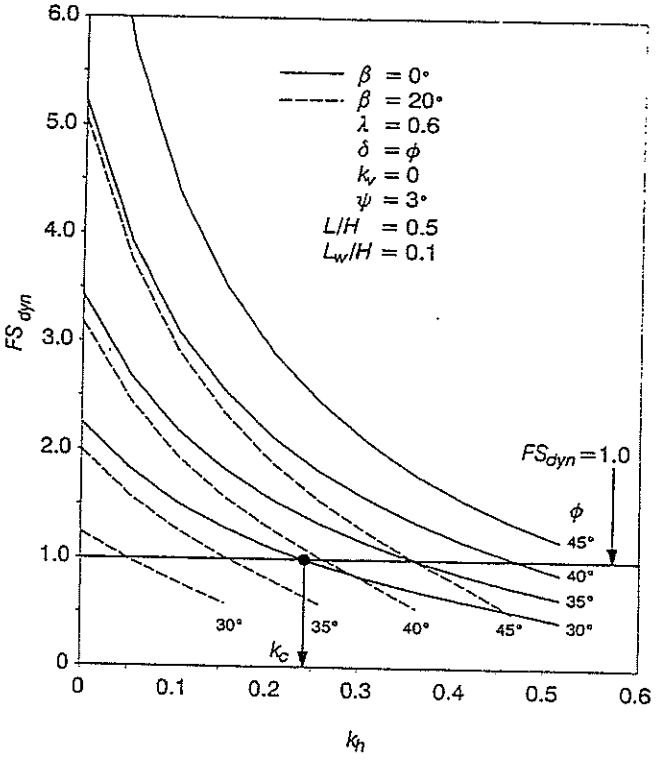

Fig. 7. Critical acceleration coefficient k_c for base sliding of composite gravity mass versus soil friction angle ϕ, vertical acceleration coefficient k_v, backslope angle β, and reinforcement ratio L/H.

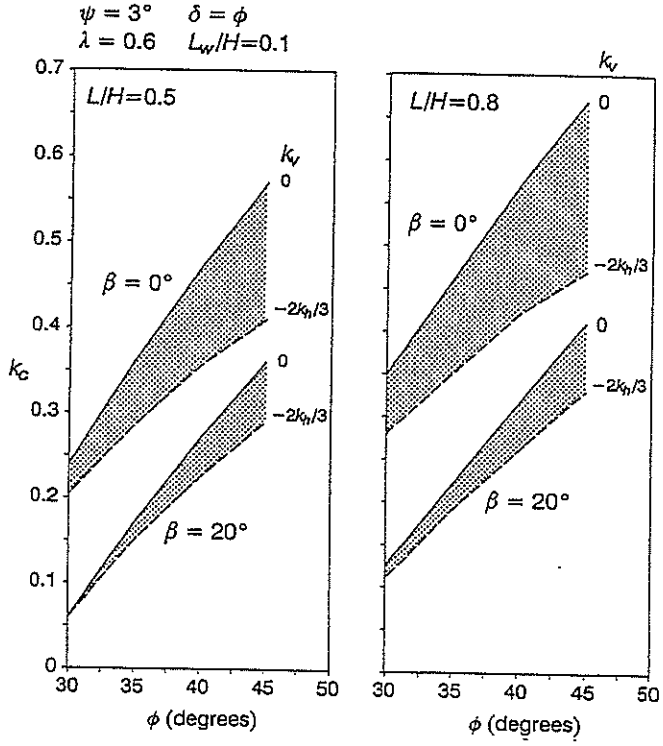

backslope angle (β). For example, letting $\beta = 0$, $L/H = 0.5$, and $k_v = 0$ results in values of k_c that increase from 0.24 to 0.57 as ϕ increases from 30 to 45°. For the same input parameters and $\beta = 20°$, the value of k_c increases from 0.06 to 0.36. The effect of increasing the reinforcement ratio (L/H) is to increase the value of the critical acceleration coefficient (k_c). For a soil friction angle $\phi = 35°$, $\beta = 0°$, and $k_v = 0$, an increase in the L/H ratio from 0.5 to 0.8 (60% increase) results in an increase in the value of k_c from 0.36 to 0.46 (30% increase). The data also show that for decreasing values of k_v (i.e., increasing magnitude of upward acceleration of the sliding mass) there is a resulting decrease in the value of the critical horizontal acceleration coefficient (k_c).

Critical acceleration against internal sliding along soil–geosynthetic interface

The free body diagram for internal sliding is shown in Fig. 8. Internal sliding of a segmental retaining wall refers to horizontal sliding of a portion of the reinforced soil mass along a soil–geosynthetic interface and through the facing column at a depth z below the crest of the wall.

The destabilizing forces are the dynamic active earth force (P_{AE}) acting at the back of the sliding soil mass plus the inertial force $P_I = k_h \lambda W_z$. Here, $W_z = W_s + W_w$ is the total weight of the sliding mass due to the reinforced soil weight (W_s) and weight of the facing column (W_w). The inertial force P_I is assumed to act at the centre of gravity of the sliding mass above the soil–geosynthetic interface. The resisting force comprises two components: one component is due to the resistance R_s mobilized along the soil–geosynthetic sliding interface, calculated as

$$[8] \qquad R_s = W_s(1 - k_v)\tan \phi_{ds}$$

where ϕ_{ds} is the soil–geosynthetic interface friction angle; the second component is due to the shear resistance developed at the block–geosynthetic interface within the wall facing at the same depth. The expression for interface shear capacity (eq. 1) can be modified to account for vertical facing inertial forces (upward) as follows:

$$[9] \qquad V_u = a_u + W_w(1 - k_v)\tan \lambda_u$$

Thus, the dynamic factor of safety against internal sliding can be calculated as

$$[10a] \qquad FS_{dyn} = \frac{V_u + R_s}{P_{AE}\cos(\delta - \psi) + P_I} = \frac{\dfrac{a_u}{\gamma z^2} + \left(\dfrac{L - L_w}{z} c_2 \tan \phi_{ds} + \dfrac{L_w}{z}\tan \lambda_u\right)(1 - k_v)}{\dfrac{1}{2}K_{AE}(1 - k_v)c_1^2 \cos(\delta - \psi) + k_h\lambda\left(\dfrac{L - L_w}{z}c_2 + \dfrac{L_w}{z}\right)}$$

Fig. 8. Free body diagram of sliding mass along a soil–geosynthetic interface and through the facing column at depth z below crest of wall.

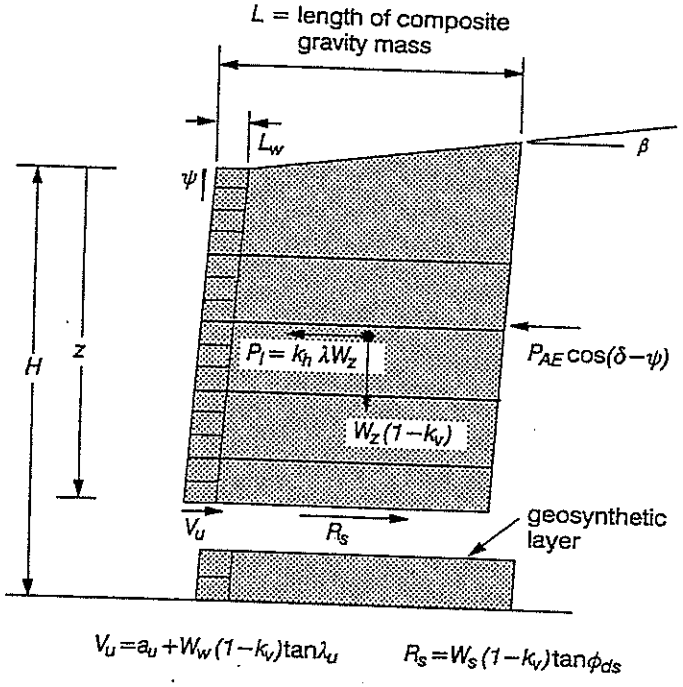

where

$$[10b] \quad c_1 = 1 + \frac{L - L_w}{z}\tan\beta$$

and

$$[10c] \quad c_2 = 1 + \frac{L - L_w}{2z}\tan\beta$$

For a given set of wall parameters, the above equation can be solved iteratively to find the critical acceleration coefficient against internal sliding, which is the value of k_h corresponding to $FS_{dyn} = 1.0$ in eq. 10*a*. Solutions to eq. 10*a* are illustrated in Fig. 9 for an example structure that has a height $H = 6$ m and five equally spaced reinforcement layers. The shear-capacity parameters used in Fig. 9 are interpreted from Fig. 3*b* for group 6 data representing relatively poor block–geosynthetic shear-capacity systems. As may be expected, Fig. 9 shows that the deepest interface layer is the most critical layer for internal sliding. For the shear-capacity parameters used, the smallest critical acceleration coefficient for internal sliding is $k_c = 0.38$ for $k_v = 0$, and $k_c = 0.31$ for $k_v = -2k_h/3$. As in the base sliding case, the effect of combined horizontal and vertical acceleration ($k_v = -2k_h/3$) is to reduce the magnitude of the critical horizontal acceleration coefficient.

Typical solutions for the critical acceleration coefficient (k_c) for internal sliding of the same example wall are shown in Fig. 10 using average shear-capacity values for the three groups of block–geosynthetic systems shown in Fig. 3*b*. The data in Fig. 10 indicate that, despite the large differences in shear capacity for the three data groups, the differences in the corresponding values of k_c are small. For example, at the deepest layer ($z/H = 0.9$), $k_c = 0.38$ using group 6 shear data and $k_c = 0.43$ using group 4 shear data.

Fig. 9. Influence of horizontal acceleration coefficient k_h and normalized depth of sliding interface z/H on factor of safety against internal sliding.

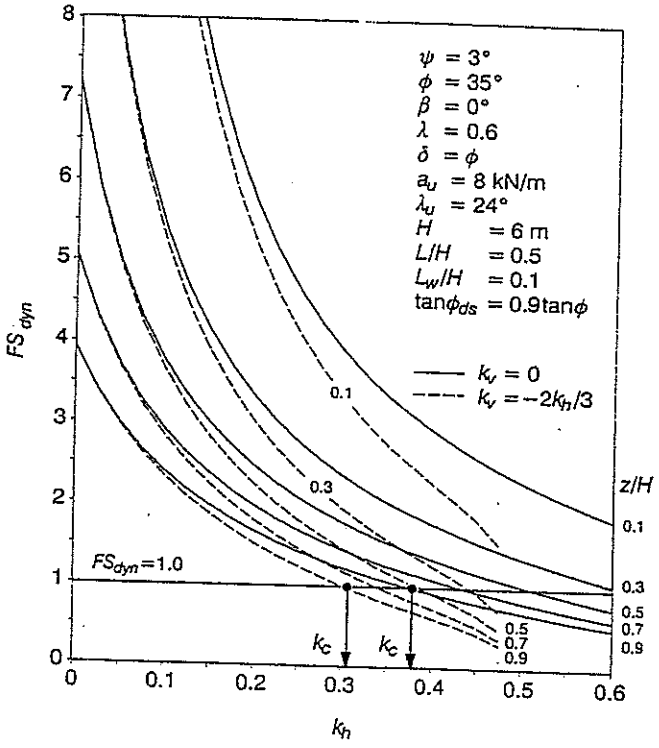

An implication to seismic design is that for typical facing units on the market today, available facing shear capacity is not critical in the design of geosynthetic-reinforced segmental retaining walls against internal sliding modes of failure. Although not demonstrated, the magnitude of the coefficient of direct sliding ($\tan\phi_{ds}$) has a more critical influence on k_c than facing interface shear capacity. The reason is clearly due to the typically small ratio of L_w/L in most reinforced segmental retaining wall systems.

Critical acceleration against block interface shear through facing column

Sliding at block–geosynthetic or block–block interfaces may occur when the shear capacities at these interfaces are exceeded. The influence of interface shear transmission on facing column stability can be analyzed by treating the facing column as a beam in which the integrated lateral pressure (i.e., distributed load illustrated in Fig. 4) must equal the sum of the reactions (forces in reinforcement layers). The calculation of interface shear force under dynamic loading must also include the effect of the wall inertia. The general approach is illustrated in Fig. 11. The total force carried by reinforcement layers above interface j is calculated as the area *ABCD* of the lateral earth pressure distribution plus the facing column inertial force over the same height. The out-of-balance force (interface shear force) at interface j is equal to the sum of the incremental column inertial force $k_h \Delta W_w^j$ plus the force due to area *CDEF* in the figure. The partitioning of forces illustrated in the figure is a direct result of the contributory-area

approach used to assign tensile loads to reinforcement layers in conventional static analyses (Christopher et al. 1989; Simac et al. 1993; Bathurst and Simac 1994). The locally maximum interface shear forces, and hence the most critical acceleration against relative sliding of facing units, will occur at reinforcement elevations which act as supports in the beam analog model. The expression for the dynamic factor of safety against interface shear-capacity failure at a reinforcement layer is given by

$$[11] \quad FS_{dyn} = \frac{a_u + W_w(1 - k_v)\tan \lambda_u}{\left[0.8\Delta K_{dyn} \cos(\delta - \psi) + (K_A - 0.6\Delta K_{dyn})\cos(\delta - \psi)\left(\frac{z}{H} - \frac{S_v}{4H}\right) + k_h \frac{L_w}{H}\right]\frac{\gamma H S_v}{2}}$$

where S_v is the height of the contributory area of the considered reinforcement layer at depth z. For the block–geosynthetic interface at the topmost reinforcement layer, S_v is taken as the depth from the crest of the wall to the mid-elevation between the two topmost reinforcement layers.

Figure 12 illustrates solutions to eq. 11 for the previous example wall problem assuming facing-unit systems with relatively large interface shear capacity (group 1 data in Fig. 3*a*) and relatively weaker facing units with a geosynthetic inclusion (group 6 data in Fig. 3*b*). The maximum value of k_h for any curve in Fig. 12 corresponds to the condition $\phi - \theta = 0$ (see eq. 3). The curves in Fig. 12 show that the dynamic factor of safety against interface shear decreases rapidly as the horizontal acceleration coefficient increases. The curves also show that the factor of safety against interface shear decreases with depth of the facing interface below the crest of the wall for the static loading condition ($k_h = 0$). However, under seismic loading conditions, the trend in the curves is reversed for $k_h \geq 0.15$ for large interface shear systems and $k_h \geq 0.10$ for relatively weaker interface shear systems. Once this threshold value of k_h is exceeded, the most critical interface is located at the topmost interface layer (i.e., $z/H = 0.1$ in the example calculations). The threshold value for k_h in Fig. 12 is independent of the elevation of reinforcement layers, provided that the height of the top unreinforced portion of the facing column is equal to half the height of the contributory area (i.e., $S_v/2$). If the contributory area of the topmost layer is increased, the factor of safety against interface sliding at the topmost block–reinforcement interface will be further reduced.

Figure 13 shows computed critical horizontal coefficient (k_c) values plotted against different normalized interface depths using the same interface shear data as above. The value of critical acceleration coefficient k_c against interface sliding is greatly influenced by available interface shear capacity, particularly at the top of the wall. At the topmost interface ($z/H = 0.1$ in the example), the value of k_c for the large shear capacity system is 2–2.5 times greater than for the relatively poorer interface shear system.

It is convenient to rewrite eq. 11 in the following form:

$$[12] \quad FS_{dyn} = \frac{U}{\left[0.8\Delta K_{dyn} \cos(\delta - \psi) + (K_A - 0.6\Delta K_{dyn})\cos(\delta - \psi)\left(\frac{z}{H} - \frac{S_v}{4H}\right) + k_h \frac{L_w}{H}\right]}$$

where U is a nondimensional interface shear capacity quantity expressed by

$$[13] \quad U = \frac{V_u}{\frac{1}{2}\gamma H S_v} = \frac{a_u + W_w(1 - k_v)\tan \lambda_u}{\frac{1}{2}\gamma H S_v}$$

Rewriting eq. 13 yields:

$$[14] \quad U = \frac{V_u}{\frac{1}{2}\gamma H S_v} = \frac{a_u}{\frac{1}{2}\gamma H S_v} + \frac{2L_w \tan \lambda_u}{S_v}\left(\frac{z}{H}\right)(1 - k_v)$$

To examine the effect of interface shear capacity on column interface shear stability, eq. 12 has been used to calculate k_c for a range of U values at three interface elevations ($z/H = 0.1$, 0.5, and 0.9) assuming the presence of a geosynthetic inclusion. The results are presented in Fig. 14. The curves show that for the case $k_v = 0$, the computed values of the critical acceleration coefficient are very sensitive to the magnitude of U for $U < 1$. For $k_v = -2k_h/3$, values of k_c are sensibly constant for $U > 0.5$. The most critical elevation occurs at the top reinforcement layer (i.e., $z/H = 0.1$). The range of critical acceleration coefficient values ($k_c = 0.21$–0.46) at this elevation calculated using all available shear-test data (shaded region in Fig. 14) is also shown in the figure. This range shows that relatively large critical horizontal acceleration values for column shear failure are possible with segmental retaining wall systems on the market today, even with the presence of a geosynthetic inclusion at the shear surface. An implication for design is that selection of a segmental retaining wall system with efficient shear capacity can significantly improve resistance to facing shear failure under seismic loading. An alternative strategy for a prescribed segmental retaining wall facing unit type is to increase the magnitude of normalized shear capacity (U) by reducing the reinforcement spacing (S_v).

Fig. 10. Critical horizontal acceleration coefficient k_c for internal sliding for segmental walls with a range of block–geosynthetic interface shear capacities.

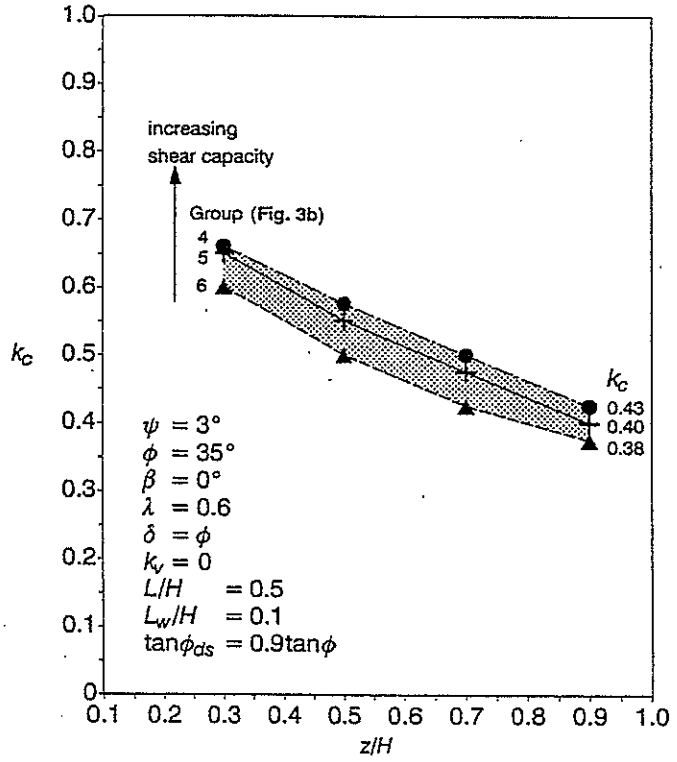

Calculation of permanent displacements

The permanent displacement of a geosynthetic-reinforced segmental soil retaining wall due to the sliding or shear mechanisms introduced earlier can be estimated using one of two general approaches. For a given input acceleration time history, Newmark's double-integration method (Newmark 1965) for a sliding block can be used to calculate the permanent displacement. However, if the input acceleration data are specified only by characteristic parameters such as the peak ground acceleration and the peak ground velocity, then empirical methods that correlate the expected permanent displacement and the characteristic parameters of the earthquake are required. Alternatively, if the tolerable permanent displacement of the structure is specified, based on serviceability criteria, the wall can then be designed using the empirical-method approach so that expected permanent displacements do not exceed specified values.

Newmark's double-integration method

Most displacement-based methods have been formulated based on the sliding-block theory proposed by Newmark (1965). According to this theory, the potential sliding soil body is treated as a rigid–plastic monolithic mass under the action of seismic forces. Permanent displacement of the mass takes place whenever the seismic force acting on the soil mass (plus the existing static force) overcomes the available resistance along the potential sliding surface. The corresponding acceleration that causes this seismic force is the critical acceleration of the sliding soil mass.

Fig. 11. Calculation of dynamic interface shear force acting at a reinforcement elevation. F_{dyn}, dynamic force in reinforcement layer; S_{dyn}, dynamic interface shear force; N, total number of reinforcement layers; M, total number of facing units.

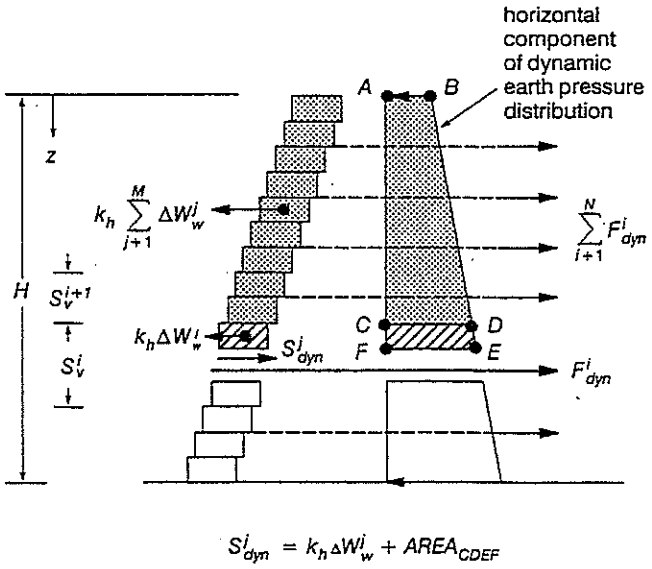

$$S_{dyn}^i = k_h \Delta W_w^i + AREA_{CDEF}$$

Given an earthquake record, the accumulated permanent displacement of the sliding soil body is computed by numerically integrating twice the acceleration time history, with the critical acceleration used as the reference datum. This procedure is illustrated in Fig. 15, where g is the gravitational constant, $a(t)$ is the horizontal ground acceleration function with time t, $a_m = k_m g$ (where k_m is the peak horizontal acceleration coefficient) is the peak value of $a(t)$, and $a_c = k_c g$ is the critical horizontal acceleration of the sliding block. For a given ground acceleration time history and a known critical acceleration of the sliding mass, the earthquake-induced displacement is calculated by integrating those portions of the acceleration history that are above the critical acceleration and those portions that are below until the relative velocity between the sliding mass and the sliding base reduces to zero.

Empirical displacement methods

Newmark's sliding-block theory has been widely used to establish empirical relationships between the expected permanent displacement and characteristic seismic parameters of the input earthquake by integrating existing acceleration records. The critical acceleration ratio, which is the ratio of the critical acceleration ($k_c g$) of the sliding block to the peak horizontal acceleration ($k_m g$) of the earthquake, has been shown to be an important parameter that affects the magnitude of the permanent displacement. Thus, the seismic displacement of a potential sliding soil mass computed using Newmark's theory has been traditionally correlated with the critical acceleration ratio (k_c/k_m) and other representative characteristic seismic parameters such as the peak ground acceleration ($k_m g$), the peak ground velocity (v_m), and the predominant period (T) of the acceleration

Fig. 12. Influence of horizontal acceleration coefficient k_h, normalized depth of shear interface z/H, interface shear capacity, and vertical acceleration coefficient k_v on factor of safety against interface shear failure at facing column.

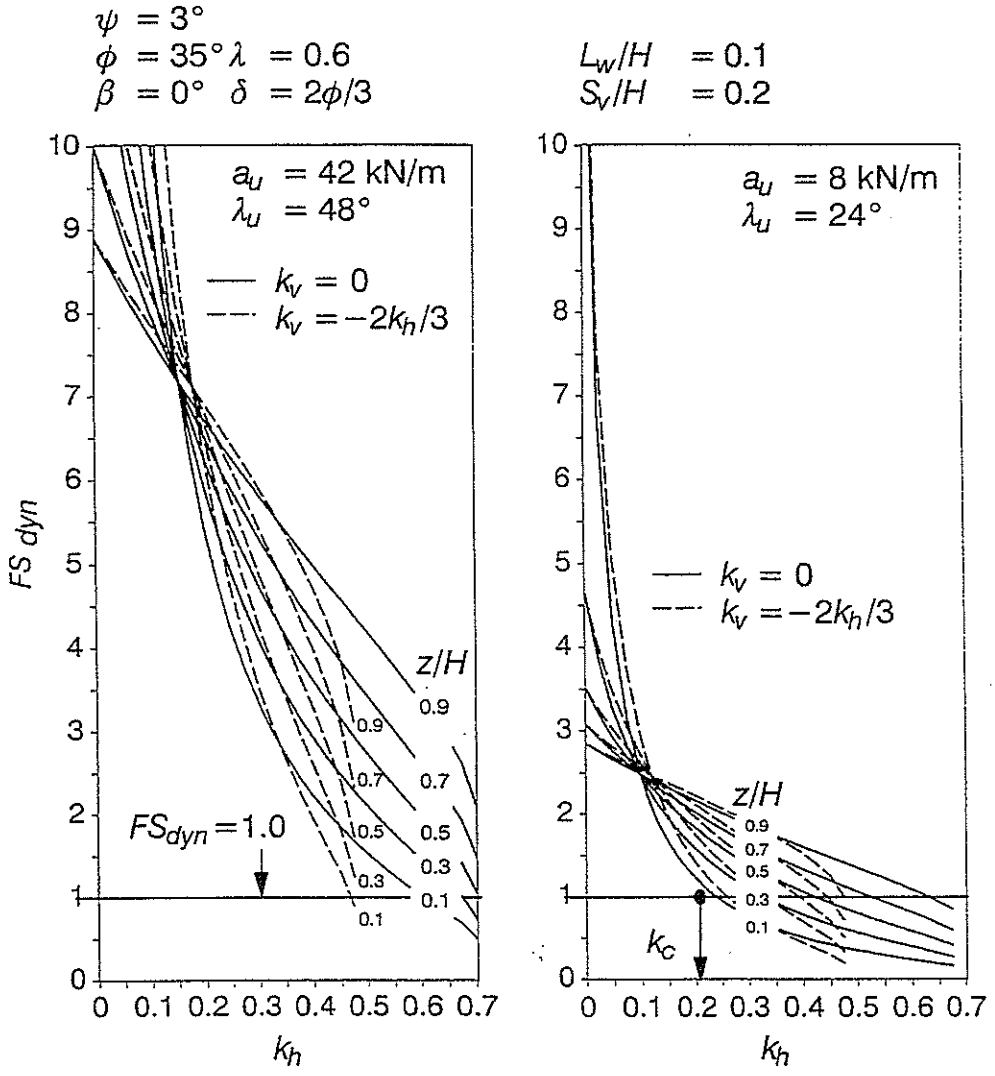

(a) facing system with relatively large interface shear capacity (Group 1 data in **Fig. 3a**)

(b) facing system with relatively low interface shear capacity (Group 6 data in **Fig. 3b**)

spectrum (e.g., Newmark 1965; Sarma 1975; Franklin and Chang 1977). The writers have reformulated a number of existing displacement methods based on nondimensionalized displacement terms that are common to the methods and divided them into two separate categories based on the characteristic seismic parameters referenced in each method (Cai and Bathurst 1996). The first category of methods uses the peak ground acceleration ($k_m g$) and peak ground velocity (v_m) as characteristic parameters, and the second category of methods uses the peak ground acceleration ($k_m g$) and the predominant period (T) of the ground-acceleration spectrum.

For brevity, only the first category of methods is presented in Fig. 16. These methods give correlations between the dimensionless displacement term $d/(v_m^2/k_m g)$, where d is the actual expected permanent displacement, and the critical acceleration ratio (k_c/k_m). In Fig. 16, there are three upper bound displacement curves (a, c, e) and two mean displacement curves (b, d) that are derived based on different sources of earthquake data.

It should be pointed out, however, that since these methods have been formulated based on different earthquake data, the selection of which method to use should be based on careful evaluation of the characteristics of the earthquake record and the site conditions under consideration. It should also be noted that the values of permanent displacement given by each method are only order-of-magnitude estimates rather than accurate predictions. Engineering judgement plays an important role in the interpretation of results using the methods given in Fig. 16.

Table 1. Material properties for example reinforced segmental retaining wall.

Material–interface	Properties	Values
Soil	Friction angle (ϕ)	30°, 35°, 40°
	Unit weight (γ)	20 kN/m^3
Geosynthetic	Index strength (ASTM D-4595)	39.5 kN/m
	Design strength	16.5 kN/m
Soil–geosynthetic	Coefficient of direct sliding	0.9 tan ϕ
Segmental block	Width (toe to heel)	600 mm
	Height	200 mm
	Length	450 mm
	Infilled block mass	117 kg
Block–block interface shear[a]	a_u	42 kN/m
	λ_u	48°
Block–geosynthetic interface shear[b]	a_u	8 kN/m
	λ_u	24°

[a]Group 1 data, Fig. 3*a*.
[b]Group 6 data, Fig. 3*b*.

Example application

An actual geosynthetic-reinforced segmental retaining wall is shown in Fig. 17 and is used here to demonstrate the application of the sliding-block and empirical methods to estimate wall deformations. The wall is 6 m high and has 30 segmental masonry block units and 8 layers of geogrid reinforcement extending to 4.3 m into the backfill soil from the front face of the wall (Bathurst et al. 1993*b*). The material properties of the wall components are given in Table 1. Interface shear-capacity test data are not available for this structure and the writers have assumed group 6 data in Fig. 3*b* (the worst case) for the properties of the facing units at geosynthetic interfaces for demonstration purposes only. At block to block interfaces, group 1 data have been assumed (best case). To investigate the influence of the shear strength of the backfill soil on the seismic displacement of the wall, three values of soil friction angle (ϕ = 30, 35, and 40°) were used in the calculations.

It should be noted that the material properties and tensile design strength for the geosynthetic reinforcement are for static load conditions. No attempt has been made to adjust any parameter for the influence of rapid cyclic loading. In practice, the design strength of the reinforcement is typically increased by 33% to account for the short duration of peak seismic loading. Recommended practice for adjusting component design strengths for seismic loading conditions is discussed in the paper by Bathurst and Cai (1995).

The east–west (90°) horizontal ground acceleration component recorded at Newhall Station (California Strong Motion Instrumentation Program) reported during the 17 January 1994 Northridge earthquake (M = 6.7) was used as the input earthquake data. The horizontal ground acceleration, ground velocity, and acceleration spectrum are shown in Fig. 18. The peak characteristics of ground motion are also indicated in the figure. In the calculations, it was assumed that the inertial forces created by the positive components of the acceleration (k_m = 0.60) act outward from the wall. It should be noted that using $k_h = k_m = 0.6$ in pseudostatic seismic stability analyses represents a very extreme loading but is introduced here for illustration purposes only. For example, on the west coast of British Columbia (the most seismically active area of Canada), the typical maximum peak horizontal ground acceleration on rock, based on a 10% probability of exceedance in

Fig. 13. Critical horizontal acceleration coefficient k_c versus normalized interface depth below crest of wall z/H, interface shear capacity, and vertical acceleration coefficient k_v. Solution limit corresponds to $\phi - \theta = 0$ in [3].

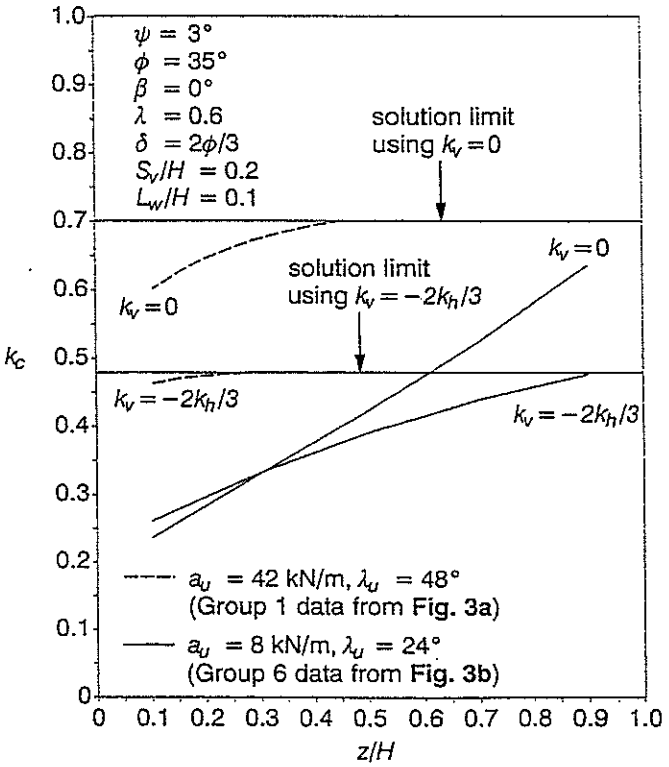

Fig. 14. Critical acceleration coefficient k_c versus normalized interface shear capacity U for interface locations with a geosynthetic inclusion.

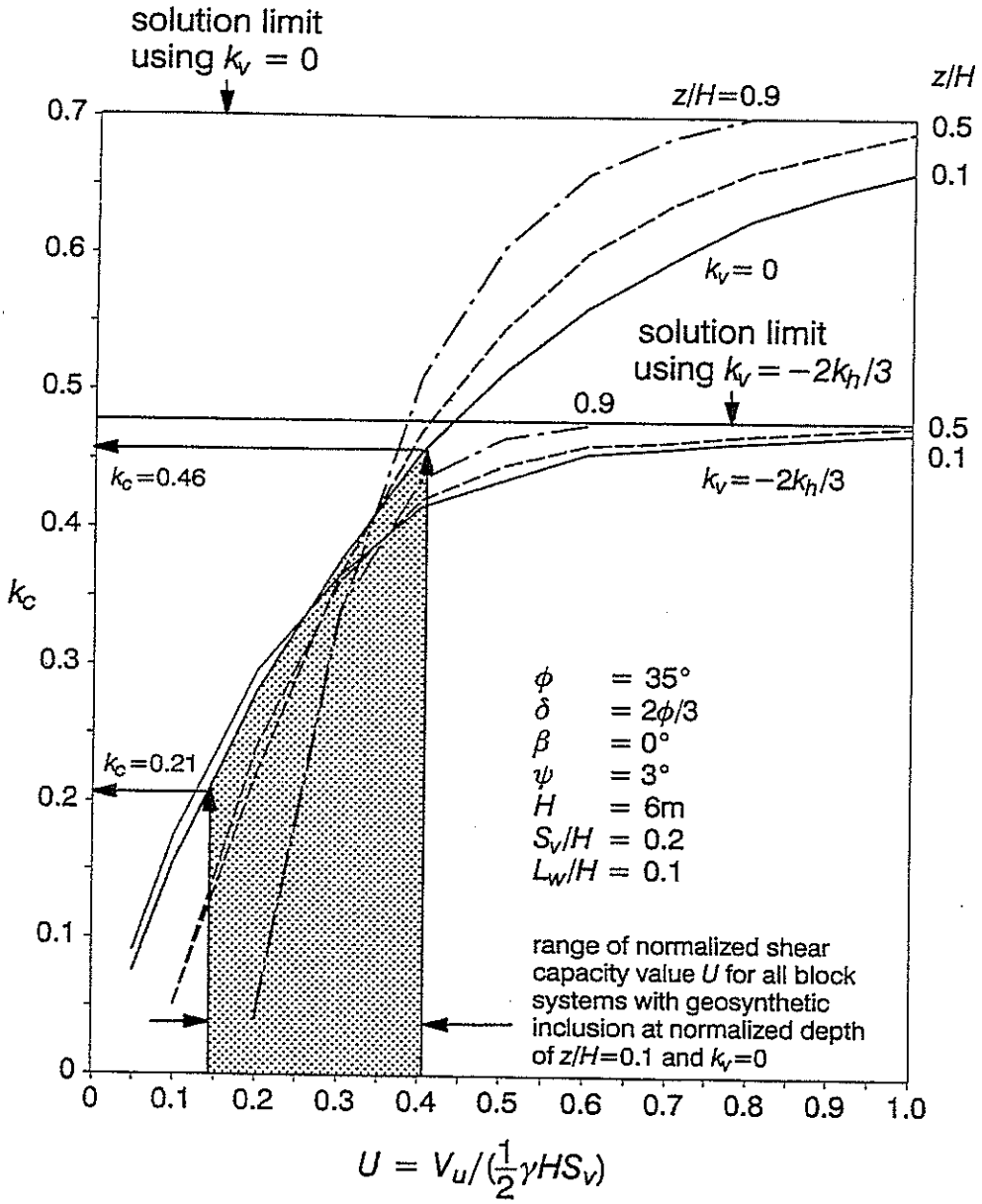

50 years, is $a_m = 0.32g$ (Canadian Geotechnical Society 1992). For the western United States a value of $a_m = 0.4g$ based on the same criteria is a representative upper limit for structures on rock (Kramer 1996).

Static and dynamic factors of safety

Factors of safety against translational failure modes identified in Fig. 2 were calculated using a software program that implements the current limit-equilibrium methodology recommended by the NCMA for routine geosynthetic-reinforced segmental retaining walls under static loading (Bathurst and Simac 1995). Static factors of safety against external (base) sliding of the reinforced soil mass are FS_{sta} = 3.40, 5.24, and 8.06 for ϕ = 30, 35, and 40°, respectively. The static factors of safety against internal sliding and interface shear at geosynthetic elevations are plotted in Fig. 19. Calculated factors of safety for base sliding, internal sliding, and block interface shear exceed factors of safety under static loading conditions recommended by the NCMA (Simac et al. 1993; Bathurst et al. 1993*a*).

The values of dynamic factor of safety against external sliding under a peak ground acceleration coefficient of k_h = 0.60 were calculated to be FS_{dyn} = 0.38, 0.62, and 0.86 for ϕ = 30, 35, and 40°, respectively. Thus, base sliding is anticipated for the range of soil friction angles investigated.

The dynamic factors of safety against internal sliding and block interface shear at reinforcement elevations for a peak acceleration of k_h = 0.60 are plotted in Fig. 20. The geosynthetic–soil interface elevations at which sliding displacement will occur correspond to factor of safety values less

Fig. 15. Illustration of Newmark's sliding-block method to calculate permanent displacement of sliding earth structure (unidirectional displacement).

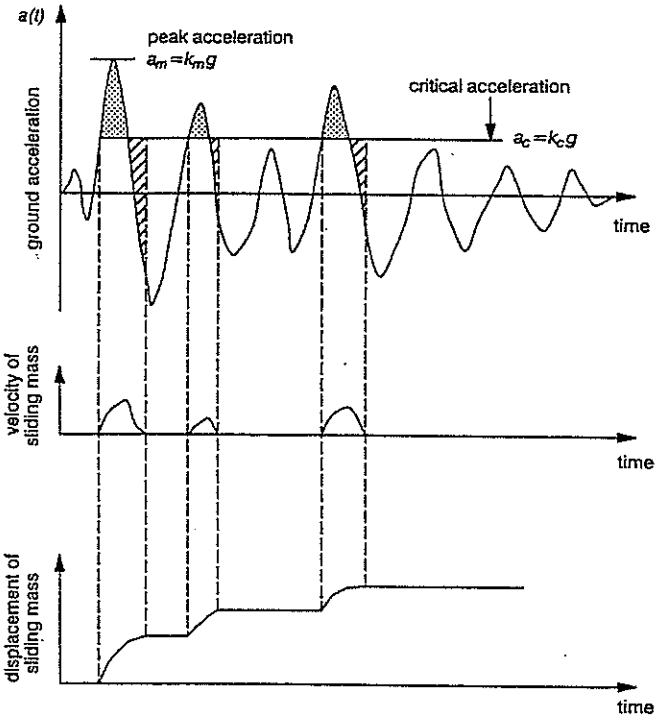

Table 2. Permanent displacements due to base sliding.

Soil friction angle, ϕ (°)	Critical acceleration ratio (k_c/k_m)	Calculated permanent displacement[a] (mm)	Estimated permanent displacement[b] (mm)
30	0.55	48	54
35	0.72	11	15
40	0.90	0.6	4

[a]Newmark's double-integration method.
[b]Empirical method e.

than $FS_{dyn} = 1.0$ for both internal sliding and block interface sliding mechanisms. The data show that internal sliding is anticipated at the lower interface elevations and block interface shear is anticipated at the higher interface layers.

Critical accelerations and permanent displacements

External sliding

The values of critical acceleration coefficients against external sliding calculated using eq. 7 with soil friction angles of $\phi = 30$, 35, and 40° are $k_c = 0.33$, 0.43, and 0.54, respectively. These values are all less than the peak ground acceleration coefficient of $k_m = 0.6$ shown in Fig. 18. The corresponding critical acceleration ratios are $k_c/k_m = 0.55$, 0.72, and 0.90. Permanent displacements due to base sliding (external sliding) calculated using the Newmark's double-integration procedure are given in Table 2. Method e in Fig. 16 is also used to estimate the permanent base sliding displacement and the results of this calculation are also given in Table 2.

Table 3. Permanent displacement due to internal sliding at geosynthetic-reinforcement elevations.

Layer number	Critical acceleration ratio (k_c/k_m)	Calculated permanent displacement[a] (mm)	Estimated permanent displacement[b] (mm)
		$\phi = 30°$	
7, 8	>1	0	0
6	~1	0	0
5	0.92	0.31	3.45
4	0.83	2.80	6.70
3	0.73	10.0	14.0
2	0.67	17.6	21.9
1	0.58	37.4	43.2
Σ		68	89
		$\phi = 35°$	
5–8	>1	0	0
4	~1	0	0
3	0.88	1.08	4.64
2	0.82	3.27	7.21
1	0.73	10.0	14.0
Σ		14	26
		$\phi = 40°$	
3–8	>1	0	0
2	~1	0	0
1	0.90	0.6	4
Σ		0.6	4

[a]Newmark's double-integration method.
[b]Empirical method e.

Internal sliding

The values of critical acceleration coefficient against internal sliding at reinforcement elevations are plotted in Fig. 21*a*. It can be seen that the unreinforced portion of the wall above the topmost reinforcement layer (layer 8) has the greatest resistance to internal sliding. The calculated permanent displacements using Newmark's integration method and the empirical method e at the geosynthetic elevations where the critical accelerations are exceeded are given in Table 3. When the friction angle of the soil is taken as $\phi = 30°$, permanent displacements due to internal sliding occur at all but the top three reinforcement elevations. When $\phi = 35°$, permanent displacements develop at the bottom three reinforcement elevations, and when $\phi = 40°$ permanent displacements occur only at the bottom reinforcement layer. The summary data in Table 3 show that the amount of permanent displacement due to internal sliding diminishes rapidly with an increase in soil shear strength.

It is important to note that for the range of soil friction angles and the block to geosynthetic interface properties

Fig. 16. Nondimensionalized displacement in terms of $d/(v_m^2/k_m g)$ versus critical acceleration ratio k_c/k_m (after Cai and Bathurst 1996).

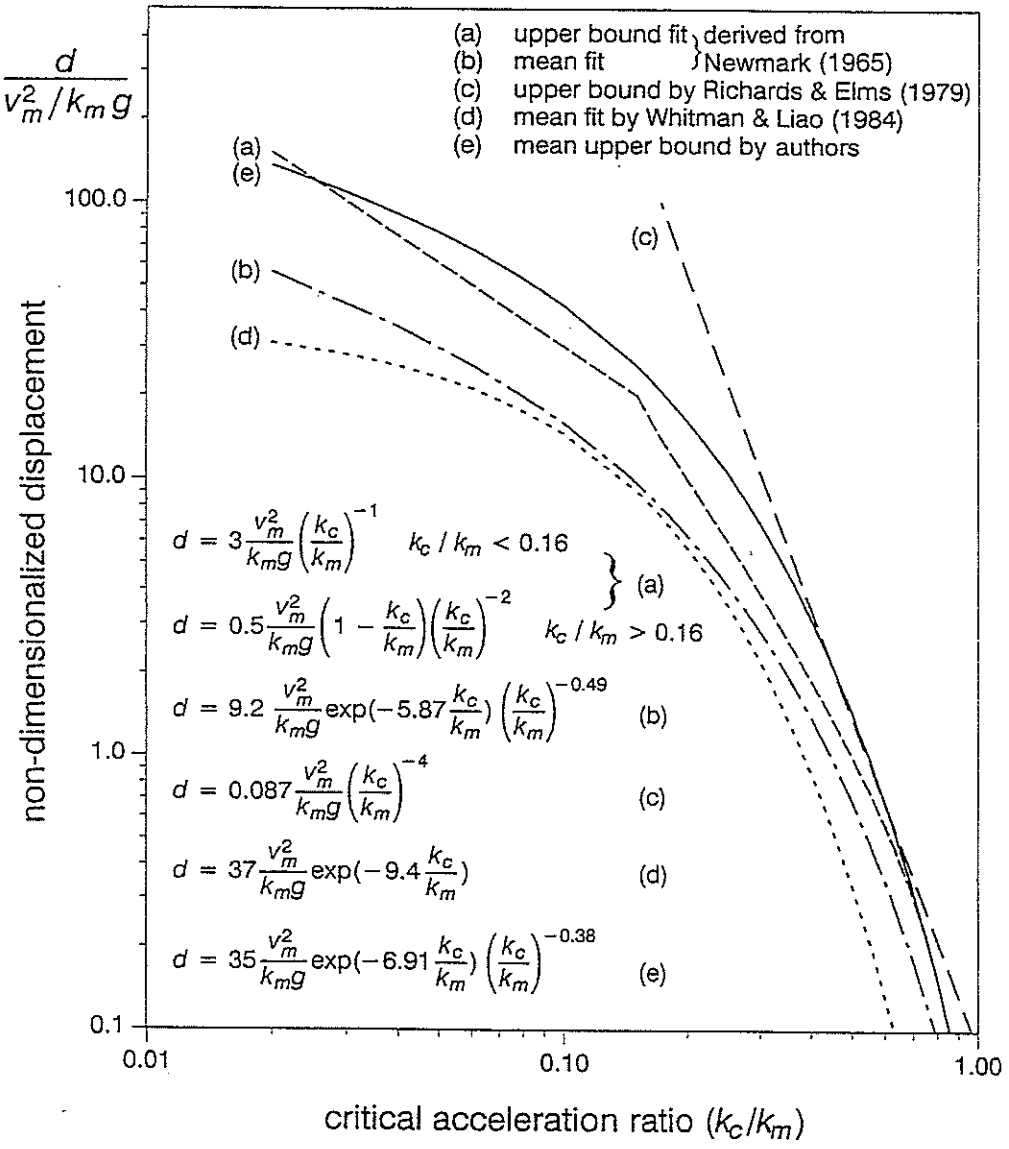

used, Fig. 21*a* shows that the wall is capable of withstanding peak horizontal accelerations of 0.35*g*, 0.44*g*, and 0.54*g*, without experiencing any permanent displacement due to internal sliding.

Block interface shear

Values of critical acceleration for block interface shear at geosynthetic elevations are plotted in Fig. 21*b*. Although the unreinforced portion of the wall above the topmost reinforcement layer has the largest resistance to internal sliding (Fig. 21*a*), its resistance to localized shear at the facing is the lowest. For $\phi = 30°$, relative block interface movement occurs at the top four reinforcement elevations, whereas for $\phi = 35$ and 40°, relative block interface movement occurs at the top three reinforcement elevations. The displacement results calculated using Newmark's method and the empirical method e are given in Table 4. The results in the table show that at the topmost reinforcement elevation (layer 8), the permanent displacement due to facing interface shear sliding is large due to the relatively small critical acceleration value ($k_c/k_m < 0.5$). However, these displacements decrease rapidly with increasing depth below the wall crest and become negligible below layer 6, particularly for backfill soils with large soil friction angles. It should be emphasized here that the high permanent displacements at the top reinforcement layers are a direct result of the poor interface shear properties used (group 6 data) in the analyses and the extremely high value of the peak horizontal acceleration ($k_m = 0.6$). Under these conditions, it is the top portion of a segmental retaining wall that is most susceptible to failure manifested as unacceptably large outward movement.

Similar to the observations made with respect to internal sliding, Fig. 21*b* shows that the wall is capable

Fig. 17. Example geosynthetic-reinforced segmental soil retaining wall (after Bathurst et al. 1993*b*).

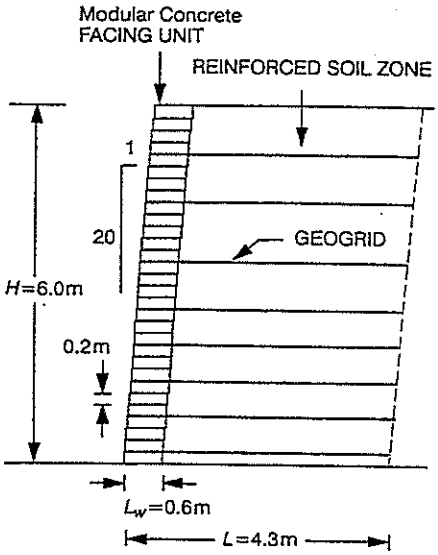

Layer no.	z/H	S_v/H
8	0.133	0.2
7	0.267	0.15
6	0.433	0.15
5	0.567	0.117
4	0.667	0.1
3	0.767	0.1
2	0.867	0.1
1	0.967	0.083

of withstanding peak horizontal accelerations in the range of 0.25–0.28g for the three soil friction angles used without experiencing any facing interface shear sliding.

Total permanent wall displacement

The total permanent displacement at the wall face at each elevation from the initial static position is estimated by adding the layer displacement to the cumulative displacement below that layer. The layer displacement is taken as the larger of the facing shear displacement or internal sliding at that layer. The controlling mechanism is illustrated in Table 5 where cumulative displacements for each analysis have been summarized.

The serviceability (relative deformation) criterion for the interpretation of interface shear capacity between segmental units with and without a geosynthetic inclusion is taken as 2% of the height of the block unit according to NCMA guidelines (Simac et al. 1993). This criterion can be compared with the maximum seismic-induced out-of-alignment displacement, which is 4.0, 2.4, and 1.4% for backfill soils with ϕ = 30, 35, and 40°, respectively, using Newmark's method. Hence for the strongest backfill this criterion is satisfied despite a very large ground acceleration in combination with a very poor interface system. The magnitudes of the seismic-induced displacements can also be referenced to construction-induced out-of-alignment displacement, which has been estimated to be about 1–1.5% of the height of the wall for well-constructed segmental retaining walls due to the incremental construction procedure and compaction of soil behind each facing course (Bathurst et al. 1995).

A similar set of analyses carried out with typical segmental retaining wall systems with better interface shear resistance showed that interface shear deformations were much smaller and were well within the 2% serviceability criterion. Indeed, for the best interface shear systems, combined with a backfill soil with ϕ = 40°, the maximum

Fig. 18. Northridge 1994 earthquake data recorded at Newhall Station (90°). Original data from the California Strong Motion Instrumentation Program (California Division of Mines and Geology).

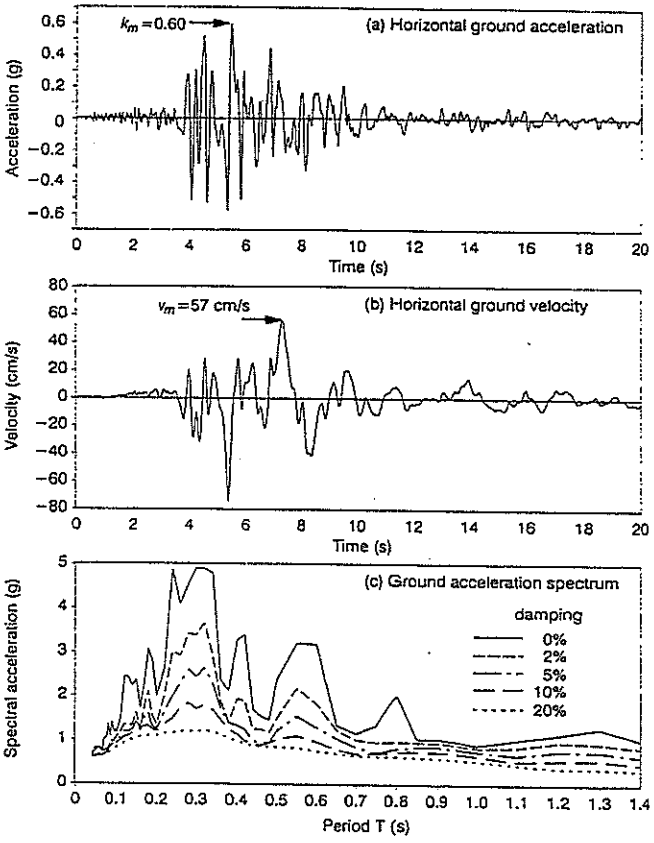

Fig. 19. Static factors of safety against internal sliding and block–geosynthetic interface shear for example reinforced SRW structure.

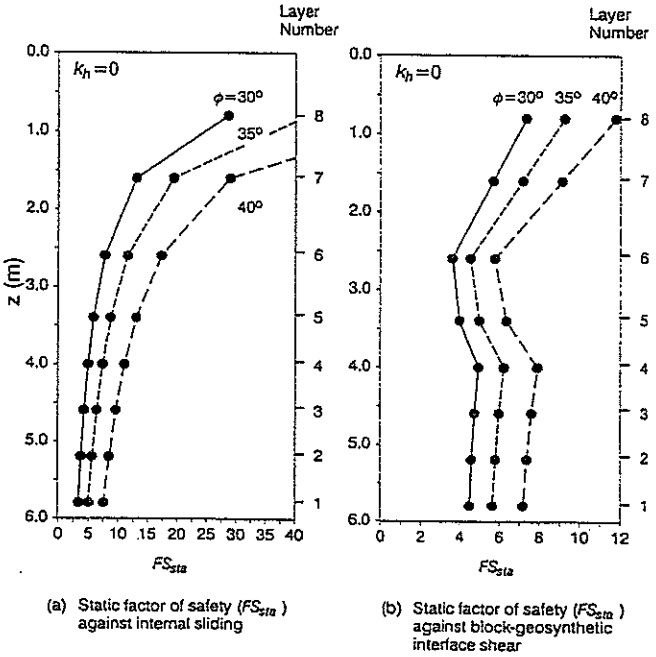

Fig. 20. Dynamic factors of safety against internal sliding and block–geosynthetic interface shear for example reinforced SRW structure.

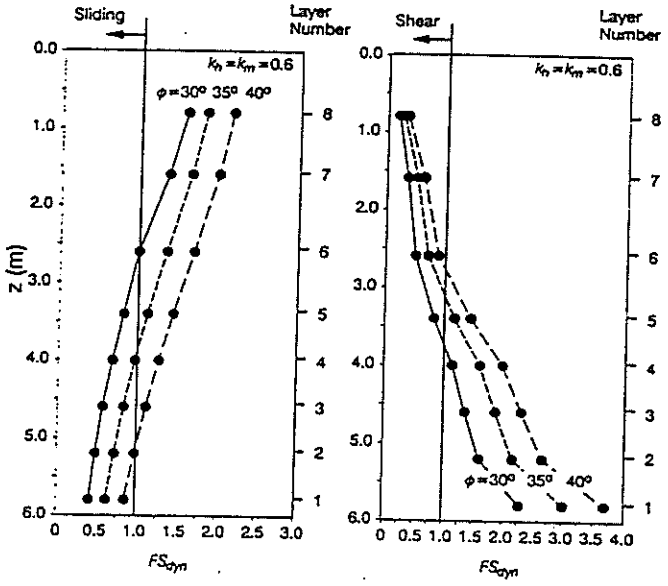

(a) Dynamic factor of safety (FS_{dyn}) against internal sliding

(b) Dynamic factor of safety (FS_{dyn}) against block-geosynthetic interface shear

Fig. 21. Critical accelerations against internal sliding and interface block–geosynthetic shear for example reinforced SRW structure.

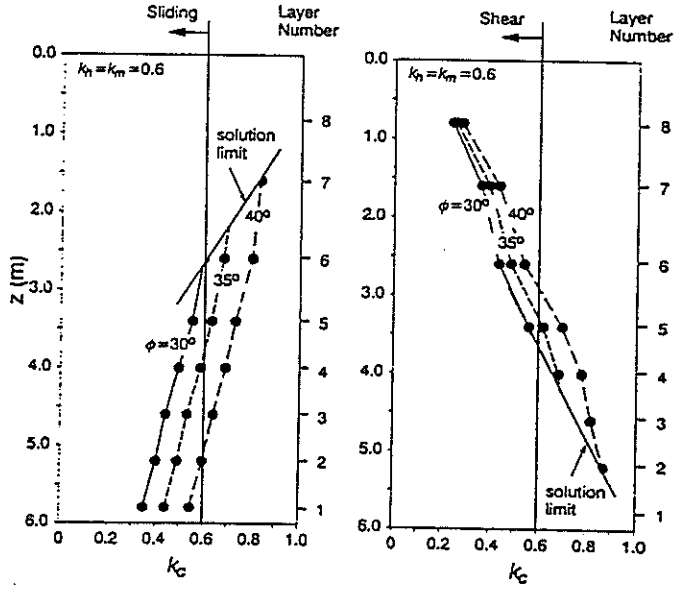

(a) Critical acceleration coefficient against internal sliding

(b) Critical acceleration coefficient against block-geosynthetic interface shear

out-of-alignment displacements were only a few millimetres. Taken together the results of analyses suggest that deformation-resistant reinforced segmental retaining walls can be constructed for walls 6 m or less in height using good quality backfill soils and segmental retaining wall systems on the market today that have good interface shear capacity.

Table 4. Perman shear at geosynt

Layer number	Crit accele ratio (k_c/k_m)	displacement[a] (mm)	nt displacement[b] (mm)
		ϕ = 30°	
8	0.40	128	172
7	0.60	31.7	37.3
6	0.73	10.0	14.0
5	0.93	0.2	3.21
1–4	>1	0	0
Σ		170	226
		ϕ = 35°	
8	0.43	107	136
7	0.67	17.6	21.9
6	0.81	3.80	7.76
1–5	>1	0	0
Σ		128	166
		ϕ = 40°	
8	0.47	84.2	100
7	0.73	10.0	14.0
6	0.90	0.6	4.0
1–5	>1	0	0
Σ		95	118

[a]Newmark's double-integration method.
[b]Empirical method e.

Comparison of Newmark's method and empirical method to calculate permanent displacements

Newmark's method and the empirical approach (method e) give similar results for the three displacement mechanisms examined when large-displacement values are calculated (i.e., backfill soils with ϕ = 30 and 35°). The order-of-magnitude accuracy of the empirical method (compared with Newmark's method) is satisfied for all large-displacement results. The discrepancies for analyses with ϕ = 40° are larger but the errors are of little practical consequence because of their small magnitudes.

Implications to design

The paper examines conventional displacement methods that have been adapted for the special case of geosynthetic-reinforced segmental retaining wall structures. The implications of the study to the analysis, design, and performance of these structures can be summarized as follows:

(1) The dry-stacked facing-column units that are a distinguishing feature of geosynthetic-reinforced segmental retaining wall systems perform a structural function by resisting horizontal displacements under both static and seismic loading conditions. The influence of interface shear

Table 5. Total permanent displacement (mm) considering all displacement mechanisms.

	$\phi = 30°$		$\phi = 35°$		$\phi = 40°$	
Layer number	Newmark's method	Empirical method	Newmark's method	Empirical method	Newmark's method	Empirical method
8	286[a]	370[a]	154[a]	206[a]	86[a]	126[a]
7	158[a]	198[a]	47[a]	70[a]	12[a]	26[a]
6	126[a]	160[a]	29[a]	49[a]	1.8	12
5	116	146	25	41	1.2	8
4	116	140	25	41	1.2	8
3	113	133	25	41	1.2	8
2	103	119	24	36	1.2	8
1	85.4	97	21	29	1.2	8
Base sliding	48	54	11	15	0.6	4

[a]Controlling mechanism is facing shear, otherwise internal sliding controls.

capacity, particularly with respect to stability of the facing column, must be evaluated during design.

(2) The available shear capacity from segmental retaining wall products on the market today varies widely. Product specific shear testing is required to ensure that representative shear capacity parameters are used for design.

(3) The presence of a geosynthetic inclusion at the interface between segmental retaining wall units may reduce the interface shear capacity to lower values than for block to block interfaces, particularly for systems that derive significant shear capacity through friction.

(4) The top unreinforced portion of a geosynthetic-reinforced segmental retaining wall is typically the least stable portion of the structure with respect to facing-column stability under seismic loading. The number of reinforcement layers close to the top of the wall may have to be increased from the number required for a static loading environment in order to ensure an acceptable margin of safety against both horizontal movements and collapse during a seismic event.

(5) Empirical displacement methods that are used to estimate wall deformations can at best provide order-of-magnitude estimates. Predicted values can be expected to vary greatly depending on the empirical method selected. In practice, these methods are best suited to making relative performance comparisons between nominally identical wall structures constructed with different candidate block systems.

Discussion and concluding remarks

This paper deals with only the calculation of permanent displacements related to a narrow set of failure mechanisms for reinforced segmental retaining walls (external sliding, internal sliding, and block interface shear failure). These are the only mechanisms that can be treated using conventional sliding-block methods. The remaining failure mechanisms (Fig. 2) can be evaluated using a pseudostatic limit-equilibrium approach as outlined in the paper by Bathurst and Cai (1995). However, pseudostatic methods adapted to segmental retaining wall structures can only be used to estimate factors of safety against collapse.

An important assumption in the current paper is that the base acceleration at each geosynthetic elevation is the same as the ground acceleration. This may have introduced unquantifiable errors, since response acceleration may be amplified with height above the base of the wall. However, finite element analysis (Cai and Bathurst 1995) has shown that variations in the peak values of the response acceleration along the height of a 3.2 m high geosynthetic-reinforced segmental retaining wall are generally small and any error introduced from this approximation may be insignificant. For higher walls the possibility of acceleration amplification is greater and more research is required to develop rules to estimate ground amplification with wall height. However, it should be noted that the possibility of acceleration amplification is considered in part by adopting a dynamic earth pressure increment distribution that has a maximum value at the top of structure as illustrated in Fig. 4.

It is important to note that the example calculations in the current study required relatively high horizontal accelerations to generate significant displacements. The qualitatively good performance of several geosynthetic-reinforced segmental retaining walls has been recorded in the literature. For example, one wall is estimated to have experienced peak horizontal ground accelerations as high as 0.5g during the Northridge earthquake in California on 17 January 1994 but did not exhibit any signs of facing-column movement (Bathurst and Cai 1995). It appears that geosynthetic-reinforced segmental retaining walls can be constructed to be earthquake resistant under significant seismic loading.

Acknowledgements

The funding for the work reported in the paper was provided by the Department of National Defence (DND, Canada) through an Academic Research Program (ARP) grant awarded to the second author and by the Directorate Infrastructure Support (DIS/DND).

References

Allen, T.M. 1993. Issues regarding design and specification of segmental block-faced geosynthetic walls. Transportation Research Record No. 1414, pp. 6–11.

Bathurst, R.J., and Cai, Z. 1995. Pseudo-static seismic analysis of geosynthetic-reinforced segmental retaining walls. Geosynthetics International, 2(5): 787–830.
Bathurst, R.J., and Simac, M.R. 1993. Laboratory testing of modular unit-geogrid facing connections. *In* Geosynthetic soil reinforcement testing procedures. *Edited by* S.C.J. Cheng. American Society for Testing and Materials, Special Technical Publication 1190, pp. 32–48.
Bathurst, R.J., and Simac, M.R. 1994. Geosynthetic reinforced segmental retaining wall structures in North America (invited keynote paper). Proceedings of the 5th International Conference on Geotextiles, Geomembranes and Related Products, 6–9 Sept. 1994, Singapore.
Bathurst, R.J., and Simac, M.R. 1995. Software for segmental retaining walls. Geotechnical Fabrics Report, 13(7): 20–21.
Bathurst, R.J., Simac, M.R., and Berg, R.R. 1993*a*. Review of the NCMA segmental retaining wall design manual for geosynthetic-reinforced structures. Transportation Research Record, No. 1414, pp. 16–25.
Bathurst, R.J., Simac, M.R., Christopher, B.R., and Bonczkiewicz, C. 1993*b*. A database of results from a geosynthetic reinforced modular block soil retaining wall. Proceedings of Soil Reinforcement: Full Scale Experiments of the 80's, 18–19 Nov. 1993, Paris, France, International Society of Soil Mechanics and Foundation Engineering — l'École nationale des ponts et chaussées, pp. 341–365.
Bathurst, R.J., Simac, M.R., and Sandri, D. 1995. Lessons learned from the construction performance of a 14 m high segmental retaining wall. *In* Proceedings of Geosynthetics: Lessons Learned from Failures, 20 Feb. 1995, Nashville, Tenn. *Edited by* J.P. Giroud. pp. 21–34.
Bonaparte, R., Schmertmann, G.R., and Williams, N.D. 1986. Seismic design of slopes reinforced with geogrids and geotextiles. Proceedings of the 3rd International Conference on Geotextiles, Vienna, Austria. Vol. 2, pp. 273–278.
Cai, Z., and Bathurst, R.J. 1995. Seismic response analysis of geosynthetic reinforced soil segmental retaining walls by finite element method. Computers and Geotechnics, 17(4): 523–546.
Cai, Z., and Bathurst, R.J. 1996. Deterministic sliding block methods for estimating seismic displacements of earth structures. Soil Dynamics and Earthquake Engineering, 15(4): 255–268.
Canadian Geotechnical Society. 1992. Canadian foundation engineering manual. 3rd ed. Canadian Geotechnical Society, Toronto, Ont.
Chida, S., Minami, K., and Adach, K. 1982. Test de stabilité de remblais en Terre Armée [translated from Japanese].
Christopher, B.R., Gill, S.A., Giroud, J.P., Juran, I., Schlosser, F., Mitchell, J.K., and Dunnicliff, J. 1989. Reinforced soil structures: Vol. I. Design and construction guidelines. Federal Highway Administration, Report FHWA-RD-89-043, Washington, D.C.
Collin, J.G., Chouery-Curtis, V.E., and Berg, R.R. 1992. Field observations of reinforced soil structures under seismic loading. Proceedings of the International Symposium on Earth Reinforcement, Fukuoka, Japan. Vol. 1, pp. 223–228.
Ebling, R.M., and Morrison, E.E. 1993. The seismic design of waterfront retaining structures. Naval Civil Engineering Laboratory, Technical Report ITL-92-11 NCEL TR-939, Port Huenene, Calif.
Eliahu, U., and Watt, S. 1991. Geogrid-reinforced wall withstands earthquake. Geotechnical Fabrics Report, 9(2): 8–13.
Franklin, A.G., and Chang, F.K. 1977. Permanent displacement of earth embankments by Newmark sliding block analysis. United States Waterways Experiment Station, Vicksburg, Miss., Miscellaneous Paper S-71-17.
Kramer, S.L. 1996. Geotechnical earthquake engineering. Prentice Hall, Inc., Englewood Cliffs, N.J.
Newmark, N.M. 1965. Effect of earthquakes on dams and embankments. Géotechnique, 15(2): 139–159.
Okabe, S. 1926. General theory of earth pressure. Journal of the Japanese Society of Civil Engineers, 12(1): 1277–1323.
RECO. 1991. Reinforced earth structures in seismic regions. Reinforced Earth Company (RECO), Terre Armée Internationale, Paris, France, Miscellaneous Report.
Richards, R., and Elms, D.G. 1979. Seismic behavior of gravity retaining walls. ASCE Journal of the Geotechnical Engineering Division, 105(GT4): 449–464.
Sandri, D. 1994. Retaining walls stand up to the Northridge earthquake. Geotechnical Fabrics Report, 12(4): 30–31.
Sarma, S.K. 1975. Seismic stability of earth dams and embankments. Géotechnique, 25(4): 743–761.
Seed, H.B., and Whitman, R.V. 1970. Design of earth retaining structures for dynamic loads. ASCE Specialty Conference: Lateral Stresses in the Ground and Design of Earth Retaining Structures, Cornell University, Ithaca, N.Y., 22–24 June, pp. 103–147.
Segrestin, P., and Bastick, M. 1988. Seismic design of reinforced earth retaining walls — the contribution of finite element analysis. Proceedings of the International Geotechnical Symposium on Theory and Practice of Earth Reinforcement, Fukuoka, Japan, 5–7 October, 1988, pp. 577–582.
Simac, M.R., Bathurst, R.J., and Goodrum, R.A. 1991. Design and analysis of three reinforced soil retaining walls. Geosynthetics '91, Atlanta, Ga., 26–28 February 1991, Vol. 2, pp. 781–798.
Simac, M.R., Bathurst, R.J., Berg, R.R., and Lothspeich, S.E. 1993. National Concrete Masonry Association segmental retaining wall design manual. National Concrete Masonry Association, Herndon, Va.
Steedman, R.S., and Zeng, X. 1990. The influence of phase on the calculation of pseudo-static earth pressure on a retaining wall, Géotechnique, 40(1): 101–112.
Stewart, J.P., Bray, J.D., Seed, R.B., and Sitar, N. 1994. Preliminary report on the principal geotechnical aspects of the January 17, 1994 Northridge earthquake. University of California at Berkeley, Earthquake Engineering Research Center, Report UCB/EERC-94/08.
Whitman, R.V. 1990. Seismic design and behavior of gravity retaining walls. ASCE Specialty Conference: Design and Performance of Earth Retaining Structures, Ithaca, N.Y. ASCE Geotechnical Special Publication No. 25, pp. 817–842.
Whitman, R.V., and Liao, S. 1984. Seismic design of gravity retaining walls. Proceedings of the 8th World Conference on Earthquake Engineering, San Francisco, Calif., Vol. 3. pp. 533–540.

List of symbols

$a(t)$	ground acceleration with time t (m/s^2)
a_c	critical horizontal acceleration of sliding block (m/s^2)
a_m	peak horizontal ground acceleration (m/s^2)
a_u	minimum interface shear strength (N/m)
a_1, a_2	geometric constants (dimensionless)
d	permanent displacement (empirical methods) (m)
F_{dyn}	dynamic force in reinforcement layer (N/m)
FS_{dyn}	factor of safety under dynamic loading (dimensionless)
g	gravitational constant (m/s^2)
H	wall height (m)

K_A static active earth pressure coefficient calculated using Coulomb earth pressure theory (dimensionless)

K_{AE} dynamic active earth pressure coefficient calculated using Mononobe–Okabe method (dimensionless)

k_h horizontal seismic coefficient (dimensionless)

k_c critical horizontal seismic coefficient (dimensionless)

k_m peak horizontal acceleration coefficient (dimensionless)

k_v vertical seismic coefficient (dimensionless)

L base width of reinforced soil zone plus facing column (m)

L_W width of facing column (m)

m ratio of moment arm of dynamic active earth force to wall height (dimensionless)

N_n normal load (N/m)

P_A static active earth force (N/m)

P_{AE} dynamic active earth force (N/m)

P_I seismic inertial force (N/m)

R frictional resistance (N/m)

R_s frictional resistance along the soil–geosynthetic sliding interface (N/m)

U normalized interface shear capacity (dimensionless)

S_{dyn} dynamic interface shear force (N/m)

S_v contributory area (m^2/m)

T period (s)

t time (s)

W_H total weight of composite mass (= W_w + W_s) (N/m

W_s weight of reinforced soil mass (N/m)

W_w weight of facing column (N/m)

W_z weight of composite mass to depth z below crest o wall (N/m)

z depth from crest of wall (m)

V_u interface shear capacity (N/m)

v_m peak horizontal velocity (m/s)

β wall backslope angle (°)

ΔK_{dyn} dynamic earth pressure coefficient incremen (dimensionless)

ΔP_{dyn} dynamic force increment (N/m)

ΔW_w incremental weight of facing column (N/m)

δ interface friction angle (°)

ϕ friction angle of soil (°)

ϕ_{ds} geosynthetic–soil interface friction angle (°)

γ soil or facing-column unit weight (N/m^3)

λ inertial force reduction factor for gravity mass ir external and internal sliding stability calculations (dimensionless)

λ_u interface friction angle between facing units (°)

θ inertia angle (°)

ψ wall inclination angle (°)

Appendix E

Local Stability of GRS Walls with Segmental Precast Concrete Unit Facing

Appendix E Local Stability of GRS Walls with Segmental Precast Concrete Unit Facing

E1. General

Properties of segmental precast concrete units affect the local stability of GRS walls. Requirements with respect to minimum compressive strength, manufacturing tolerances and other properties of segmental precast concrete units are given in the NCMA Concrete Masonry Standards (NCMA 1998a). Additional consideration should be given to segmental unit strength properties and durability resistance for structures in aggressive environments.

The facing units and facing connections between the facing and reinforcements should be designed to the same durability criteria as the overall structure.

The following mechanisms create shear connections between segmental units:

- built-in mechanical interlock (shear keys, leading/trailing lips, etc.);
- mechanical connectors (pins or clips linking successive vertical courses of units);
- for flat interfaces: shear resistance due to friction between segmental units and geosynthetic reinforcement and to friction between geosynthetic reinforcement and granular material filling unit cavities (for units with cavities).

In the design of GRS structures, properties of segmental facing are described by the following parameters:

- Size, shape, weight, strength and durability of segmental units;
- Shear capacity of the interface between successive courses of segmental units (V_u kN/m);
- Connection strength developed between segmental units and a layer of geosynthetic reinforcement (T_{cl} kN/m).

Both the shear capacity V_u and the connection strength T_{cl} are a function of wall height, type of segmental unit and infill, and properties of geosynthetic reinforcement (if geosynthetic is present between courses of segmental units). Values of T_{cl} and V_u should be calculated based on the results of large scale testing of connection details in accordance with NCMA Test Method SRWU-1: Determination of Connection Strength Between Geosynthetic and Segmental Concrete Units, and NCMA Test Method SRWU-2: Determination of Shear Strength between Segmental Concrete Units (NCMA 1997) respectively.

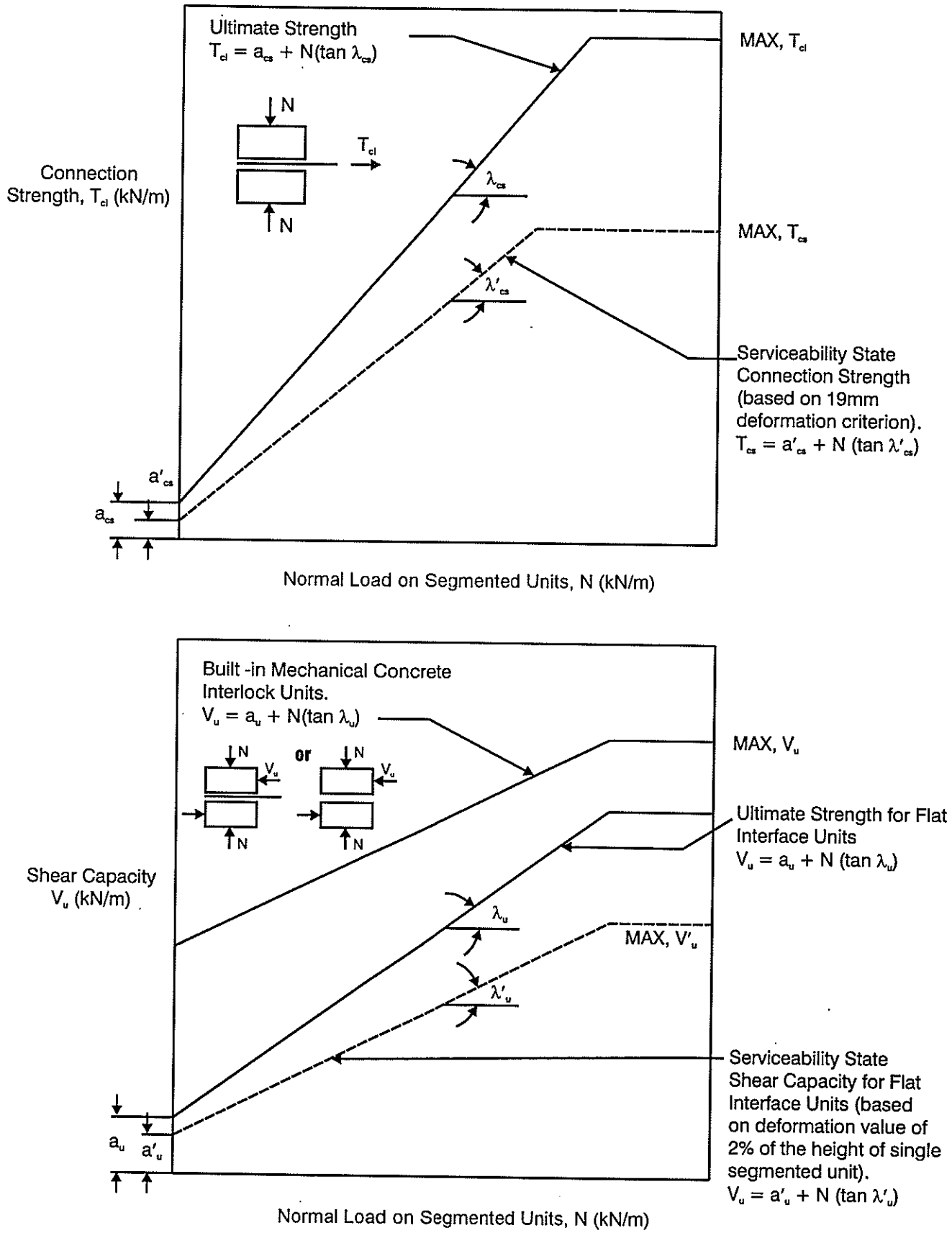

Figure E1 **Typical interpretation of connection strength and shear capacity test data (NCMA 1997).**

04/12/00

CAD FILE 3401650SK18.CDR MT

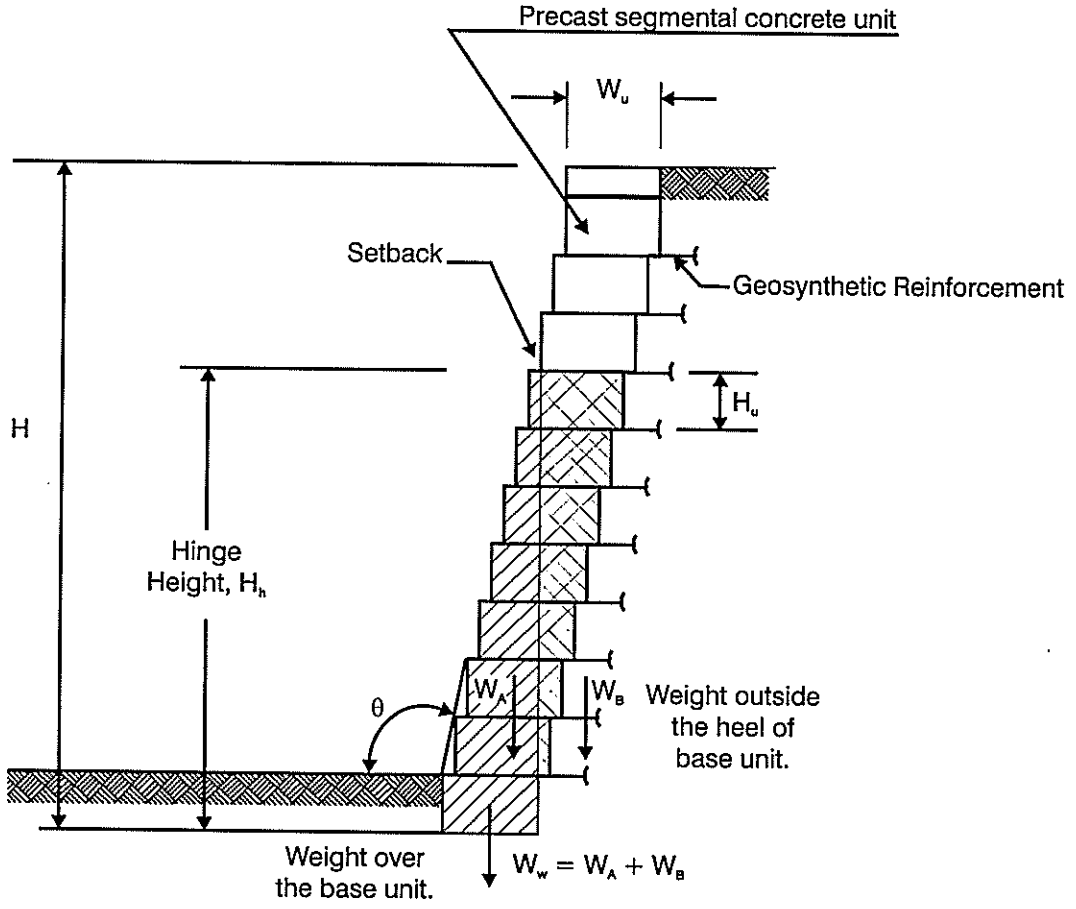

Hinge Height H_h is related to the maximum number of concrete units that can be stacked in an isolated column at a facing inclination of θ without toppling:

$H_h = 2(W_u - G_u) / \tan(\theta\text{-}90°)$

Only the weight ($W_w = W_A + W_B$) of all concrete units within H_h will be considered to act at the base of the lowermost SRW unit. The same concept is applied to assess the full weight of unit column acting on any concrete unit at any elevation (z) in the wall face.

H_u is the concrete facing block unit height
W_u is the concrete facing block unit width, front to back
G_u is the distance to the center of gravity of a horizontal segmental facing concrete unit, including aggregate fill, measured from the front of the unit
θ is the wall batter due to setback per course
H is the total height of the wall
H_h is the hinge height.

Figure E2 Hinge height for GRS walls with segmental precast concrete unit facing.

Typical interpretation of connection strength and shear capacity test data is shown on Figure E1. Both the connection strength and the shear capacity are bilinear functions of the normal load on segmental units and, therefore, can be described by linear equation (for low normal loads) and a constant maximum value (for high normal loads). The strength/shear capacity failure (solid lines on Figure E1) and the performance failure in terms of the specified deformation criteria (dashed lines on Figure E1) are separately considered.

The so-called "hinge height" concept is used to calculate normal pressures at the wall base, or pressures between two successive courses of segmental units at any level in the wall facing (Figure E2).

The hinge height (H_h) is the total height of the maximum number of segmental units that can be stacked in an isolated column at a facing inclination θ to the horizontal without toppling. It is assumed that only the weight of segmental units located within the hinge height H_h is transferred to the wall base. The "hinge height" concept is also used to assess vertical pressures between two successive courses of segmental units at any elevation in the wall facing, and to calculate the shear capacity V_u and the connection strength T_{cl}.

E2. Analysis of Local Stability

The local stability analysis should be carried out to ensure that the segmental unit facing is stable at all elevations above the toe of the wall and that connections between the facing units and reinforcement layers are not overstressed.

The following failure modes should be considered (Figure E3(a)–(e)):

- Shear failure (bulging of the facing column; Figure E3(a));
- Connection failure (rupture or slippage of the reinforcement; Figure E3(b));
- Local overturning (Figure E3(c));
- Failure of the unreinforced crest of the wall (above the highest reinforcement layer) by either shear or overturning (Figure E3(e)(d)).

E2.1 Shear Failure

Bulging of a segmental unit facing occurs when one or a number of segmental concrete units do not maintain their original relative position with respect to the units above and below them. To prevent bulging failure, the friction resistance between the segmental units should be sufficient to resist the shear forces acting in the facing column.

The shear forces on the segmental block interface are assessed by treating the facing column as a vertical beam. A simplified loading case (assuming a horizontal backfill slope and no surcharge loads) is shown on Figure E4.

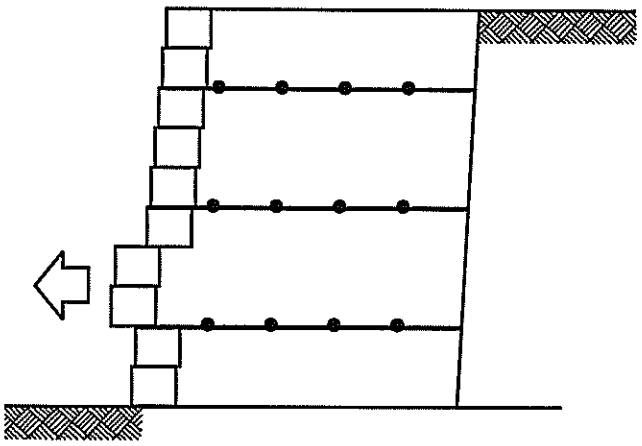

a) Shear Failure (Bulging)

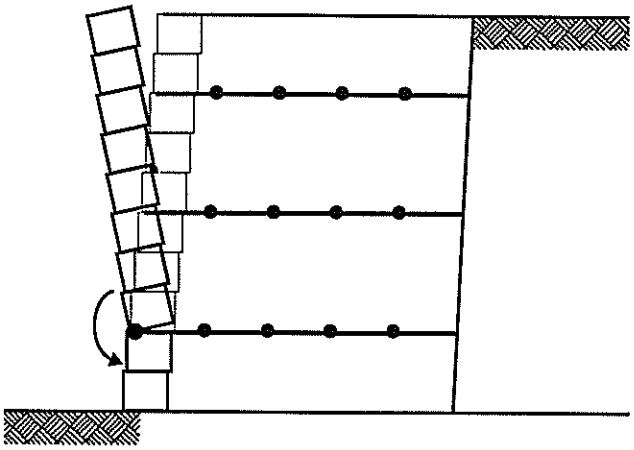

c) Local Overturning

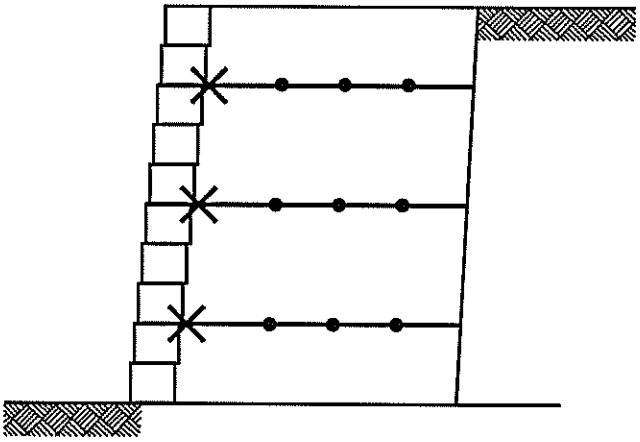

b) Connection Failure

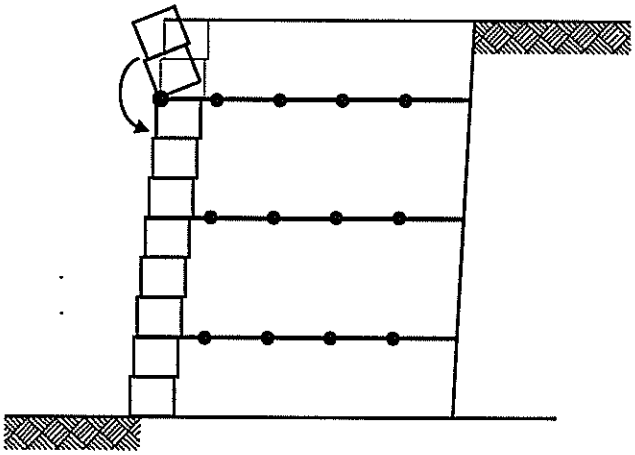

d) Crest Toppling

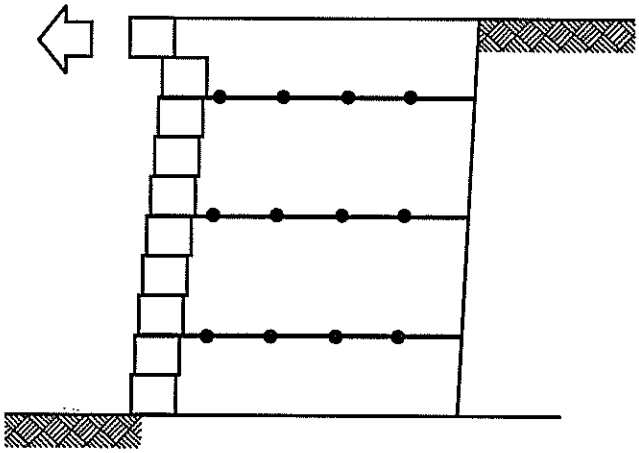

e) Crest Sliding Failure

Figure E3 Local stability failure modes for segmental GRS walls.

In general, the bulging stability should be checked for each segmental unit interface in the wall facing as follows:

- for the ultimate limit state

$$F^*_h - \sum_{j+1}^{n} F^*_i \leq \Phi_1 V_u \qquad \text{(E1)}$$

- for the serviceability limit state

$$F^*_h - \sum_{j+1}^{n} F^*_i \leq \Phi_2 V'_u \qquad \text{(E2)}$$

where:

F^*_h is the resultant of all factored horizontal disturbing forces including:

– the factored active thrust $F^*_A(z)$;

– the factored horizontal force due to sloping backfill $K_{ar}\sigma^*_{bs}z$ (refer to Section 3.4.1 of this report);

– factored horizontal forces due to concentrated loads on the top of the wall calculated as horizontal pressures $\Delta\sigma^*_h$ (Figure 3.5a) and $K_{ar}\Delta\sigma^*_v$ (Figure 3.4a) integrated over the height z of the facing column above the sliding surface (Figure E4);

– the factored inertia force $\Delta F^*_{AE}(z)$ due to the weight of the reinforced backfill (for seismic conditions only);

– the factored inertia force $F^*_w(z)$ due to the weight of the segmental facing column above the sloping surface (for seismic conditions only).

Load factors are given in Table 2.4.

ΣF^*_i is the sum of the design tensile forces in the layers of geosynthetic reinforcement above the interface considered (refer to Section 3.4.2);

V_u, V'_u are the peak shear capacity and the serviceability state shear capacity between successive courses of segmental units (refer to Section E1).

In the calculations of V_u and V'_u, the normal load on segmental units (Figure E1) should be taken as the lesser of the facing column weight within the hinge height H_h (Figure E2) and the weight of the full column above the sliding surface.

Φ_1, Φ_2 are the reduction factors for the ultimate limit state and serviceability limit state respectively:

– for static conditions: $\Phi_1 = \Phi_2 = 1.0$,

– for seismic conditions: $\Phi_1 = 0.9$ and $\Phi_2 = 1.0$.

Very often, disturbing forces under seismic conditions are too high and therefore one or both of the conditions in equations E1, E2 cannot be satisfied. In such cases deformations of the wall facing should be assessed using the deformation analysis method (Appendix D).

For structure performance category 3 (Table A5, Appendix A1.10), the shear capacity of the segmental block interface shall not be fully dependent on frictional resistance between the segmental units. Shear resisting devices such as shear keys, pins, etc., shall be used.

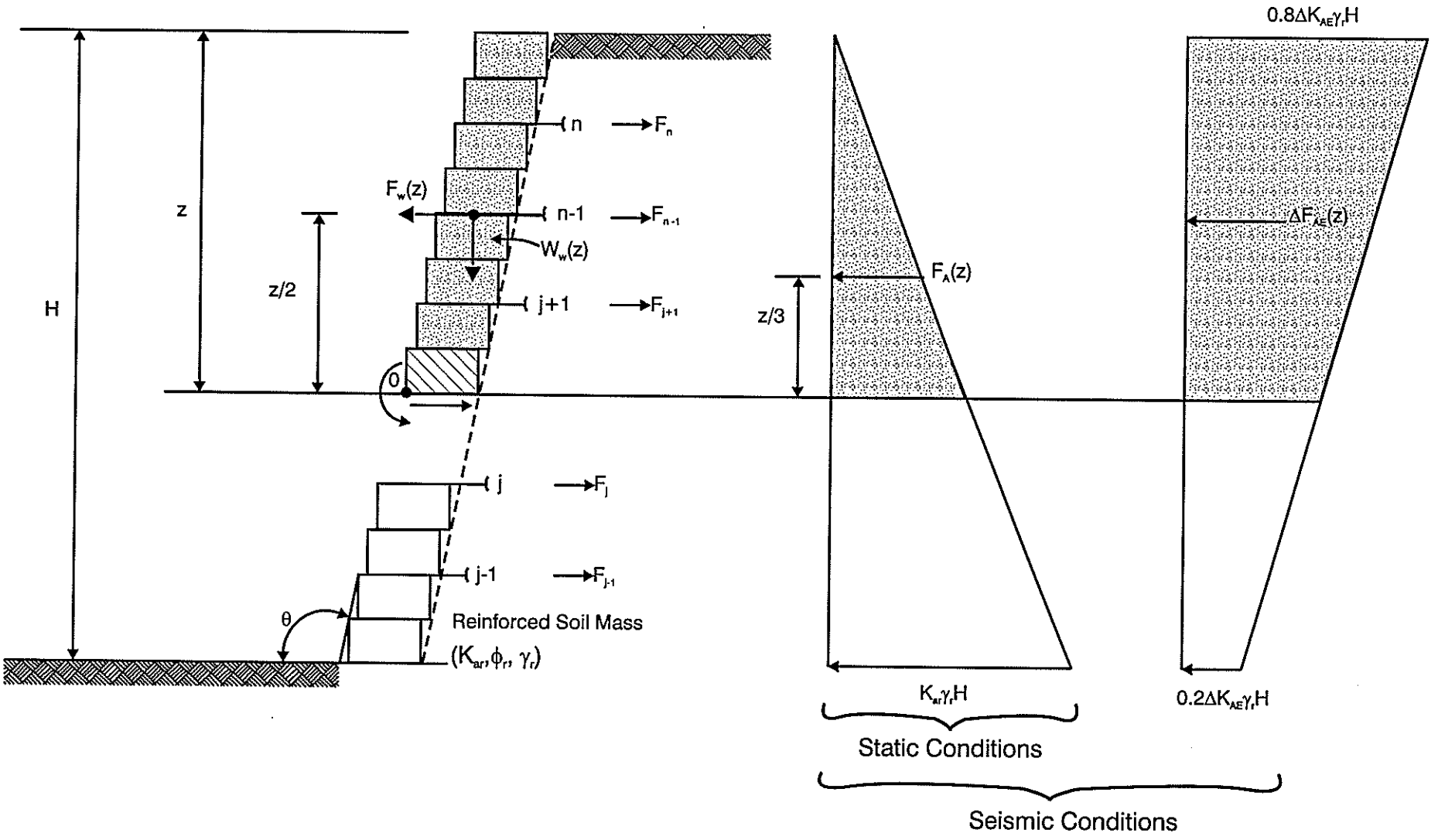

Figure E4 Forces for local stability analysis.

E2.2 Connection Failure

The strength of the connection between geosynthetic reinforcement and segmental unit blocks should be checked for each reinforcement layer as follows:

- for ultimate limit state:

$$F^*_j \leq \Phi_1 T_{cl} \quad \text{(E3)}$$

- for serviceability limit state:

$$F^*_j \leq \Phi_2 T'_{cl} \quad \text{(E4)}$$

where:

F^*_j is the design tensile force in a layer of geosynthetic reinforcement, Equations 30 and 34 (refer Sections 3.4.2, 3.5.1 respectively; and Table 2.4 for load factors);

T_{cl}, T'_{ce} are peak connection strength and serviceability connection strength between segmental units and a layer of geosynthetic reinforcement (refer to Section E1 and Figure E1);

Φ_1, Φ_2 are the reduction factors for the ultimate limit state and the serviceability limit state respectively:

– for static conditions: $\Phi_1 = \Phi_2 = 1.0$,

– for seismic conditions: $\Phi_1 = 0.9$ but the serviceability limit state is not considered.

In the calculations of T_{cl} and T'_{cl}, the normal load on segmental unit–reinforcement layer interface (Figure E1) should be taken as the lesser of the facing column weight within the hinge height H_h (Figure E2) and the weight of the full column above the reinforcement layer being considered.

E2.3 Local Overturning

The stability of local overturning of the segmental facing column against local overturning should be checked for seismic conditions as follows:

$$M^*_d \leq \Phi M^*_r \quad \text{(E5)}$$

where:

M^*_d is the resultant of all driving moments of factored forces about the toe (point O on Figure E4) of the facing unit considered;

M^*_r is the resultant of all restoring moments of factored forces about the toe of the facing unit considered;

Φ is the reduction factor for overturning under seismic conditions $\Phi = 0.9$.

The forces shown on Figure E4 and discussed in Section E2.1 should be considered in the overturning stability analysis.

E2.4 Unreinforced Crest Failure

The unreinforced column of the segmental facing units above the highest reinforcement layer has a potential to fail by internal sliding (shear) and/or overturning or crest toppling (Figure E3(e)(d)). Therefore, sliding and overturning stability analyses should be undertaken for each segmental block interface above the highest reinforcement layer.

The sliding stability analyses is identical to that described in Section E2.1 but the summation term should be excluded from Equations E1 and E2.

The overturning stability analysis is identical to that described in Section E2.3. Same forces should be considered except for the tensile forces in geosynthetic reinforcement.

Appendix F

Guideline Specifications for GRS Structures

Appendix F Guideline Specifications for GRS Structures

F1. Specification for GRS Structure (Method & Material Specification)

1. Description

Work shall consist of furnishing all materials, labour, equipment and supervision to install a GRS system in accordance with this specification and reasonably close conformity with the lines, grades, design and dimensions shown on the drawings.

2. Geosynthetic Reinforcement Material

2.1 *Acceptable Suppliers:* The specific geosynthetic reinforcement material and supplier shall be approved by the Engineer. The Contractor/Supplier submitted package should satisfactorily address the items listed in Appendix C.

2.2 *Materials:* The geosynthetic reinforcement shall be a regular network of integrally connected polymer tensile elements with aperture geometry sufficient to permit significant mechanical interlock with the surrounding soil or rock. The geosynthetic reinforcement structure shall be dimensionally stable and able to retain its geometry under construction stresses and shall have high resistance to damage during construction, to ultraviolet degradation and to all forms of chemical and biological degradation encountered in the soil being reinforced.

2.3 *GRS Design Criteria:* The geosynthetics shall have design tensile strengths, pullout and direct shear parameters and other properties as shown on the drawings for the backfills and soil type(s) indicated.

2.4 *Permeability:* The permeability of a geotextile reinforcement shall be greater than the permeability of the fill soil.

2.5 *Certification:* The Contractor shall submit a manufacturer's certification that the geosynthetics supplied meet the respective index criteria set when geosynthetic was approved by the Engineer, measured in full accordance with all test methods and standards specified. In case of dispute over validity of values, the Engineer can require the Contractor to supply test data from an approved laboratory to support the certified values submitted.

2.6 *Quality Assurance/Index Properties:* Testing procedures for measuring design properties require elaborate equipment, tedious set-up procedures and long durations for testing. These tests are inappropriate for quality assurance (QA) testing of geosynthetic reinforcements received on site.

In lieu of these tests for design properties, a series of index criteria may be established for QA testing. These index criteria include mechanical and geometric properties that directly impact the design strength and soil interaction behaviour of geosynthetics. QA testing should measure the respective index criteria set when geosynthetic was approved by the Engineer.

3. Construction

3.1 *Delivery, Storage and Handling:* The Contractor shall check the geosynthetic upon delivery to ensure that the proper material has been received. During all periods of shipment and storage the geosynthetic shall be protected from temperatures greater than 60 degrees Celsius, mud, dirt, dust and debris. The Contractor shall follow manufacturer's recommendations in regard to protection from direct sunlight.

At the time of installation geosynthetic shall be rejected if it has defects, tears, punctures, flaws, deterioration or damage incurred during manufacture, transportation or storage. If approved by the Engineer, torn or punctured sections may be repaired by placing a patch over the damaged area. Any geosynthetic damaged during storage or installation shall be replaced by the Contractor at no extra cost.

3.2 *On-Site Representative:* Geosynthetic reinforcement material suppliers shall provide a qualified and experienced representative on site, for a minimum of three days, to assist the Contractor at the start of construction. If there is more than one GRS structure on a project then this criteria will apply to construction of the initial structure only. The representative shall also be available on an as-needed basis, as requested by the Engineer, during construction of the remaining structures.

3.3 *Site Excavation:* All areas immediately beneath the installation area for the geosynthetic reinforcement shall be properly prepared as detailed on the drawings, specified elsewhere within the specifications, or directed by the Engineer. Subgrade surface shall be level, free from deleterious materials, loose or otherwise unsuitable soils. Prior to placing of geosynthetic reinforcement, subgrade shall be proofrolled to provide a uniform and firm surface. Any soft areas, as determined by the Engineer, shall be excavated and replaced with suitable compacted soils. Foundation surface shall be inspected and approved by the Engineer prior to fill placement. Benching the backcut into competent soil is recommended to improve stability.

3.4 *Geosynthetic Placement:* The geosynthetic reinforcement shall be installed in accordance with the manufacturer's recommendations. The geosynthetic reinforcement shall be placed within the layers of the compacted soil as shown on the drawings or as directed.

The geosynthetic reinforcement shall be placed in continuous, longitudinal strips in the direction of main reinforcement. However, if the Contractor is unable to complete a required length with a single continuous length of geogrid, a joint may be made with the Engineer's approval. Only one joint per length of geogrid shall be allowed. This joint shall be made for the full width of strip by using a similar material with similar strength. Joints in geogrid reinforcement shall be pulled and held taut during fill placement. Joints shall not be used with geotextiles.

Adjacent strips, in the case of 100% coverage in plan view, need not be overlapped. The minimum horizontal coverage is 50% with horizontal spacings between reinforcement no greater than 1 m. Horizontal coverage of less than 100% shall not be allowed unless specifically detailed in the construction drawings.

Adjacent rolls of geosynthetic reinforcement shall be overlapped or mechanically connected where exposed in a wraparound face system, as applicable.

Place only that amount of geosynthetic reinforcement required for immediately pending work to prevent undue damage. After a layer of geosynthetic reinforcement has been placed, the next succeeding layer of soil shall be placed and compacted as appropriate. After the specified soil layer has been placed, the next geosynthetic reinforcement layer shall be installed. The process shall be repeated for each subsequent layer of geosynthetic reinforcement and soil.

Geosynthetic reinforcement shall be placed to lay flat and pulled tight prior to backfilling. After a layer of geosynthetic reinforcement has been placed, suitable means, such as pins or small piles of soil, shall be used to hold the geosynthetic reinforcement in position until the subsequent soil layer can be placed. Under no circumstances shall a track-type vehicle be allowed on the geosynthetic reinforcement before at least 150 mm of soil has been placed.

During construction, the surface of the fill should be kept approximately horizontal. Geosynthetic reinforcement shall be placed directly on the compacted horizontal fill surface. Geosynthetic reinforcements are to be placed within 75 mm of the design elevations and extend the length as shown on the elevation view, unless otherwise directed by the Engineer. Correct orientation of the geosynthetic reinforcement shall be verified by the Contractor.

3.5 *Fill Placement:* Appropriate specification for grading, plasticity, index and other properties of fill material should be included. Fill shall be compacted as specified by project specifications or to at least 95% of the maximum density determined in accordance with Test 4.1.2 New Zealand heavy compaction test, NZS 4402:1986.

Density testing shall be made every 1,000 cubic metres of soil placement or as otherwise specified by the Engineer or contract documents.

Backfill shall be placed, spread and compacted in such a manner to minimise the development of wrinkles and/or displacement of the geosynthetic reinforcement.

Fill shall be placed in 300 mm maximum lift thickness where heavy compaction equipment is to be used and 150 mm maximum uncompacted lift thickness where hand-operated equipment is used.

Backfill shall be graded away from the face of the structure and rolled at the end of each workday to prevent ponding of water on the surface of the reinforced soil mass.

Tracked construction equipment shall not be operated directly upon the geosynthetic reinforcement. A minimum fill thickness of 150 mm is required prior to operation of tracked vehicles over the geosynthetic reinforcement. Turning of tracked vehicles should be kept to a minimum to prevent tracks from displacing the fill and the geosynthetic reinforcement.

If recommended by the geogrid manufacturer and approved by the Engineer, rubber-tired equipment may pass over the geogrid reinforcement at slow speeds, less than 2 km/h. Sudden braking and sharp turning shall be avoided.

3.5 *Erosion Control Material Installation* (Erosion Control Material Specification should be included, if appropriate).

3.6 *Geosynthetic Drainage Composite* (Drainage Composite Material Specification should be included, if appropriate).

3.7 *Final Geometry Verification:* The Contractor shall confirm that as-built structure geometrics conform to geometries shown on construction drawings (required tolerances should be specified by the Engineer).

4. Method of Measurement

The unit of measurement for furnishing the GRS structure shall be the vertical square metre of face. Payment shall cover supply and installation of the GRS system. Excavation of unsuitable materials and replacement with select fill, as directed and approved in writing by the Engineer, shall be paid for under separate pay items.

5. Basis of Payment

The accepted quantities of GRS structure will be paid for per vertical square metre in place.

F2. Specification for GRS Structure (Performance Specification)

1. Description

Work shall consist of design, furnishing all materials, labour, equipment and supervision and construction of a GRS structure in accordance with this specification and in reasonably close conformity with the lines, grades, design and dimensions shown on the drawings. Supply of geosynthetic reinforcement, drainage composite and erosion control materials and site assistance are all to be furnished by the GRS system Supplier/Contractor. The Contractor shall also provide evidence of building consent approval by the local consent authority.

2. GRS System

2.1 *Acceptable Suppliers:* proposed materials/system shall be reviewed and accepted by the Engineer. The material/system supplier submitted package should satisfactorily address the items listed in Appendix C.

2.2 *Materials:* only those geosynthetic reinforcement, drainage composite and erosion mat materials accepted by the Engineer shall be utilised. (Generic specifications for soil reinforcement, drainage composite and geosynthetic erosion mat materials should be included.)

2.3 *Design Criteria:* (project-specific design criteria should be specified and may include required design life, structure category, minimum soil reinforcement length, foundation soil parameters, required minimum embedment for the structure, post-construction settlement control, etc.).

2.4 *Design Submittal:* the Contractor shall submit three (3) sets of detailed design calculations, construction drawings and specifications for approval within twenty (20) days of authorisation to proceed and at least forty (40) days prior to the beginning of GRS structure construction.

2.5 *Material Submittal:* the Contractor shall submit three (3) sets of manufacturer's certification that indicate the geosynthetic soil reinforcement, drainage composite and geosynthetic erosion mat meet the requirements set forth in the respective material specifications, for approval at least twenty (20) days prior to the start of GRS structure construction.

3. Construction

3.1 *Delivery, Storage and Handling:* The Contractor shall check the geosynthetic upon delivery to ensure that the proper material has been received. During all periods of shipment and storage the geosynthetic shall be protected from temperatures greater than 60 degrees Celsius, mud, dirt, dust and debris. The Contractor shall follow manufacturer's recommendations in regard to protection from direct sunlight.

At the time of installation geosynthetic shall be rejected if it has defects, tears, punctures, flaws, deterioration or damage incurred during manufacture, transportation or storage. If approved by the Engineer, torn or punctured sections may be repaired by placing a patch over the damaged area. Any geosynthetic damaged during storage or installation shall be replaced by the Contractor at no extra cost.

3.2 *On-Site Representative:* Geosynthetic reinforcement material suppliers shall provide a qualified and experienced representative on site, for a minimum of three (3) days, to assist the Contractor at the start of construction. If there is more than one GRS structure on a project then this criteria will apply to construction of the initial structure only. The representative shall also be available on an as-needed basis, as requested by the Engineer, during construction of the remaining structures.

3.3 *Site Excavation:* All areas immediately beneath the installation area for the geosynthetic reinforcement shall be properly prepared as detailed on the drawings, specified elsewhere within the specifications, or directed by the Engineer. Subgrade surface shall be level, free from deleterious materials, loose or otherwise unsuitable soils. Prior to placing of geosynthetic reinforcement, subgrade shall be proofrolled to provide a uniform and firm surface. Any soft areas, as determined by the Engineer, shall be excavated and replaced with suitable compacted soils. Foundation surface shall be inspected and approved by the Engineer prior to fill placement. Benching the backcut into competent soil is recommended to improve stability.

3.4 *Geosynthetic Placement:* The geosynthetic reinforcement shall be installed in accordance with the manufacturer's recommendations. The geosynthetic reinforcement shall be placed within the layers of the compacted soil as shown on the drawings or as directed.

The geosynthetic reinforcement shall be placed in continuous, longitudinal strips in the direction of main reinforcement. However, if the Contractor is unable to complete a required length with a single continuous length of geogrid, a joint may be made with the Engineer's approval. Only one joint per length of geogrid shall be allowed. This joint shall be made for the full width of strip by using a similar material with similar strength. Joints in geogrid reinforcement shall be pulled and held taut during fill placement. Joints shall not be used with geotextiles.

Adjacent strips, in the case of 100% coverage in plan view, need not be overlapped. The minimum horizontal coverage is 50% with horizontal spacings between reinforcement no greater than 1 m. Horizontal coverage of less than 100% shall not be allowed unless specifically detailed in the construction drawings.

Adjacent rolls of geosynthetic reinforcement shall be overlapped or mechanically connected where exposed in a wraparound face system, as applicable.

Place only that amount of geosynthetic reinforcement required for immediately pending work to prevent undue damage. After a layer of geosynthetic reinforcement has been placed, the next succeeding layer of soil shall be placed and compacted as appropriate. After the specified soil layer has been placed, the next geosynthetic reinforcement layer shall be installed. The process shall be repeated for each subsequent layer of geosynthetic reinforcement and soil.

Geosynthetic reinforcement shall be placed to lay flat and pulled tight prior to backfilling. After a layer of geosynthetic reinforcement has been placed, suitable means, such as pins or small piles of soil, shall be used to hold the geosynthetic reinforcement in position until the subsequent soil layer can be placed. Under no circumstances shall a track-type vehicle be allowed on the geosynthetic reinforcement before at least 150 mm of soil has been placed.

During construction, the surface of the fill should be kept approximately horizontal. Geosynthetic reinforcement shall be placed directly on the compacted horizontal fill surface. Geosynthetic reinforcements are to be placed within 75 mm of the design elevations and extend the length as shown on the elevation view, unless otherwise directed by the Engineer. Correct orientation of the geosynthetic reinforcement shall be verified by the Contractor.

3.5 *Fill Placement:* Appropriate specification for grading, plasticity, index and other properties of fill material should be included. Fill shall be compacted as specified by project specifications or to at least 95% of the maximum density determined in accordance with Test 4.1.2 New Zealand heavy compaction test, NZS 4402:1986.

Density testing shall be made every 1,000 cubic metres of soil placement or as otherwise specified by the Engineer or contract documents.

Backfill shall be placed, spread and compacted in such a manner to minimise the development of wrinkles and/or displacement of the geosynthetic reinforcement.

Fill shall be placed in 300 mm maximum lift thickness where heavy compaction equipment is to be used and 150 mm maximum uncompacted lift thickness where hand-operated equipment is used.

Backfill shall be graded away from the face of the structure and rolled at the end of each workday to prevent ponding of water on the surface of the reinforced soil mass.

Tracked construction equipment shall not be operated directly upon the geosynthetic reinforcement. A minimum fill thickness of 150 mm is required prior to operation of tracked vehicles over the geosynthetic reinforcement. Turning of tracked vehicles should be kept to a minimum to prevent tracks from displacing the fill and the geosynthetic reinforcement.

If recommended by the geogrid manufacturer and approved by the Engineer, rubber-tired equipment may pass over the geogrid reinforcement at slow speeds, less than 2 km/h. Sudden braking and sharp turning shall be avoided.

3.5 *Erosion Control Material Installation* (Erosion Control Material Specification should be included, if appropriate).

3.6 *Geosynthetic Drainage Composite* (Drainage Composite Material Specification should be included, if appropriate).

3.7 *Final Geometry Verification:* The Contractor shall confirm that as-built structure geometrics conform to geometries shown on construction drawings (required tolerances should be specified by the Engineer).

4. Method of Measurement

Measurement of Geosynthetic Reinforced Soil Structure is on a vertical square metre basis.

Payment shall cover GRS structure design, supply and installation of geosynthetic soil reinforcement, reinforced soil fill, drainage composite and geosynthetic erosion mat. Excavation of any unsuitable materials and replacement with select fill, as directed by the Engineer, shall be paid under a separate pay item.

Quantities of reinforced soil structure as shown on the plans may be increased or decreased at the direction of the Engineer based on construction procedures and actual site conditions.

5. Basis of Payment

The accepted quantities of geosynthetic reinforced soil structure will be paid for per vertical square metre in place.

Appendix G

Worked Examples for GRS Walls

Appendix G Worked Examples for GRS Walls

G1 Example 1: Example of Gravity Load Design Calculation of a GRS wall with Modular Block Facing

A typical GRS wall design will be illustrated using the design procedures outlined in these Guidelines. The wall has modular block facing. Details of the proposed wall are given in Table G1 and a section is shown in Figure G1.

Table G1 Design parameters for GRS walls with modular block facings.

Description	Symbol	Parameter	Units
Wall, Backfill and Foundation Soil			
Wall Height	H	2.4	m
Inclination of the Wall face from Horizontal	θ	93	Degrees
Backfill Slope Angle	β	18	Degrees
Angle of Internal Friction for Reinforced Backfill	ϕ_r	28	Degrees
Cohesion of Reinforced Backfill	c_r	0	kPa
Unit Weight of Reinforced Backfill	γ_r	19	kN/m^3
Angle of Internal Friction for Retained Backfill	ϕ_f	28	Degrees
Cohesion of Retained Backfill	c_f	0	kPa
Unit Weight of Retained Backfill	γ_f	19	kN/m^3
Angle of Internal Friction for Foundation Soil	ϕ	28	Degrees
Cohesion of Foundation Soil	c	0	kPa
Unit Weight of Foundation Soil	γ	19	kN/m^3
Modular Blocks			
Modular Block Height	H_u	150	mm
Modular Block width	W_u	305	mm
Unit Weight of Modular Block	γ_u	19	kN/m^3
Apparent Minimum Shear Capacity Between Modular Blocks	a_u	5.836	kN/m
Apparent Angle of Friction between Modular Blocks	λ_u	30	Degrees
Apparent Minimum Connection Strength Between Geogrid and Modular Bocks	a_{cs}	4.973	kN/m
Apparent Angle of Friction for Connection Strength Between Geogrid and Modular Blocks	λ_{cs}	43	Degrees
Geosynthetic Reinforcement			
Ultimate Tensile Strength of Geogrid	T_{ult}	38.3	kN/m
Uncertainty Factor (Manufacturing)	Φ_m	1	-
Reduction Factor for Creep Deformation	Φ_{cr}	0.63	-
Uncertainty Factor (Extrapolation)	Φ_e	1.0	-
Reduction Factor (Installation Damage)	Φ_i	0.85	-

Reduction Factor (Chemical Degradation)	Φ_{rch}	1.0	-
Reduction Factor (Biological Degradation)	Φ_{rb}	1.0	-
Uncertainty Factor (Overall Degradation)	Φ_d	0.95	-
Reduction Factor (joints, seams, connections)	Φ_j	1.0	-
Reduction Factor Associated with Ramification of Failure	Φ_n	1.0	-
Scale Effect Correction Factor	α	1.0	-
Pullout Resistance Factor	F^*	0.371	-
Soil-Reinforcement Interface Friction Angle	ρ	26	Degrees
Load Factors and Reduction Factors			
Load Factors	α_i	As recommended by appropriate sections of the Guidelines	-
Reduction Factors	Φ_i	As recommended by appropriate sections of the Guidelines	-

Wall Height

Wall height above the ground surface level: H=2.4m
Minimum required embedment (Table 2.1): H/10=0.24m
Minimum required embedment (Section 2.5): 0.5m
Wall height above the subgrade level: $H=2.4_m + 0.5m=2.9m$

Consider external stability of the wall.

G1.1 Select Reinforcement Length

Try Block width $B = (L+W_u) \approx 0.7\text{-}0.8H_{tot}$

Assume L = 1.7m (ie $B/H_{tot} \approx 0.7$)
B = 1.7+0.305=2.005 m

G1.2 Calculate the force due to active soil thrust

Calculate the height over which the soil pressures are considered to act.

$$h^* = H\text{-}h = \frac{L\sin\theta\sin\beta}{\sin(180-\beta-\theta)} =$$

$$= \frac{1.7^\circ \sin 93^\circ \sin 18^\circ}{\sin(180-18-93)} = 0.56 \text{ m}$$

$$H_{tot} + h^* = 2.9 + 0.56 = 3.46\text{m}$$

Calculate K_{af} (Equation 3):

$$K_{af} = \cos\beta \left[\frac{\cos\beta\beta - \sqrt{\cos^2\beta - \cos^2\phi_f}}{\cos\beta + \sqrt{\cos^2\beta - \cos^2\phi_f}} \right] =$$

$$= \cos 18^\circ \left[\frac{\cos 18^\circ - \sqrt{\cos^2 18^\circ - \cos^2 28^\circ}}{\cos 18^\circ + \sqrt{\cos^2 18^\circ - \cos^2 28^\circ}} \right] = 0.436$$

Total active soil force:
$F_A = 0.5\ K_{af}\ \gamma_f\ h^2 = 0.5 \times 0.436 \times 19 \times 3.46^2 = 49.59$ kN/m

Horizontal component of the total active soil force:
$F_{ah} = F_A \cos(\delta + 90^\circ - \theta)$

Assuming $\delta = \beta$:
$F_{Ah} = F_A \cos(\beta + 90^\circ - \theta) = 49.59 \times \cos(18^\circ + 90^\circ - 93^\circ) = 47.90$ kN/m

Location of the horizontal component above the subgrade level:
$y_{Ah} = 3.46/3 = 1.15$m

G1.3 Forward Sliding

Driving force:
$F_h^* = F_{Ah}^* = \alpha F_{Ah} = 1.5 \times 47.90 + 71.85$ kN/m

α is the load factor from Table 2.4, load combination B

Weight of the reinforced block:
$V_1 = B \times H_{tot} \times \gamma_r = 2.005 \times 2.9 \times 19 = 110.48$ kN/m

$$V_2 = \frac{\gamma_f L h^*}{2} = (19 \times 1.7 \times 0.56)/2 = 9.04 \text{ kN/m}$$

Vertical factored force:
$F_v^* = \alpha(V_1 + V_2) = 1.0 \times (110.48 + 9.04) = 119.52$ kN/m
where:
α is the load factor from Table 2.4 (in the Guidelines).

Factored resisting force:

A. Sliding along the foundation soil

$\Phi F_v^* \tan \phi = 1.0 \times 119.52 \times \tan 28° = 63.55$ kN/m

where:

Φ is the reduction factor for sliding (Section 3.1.2 in the Guidelines)

B. Sliding along the reinforced backfill

As above, because in our example $\phi = \phi_r = 28°$

$\Phi F_v^* \tan\phi_r = 63.55$ kN/m

C. Sliding along soil reinforcement interface

Ultimate soil-geosynthetic interaction strength

$T_{i,2} = (\tan \rho)\ \alpha\ \sigma^*_v\ L_e = (\tan \rho)\ \alpha\ F_v^* =$

$= (\tan 26°) \times 1.0 \times 119.52 = 58.29$ kN/m

Factored soil-geosynthetic interaction strength:

$T^*_{di,2} = T_{i,2}\ \Phi\ \Phi_n = 58.29 \times 0.8 \times 1.0 = 46.63$ kN/m

Check conditions (7) and (8):

$F_h^* = 71.85$ kN/m $\leq \Phi F_v^* \tan \phi = 63.55$ kN/m

$F_h^* = 71.85$ kN/m $\leq T_{di,2}^* = 46.63$ kN/m

The conditions are not satisfied

Assume L = 2.8 m

B = 2.8 + 0.305 = 3.105 m

$h^* = 0.92$

$H_{tot} + h^* = 2.9 + 0.92 = 3.82$ m

$F_A = 0.5 \times 0.436 \times 19 \times 3.82^2 = 60.44$ kN/m

$F_{Ah} = 60.44 \times \cos (18° + 90° - 93°) = 58.38$ kN/m

$y_{Ah} = 3.82/3 = 1.27$m

$F_h^* = F_{hA}^* = 1.5 \times 58.38 = 87.57$ kN/m

$V_1 = 3.105 \times 2.9 \times 19 = 171.09$ kN/m

$V_2 = (19 \times 2.8 \times 0.92)/2 = 24.47$ kN/m

$F_v^* = 1.0\ (171.09 + 24.47) = 195.56$ kN/m

A. $\Phi F_v^* \tan\phi = 1.0 \times 195.56 \times \tan 28° = 103.98$ kN/m

B. As above.

C. $T_{i,2} = \tan 26° \times 1.0 \times 195.56 = 95.38$ kN/m
$T_{di,2}^{*} = 95.38 \times 0.8 \times 1.0 = 76.30$ kN/m
Check Conditions (7) and (8)

87.57 kN/m ≤ 103.98 kN/m (7)
87.57 kN/m ≤ 76.30 kN/m (8)

Condition (7) is satisfied. Condition (8) is not satisfied if the lowest geogrid layer is placed at the base of the wall. As shown in further calculations (refer to Section G1.13), condition (8) will be satisfied if the lowest geogrid layer is placed 0.3 m above the base of the wall and the friction force between the modular blocks is taken into account.

G1.4 Bearing Capacity

Assess ultimate bearing capacity of soil. Equation 4.6.4 from Manuals for the Design of Bridge Foundations (NCHRP 1991) is used here. Any other appropriate method can also be used.

$q_u = 0.5\gamma B' N_{\gamma m} + \gamma D_f N_{qm}$
where:
B' is the reduced effective width of the wall base
$N_{\gamma m} = N_\gamma s_\gamma c_\gamma i_\gamma d_\gamma$
$N_\gamma = 17$ (bearing capacity factor)
$s_\gamma = 0.96$ (footing shape factor)
$c_\gamma = 0.96$ (soil compressibility factor)
i_γ is a function of load inclination
$d_\gamma = 1.0$ (embedment factor)

$N_{qm} = N_q s_q c_q i_q d_q$

$N_q = 15$ (bearing capacity factor)
$s_q = 1.05$ (footing shape factor)
$c_q = 0.96$ (soil compressibility factor)
i_q is a function of load inclination
$d_q = 1.0$ (embedment factor)

$D_f = 0.5$m (embedment depth)

Determine the eccentricity:
$F_{Av} = 60.44 \sin (18°+90°-93°) = 15.64$ kN/m =
$x_{v1} = [B + H_{tot} \tan (\theta - 90°)]/2 =$
$= [3.105 + 2.9 \times \tan (93°-90°)]/2 = 1.628$ m
$x_{v2} = H_{tot} \tan (\phi - 90°) + W_u + 2L/3 =$
$= 2.9 \times \tan (93°-90°) + 0.305 + 2 \times 2.8/3 = 2.324$ m

$x_{Av} = B + y_{Ah} \tan (\theta - 90°) =$
$= 3.105 + 1.27 \tan (93°-90°) = 3.172$ m

$$e = \frac{F_{Ah}^{*} y_{Ah} - V_1^{*}(x_{v1} - B/2) - V_2^{*}(x_{v2} - B/2) - F_{Av}^{*}(x_{Av} - B/2)}{V_1^{*} + V_2^{*} + F_{Av}^{*}} =$$

$$= \frac{87.5x1.27 - 1.5x171.09(1.628 - 3.105/2) - 1.5x24.47(2.324 - 3.105/2) - 1.5x15.64(3.172 - 3.105/2)}{1.5x171.09 + 1.5x24.47 + 1.5x15.64} =$$

= 0.081m
(all forces are factored as per Combination A, Table 2.4 in Guidelines).

$\sigma_v^{*} = F_v^{*}/(B\text{-}2\ e) = (V_1^{*} + V_2^{*} + F_{Av}^{*})/ (B\text{-}2\ e) =$
$= 316.80/(3.105\text{-}2x0.081) = 107.65$ kPa

Calculate q_u:
$F_h^{*}/F_v^{*} = 87.57/316.80 = 0.28$

Therefore $i_\gamma = 0.38$; $i_q = 0.53$

$B' = B\text{-}2e = 3.105 - 2 \times 0.081 = 2.943$m
$N_{\gamma m} = 17 \times 0.96 \times 0.96 \times 0.38 \times 1.0 = 5.953$
$N_{qm} = 15 \times 1.05 \times 0.96 \times 0.53 \times 1.0 = 8.014$
$q_u = 0.5x\ 19 \times 2.943 \times 5.953 + 19 \times 0.5 \times 8.014 = 242.57$ kPa

Check Condition (11) in Guidelines:

$$\sigma_v^{*} = \frac{F_v^{*}}{B'} = \frac{316.80}{2.943} = 107.65 \text{ kPa} \le \Phi q_u = 0.6 \times 242.57 = 145.54 \text{ kPa}$$

The condition is satisfied.

G1.5 Overturning

Driving moments:
$M_d^{*} = F_{Ah}^{*}\ y_{Ah} = \alpha\ F_{Ah}\ y_{Ah} = 1.5 \times 58.38 \times 1.27$
$= 111.21$ kNm/m

Restoring moments:
$M_r^{*} = \alpha V_1 x_{v1} + \alpha\ V_2\ x_{v2} + \alpha F_{Av}\ x_{av} =$
$= 1 \times 171.09 \times 1.628 + 1 \times 24.47 \times 2.342 + 1 \times 15.64 \times 3.172 =$
$= 389.45$ kNm/m

Check Condition (12) in Guidelines:
$M^{*}_d = 111.21$ kNm/m $\le \Phi\ M_r^{*} = 0.75 \times 385.45 = 289.09$ kNm/m

The condition is satisfied.

Consider internal stability of the wall.

G1.6 Lateral Soil Pressures caused by Reinforced Backfill and Imposed Surcharge Loads

From Equation (27) in Guidelines:
$K_{ar} = \tan^2 (45° - \phi r/2) = \tan^2 (45°-28°/2) = 0.36$

Calculate load due to sloping backfill (refer to Figure 3.9 in Guidelines):
$\sigma_{bs} = 0.5\ L\ \gamma_f \tan \beta = 0.5 \times 2.8 \times 19 \times \tan 18° =$
$= 8.64$ kPa

Horizontal design soil pressures:
$\sigma_{hj} = \sigma_{h,a} + K_{ar}\ \sigma_{bs} =$
$= K_{ar}\ \gamma_r\ z_j + K_{ar}\ \sigma_{bs} =$
$= 0.36 \times 19 \times z_j + 0.36 \times 8.64 = 3.11 + 6.84z$ kPa

G1.7 Design Tensile Strength of Geogrid

$T^*_d = T_{ult}\ \Phi_m\ \Phi_{rc}\ \Phi_e\ \Phi_i\ \Phi_{rch}\ \Phi_{rb}\ \Phi_d\ \Phi_j\ \Phi_n =$
$= 38.3 \times 1 \times 0.63 \times 1.0 \times 0.85 \times 1.0 \times 1.0 \times 0.95 \times 1.0 \times 1.0 =$
$= 19.48$ kN/m

G1.8 Minimum Number of Reinforcement Layers Required

Pressure distribution:
Top of facing: $\sigma_{ht} = 3.11$ kPa
Bottom of facing: $\sigma_{hb} = 3.11 + 6.84z = 3.11 + 6.84 \times 2.9 = 22.95$ kPa

Total factored force: $\Sigma F_j^* = \alpha\ 0.5(\sigma_{ht} + \sigma_{hb}) \times H_{tot} =$
$= 1.5 \times 0.5\ (3.11 + 22.95) \times 2.95 = 56.68$ kN/m
where:
$\alpha = 1.5$ – load factor

Minimum number of geogrid reinforcement required:

$$N = \frac{\Sigma F_j^*}{T_d^*} = \frac{56.68}{19.48} = 2.91$$

For GRS walls with modular block facing recommended spacings between geogrid layers is normally advised by modular block manufacturers. Recommended spacing is governed by shear and connection strength capacity of modular blocks. Assume a maximum spacing of 600 mm for our wall.

G1.9 Reinforcement Layout

Select the following trial reinforcement layout:

$z_1 = 2.6$ m	$S_{v1} = 0.6$ m
$z_2 = 2.0$ m	$S_{v2} = 0.6$ m
$z_3 = 1.4$ m	$S_{v3} = 0.6$ m
$z_4 = 0.8$ m	$S_{v4} = 0.6$ m
$z_5 = 0.2$ m	$S_{v5} = 0.5$ m

G1.10 Tensile Loads Applied to Each Layer

$F_1 = \sigma_{h1} S_{v1} = (3.11 + 6.84 \times 2.6) \times 0.6 = 12.54$ kN/m
$F_2 = \sigma_{h2} S_{v2} = (3.11 + 6.84 \times 2.0) \times 0.6 = 10.07$ kN/m
$F_3 = \sigma_{h3} S_{v2} = (3.11 + 6.84 \times 1.4) \times 0.6 = 7.61$ kN/m
$F_4 = \sigma_{h4} S_{v4} = (3.11 + 6.84 \times 0.8) \times 0.6 = 5.15$ kN/m
$F_5 = \sigma_{h5} S_{v5} = (3.11 + 6.84 \times 0.25) \times 0.5 = 2.41$ kN/m

$F_1^* = \alpha F_1 = 1.5 \times 12.54 = 18.81$ kN/m
$F_2^* = \alpha F_2 = 1.5 \times 10.07 = 15.12$ kN/m
$F_3^* = \alpha F_3 = 1.5 \times 7.61 = 11.42$ kN/m
$F_4^* = \alpha F_4 = 1.5 \times 5.15 = 7.73$ kN/m
$F_5^* = \alpha F_5 = 1.5 \times 2.14 = 3.21$ kN/m

G1.11 Tensile Strength

All factored forces F_j^* are less than $T_d^* = 19.48$ kN/m. Therefore condition (31) is satisfied.

G1.12 Pullout

Calculate the adherence length in the resistance zone behind the failure surface.

Inclination of the failure surface using the equation on Figure 3.9 in Guidelines:
$\phi_r = 28°$; $\delta = \beta = 18°$; $\theta = 93°$

$\tan(\psi - \phi_r) =$

$$= \frac{-\tan(28-18) + \sqrt{\tan(28-18)[\tan(28-18) + \cot(28+93-90)][1 + \tan(18+90-93)\cot(28+93-90)]}}{1 + \tan(18+90-93)[\tan(28-18) + \cot(28+93-90)]},$$

$\tan(\psi - \phi_r) = 0.341$

$\psi - 28° = 18.8$
$\psi = 46.8°$

Adherence length past the failure plane:
$L_{e,j} = L - (H_{tot} - z_j) \tan(90-\psi) + (H_{tot} - z_j) \tan(\theta - 90°)$

$L_{e,1} = 2.8 - (2.9-2.6) \times \tan(90°-46.8°) + (2.9-2.6) \tan(93°-90°) = 2.53$ m
$L_{e,2} = 2.8 - (2.9-2.0) \times \tan(90°-46.8°) + (2.9-2.0) \tan(93°-90°) = 2.00$ m
$L_{e,3} = 2.8 - (2.9-1.4) \times \tan(90°-46.8°) + (2.9-1.4) \tan(93°-90°) = 1.47$ m
$L_{e,4} = 2.8 - (2.9-0.8) \times \tan(90°-46.8°) + (2.9-0.8) \tan(93°-90°) = 0.94$ m
$L_{e,5} = 2.8 - (2.9-0.2) \times \tan(90°-46.8°) + (2.9-0.2) \tan(93°-90°) = 0.41$ m

Average depth of overburden $z_{p,j}$ (refer to Figure 3.9 in Guidelines):
$z_{p,j} = z_j + [0.5\ L_{e,j} + (H_{tot}-z_j)/\tan\psi - H\ H_{tot}\ (\phi-90°)]\ \tan\beta$

$z_{p,1} = 2.6 + [0.5 \times 2.53 + (2.9-2.6)/\tan46.8° - 2.9 \tan(93°-90°)]\ \tan18° = 3.05$ m
$z_{p,2} = 2.9 + [0.5 \times 2.0 + (2.9-2.0)/\tan46.8°-2.9 \tan(93°-90°)]\ \tan18° = 2.55$ m
$z_{p,3} = 1.4 + [0.5 \times 1.47 + (2.9-1.4)/\tan46.8°-2.9 \tan(93°-90°)]\tan18° = 2.05$ m
$z_{p,4} = 0.8 + [0.5 \times 0.94 + (2.9-0.8)/\tan46.8°-2.9 \tan(93°-90°)]\tan18° = 1.55$ m
$z_{p,5} = 0.2 + [0.5 \times 0.41 + (2.9-0.2)/\tan46.8°-2.9 \tan(93°-90°)]\tan18° = 1.05$ m

Calculate the design soil reinforcement interaction strength for pullout (Equations A5 and A7 in Appendix A):
$T_{i,1} = F^*\ \sigma_v^*\ L_c\ C;\ C = 2$
$T^*_{di,1} = T_{i,1}\ \Phi\ \Phi_n = \Phi\ \Phi_n F^*\ \alpha\ \sigma_v^*\ L_e\ C$
$\Phi = 0.8\quad \Phi_n = 1.0$

$j = 1\quad T^*_{di,1} = 0.8 \times 1.0 \times 0.371 \times 1.0 \times (3.05 \times 19) \times 2.53 \times 2 = 87.03$ kN/m
$j = 2\quad T^*_{di,1} = 0.8 \times 1.0 \times 0.371 \times 1 \times (2.55 \times 19) \times 2.0 \times 2 = 57.52$ kN/m
$j = 3\quad T^*_{di,1} = 0.8 \times 1.0 \times 0.371 \times 1 \times (2.05 \times 19) \times 1.47 \times 2 = 33.99$ kN/m
$j = 4\quad T^*_{di,1} = 0.8 \times 1.0 \times 0.371 \times 1 \times (1.55 \times 19) \times 0.94 \times 2 = 16.43$ kN/m
$j = 5\quad T^*_{di,1} = 0.8 \times 1.0 \times 0.371 \times 1 \times (1.05 \times 19) \times 0.41 \times 2 = 4.86$ kN/m

All factored forces F_j^* (refer to Section G1.10) are less than $T^*_{di,1}$ for each layer of geosynthetic reinforcement. Therefore condition (32) is satisfied.

G1.13 Internal Sliding Failure

The potential for an internal sliding failure should be checked at each geosynthetic reinforcement level. Destabilising force $F^*_{h,z}$ increases proportionately with z_j^2. Resisting force increases proportionately with z_j. Therefore, if condition (33) is satisfied for the lowest reinforcement layer, then all other reinforcement layers will have adequate resistance to internal sliding failure.

(This statement may not be correct for other GRS walls. For GRS walls with non-uniform lengths of reinforcement layers, non-uniform backfill materials etc., sliding along all reinforcement layers should be checked.)

Check lowest layer.
Driving force:
$F_A = 0.5\ K_{af}\ \gamma_f h^2 = 0.5\ K_{af}\ \gamma_f (H_{tot} + h^* - 2H_u)^2 =$
$= 0.5 \times 0.436 \times 19 \times (3.82-2 \times 0.15)^2 =$
$= 51.32$ kN/m

$F_{Ah} = F_A \cos(\beta + 90° - \phi) = 51.32 \cos(18° + 90° - 93°) =$
$= 49.57$ kN/m

$F^*_{h,z1} = \alpha F_{Ah} = 1.5 \times 49.57 = 74.36$ kN/m

From Section G1.3:
$V_2 = 24.47$ kN/m
$V_1 = B \times (H_{tot}-2H_u)\,\gamma_f = 3.105 \times (2.9-2\times0.15) \times 19 = 153.39$ kN/m
$F_v^* = L\,(V_1 + V_2) = 1.0(24.47 + 153.39) = 177.86$ kN/m
$T_{i,2} = (\tan\rho)\,\alpha\,F_v^* = \tan 26° \times 1 \times 177.86 = 86.75$ kN/m
$T_{di,2}^* = \Phi\,\Phi_n\,T_{i,2} = 0.8 \times 1 \times 86.75 = 69.40$ kN/m

In Condition (33) $T_{fr}^* = V_u$ is the design shear resistance provided by the wall facing (refer to Appendix E).

For the lowest layer of reinforcement (z_1=2.6m), V_u can be calculated using recommendations given on Figure E1 (Appendix E):
$T_{fr}^* = V_u = a_u + N\tan\lambda_u =$
$= 5.836 + (2.6\times0.305\times19)\tan 30° = 14.53$ kN/m

Check Condition (33):
$F_{h,z1}^* = 74.36$ kN/m $\leq T_{di,2}^* + T_{fr}^* = 69.40+14.53 = 83.93$ kN/m

Therefore Condition (33) is satisfied.

Condition (33) for the lowest layer of reinforcement is completely identical to condition (8) analysed in G1.3. Therefore condition (8) for the chosen reinforcement layout is also satisfied.

G1.14 Local Stability

A. Shear failure (bulging of the facing column)
Hinge height (Figure E2):

$H_h = 2(W_u-G_u)/\tan(\theta-90°) =$
$= 2(0.305-0.1525)/\tan(93°-90°) = 5.82$ m

As hinge height is higher than the total height of the GRS wall, it will not be used in further analysis.

Horizontal disturbing forces at different elevations are as follows:
$z = z_j$ $\quad F_h^* = \alpha\,0.5\,(\sigma_{ht}+\sigma_{h,z})\,z_j$
$\sigma_{ht} = 3.11$ kPa; $\sigma_{h,z} = 3.11 + 6.84z_j$ kPa; α = 1.5-load factor
(similar to equations used in Section G1.6)

$z = z_1 = 2.6$m $\quad F_h^* = 1.5\times0.5(3.11+3.11+6.84\times2.6)\times 2.6 = 46.81$ kN/m
$z = z_2 = 2.0$m $\quad F_h^* = 1.5\times0.5(3.11+3.11+6.84\times2.0)\times 2.0 = 29.85$ kN/m
$z = z_3 = 1.4$m $\quad F_h^* = 1.5\times0.5(3.11+3.11+6.84\times1.4)\times 1.4 = 16.58$ kN/m
$z = z_4 = 0.8$m $\quad F_h^* = 1.5\times0.5(3.11+3.11+6.84\times0.8)\times 0.8 = 7.02$ kN/m
$z = z_5 = 0.2$m $\quad F_h^* = 1.5\times0.5(3.11+3.11+6.84\times0.2)\times 0.2 = 1.14$ kN/m

From previous calculations:
$z = z_1 = 2.6m$ $F_1^* = 18.81$ kN/m
$z = z_2 = 2.0m$ $F_2^* = 15.12$ kN/m
$z = z_3 = 1.4m$ $F_3^* = 11.42$ kN/m
$z = z_4 = 0.8m$ $F_4^* = 7.73$ kN/m
$z = z_5 = 0.2m$ $F_5^* = 3.21$ kN/m

Modular block shear capacity:
$V_u = a_u + N \tan \lambda_u$; $N = \gamma_u z W_u$

$V_u = 5.836+19 \text{ z } 0.305 \tan 30° = 5.836+3.346z$ kN/m

$z = z_1 = 2.6m$ $V_u = 14.53$ kN/m
$z = z_2 = 2.0m$ $V_u = 12.53$ kN/m
$z = z_3 = 1.4m$ $V_u = 10.52$ kN/m
$z = z_4 = 0.8m$ $V_u = 8.51$ kN/m
$z = z_5 = 0.2m$ $V_u = 6.51$ kN/m

Check Condition (E1) at levels $z = z_j$:
$z = z_1$ $F_h^* - \Sigma F_i^* = 46.81-(15.12+11.42+7.73+3.21) = 9.33 \text{ kN/m} \leq \Phi V_u = 14.53$kN/m
$z = z_2$ $F_h^* - \Sigma F_i^* = 29.85-(11.42+7.73+3.21) = 7.49 \text{ kN/m} \leq \Phi V_u = 12.53$ kN/m
$z = z_3$ $F_h^* - \Sigma F_i^* = 16.58-(7.73+3.21) = 5.64 \text{ kN/m} \leq \Phi V_u = 10.52$ kN/m
$z = z_4$ $F_h^* - \Sigma F_i^* = 7.02-(3.21) = 3.81 \text{ kN/m} \leq \Phi V_u = 8.51$ kN/m
$z = z_5$ $F_h^* - \Sigma F_i^* = 1.14- 0 = 1.14 \text{ kN/m} \leq \Phi V_u = 6.51$ kN/m

Therefore Condition (E1) is satisfied at all levels.

B. Connection failure

Tensile loads (from previous calculations):
$F_1^* = 18.81$ kN/m
$F_2^* = 15.12$ kN/m
$F_3^* = 11.42$ kN/m
$F_4^* = 7.73$ kN/m
$F_5^* = 3.21$ kN/m

Connection strength:
$T_{cl} = a_{cs} + N (\tan \lambda_{cs})$; $N = \gamma_u \text{ z } W_u$
$T_{cl} = 4.973+19 \text{ z } 0.305 \tan 43° = 4.973+5.404z$ kN/m

Check Condition (E3):
$F_1^* = 18.81 \text{ kN/m} \leq \Phi_1 T_{cl} = 1.0x(4.973+5.404x2.6) = 19.02$ kN/m
$F_2^* = 15.12 \text{ kN/m} \leq \Phi_1 T_{cl} = 1.0x(4.973+5.404x2.0) = 15.78$ kN/m
$F_3^* = 11.42 \text{ kN/m} \leq \Phi_1 T_{cl} = 1.0x(4.973+5.404x1.4) = 12.54$ kN/m
$F_4^* = 7.73 \text{ kN/m} \leq \Phi_1 T_{cl} = 1.0x(4.973+5.404x0.8) = 9.30$ kN/m
$F_5^* = 3.21 \text{ kN/m} \leq \Phi_1 T_{cl} = 1.0x(4.973+5.404x0.2) = 6.05$ kN/m

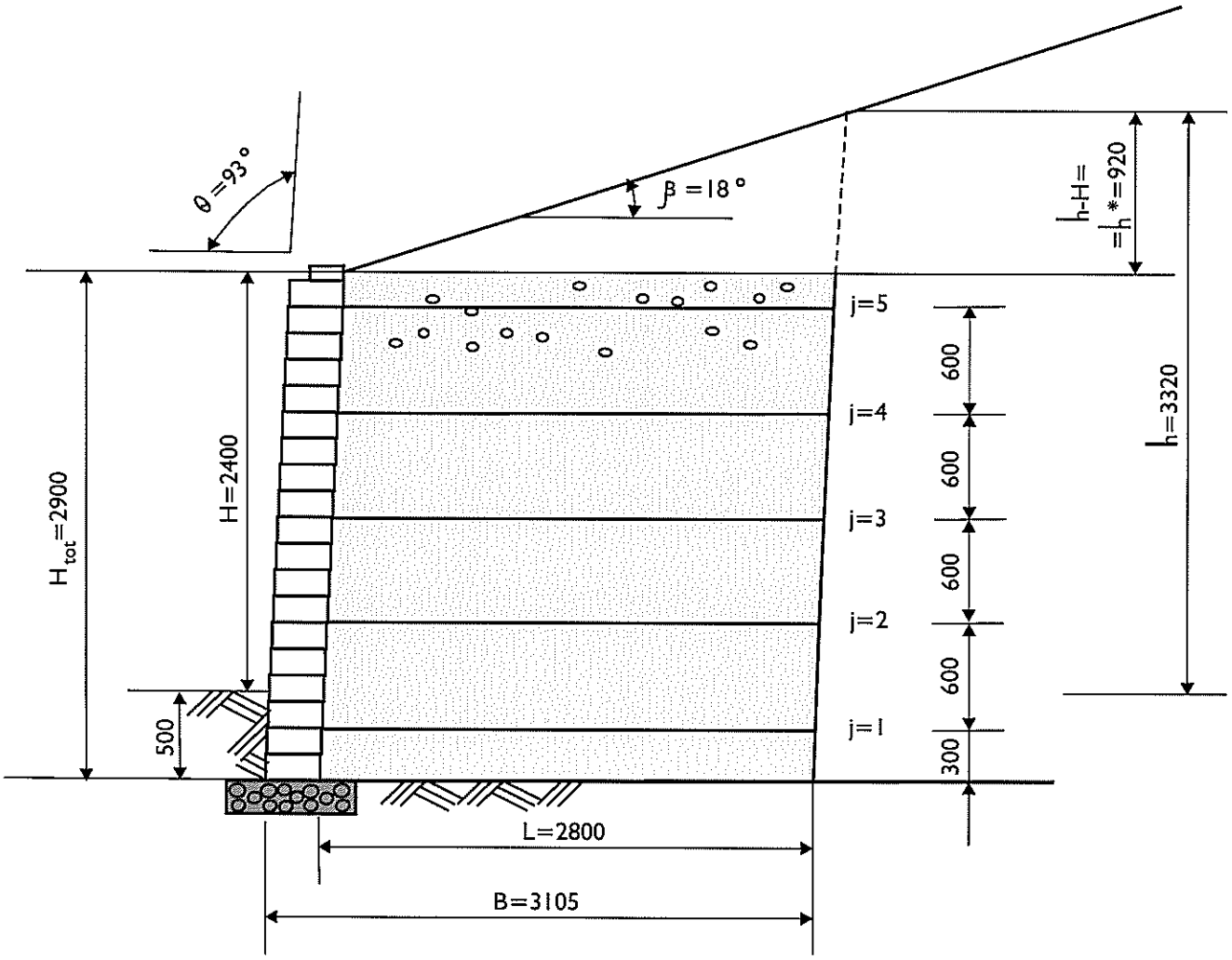

Figure G1: Final Reinforcement Layout

13/8/02
CAD FILE 3401650SK28.CDR AM/LG

Therefore Condition (E3) is satisfied for all connections.

Stability of unreinforced crest against failure should also be checked (refer to E2.4). In our example the unreinforced crest comprises one block only.

Shear:
$F^* = \alpha\ 0.5\ (3.11+6.84z)$ (Refer to G1.14,A)
$F^* = 1.5x0.5\ (3.11+3.11+6.84x0.2)0.2 = 1.14$ kN/m
$V_u = 6.51$ kN/m
$F^* \leq V_u$

Therefore internal sliding by shear will not occur. In our case this check appears to be completely identical to the check of condition (E1) for layer $z=z_5$.

It can also be shown that overturning of the unreinforced crest comprising one block only is not a problem.

The final wall design is shown on Figure G1.

G2 Example 2: Example of Seismic Design of a GRS wall with Wrap-around Facing

In this example the design of the reinforcement layout for a GRS wall with a vertical wrap around facing and subjected to earthquake loading is illustrated. Details of the proposed wall are given in Table G2 and a section is shown in Figure G2.

Table G2 Design parameters for GRS walls with wrap around facing.

Description	Symbol	Parameter	Units
Wall, Backfill and Foundation Soil			
Wall Height	H	2.3	m
Inclination of the Wall Face from Horizontal	θ	90	degrees
Backfill Slope Angle	β	0	Degrees
Angle of Internal Friction for Reinforced Backfill	ϕ_r	37	Degrees
Cohesion of Reinforced Backfill	c_r	0	kPa
Unit Weight of Reinforced Backfill	γ_r	19	kN/m^3
Angle of Internal Friction for Retained Backfill	ϕ_f	30	Degrees
Cohesion of Retained Backfill	c_f	0	kPa
Unit Weight of Retained Backfill	γ_f	19	kN/M^3
Angle of Internal Friction for Foundation Soil	ϕ	30	Degrees
Cohesion of Foundation Soil	c	0	kPa
Unit Weight of Foundation Soil	γ	19	kN/m^3

Geosynthetic Reinforcement			
Ultimate Tensile Strength of Geogrid	T_{ult}	38.3	kN/m
UncertaintyFactor (Manufacturing)	Φ_m	1	-
Reduction Factor for Creep Deformation	Φ_{cr}	0.63	-
Uncertainty Factor (Extrapolation)	Φ_e	1.0	-
Reduction Factor (Installation Damage)	Φ_i	0.87	-
Reduction Factor (Chemical Degradation)	Φ_{rch}	1.0	-
Reduction Factor (Biological Degradation)	Φ_{rb}	1.0	-
Uncertainty Factor (Overall Degradation)	Φ_d	0.95	-
Reduction Factor (joints, seams, connections)	Φ_j	1.0	-
Reduction Factor Associated with Ramification of Failure	Φ_n	1.0	-
Scale Effect Correction Factor	α	1.0	-
Pullout Resistance factor	F^*	0.371	-
Soil-Reinforcement Interface Friction Angle	ρ	26°	-
Seismic Load			
Peak Horizontal Ground Acceleration Coefficient	PGA	0.3	-
Load Factors and Reduction Factors			
Load Factors	α_i	As recommended by appropriate sections of the Guidelines	-
Reduction Factors	Φ_i	As recommended by appropriate sections of the Guidelines	-

Wall height:
Wall height above the ground surface level: H = 2.3 m
Minimum embedment requirement (Table 2.1): H/10 =0.23 m
Minimum embedment required (Section 2.5): 0.5 m
Wall height above the subgrade level: H_{tot} = 2.3+0.5 =2.8m

Note: Manufacturer's recommendations with respect to secondary reinforcement (where appropriate) should be taken into account.

G2.1 Seismic Loading

Our retaining wall is a wall with an unrestrained base. Therefore according to Equations (14) and (15) in the Guidelines:

$a_{h,ext}$ = 0.6 PGA = 0.6x0.3 = 0.18
$a_{h,int}$ = (1.3-PGA)PGA = (1.3-0.3) x 0.3 = 0.3

Assume $a_v = 0$. From Equation (18):

$$\xi_{ext} = \tan^{-1}\frac{a_{h,ext}}{1 \pm a_v} = \tan^{-1}\frac{0.18}{1 \pm 0.0} = 10.20°$$

$$\xi_{int} = \tan^{-1}\frac{a_{h,ext}}{1 \pm a_v} = \tan^{-1}\frac{0.3}{1 \pm 0} = 16.70°$$

The coefficient of active soil pressure for static conditions (Equations 2 and 27):
$K_{af} = \tan^2(45\text{-}\phi_f/2) = \tan^2(45\text{-}30/2) = 0.33$
$K_{ar} = \tan^2(45\text{-}\phi_r/2) = \tan^2(45\text{-}37/2) = 0.25$

The Mononobe – Okabe earth pressure coefficient (Equation 17):
Retained fill:

$$K_{AE} = \frac{\cos^2(\phi - \xi - 90 + \theta)}{\cos\xi\cos^2(90-\theta)\cos(I + 90 - \theta + \xi)\left[1 + \sqrt{\frac{\sin(\phi + I)\sin(\phi - \xi - I)}{\cos(I + 90 - \theta + \xi)\cos(I - 90 + \theta)}}\right]^2} =$$

$$= \frac{\cos^2(30 - 10.20 - 90 + 90)}{\cos 10.20\cos^2(90-90)\cos(0 + 90 - 90 + 10.20)\left[1 + \sqrt{\frac{\sin(30+0)\sin(30 - 10.20 - 0)}{\cos(0 + 90 - 90 + 10.20)\cos(0 - 90 + 90)}}\right]^2} =$$

Reinforced fill: $K_{AE} =$

$$= \frac{\cos^2(37 - 16.70 - 90 + 90)}{\cos(16.70)\cos^2(90-90)\cos(0 + 90 - 90 + 16.70)\left[1 + \sqrt{\frac{\sin(37+0)\sin(37 - 16.70)}{\cos(0 + 90 - 90 + 16.70)\cos(0 - 90 + 90)}}\right]^2} =$$

$= 0.45$

Calculate the seismic soil pressure coefficient increment (Equation 21):
Retained Fill:
$\Delta K_{AE} = (1+0)\ 0.46\text{-}0.33 = 0.13$

Reinforced fill:
$\Delta K_{AE} = (1+0)\ 0.45\text{-}0.25 = 0.2$

G2.2 Forces Acting on the Reinforced Block

Assume L = 2.6 m (B = L = 2.6m)

Weight of the reinforced block:
$V_1 = B \times H_{tot}\ \gamma_r = 2.6 \times 2.8 \times 19 = 138.38$ kN/m

The active soil thrust:
$F_A = 0.5\ K_{af}\ \gamma_f\ H^2_{tot} = 0.5 \times 0.33 \times 19 \times 2.8^2 = 24.58$ kN/m

Total inertia force of the reinforced block:
$F_{IR} = F_{ir}+F_{is} = F_{ir}+0 = 0.5\ a_{h,ext}\gamma_r\ H_{tot}^2 = 0.5x0.18x19x2.8^2 = 13.41$ kN/m

Seismic thrust (Equation 26):
$F'_{AE} = F_A + 0.5\ \Delta F_{AE} = F_A + 0.5\ (0.5\Delta K_{AE}\ \gamma_f\ H^2_{tot}) = 24.58+0.5(0.5x0.13x19x2.8^2) =$
$= 29.42$ kN/m

G2.3 Forward Sliding

Factored driving force:
$F_h^* = \alpha F_{IR} + \alpha F'_{AE} = 1x13.41+1.0x29.42 = 42.83$ kN/m
($\alpha = 1.0$, Table 2.4 of the Guidelines)

Factored vertical force:
$F_v^* = \alpha V_1 = 1.0x138.38 = 138.38$ kN/m
($\alpha = 1.0$, Table 2.4 of the Guidelines)

Factored resisting force:
A. Sliding along the Foundation soil (Equation 7)
$\Phi\ F_v^*\ \tan\phi = 0.9 \times 138.38 \times \tan 30° = 71.90$ kN/m
where $\Phi = 0.9$ (refer to Section 3.3 of the Guidelines)

B. Sliding along the Reinforced Backfill
$\Phi\ F_v^*\ \tan\phi_r = 0.9x138.38x\ \tan 37° = 93.85$ kN/m
where: $\Phi = 0.9$ (refer to Section 3.3)

C. Sliding along Soil-Reinforcement Interface
Ultimate interface soil-geosynthetic interaction strength (Equation A8):
$T_{i,2} = (\tan\rho)\ \alpha\sigma_v^*\ L_e = (\tan\rho)\ \alpha F_v^* =$
$= (\tan 26°) \times 1.0x138.38 = 67.49$ kN/m

Factored soil-geosynthetic interaction strength (Equation A6):
$T^*_{di,2} = T_{i,2}\ \Phi\ \Phi_n = 67.49x0.8x1.0 = 54.00$ kN/m

Check Conditions (7), (8):
$F_h^* = 42.83$ kN/m $\le \Phi\ F_v^*\ \tan\phi = 71.90$ kN/m
$F_h^* = 42.83$ kN/m $\le \Phi\ F_v^*\ \tan\phi_r = 93.85$ kN/m
$F_h^* = 42.83$ kN/m $\le T^*_{di,2} = 54.00$ kN/m

The conditions are satisfied.

G2.4 Bearing Capacity

Assess ultimate bearing capacity of soil (NCHRP 1991):
$q_u = 0.5\gamma\ B'\ N_{\gamma m} + \gamma\ D_f\ N_{qm}$

where:
$N_{\gamma m} = N_\gamma\, s_\gamma\, c_\gamma\, i_\gamma\, d_\gamma$
B' is the reduced effective width of the wall base
$N_\gamma = 22$ (bearing capacity factor)
$s_\gamma = 0.96$ (footing shape factor)
$c_\gamma = 0.68$ (soil compressibility factor)
i_γ is a function of load inclination
$d_\gamma = 1.0$ (embedment factor)

$N_{qm} = N_q\, s_q\, c_q\, i_q\, d_q$

$N_q = 18$ (bearing capacity factor)
$s_q = 1.06$ (footing shape factor)
$c_q = 0.68$ (soil compressibility factor)
i_q is a function of load inclination
$d_q = 1.0$ (embedment factor)

$D_f = 0.5$m (embedment depth)

Determine the eccentricity:
$x_{vl} = 1.3$ m
$y_{Ah} = H_{tot}/3 = 2.8/3 = 0.93$ m

$y_{AE.h} = 0.6\, H_{tot} = 0.6 \text{x} 2.8 = 1.68$ m

$e = (F_A^*\, y_{Ah} + 0.5 \Delta F_{AE}^*\, y_{AE,h} - V_l^*(x_{vl}-0.5B) + 0.5\, H_{tot}\, F_{ir}^*) / V_l^* =$

$$= \frac{24.58x0.93 + 0.5x(0.5x0.13x19x2.8^2)x1.68 - 0 + 0.5x2.8x13.41}{138.38} =$$

$= 0.36$ m

$\sigma^* = F_v^*/(B-2e) = 138.38/(2.6-2\text{x}0.36) =$
$= 73.6$ kPa

Calculate q_u:
$F_h^*/F_v^* = (29.42+13.41) / 138.38 = 0.31$

Therefore $i_\gamma = 0.34$ $\quad i_q = 0.49$

$B' = B-2e = 2.6-2\text{x}0.22 = 2.16$m

$N_{\gamma m} = 22 \text{ x } 0.96 \text{ x } 0.68 \text{ x } 0.34 \text{ x } 1.0 = 4.88$
$N_{qm} = 18 \text{ x } 1.06 \text{ x } 0.68 \text{ x } 0.49 \text{ x } 1.0 = 6.36$
$q_u = 0.5\text{x } 19 \text{ x } 2.16 \text{ x } 4.88 + 19 \text{ x } 0.5 \text{ x } 6.36 = 160.56$ kPa

Check Condition (11)
$\sigma_v^* = 73.6$ kPa $\leq \Phi q_u = 0.7 \times 160.56 = 112.39$ kPa
Note that $\Phi = 0.7$ (refer to Section 3.3)

The condition is satisfied.

G2.5 Overturning

Driving moments:
$M_d^* = F_A^* y_{Ah} + 0.5\ \Delta F_{AE}^* y_{AE,h} + 0.5\ H_{tot} F_{ir}^* =$
$= 24.58 \times 0.93 + 0.5 \times (0.5 \times 0.13 \times 19 \times 2.8^2) \times 1.68 + 0.5 \times 2.8 \times 13.41 =$
$= 49.77$ kNm/m

$M_r^* = V_I^* x_{vI} = 138.38 \times 1.3 = 179.89$ kNm/m

Check Condition (12):
$M_d^* = 49.77$ kNm/m $\leq \Phi\ M_r^* = 0.9 \times 179.89 = 161.9$ kNm/m

Note that $\Phi = 0.9$ (refer to Section 3.3 of Guidelines)

The condition is satisfied.

Consider internal stability of the wall.

G2.6 Lateral Soil Pressures

For reinforced fill from previous calculations:
$K_{ar} = 0.25$
$K_{AE} = 0.45$
$\Delta K_{AE} = 0.2$

Horizontal design soil pressure:

$$\sigma_h^* + \Delta\sigma_{h,AE}^* = \alpha(K_{ar}\ \gamma_r\ z) + \alpha(0.8\text{-}0.6\ \frac{z}{H})\ \Delta K_{AE}\ \gamma_r\ H_{tot} \cos\beta =$$

$$= 1.0\text{x}0.25\text{x}19 \text{ x } z + 1.0\ (0.8\text{-}0.6\ \frac{z}{2.8})\ 0.2\text{x}19\text{x}2.8\text{x}1.0 =$$

$= 2.47z + 8.51$ kPa

G2.7 Design Tensile Strength of Geosynthetic

$T_d^* = T_{ult}\ \Phi_m\ \Phi_{rc}\ \Phi_e\ \Phi_i\ \Phi_{rch}\ \Phi_{rb}\ \Phi_d\ \Phi_j\ \Phi_n =$
$= 38.3\text{x}1.0\text{x}1.0\text{x}1.0\text{x}0.85\text{x}1.0\text{x}1.0\text{x}0.95\text{x}1.0\text{x}1.0 = 30.93$ kN/m

Note that $\Phi_{rc} = 1.0$ should be used (refer to Section 3.5.2 of the Guidelines)

G2.8 Minimum Number of Reinforcement Layers Required

Top of facing: $\sigma_t^* = 8.51$ kPa

Bottom of facing: $\sigma_b^* = 2.47z + 8.51 = 2.47 \times 2.8 + 8.51 = 15.43$ kPa

Total factored force: $\Sigma F_j^* = 0.5(\sigma_t^* + \sigma_b^*) H_{tot} =$

$= 0.5x (8.51 + 15.43) \times 2.8 = 33.5$ kN/m

Minimum number of geogrid layers required:

$$N = \frac{\Sigma F_j^*}{T_d^*} = \frac{33.5}{30.93} = 1.1$$

For GRS walls with wrap around facing, maximum spacing between layers of primary reinforcement (i.e. geogrid layers providing strength and intergrity to the whole wall) is normally advised by manufacturers.

If intermediate (or so-called secondary) reinforcement (refer to Section 4.4 of the Guidelines) is not used, maximum spacing between primary reinforcement layers of 0.6 m is typically recommended.

G2.9 Reinforcement Layout

Select the following trial reinforcement layout:

$z_1 = 2.8$ m	$S_{v1} = 0.3$ m
$z_2 = 2.2$m	$S_{v2} = 0.6$ m
$z_3 = 1.6$ m	$S_{v3} = 0.6$ m
$z_4 = 1.0$ m	$S_{v4} = 0.6$ m
$z_5 = 0.4$ m	$S_{v5} = 0.7$ m

G2.10 Tensile Loads applied to each Geogrid Layer

$F_1^* = F_1 = \sigma_{h1} S_{v1} = (2.47 \times 2.65 + 8.51) \times 0.3 = 4.52$ kN/m

$F_2^* = F_2 = \sigma_{h2} S_{v2} = (2.47 \times 2.2 + 8.51) \times 0.6 = 8.37$ kN/m

$F_3^* = F_3 = \sigma_{h3} S_{v3} = (2.47 \times 1.6 + 8.51) \times 0.6 = 7.48$ kN/m

$F_4^* = F_4 = \sigma_{h4} S_{v4} = (2.47 \times 1.0 + 8.51) \times 0.6 = 6.59$ kN/m

$F_5^* = F_5 = \sigma_{h5} S_{v5} = (2.47 \times 0.35 + 8.51) \times 0.7 = 6.56$ kN/m

G2.11 Tensile Strength

$T_d^* = 30.93$ kN/m (refer to Section G2.7)

All factored forces F_j^* are less than T_d^* therefore condition (36) of the Guidelines is satisfied.

G2.12 Pullout

Adherence length past the failure plane:

$L_{e,j} = L - (H_{tot} - z_j) \tan(90° - \psi)$

$\psi = 45° + \phi/2 = 45 + 37/2 = 63.5°$

$\tan(90° - 63.5°) = 0.499$

$L_{e,1}$ = 2.6 - (2.8-2.8) x 0.499 = 2.6 m
$L_{e,2}$ = 2.6 - (2.8-2.2) x 0.499 = 2.30 m
$L_{e,3}$ = 2.6 – (2.8-1.6) x 0.499 = 2.00 m
$L_{e,4}$ = 2.6 – (2.8-1.0) x 0.499 = 1.70 m
$L_{e,5}$ = 2.6 - (2.8-0.4) x 0.499 = 1.40 m

Depth of overburden: for horizontal backfill $z_{pj} = z_j$

Calculate the design soil-reinforcement interaction strength for pullout (refer to Equations A5 and A7, Appendix A):
$T_{i,1} = F^* \alpha \sigma^*_v L_e C$; $C = 2$
$T^*_{di,1} = T_{i,1} \Phi \Phi_n = \Phi \Phi_n F^* \alpha \sigma^*_v L_e C$

$\Phi = 0.8$ $\Phi_n = 1.0$

j = 1 $T_{di,1}^*$ = 0.8x1.0x0.371x1.0x(19x2.8)x2.6x2 = 82.1 kN/m
j = 2 $T_{di,1}^*$ = 0.8x1.0x0.371x1.0x(19x2.2)x2.3x2 = 57.1 kN/m
j = 3 $T_{di,1}^*$ = 0.8x1.0x0.371x1.0x(19x1.6)x2.0x2 = 36.1 kN/m
j = 4 $T_{di,1}^*$ = 0.8x1.0x0.371x1.0x(19x1.0)x1.7x2 = 19.2 kN/m
j = 5 $T_{di,1}^*$ = 0.8x1.0x0.371x1.0x(19x0.4)x1.4x2 = 6.3 kN/m

Factored forces F_1, F_2, F_3 and F_4 are less than $T_{di,1}$ (j = 1,2,3,4) and therefore condition (37) is satisfied. For the 5th layer, F_5 is slightly higher than $T_{di,1}^*$ j = 5. Therefore the layer should be longer than 2.6 m.

The adherence length required is:
$L_e = F_5^*/\Phi \Phi_n F^* \alpha\sigma^*_v C) = 6.56/(0.8x1.0x0.371x1x19x0.4x2) = 1.45$ m

i.e. 0.05 m extra length (1.45 m – 1.40 m = 0.05 m) is required. This extra length is only 3.6% of the original adherence length and will not substantially change the design soil-reinforcement interaction strength for pullout ($T_{di,1}^*$, j=5). Therefore the geogrid length for layer 5 can be left without amendments.

G2.13 Internal Sliding Failure

The potential for an internal sliding failure should be checked at each geosynthetic reinforcement level.

G2.13.1 *Lateral soil pressures at the rear of the GRS block*

Note that only 50% of the external seismic thrust increment $\Delta F_{AE}(z)$ should be considered for the internal sliding stability calculation.
K_{af} = 0.33
ΔK_{AE} = 0.13

Horizontal design soil pressure:

$\sigma_h^* + 0.5\ \sigma_{h\ AE}^* = \alpha(K_{af}\ \gamma_f\ z) + 0.5\alpha(0.8\text{-}0.6\ \frac{z}{H})\ \Delta K_{AE}\ \gamma_f\ H \cos\beta =$

$= 1.0x\ (0.33x19x\ z) + 0.5x1.0x(0.8\text{-}0.6\ \frac{z}{2.8})\ x\ 0.13x19x2.8x1 =$

$= 5.529z + 2.77$ kPa

G2.13.2 *Destabilising Forces*

$F_{h,z}^* = F_{IR}(z) + F_A(z) + 0.5\ \Delta\ F_{AE}(z)$

$F_{IR}(z) = 0.5a_{h,ext}\ \gamma_r\ z^2 = 0.5x0.18x19xz^2 = 1.71z^2$ kN/m

$F_A(z) + 0.5\ \Delta\ F_{AE}(z) = 0.5\ x\ (2.77 + 5.529z + 2.77)z =$

$= 2.77 + 2.76z^2$ kN/m

j = 1 $F_{h,z}^* = 1.71x(2.8)^2 + 2.77\ x\ 2.8 + 2.76\ x\ (2.8)^2 = 42.8$ kN/m
j = 2 $F_{h,z}^* = 1.71\ x\ (2.2)^2 + 2.77\ x\ 2.2 + 2.76\ x\ (2.2)^2 = 27.73$ kN/m
j = 3 $F_{h,z}^* = 1.71\ x\ (1.6)^2 + 2.77\ x\ 1.6 + 2.76\ x\ (1.6)^2 = 15.88$ kN/m
j = 4 $F_{h,z}^* = 1.71\ x\ (1.0)^2 + 2.77\ x\ 1.0 + 2.76\ x\ (1.0)^2 = 7.24$ kN/m
j = 5 $F_{h,z}^* = 1.71\ x\ (0.4)^2 + 2.77\ x\ 0.4 + 2.76\ x\ (0.4)^2 = 1.82$ kN/m

G2.13.3 *Design soil reinforcement interaction strength for direct shear*

$T^*_{di,2} = T_{i,2}\ \Phi\ \Phi_n$; $T_{i,2} = (\tan\rho)\ \alpha\ \sigma^*_v\ L_e$

$Tdi,_2^* = \Phi\ \Phi_n\ (\tan\rho)\ \alpha\ \sigma^*_v\ L = 0.8x1.0x(\tan 26°)\ x\ 1x\ (19x\ z)2.6 =$

$= 19.28z$ kN/m

j = 1 $T_{di,2}^* = 19.28x2.8 = 53.98$ kN/m
j = 2 $T_{di,2}^* = 19.28x2.2 = 42.41$ kN/m
j = 3 $T_{di,2}^* = 19.28x1.6 = 30.85$ kN/m
j = 4 $T_{di,2}^* = 19.28x1.0 = 19.28$ kN/m
j = 5 $T_{di,2}^* = 19.28x0.4 = 7.71$ kN/m

As $T_{di,2}^* > F_{h,z}^*$ for all j (j = 1-5), Condition (33) of the Guidelines is satisfied.

The final design is shown on Figure G2.

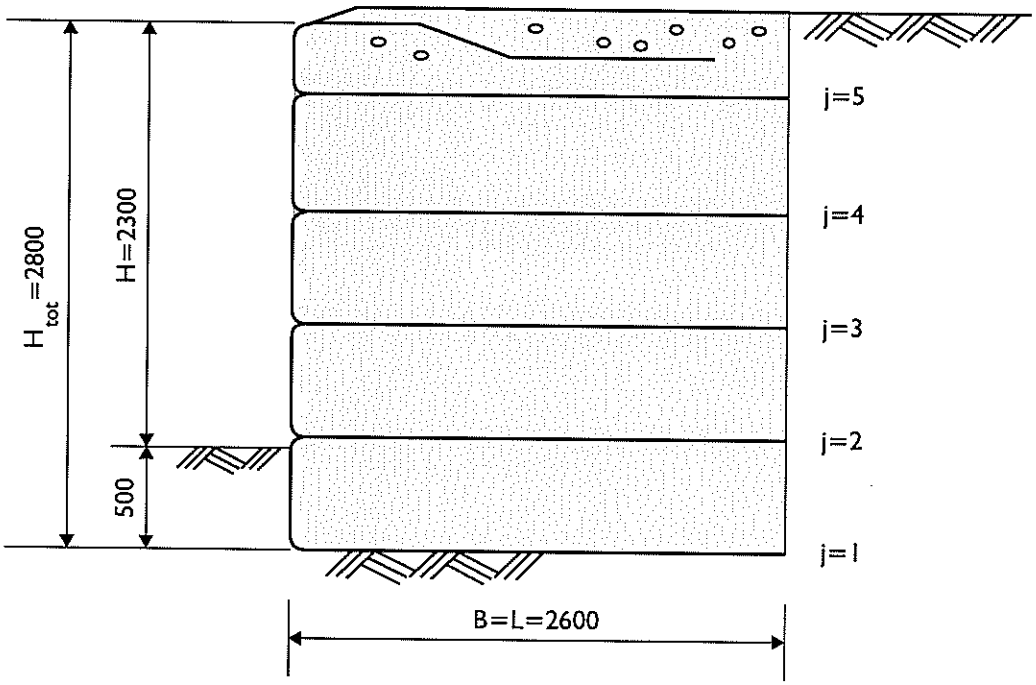

Figure G2: Final Reinforcement Layout

13/8/02
CAD FILE 3401650SK27.CDR AM/LG

Appendix H

Design Charts and Worked Examples for GRS Slopes

Application of Revised Design Charts for Steep Reinforced Slopes

R. A. Jewell

Department of Engineering Science, University of Oxford, Parks Road, Oxford, UK

ABSTRACT

After several years of application and after further research studies, earlier published design charts for steep reinforced slopes have been fully revised and extended to provide greater economy and flexibility in design. The charts now extend to the vertical case and are valid for the full range of polymer reinforcement materials including geotextiles and polymer grids. Savings in reinforcement quantities in the range 20% to 30% are typical. This paper describes the practical application of the revised charts and is illustrated by worked examples.

NOTATION

B	Depth (or thickness) of grid reinforcement bearing surfaces
c'_d	Design value of effective cohesion in the soil
f_b	Bond coefficient between soil and reinforcement (eqn (4))
f_c	Overall factor reflecting the seriousness of the limit state
f_d	Partial factor to allow for effects of mechanical damage
f_{ds}	Direct sliding coefficient for soil over a reinforcement layer (eqn (3))
f_{env}	Partial factor to allow for effects of chemical and micro-biological environment
f_m	Partial factor between the *allowable* and *limiting* reinforcement forces
f_{sf}	Coefficient of skin friction ($=\tan\delta/\tan\phi'$)
FS_s	Factor of safety on peak shearing resistance ($=\tan\phi'_p/\tan\phi'_d$)

H	Height of slope
H'	Effective height of slope to allow for surcharge ($=H + q_{sv}/\gamma_d$)
K_d	Design value of earth pressure coefficient
K_{Req}	Earth pressure coefficient giving minimum required reinforcement force
L_B	Bond length for reinforcement at the base of the slope (eqn (6))
L_R	Reinforcement length
$(L_R/H)_{ds}$	Minimum required length for satisfactory direct sliding equilibrium
$(L_R/H)_{ovrl}$	Minimum required length for satisfactory internal and overall equilibrium
P_{all}	Allowable reinforcement force ($=P_{lim}/f_m$) (eqn (2))
P_{lim}	Limiting reinforcement force capacity (see Section 3.2)
P^{Field}	Reinforcement force for *Field* conditions (eqn (1))
P^{Ref}	Reinforcement force for laboratory *Reference* conditions (eqn (1))
q_{sv}	Uniform vertical surcharge
r_u	Pore water pressure coefficient ($=u/\gamma z$)
s_h	Horizontal spacing between reinforcement members
s_v	Vertical spacing between reinforcement layers
S	Spacing between reinforcement grid bearing surfaces
t_d	Design time under load for reinforcement
T_d	Design temperature
W_r	Width of reinforcement
z	Depth below the ground surface
z_{crit}	Critical depth below the slope crest ($=HL_B/L_R$)
α_s	Proportion of reinforcement plane area that is solid
α_b	Proportion of total reinforcement bearing surface available
β	Slope angle from the horizontal
γ	Unit weight of soil
γ_d	Design value of unit weight
γ_{max}	Maximum unit weight of soil
δ	Angle of shearing resistance between soil and plane reinforcement surface
σ_{av}	Available stress in the soil from the reinforcement
σ'_b	Effective bearing stress acting on reinforcement bearing surfaces (eqn (5))
σ'_n	Effective stress normal to the plane of the reinforcement
σ_{Req}	Required stress in the soil to be provided by reinforcement
ϕ'	Effective angle of friction

ϕ'_{cs}	Critical state or large strain angle of shearing resistance
ϕ'_d	Design value of effective angle of shearing resistance
ϕ'_p	Peak effective angle of shearing resistance
$(\ )_{chart}$	Value of a parameter determined from the design charts
$(\ )_d$	Design value of a parameter

1 INTRODUCTION

An analysis for steep reinforced slopes was developed in the early eighties and used to derive design charts.[1] Confidence in the use of geotextiles and polymer grids to reinforce steep slopes has increased markedly since that time, and now work on drafting national and international standards and codes of practice is well advanced.[2,3]

The steep reinforced slopes designed using the charts have performed satisfactorily, although the reinforcement forces (and measured deformations) have been smaller than those anticipated in the design calculation.[4,5]

In the light of the above, the design charts and their theoretical basis have been reassessed to see whether reinforced slopes might be designed with less reinforcement material, but with the same level of safety. This study has resulted in a revised design method,[6] and accompanying revised charts (see Appendices 1–3) for steep reinforced slopes which supersede those published in 1984,[1] and offer greater economy and flexibility.

This paper describes and illustrates by worked examples the practical application of the revised design method and charts, the theoretical basis of which was described at the recent UK symposium on reinforced embankments.[7]

2 DEFINITION OF PARAMETERS

The definitions for the steep reinforced slope cases described by the charts are summarised in Fig. 1. Uniform fills sloping at an angle β from the horizontal in the range $90° > \beta > 30°$ are allowed, extending the previous work from $\beta = 80°$ to the vertical. The fill slopes are assumed to rest on a competent, level foundation and have a level crest. Uniform vertical surcharge loading on the crest is allowed, but, as in the previous charts, point loads and earthquakes are not included.

The critical equilibrium for steep reinforced slopes is usually governed by *long-term* stability conditions. The soil strength is thus described in terms of an effective frictional shearing resistance, (ϕ', $c' = 0$). The

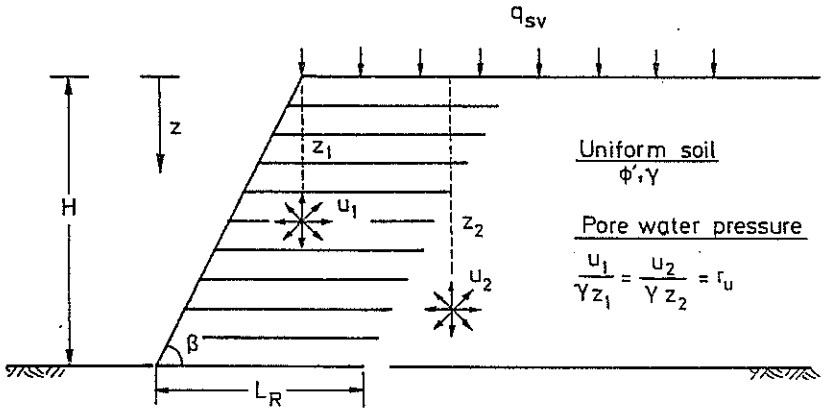

Fig. 1. Definitions for steep reinforced slopes.

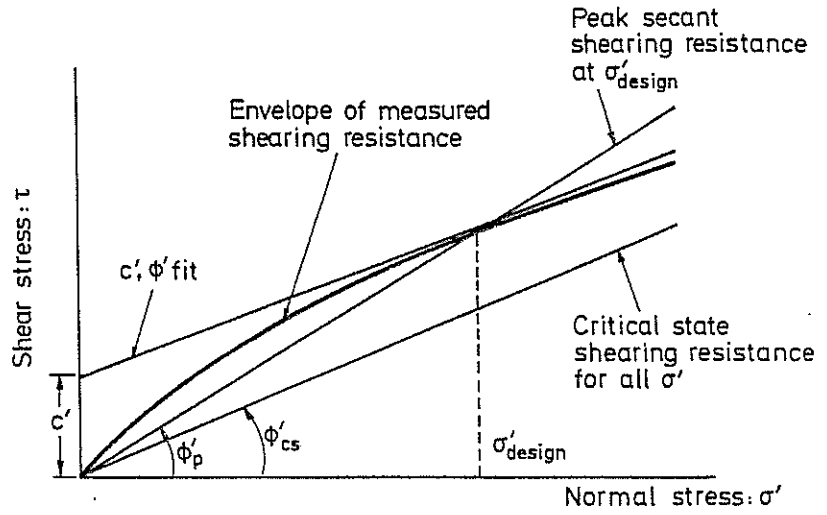

Fig. 2. Curved envelope of shearing resistance showing a peak secant angle of friction ϕ'_p at σ'_d, and a conventional (c', ϕ') fit to the data.

curvature of the Mohr–Coulomb envelope of *peak shearing resistance* for a soil tested at one density but over a range of effective stresses is taken into account by the choice of a secant angle of shearing resistance ϕ'_p at an appropriate stress, rather than by (c', ϕ') parameters fitted to the data (Fig. 2).

In line with the earlier work, the use of the large strain or *critical state shearing resistance* ϕ'_{cs} will be recommended for the design of soil slopes reinforced by polymer reinforcement materials (Section 3.1). The critical state angle of friction for a soil is constant over the practical range of effective stress.

Pore water pressures are an important aspect of slope behaviour and are allowed for in the charts by the non-dimensional *pore water pressure coefficient* $r_u = u/\gamma z$ introduced by Bishop and Morgenstern.[8] This

approach identifies the magnitude of the pore water pressure u, at a depth z, simply as a function of the overburden pressure γz (Fig. 1). The coefficient r_u is not an ideal description for the pattern of pore water pressures which might develop with water infiltration or flow through a slope, but it is the only non-dimensional parameter available to describe pore water pressures for use in charts.

The interaction between the soil and the horizontal reinforcement layers is described in terms of a *bond coefficient* f_b, which governs the rate of load transfer between the reinforcement and the soil (i.e. the bond length for a reinforcement layer). A separate *direct sliding coefficient* f_{ds} applied to the soil shearing resistance governs the resistance to shear failure $f_{ds} \tan \phi'$ either immediately above or below a layer of reinforcement in the reinforced zone (Fig. 3).

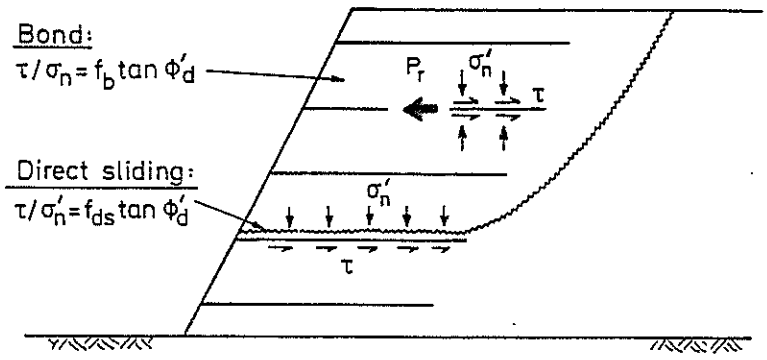

Fig. 3. Illustration of bond and direct sliding in a steep reinforced slope.

Specific values $f_b = 0{\cdot}5$ and $f_{ds} = 0{\cdot}8$ were assumed in the earlier design charts. The revised charts now allow the *bond coefficient* to take any value in the legitimate range $1 \geq f_b \geq 0$. Also, the charts are no longer restricted to geotextile and polymer grid reinforcements, and may be used for design with strip or other narrow forms of polymer reinforcement, including loop anchors.

To keep the number of charts to a minimum it has been necessary to select only one value for the *direct sliding coefficient*, and $f_{ds} = 0{\cdot}8$ has again been chosen to safely encompass most practical cases. A simple correction is applied where f_{ds} takes a lesser value (Section 3.3).

3 DESIGN VALUES FOR PARAMETERS

The revised design charts are reproduced at the end of the paper (see Appendices 1–3). As in the earlier work, there are two charts for each of three values of the pore water pressure coefficient $r_u = 0$, $0{\cdot}25$ and $0{\cdot}50$.

- The first figure in the chart gives an earth pressure coefficient K_{Req} from which the required reinforcement force for equilibrium is calculated.
- The second two figures in the chart give the minimum required reinforcement length L_R/H.

The minimum required reinforcement length satisfies internal and overall stability requirements, and prevents direct sliding through the reinforced block, as discussed by Jewell.[6]

External equilibrium involving potential failure mechanisms passing around the reinforced zone, and local bearing capacity failure in the foundation beneath the reinforced zone in very steep slopes have to be checked separately.

The focus of attention for an economical and balanced equilibrium in a steep slope is the calculation of the distribution of the maximum required stress to be supplied by the reinforcement for equilibrium in the soil. A suitable provision of reinforcement can then be made with sufficient strength and spacing so that the *minimum available stress* (from the reinforcement) exceeds the *maximum required stress* (for equilibrium in the soil) at every depth in the slope, thereby satisfying local and overall equilibrium. The revised design procedure leads directly to these distributions of required and available stress.

- The design procedure provides a margin of safety against collapse, and is equivalent to a stability analysis, or a strength limit state analysis.

For most routine slope projects, limiting the design value of the allowable reinforcement force so that the cumulative maximum tensile strain in the reinforcement will never exceed about 3% to 5% during the design life is usually sufficient to ensure satisfactory serviceability. That is, the resulting deformation should not interfere with the appearance or function of the slope.

Deformation can be more critical for reinforced soil walls, $\beta = 85° \rightarrow 90°$, either because of the support the wall provides to superstructures, or the requirement for small tolerances to preserve an attractive finish with some facing panel arrangements. Vertical and horizontal deformations for reinforced soil walls may be calculated using the charts developed by Jewell and Milligan.[9]

The selection of design values for the material properties of the soil and the reinforcement, and the selection of safety margins, is now described.

3.1 Soil properties

The recommended approach for the design of steep slopes reinforced by polymer reinforcement materials is to select a design value for the soil shearing resistance equal to the critical state shearing resistance $\phi'_d = \phi'_{cs}$.

In a compact fill reinforced by polymer materials the mobilised shearing resistance in the equilibrium condition is almost certain to exceed the critical state value. Likewise, the mobilised reinforcement force is almost certain to be less than the force calculated for the design equilibrium assuming $\phi'_d = \phi'_{cs}$ in the soil.

The ratio between the expected peak shearing resistance for the fill ϕ'_p and the critical state shearing resistance ϕ'_{cs} assumed for the design equilibrium may be considered equivalent to a lumped factor of safety on the peak strength of the soil $FS_s = \tan \phi'_p / \tan \phi'_{cs}$.

Selection of $\phi'_d = \phi'_{cs}$ also substantially removes the need to consider the influence of the reinforcement stiffness on the design equilibrium.

Typical values of the critical state strength for granular fills are in the range $\phi_{cs} = 30°$ to $35°$, and for low plasticity clay fills $\phi_{cs} = 20°$ to $25°$.

Filling and compaction is normally well controlled during construction, and the maximum expected unit weight for the soil is recommended for design $\gamma_d = \gamma_{max}$.

Pore water pressures during the design life of the slope are more variable and less well controlled. It is prudent in most cases to allow for some pore water pressure arising during the life of the slope from infiltration into the reinforced zone, or into the unreinforced soil behind. This is particularly true for less permeable fills. Long-term equilibrium pore water pressures as high as $r_u = 0{\cdot}25$ have been recorded in grassed clay fill slopes in the UK.[10]

An appropriate design value for the pore water pressure coefficient r_u is best selected by comparing the pore water pressure implied at given positions in the slope with the worst expected pore water pressure at those positions.

The slope dimensions H and β may be taken equal to their expected values for design. Inclusion of a nominal vertical surcharge of the order 10 kN/m^2 is often prudent in routine design to allow for some margin on over-filling, and other temporary loadings on the slope crest. Vertical surcharge loading is taken into account by designing the reinforcement for an equivalent slope of increased height H' (Section 4.4).

The above design values ϕ_d, $(r_u)_d$, β and H are sufficient to determine the *required earth pressure coefficient*, K_{Req}, and the *required reinforce-*

TABLE 1
Summary of Design Parameters for the Slope[a,b]

Parameter	*Notation*	*Units*
Slope height	H	m
Slope angle	β	deg
Soil friction angle	$\phi'_d = \phi'_{cs}$	deg
Soil cohesion	$c'_d = 0$	kN/m^2
Soil unit weight	$\gamma_d = \gamma_{max}$	kN/m^3
Pore water pressure	$(r_u)_d$	—

[a]Slopes rest on a level, competent foundation.
[b]Slopes have a level crest.

ment length, L_R/H, from the design charts. The design parameters are summarised in Table 1.

3.2 Reinforcement material properties

The *allowable force* P_{all} in the reinforcement must be selected to allow for conditions in the ground, at the end of the design life and at the design temperature (t_d, T_d), and for the reinforcement material having been subject to installation mechanical damage and the subsequent action of the soil chemical and micro-biological environment.

A practical procedure for evaluating this allowable force was described at the recent UK symposium by Greenwood and Jewell,[11] and their recommended partial factors are summarised in Fig. 4 and Table 2.

The load-extension properties supplied by manufacturers for polymer reinforcement materials are *Reference properties* measured on ex-works product. The characteristic value for these properties should be used for design. (Typically the characteristic value is achieved by 19 out of 20 samples.) If the mean or average value is quoted for a property (normally because of insufficient test data) it can be reduced by a factor 1·15 to make it comparable to the characteristic value. (See Jewell and Greenwood[12] for a discussion.)

Installation in the ground degrades the properties of reinforcement to lesser *Field properties* which are the appropriate ones for design. This loss in capacity is caused immediately by mechanical damage and over time by environmental degradation (chemical and microbiological).

The properties and degradation of polymer reinforcements are strongly governed by the time under load, and by the temperature, which changes the rate of reactions. The relevant reinforcement properties for design

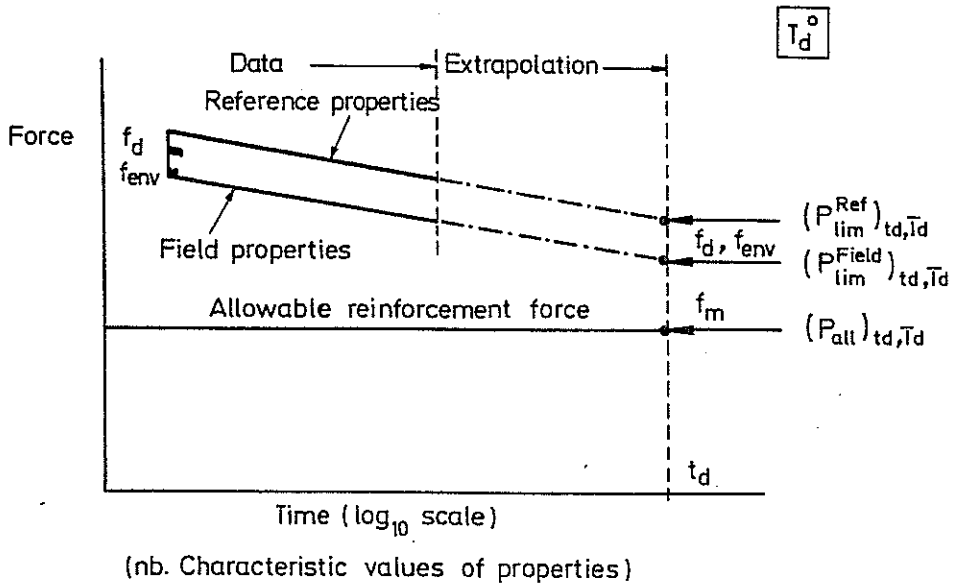

Fig. 4. Reinforcement strength characteristics at the design time and temperature (t_d, T_d), showing degradation in the ground, and the material safety margin f_m. Jewell and Greenwood.[12]

TABLE 2
Partial Safety Factors for Polymer Reinforcement (Greenwood and Jewell[12])

Mechanical damage	f_d	minimum	1·1
		typically rising to	1·6
Environmental effects	f_{env}	minimum	1·1
		outside pH range 4 to 10	[a]
Material factor	f_m	no extrapolation	1·3
		extrapolation 1 $\log_{10}$ cycle	1·5
		extrapolation 2 $\log_{10}$ cycles	2·2

[a]Yet to be determined.

must be for the material subject to a time under load (usually the design life of the slope) at a temperature appropriate to the field conditions (t_d, T_d).

Most manufacturers use the *Reference rupture strength* (i.e. the rupture strength indicated by the *Reference test data*) to establish the limiting capacity of the reinforcement for extrapolation (Fig. 4). Sometimes a maximum cumulative strain criterion is used together with the *Reference stiffness properties* to define the limiting capacity of the reinforcement. Whichever approach is followed, the resulting capacity defines the *Reference characteristic strength* or *limiting force* P_{lim}^{Ref} for the reinforcement, loaded for the design period at the design temperature, (t_d, T_d).

The corresponding *Field characteristic strength* or *limiting force* $P_{\text{lim}}^{\text{Field}}$ for the reinforcement, the value required for design, must allow for mechanical damage and environmental degradation:

$$(P_{\text{lim}}^{\text{Field}})_{t_d, T_d} = \frac{(P_{\text{lim}}^{\text{Ref}})_{t_d, T_d}}{f_d f_{\text{env}}} \tag{1}$$

where f_d and f_{env} are partial factors, evaluated for the actual reinforcement product, to allow for the anticipated degradation in the ground.

The *allowable force* P_{all} which can be safely assumed in the calculation of the design equilibrium is necessarily smaller than the limiting force. The margin between the allowable force and the limiting force is set by a *material factor* f_m,

$$(P_{\text{all}})_{t_d, T_d} = \frac{(P_{\text{lim}}^{\text{Field}})_{t_d, T_d}}{f_m} \tag{2}$$

Among other things, the *material factor* f_m allows for the uncertainty in the extrapolation of laboratory test data to reach the envisaged conditions at the end of the design life t_d at the design temperature T_d, as this is often beyond the practical range for tests (Table 2). (See Jewell and Greenwood[12] for a full discussion.)

Manufacturers should recommend values for f_d and f_{env}, based on tests for their own reinforcement products over the range of construction fills and soil environments in which they intend them to be used.

In the above approach to design there is provision for a final overall margin of safety to reflect the nature of the structure, and the seriousness and consequences of failure. This additional margin of safety is of the order $f_c = 1{\cdot}0 \rightarrow 1{\cdot}2$. A slope which would only cause minor inconvenience if it failed would probably be designed with $f_c = 1{\cdot}0$. A slope of great height, or a steep slope where there is pedestrian access at the crest or toe, would probably be designed with $f_c = 1{\cdot}2$.

The partial factor is applied to increase both the *required earth pressure coefficient*, K_{Req}, and the *required reinforcement length*, L_R/H, determined from the design charts.

3.3 Interaction parameters

3.3.1 Direct sliding coefficient

The *direct sliding coefficient* f_{ds} is a measure of the reduced shearing resistance $f_{ds} \tan \phi'$ for preferential sliding across the surface of a reinforcement layer. This sliding resistance is made up from skin friction, $\tan \delta$, which acts over the proportion of the plane sliding area α_s which is

solid reinforcement, and the full shearing resistance of the soil, $\tan\phi'$, which acts over the area of soil to soil contact $(1 - \alpha_s)$. Thus

$$f_{ds} \tan\phi' = \alpha_s \tan\delta + (1 - \alpha_s)\tan\phi'$$

or

$$f_{ds} = \alpha_s f_{sf} + (1 - \alpha_s) \tag{3}$$

where $f_{sf} = \tan\delta/\tan\phi'$ is the *coefficient of skin friction*.

For continuous sheet reinforcement, such as woven geotextiles, $\alpha_s = 1{\cdot}00$ so that the *direct sliding coefficient* is equivalent to the *coefficient of skin friction*, $f_{ds} = f_{sf}$. This can be measured in a modified direct shear test in which soil is sheared over the reinforcement surface.

For reinforcement grids, the *direct sliding coefficient* may either:

(a) be measured in a modified shear test with soil sheared over the grid, or
(b) be determined from the measured *coefficient of skin friction* f_{sf} for soil on the reinforcement surface, and the value of α_s from the grid geometry, substituted into eqn (3).

This latter procedure, (b), is the most practical one for slope design with reinforcement strips. Strips of width W_r spaced horizontally at s_h will cover a proportion of the plan area $\alpha_s = W_r/s_h$.

If the *direct sliding coefficient* is less than that assumed in the derivation of the design charts, if $f_{ds} \leq 0{\cdot}80$, then the required reinforcement length determined from the charts must be increased proportionately by a factor $0{\cdot}8/f_{ds}$.

3.3.2 Bond coefficient

The *bond coefficient* for reinforcement materials which develop bond through shear on plane reinforcement surface areas, such as woven and non-woven geotextiles, also equals the *coefficient of skin friction* $f_b = \tan\delta/\tan\phi' = f_{sf}$. (See eqn (4) below with $\alpha_s = 1{\cdot}00$ and $\alpha_b = 0$.)

There is no simple way to measure the bond coefficient for reinforcement materials which bond partly through bearing stress, such as grids. The bond coefficient then depends strongly on the proportions of the grid and on the shearing resistance of the soil, and can only be measured by pullout tests which are difficult to carry out satisfactorily.[13]

A method for calculating the bond coefficient for grids was derived by Jewell *et al.*[14] and has been shown to give suitable, slightly conservative values for design. The equations to calculate the bond coefficient are as follows:

$$f_b = \alpha_s\left(\frac{\tan\delta}{\tan\phi}\right) + \left(\frac{\alpha_b B}{S}\right)\left(\frac{\sigma'_b}{\sigma'_n}\right)\frac{1}{2\tan\phi'} \tag{4}$$

where α_b is the proportion of each grid bearing surface of width W_r and depth B available to the soil. S is the spacing between grid bearing members, and the bearing stress ratio σ'_b/σ'_n is given by the equation

$$\frac{\sigma'_b}{\sigma'_n} = \tan\left(\frac{\pi}{4}+\frac{\phi}{2}\right)\exp\left(\left(\frac{\pi}{2}+\phi\right)\tan\phi\right) \tag{5}$$

Currently available polymer grids typically have a bond coefficient in the range $1{\cdot}0 \geq f_b \geq 0{\cdot}3$, depending on the soil in which they are to be used.

The bond coefficient for a grid depends on the shearing resistance of the soil, and can change by a factor 2 depending on whether the grid is to be used in compacted sand fill or compacted clay fill. A typical example is for a grid with $\alpha_s = 0{\cdot}5$, $\tan\delta/\tan\phi' = 0{\cdot}6$ and $S/\alpha_b B = 20$, which would provide a bond coefficient $f_b = 0{\cdot}94$ in compacted granular fill with $\phi' = 45°$, and $f_b = 0{\cdot}51$ in compacted clay fill with $\phi' = 25°$, eqns (4) and (5).

The bond coefficient is needed to calculate the *bond length at the base of the slope* L_B/H. This parameter allows for bond in the revised design method.[6] The relevant equation is:

$$\frac{L_B}{H} = \left(\frac{P_{all}}{\gamma H^2 2W_r}\right)\left(\frac{1}{f_b\tan\phi}\right)\left(\frac{1}{1-r_u}\right) \tag{6}$$

A summary of the reinforcement and interaction parameters is given in Table 3. The steps for completing a design are described in Section 4, and illustrated by two design examples in Section 5.

TABLE 3
Summary of Reinforcement and Interaction Parameters

Design conditions	t_d, T_d	
Limiting reinforcement force	$(P_{lim}^{Ref})_{t_d,T_d}$	
Field degradation	$f_d f_{env}$	
Field limiting force	$(P_{lim}^{Field})_{t_d,T_d}$	$= (P_{lim}^{Ref})_{t_d,T_d}/f_d f_{env}$
Safety margin on reinforcement	f_m	
Allowable force	$(P_{all})_{t_d,T_d}$	$= (P_{lim}^{Field})_{t_d,T_d}/f_m$
Interaction coefficients		
Skin friction	f_{sf}	$= \tan\delta/\tan\phi'$
Direct sliding	f_{ds}	eqn (3)
Bond	f_b	eqn (4)
Constants of proportion		
Plane surface area	α_s	
Bearing surface area	α_b	

4 STEPS FOR SIMPLIFIED DESIGN

4.1 Values from the charts—Step (1)

Step 1.1 Having selected design values for the parameters, determine K_{Req} and L_R/H from the charts (Section 3.1). A linear interpolation between the charts is sufficient. If an overall partial factor f_c greater than unity is used, increase the values determined from the charts accordingly (Section 3.2).

Step 1.2 Ensure that the required length $(L_R/H)_{ds}$ is valid by checking that $f_{ds} \geq 0{\cdot}8$. If this is not the case, increase the required reinforcement length $(L_R/H)_{ds}$ by a factor $0{\cdot}8/f_{ds}$ (Section 3.3).

Step 1.3 Select the reinforcement length arrangement as follows.

(a) Where $(L_R/H)_{ovrl} > (L_R/H)_{ds}$ choose reinforcement with a constant length $L_R/H = (L_R/H)_{ovrl}$.

(b) Where $(L_R/H)_{ds} > (L_R/H)_{ovrl}$ either

(i) choose reinforcement with a constant length $L_R/H = (L_R/H)_{ds}$, or

(ii) choose reinforcement with a length varying uniformly from $(L_R/H)_{base} = (L_R/H)_{ds}$ at the base to $(L_R/H)_{crest} = (L_R/H)_{ovrl}$ at the crest.

Step 1.4 Determine the bond length at the base of the slope L_B/H from eqn (6), (Section 3.3).

4.2 Envelope of maximum required stress in the soil—Step (2)

Step 2.1 Construct the envelope of maximum required stress in the slope (Fig. 5a). The basic required stress for equilibrium is determined from the depth below the slope crest z and the required earth pressure coefficient K_{Req},

$$\sigma_{Req} = \gamma_d z K_{Req}$$

Step 2.2 A greater provision of reinforcement is needed, however, to allow for the effect of reinforcement bond on overall stability. Calculate the bond allowance, $(1 - L_B/L_R)$, and increase the design required stress throughout the slope by increasing the design earth pressure coefficient

$$K_d = \frac{K_{Req}}{1 - L_B/L_R}$$

Step 2.3 Finally, additional reinforcement is needed near the crest of the slope to allow for the influence of bond on local equilibrium close

to the face. Calculate the critical depth $z_{crit}/H = L_B/L_R$, to determine the minimum required stress at the crest of the slope

$$\sigma_{min} = \gamma_d z_{crit} K_{Req} = \gamma_d H(L_B/L_R) K_{Req}$$

4.3 Locus of minimum available stress from the reinforcement—Step (3)

Step 3.1 Now devise a reinforcement layout so that the minimum available stress at every depth z exceeds the envelope of maximum required stress calculated in step (2). The available stress, $\sigma_{av} = P_{all}/(s_v s_h)$, depends both on the reinforcement force and spacing. Either or both of these may be changed at different elevations in the slope.

Step 3.2 Two zones of reinforcement at constant spacing are often used. The maximum provision of reinforcement is set by the lowest layer in any zone. The lowest zone extends to the base of the slope where the provision of reinforcement must satisfy the inequality:

$$P_{all}/(s_v s_h) \geq \gamma_d H K_d$$

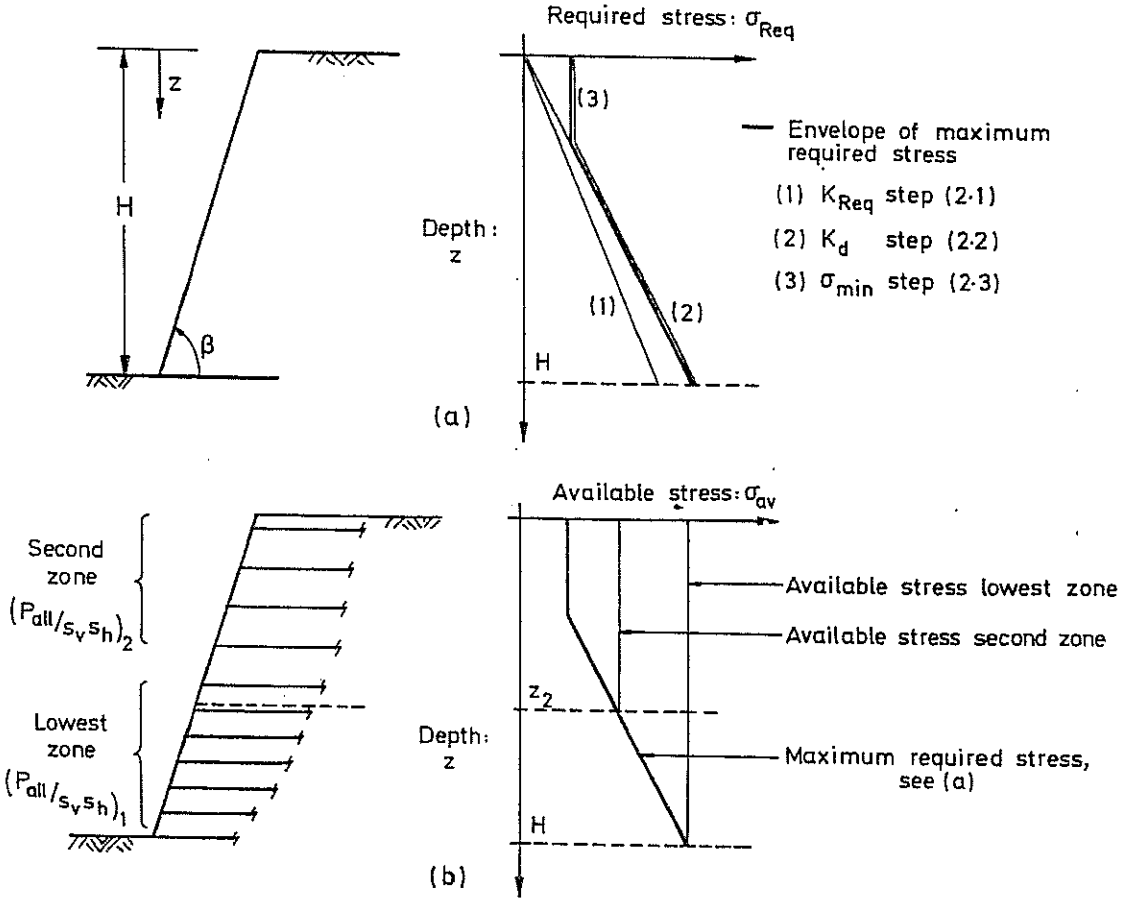

Fig. 5. Envelopes of (a) maximum required stress and (b) minimum available stress in a steep reinforced slope.

Step 3.3 If the spacing is to be changed at a depth z_2 below the slope crest, the same inequality must be satisfied but for the depth z_2 rather than H.

Step 3.4 Determine elevations for the reinforcement layers in the slope by constructing an envelope of available stress, and marking on the maximum depths at which the spacing may be changed. Now mark in the positions of the reinforcement layers working from the base of the slope and only changing the spacing once the reinforcement layer is above the maximum depth for that zone, such as z_2 in Fig. 5b.

Step 3.5 The following practical limits to the maximum vertical spacing are suggested for design:

$$(s_v)_{max} \leq \text{Minimum of } (H/8, 1\text{ m})$$

Where only limited deformation of a wrap around face is allowable in a steep slope, a reduced maximum spacing is recommended $(s_v)_{max} \leq 0{\cdot}5$ m.

4.4 Allowance for uniform vertical surcharge

Uniform vertical surcharge q_{sv} at the slope crest is allowed for by designing with an artificially greater *effective height* H'

$$H' = H + \frac{q_{sv}}{\gamma_d}$$

Design proceeds exactly as before (steps 1 to 3 above) but using H' instead of H for the slope height, and an effective depth $z' = z + q_{sv}/\gamma_d$ instead of z. The provision of reinforcement is simply terminated at the physical crest H, which occurs at an effective depth $z' = q_{sv}/\gamma_d$.

The procedure is exact for the required stresses, but is only approximate (but safe) for the required reinforcement length. The design steps are summarised in Tables 4, 5 and 6.

5 WORKED EXAMPLES

5.1 Design example 1

Data and design values

An 8 m high slope with an angle $\beta = 80°$, and with a 15 m wide crest is needed for an environmental protection scheme. The use of polymer grid reinforcement and a wrap around facing is planned. A granular fill is available on site.

TABLE 4
Required Stress

Basic required stress	K_{Req} from chart[c]
Allowance for bond	$K_d = K_{Req}/(1 - L_B/L_R)$
Minimum required stress at crest[b]	$\sigma_{min} = K_{Req}\gamma_d H'(L_B/L_R)$
Required stress at depth z'[c]	$\sigma_{Req} = K_d\gamma_d z'$
Design required stress at any depth	$\sigma_d = \text{Max}\{\sigma_{min}, \sigma_{Req}\}$

[a]Remember to allow for $f_c \geq 1{\cdot}00$.
[b]$H' = H + q_{sv}/\gamma_d$.
[c]$z' = z + q_{sv}/\gamma_d$.

TABLE 5
Reinforcement Length

Basic required lengths	$(L_R/H')_{ovrl}$ and $(L_R/H')_{ds}$ from charts[a]
If $f_{ds} \geq 0{\cdot}8$	$(L_R/H')_{ds\ design} = (L_R/H')_{ds}$
If $f_{ds} < 0{\cdot}8$	$(L_R/H')_{ds\ design} = (0{\cdot}8/f_{ds}) \times (L_R/H)_{ds}$
Minimum length at the base	$\text{Min}\{(L_R/H')_{ds\ design}, (L_R/H')_{ovrl}$
Minimum length at the crest	$(L_R/H')_{ovrl}$

[a]Remember to allow for $f_c \geq 1{\cdot}00$.

TABLE 6
Reinforcement Spacing[a]

Lowest zone at the base of the slope	$z' = H'$	$P_{all}/s_v s_h \geq K_d\gamma_d H'$
At the base of n^{th} zone of uniform reinforcement spacing	$z' = z'_n$	$P_{all}/s_v s_h \geq K_d\gamma_d z'_n$

[a]Change in reinforcement spacing either: (i) a change in reinforcement material P_{all}, or (ii) a change in the spacing (s_v, s_h), or both.

The maximum density of the fill has been measured at 21 kN/m^3, and a series of direct shear tests on the compacted fill gave peak angles of friction of the order 40° to 46°, for applied vertical stresses 100 kN/m^2 to 200 kN/m^2. The large strain or critical state angle of friction was measured in the range 30·5° to 34°. Design values $\gamma_d = 21$ kN/m^3 and $\phi'_d = 31°$ are selected from this data.

Since there is no simple means of access to the top of the slope, and the slope does not carry traffic or utilities (i.e. water pipes), it is considered adequate to design assuming zero surcharge and pore water pressure, $q_{sv} = 0$ kN/m^2 and $(r_u)_d = 0$.

The required design life is 60 years, and the site is in Northern Europe, giving the design conditions $t_d = 60$ years and $T_d = 20°C$.

A series of reinforcement grids with Index strengths in the range 110 kN/m to 35 kN/m are to be considered. The coefficient of skin friction for these grids is $f_{sf} = 0{\cdot}6$, and they all have a similar geometry with $\alpha_s = 0{\cdot}4$ and $S/\alpha_b B = 20$.

The coefficient of direct sliding can be calculated as $f_{ds} = 0{\cdot}24 + 0{\cdot}60 = 0{\cdot}84$, from eqn (3). The first component comes from shear of soil on the solid grid surfaces, and the second component comes from soil to soil shear through the grid apertures.

The bearing stress ratio in the fill is $\sigma'_b/\sigma'_n = 6{\cdot}3$, from eqn (5), so that the bond coefficient $f_b = 0{\cdot}24 + 0{\cdot}26 = 0{\cdot}50$, from eqn (4). The first component is again from surface shear, and the second component from soil bearing stress.

The reinforcement grid manufacturer recommends the following allowances for damage and environmental degradation in the reinforcement $f_d = 1{\cdot}2$ and $f_{env} = 1{\cdot}1$ for the soil and environmental conditions at the project site. These are relatively small allowances because of the benign conditions in this case. Extrapolation of the material properties test data by 1 $\log_{10}$ cycle of time is required by the manufacturer to reach the design conditions (i.e. there are stress-rupture data for up to 6 years of continuous loading) and so the appropriate material factor for design is $f_m = 1{\cdot}5$ (Table 2). The manufacturer has sufficient data to define characteristic values for the reinforcement grids as summarised in Table 7.

The expected cumulative strain in the reinforcement grids for the design conditions in the slope and the allowable loads given in Table 7 is less than 3·5% in each case.

Finally, the slope is considered not to be critical and an overall partial factor $f_c = 1{\cdot}0$ is selected for design.

TABLE 7

Characteristic Strength of the Reinforcement Grids[a] ($t_d = 60$ years and $T_d = 20°C$)

Index strength (kN/m)	*Reference strength* $((P_{lim}^{Ref})_{t_d,T_d})$	*Field strength* $((P_{lim}^{Field})_{t_d,T_d}$, *eqn (1))*	*Allowable force* (P_{all}, *eqn (2))*
110	66	50	33
80	48	36	24
55	33	25	16·5
35	21	16	10·5

[a] (i) Characteristic Index and Reference strength from manufacturer.
(ii) Field strength for degradation $f_d = 1{\cdot}2$ and $f_{env} = 1{\cdot}1$.
(iii) Material factor $f_m = 1{\cdot}5$ for 1 $\log_{10}$ cycle of extrapolation.

Design steps

Step 1.1 The basic required earth pressure coefficient $K_{Req} = 0{\cdot}23$ and the required reinforcement lengths $(L_R/H)_{ovrl} = 0{\cdot}53$ and $(L_R/H)_{ds} = 0{\cdot}28$ may be determined from the charts for the design values $(r_u)_d = 0$, $\beta = 80°$ and $\phi'_d = 31°$. The above values from the charts can be used directly as the overall partial factor $f_c = 1{\cdot}0$ (Section 3.2).

Step 1.2 The required length at the base of the slope is valid since $f_{ds} = 0{\cdot}84$.

Step 1.3 As $(L_R/H)_{ovrl} \geq (L_R/H)_{ds}$, the minimum required reinforcement length has a constant value $L_R = 0{\cdot}53 \times 8 = 4{\cdot}3$ m.

Step 1.4 Design proceeds by trial and error. Here a constant spacing $s_v = 0{\cdot}5$ m is assumed throughout the slope. The benefit of using less strong grids in the upper part of the slope will be investigated. The maximum required stress at the base of the slope is $\sigma_{Req} = K_{Req}\gamma_d H = 39$ kN/m^2. The grid reinforcement with an index strength 80 kN/m is selected for the lowest reinforcement zone as it provides a minimum available stress $\sigma_{av} = 24/0{\cdot}5 = 48$ kN/m^2 (Table 7). The bond length at the base of the slope for this reinforcement grid can be calculated $L_B/H = 0{\cdot}03$, using eqn (6).

Step 2.1 The basic required stress for equilibrium is shown in Fig. 6.

Step 2.2 For $L_R/H = 0{\cdot}53$ (step 1.2) and $L_B/H = 0{\cdot}03$ (step 1.3), $L_B/L_R = 0{\cdot}06$ and the bond allowance $(1 - L_B/L_R) = 0{\cdot}94$. This gives the design earth pressure coefficient $K_d = 0{\cdot}23/0{\cdot}94 = 0{\cdot}24$.

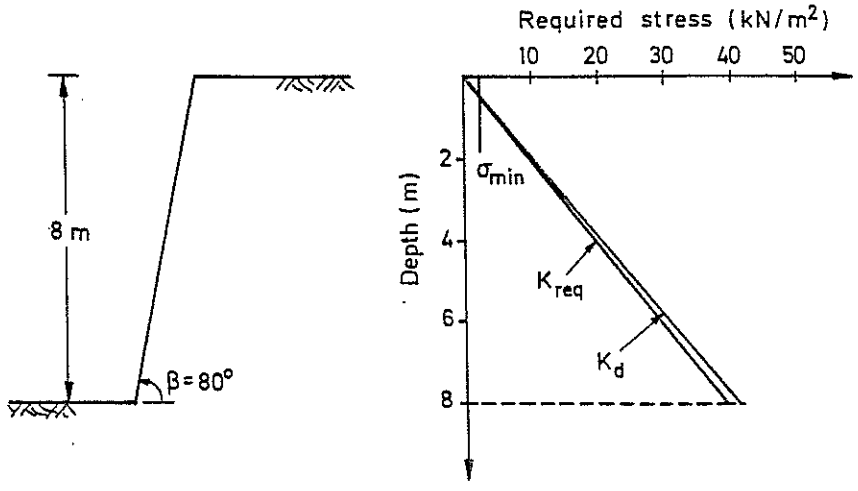

Fig. 6. Envelope of maximum required stress for design example 1.

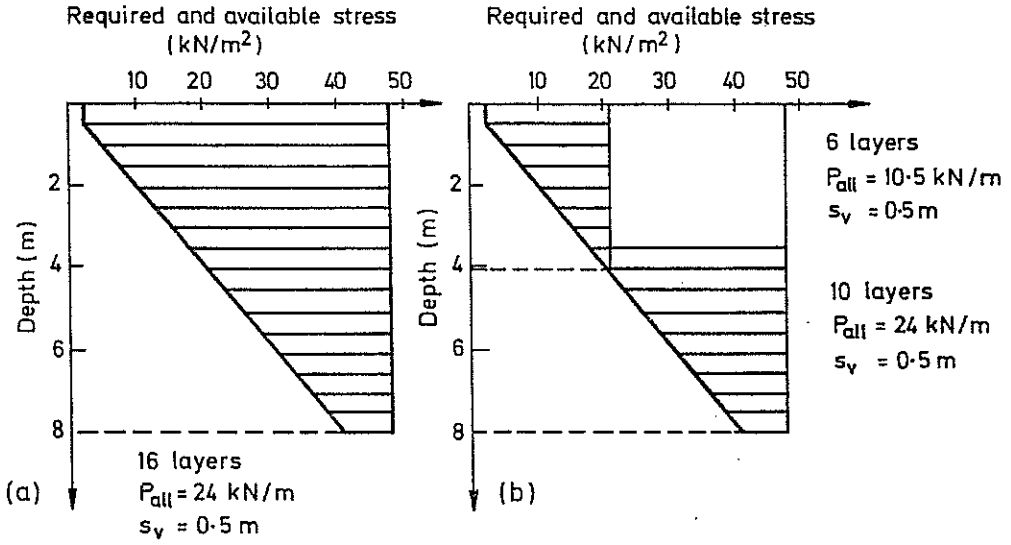

Fig. 7. Provision of minimum available stress for design example 1.

Step 2.3 For $L_B/L_R = 0{\cdot}06$, the minimum required stress is $\sigma_{min} = 2{\cdot}2$ kN/m^2 which is very small (Fig. 6).

Note that bond allowance *and the* minimum stress near the crest *seldom have a significant impact on the design of grid and geotextile reinforced slopes. The reason is that the required bond lengths for these reinforcement materials are typically short (even where the bond coefficient is relatively small, such as* $f_b < 0{\cdot}5$*) because of the rather low ratio of allowable force in the reinforcement with respect to the product of the contact area and the confining stress in the soil.*

Step 3.1 The reinforcement layout which provides a suitable locus of available stress may be devised graphically or by calculation. If a single spacing arrangement with $s_v = 0{\cdot}5$ m and $P_{all} = 24$ kN/m were adopted, for example, then $n = 8/0{\cdot}5 = 16$ layers would be required (Fig. 7a).

Steps 3 To investigate the use of less strong reinforcement near the crest of the slope where there is an excess available stress (Fig. 7a) choose the weakest grid in Table 7 with $(P_{all})_2 = 10{\cdot}5$ kN/m. At the standard spacing $s_v = 0{\cdot}5$ m this grid can provide an available stress $(\sigma_{av})_2 = 21$ kN/m^2 which is acceptable above a depth $z_2 = 21/(0{\cdot}24 \times 21) = 4{\cdot}1$ m below the crest. This enables the top 6 layers of reinforcement grid to be replaced (Fig. 7b). Use of the intermediate grid with $P_{all} = 16{\cdot}5$ kN/m can reduce further the excess available stress in the slope. For this grid, $\sigma_{av} = 33$ kN/m^2 which is permissible above a depth $z = 6{\cdot}45$ m below the slope crest. The reinforcement layout using all the grids has a constant spacing $s_v = 0{\cdot}5$ m throughout, and 5 layers

each of the two stronger reinforcement grids with a final 6 layers of the lightest grid. The three alternative reinforcement designs are summarised in Table 8, where the relative reinforcement material costs are indicated. The optimum design will depend on individual project details. While the most sophisticated layout minimises reinforcement material costs, other cost factors such as construction control and material supply arrangements can often make the simpler reinforcement layout most attractive overall. The reinforcement layout for design 3 is shown in Fig. 8.

TABLE 8
Reinforcement Design Summaries for Example 1

Index strength (kN/m)	*Cost (units)*	*Design 1 (layers)*	*Design 2 (layers)*	*Design 3 (layers)*
80	5	16	10	5
55	4			5
35	3		6	6
Relative unit cost		80	68	63
Saving over design 1		0%	15%	21%

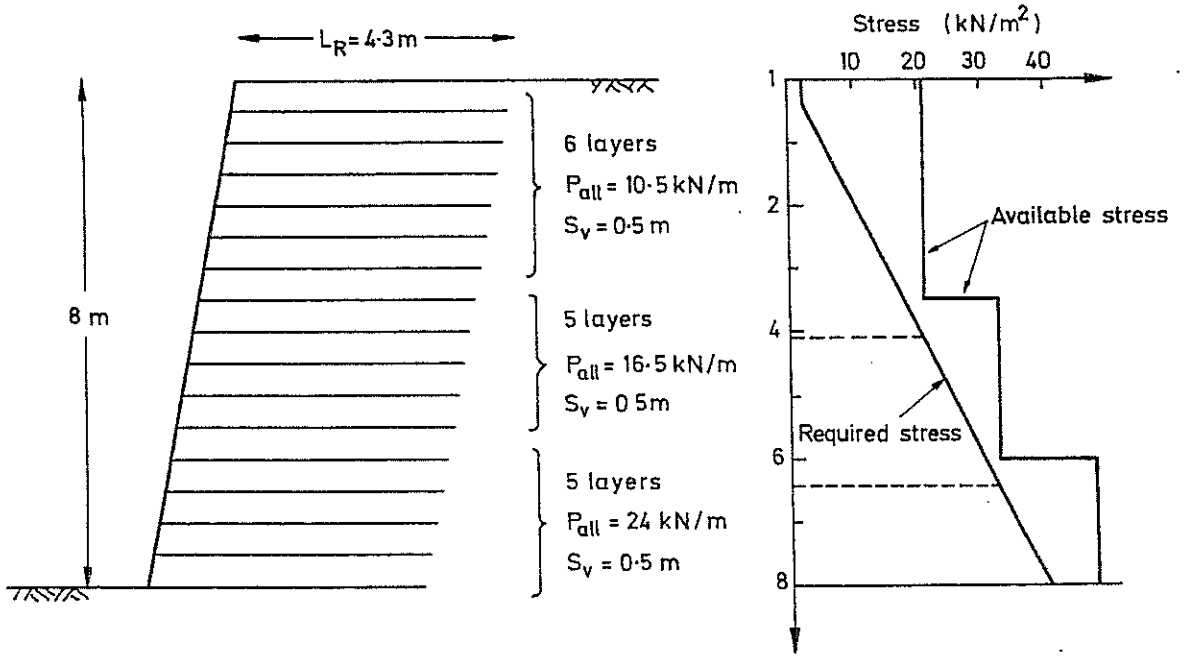

Fig. 8. Cross-section of design example 1 using all three reinforcement materials.

5.2 Design example 2

Design and design values

A 10 m high, $\beta = 65°$ slope has to be formed for a highway widening. A vegetated wrapped face is planned. The available fill is a glacial till and laboratory tests indicate an average unit weight $\gamma = 21{\cdot}2\ \text{kN/m}^3$ after compaction at optimum moisture content. The large strain shearing resistance measured in drained shear box tests and drained triaxial tests is of the order 23·5° to 26·5°. The design values selected from this data are $\gamma_d = 22\ \text{kN/m}^3$ and $\phi'_d = 24°$.

To allow for pore water pressures from water infiltration, a pore water pressure coefficient $(r_u)_d = 0{\cdot}15$ is assumed. A uniform vertical surcharge on the slope crest $q_{sv} = 15\ \text{kN/m}^2$ is assumed, which gives an effective height $H' = 10 + 15/22 = 10{\cdot}7$ m.

The reinforcement grids used on the previous project (Design example 1) are to be considered again. As it happens, the design life, degradation and material factors for the reinforcement grids for this project ($f_d = 1{\cdot}1$, $f_{env} = 1{\cdot}2$ and $f_m = 1{\cdot}5$) give the same allowable forces as before in the right-hand column of Table 7.

The skin friction and the direct sliding coefficient are also the same as before, $f_{ds} = 0{\cdot}84$. However, there is less bearing stress available because of the lower shearing resistance of the clay fill. The bearing stress ratio is $\sigma'_b/\sigma'_n = 3{\cdot}5$, from eqn (5), and the bond coefficient is $f_b = 0{\cdot}24 + 0{\cdot}21 = 0{\cdot}45$, from eqn (4).

Since the slope supports the outer edge of a highway, some additional security is required to allow for the potentially serious consequences of a failure. An overall factor $f_c = 1{\cdot}1$ is adopted.

Design steps

Step 1.1 Interpolation between the charts for $r_u = 0$ and 0·25 is required. The values of earth pressure and reinforcement length for $\beta = 65°$ and $\phi'_d = 23°$ are:

$K_{Req} = 0{\cdot}24$ and 0·37,

$(L_R/H)_{ovrl} = 0{\cdot}70$ and 0·95, and

$(L_R/H)_{ds} = 0{\cdot}70$ and 1·10 respectively.

The interpolated design values for $(r_u)_d = 0{\cdot}15$ are:

$K_{Req} = 0{\cdot}32$, $(L_R/H)_{ovrl} = 0{\cdot}85$, and $(L_R/H)_{ds} = 0{\cdot}94$.

The partial factor $f_c = 1{\cdot}1$ gives an increased required force for design $K_{Req} = 1{\cdot}1 \times 0{\cdot}32 = 0{\cdot}35$, an increased required length at the base of the slope $(L_R/H)_{ds} = 1{\cdot}1 \times 0{\cdot}94 = 1{\cdot}03$ and at the crest of the slope $(L_R/H)_{ovrl} = 1{\cdot}1 \times 0{\cdot}85 = 0{\cdot}94$.

Step 1.2 The required length at the base is valid since $f_{ds} = 0{\cdot}84$.

Step 1.3 Since $(L_R/H)_{ds} > (L_R/H)_{ovrl}$, direct sliding rather than overall stability governs the reinforcement length at the base of the slope. For reinforcement with constant length throughout the slope $L_R = 1{\cdot}03 \times 10{\cdot}7 = 11$ m.
It is permissible, for greater economy of material, to reduce the reinforcement length linearly with depth between $L_R = 11$ m at the base of the slope (see above) to $L_R = 0{\cdot}94 \times 10{\cdot}7 = 10{\cdot}1$ m at the crest.

Step 1.4 The maximum required stress at the base of the slope is $\sigma_{Req} = K_{Req}\gamma_d H' = 82$ kN/m^2. The grid reinforcement with an index strength 110 kN/m is able to provide this stress if $s_v = 33/82 = 0{\cdot}40$ m is used (Table 7).
The bond length at the base of the slope can now be calculated as $L_B/H = 0{\cdot}04$, eqn (6).

Step 2.1 The basic required stress for equilibrium is shown in Fig. 9.

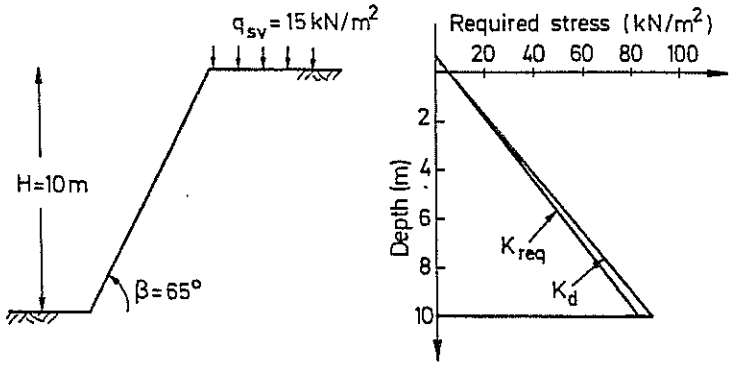

Fig. 9. Envelope of maximum required stress for design example 2.

Step 2.2 For $L_R/H = 1{\cdot}03$ (step 1.2) and $L_B/H = 0{\cdot}04$ (step 1.3), $L_B/L_R = 0{\cdot}04$ and the bond allowance $(1 - L_B/L_R) = 0{\cdot}96$. This determines the design earth pressure coefficient $K_d = 0{\cdot}35/0{\cdot}96 = 0{\cdot}37$.

Step 2.3 For $L_B/L_R = 0{\cdot}04$, the minimum required stress is $\sigma_{min} = 3{\cdot}6$ kN/m^2. (See the note at this step in Example 1.)

Step 3.1 If a single spacing arrangement with $s_v = 0{\cdot}4$ m and $P_{all} = 33$ kN/m is adopted, then $n = 10/0{\cdot}4 = 25$ layers would be required (Fig. 10a).

Steps 3 Maintaining a constant spacing $s_v = 0{\cdot}4$ m, the maximum depths to which the lighter grids may be used are as follows:
for $(P_{all})_2 = 24$ kN/m, $(\sigma_{av})_2 = 60$ kN/m^2 and $z_2' = 7{\cdot}4$ m.
for $(P_{all})_3 = 16{\cdot}5$ kN/m, $(\sigma_{av})_3 = 41$ kN/m^2 and $z_3' = 5{\cdot}1$ m.
for $(P_{all})_4 = 10{\cdot}5$ kN/m, $(\sigma_{av})_4 = 26$ kN/m^2 and $z_4' = 3{\cdot}2$ m.

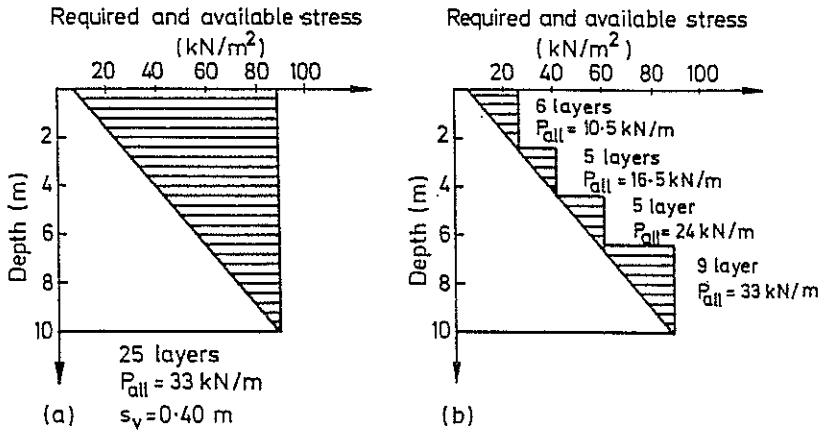

Fig. 10. Provision of minimum available stress for two alternative designs for example 2.

TABLE 9
Reinforcement Design Summaries for Example 2

Index strength (kN/m)	*Cost (units)*	*Design 1 (layers)*	*Design 2 (layers)*
110	6	25	9
80	5		5
55	4		5
35	3		6
Relative unit cost:		150	117
Saving over design 1:		0%	22%

Introducing the lighter grids would replace the top 16 layers with 5 layers each of the intermediate strength grids and 6 layers of the lightest grid (Fig. 10b). The designs are summarised in Table 9 where the maximum saving in reinforcement material cost relative to the single grid design is 22%. Design 2, adopting the constant reinforcement length, is illustrated in Fig. 11.

6 TIPS AND USEFUL NOTES FOR DESIGN

6.1 Tip for rapid preliminary estimates

To rapidly assess the quantity of reinforcement required, estimate the number of layers n_{est} of a single reinforcement type P_{all} as

$$n_{est} = \frac{K_{Req}\gamma_d(H')^2}{P_{all}}$$

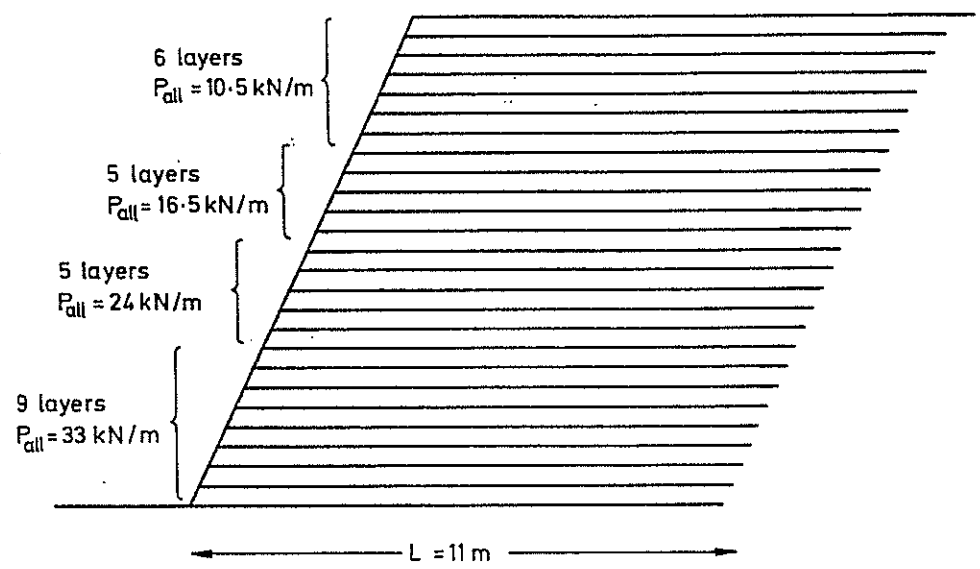

Fig. 11. Cross-section of design example 2 using all four reinforcement materials.

and estimate the spacing as

$$(s_v)_{est} = \frac{H}{n_{est}}$$

6.2 Tip for reinforcement selection

The data in Table 10 are useful for preliminary slope design where granular fills are to be used. It assumes $\phi'_d = 30°$, $\gamma_d = 20\ kN/m^3$ and $(r_u)_d = 0$.

Table 10 gives the depth to which reinforcement with allowable forces in the range $P_{all} = 40\ kN/m \rightarrow 10\ kN/m$ can be used, for slopes in the range $\beta = 90° \rightarrow 50°$.

The limiting depths given are for a unit vertical spacing $s_v = 1{\cdot}0\ m$. They should be increased by a factor 2, 3 or 5 etc., for reinforcement at spacings 0·5 m, 0·33 m or 0·20 m respectively.

TABLE 10

Depth in Metres to which Geotextile and Grid Reinforcements may be used in Slopes Formed from Granular Soils. Case $s_v = 1{\cdot}0\ m$, $\phi'_d = 30°$ and $(r_u)_d = 0$

Allowable force (P_{all}, *kN/m*)	*Slope angle* $\beta°$				
	90°	*80°*	*70°*	*60°*	*50°*
40	6·0 m	8·0 m	10·4 m	13·8 m	20·2 m
30	4·5 m	6·0 m	7·8 m	10·3 m	15·2 m
20	3·0 m	4·0 m	5·2 m	6·9 m	10·1 m
10	1·5 m	2·0 m	2·6 m	3·5 m	5·1 m

6.3 Tip on bond allowance

Unless the reinforcement form or material is changed higher in the slope, it is not necessary to recalculate the bond allowance where the reinforcement spacing or strength is changed (as in the design examples).

Also, as noted previously, bond allowance only becomes significant where a narrow width reinforcement is used, or where there is a relatively low soil shearing resistance or bond coefficient, or a relatively high pore water pressure.

6.4 Note on allowable force and spacing

A general expression for the available stress, $P_{all}/s_v s_h$, has been used in the paper. The reinforcement has a load capacity in kN and the available stress in the soil depends on the vertical and horizontal spacings between the reinforcements s_v and s_h in metres, to give an available stress in kN/m^2.

Geotextiles and grids are often used in continuous layers and their load capacity is quoted in terms of load per metre width. In the above terminology, this capacity is in terms of P_{all}/s_h.

Sometimes 1 m wide grids with an allowable load quoted in kN/m are spaced apart at a distance s_h between centres. For chart design, simply take the load capacity in kN, so that for the grids at a spacing (s_v, s_h) the available stress is $P_{all}/s_v s_h$.

The essential check is that the available stress has the correct dimensions kN/m^2.

6.5 Note on direct sliding in flatter slopes

The direct sliding mechanism of failure across the surface of the lowest layer of reinforcement becomes increasingly important for flatter slopes, lower shearing resistances and higher pore water pressures, as seen in the design charts.

The area indicated by the dotted line in the lower left corner of the charts for direct sliding is where no instability could be found using potential direct sliding mechanisms. This suggests that stability is governed solely by overall stability considerations. Care is urged in the design of slopes with these combinations of parameters, and checks on external equilibrium are particularly important.

For a slope designed with a constant reinforcement length take the greater of the two lengths required to maintain overall equilibrium and direct sliding equilibrium.

Some additional economy in reinforcement quantity is possible where

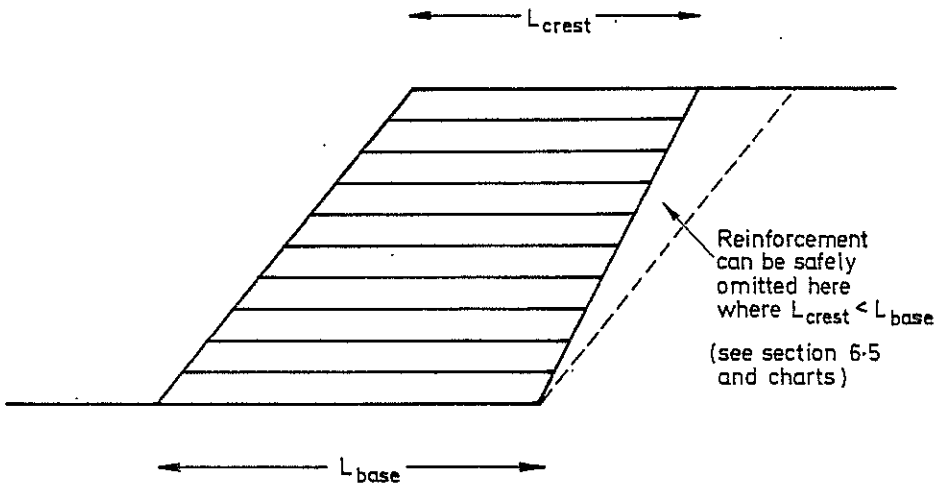

Fig. 12. Allowed shortening of reinforcement length higher in the slope where direct sliding is the critical mechanism at the base of the slope.

the length required to maintain direct sliding equilibrium is greater than the length required to maintain overall equilibrium. In such cases the reinforcement length may be linearly reduced with elevation in the slope as shown in Fig. 12.

6.6 Note on wrap around facing

When forming a wrap around face to the slope it is normally sufficient if the minimum return length is at least $3s_v$. The total length for a reinforcement layer, to include the wrap around face and the lap-back would be at least:

$$L_{total} \geq L_R + s_v \frac{(1 + 3 \sin \beta)}{\sin \beta}$$

6.7 Note on compaction stresses

For very steep slopes and walls it is advisable to consider the temporary loading near the crest of the slope which may be caused by compaction. Essentially, compaction loading may require a lateral stress in the soil of the order $\sigma_{compaction} = 10\,kN/m^2$ to $20\,kN/m^2$ to maintain equilibrium. Ingold[15] discusses the various methods to calculate compaction-induced stresses.

Routine design with geotextiles, however, often provides a sufficient quantity of reinforcement near the crest of the slope to support this magnitude of required stress. The two designs described earlier are typical

and these resulted in a minimum available stress at the crest of $\sigma_{min} = 21\ kN/m^2$ and $\sigma_{min} = 26\ kN/m^2$ respectively (Figs 7 and 10).

Note also that compaction causes relatively short-term, transient loading compared with the normal design life for a slope. Polymer reinforcement materials have a higher strength capacity for short-term loading.

7 CONCLUDING REMARKS

The practical application of revised design charts for steep reinforced slopes has been described and illustrated by two worked examples. Guidance has been given on the selection of design values for the soil and the reinforcement properties, and the partial factors of safety. These procedures revise those presented in 1984.[1]

The advantages offered by the revised design charts and design procedure include the greater flexibility and the wider range of cases allowed, the clearer and more comprehensive definition of the design parameters and safety margins, and the significant savings in the reinforcement material quantities which can be achieved.

ACKNOWLEDGEMENTS

The work on the revised design charts was encouraged and partially supported by AKZO Industrial Systems bv. The author is particularly grateful to Wim Voskamp for his helpful comments.

REFERENCES

1. Jewell, R. A., Paine, N. & Woods, R. I. Design methods for steep reinforced embankments. *Polymer grid reinforcement*, Thomas Telford, 1984, 70–81.
2. British Standards Institute. *Report on strengthened/reinforced soils and other fills*. Published Document, PD 6517: 1988, London.
3. Institution of Civil Engineers. *Specification for the use of geotextiles and related materials*. Ground Engineering Group Board, ICE (in press).
4. Jarrett, P. M. & McGown, A. *The application of polymeric reinforcement in soil retaining structures*. Kluwer Academic Publishers, Holland, 1988.
5. Fannin, R. J. & Hermann, S. Some soil and reinforcement parameters for design. *Proc. 12th Int. Conf. Soil Mechs And Fndn Engng*, Rio de Janeiro, Vol. 2, 1989, 1239–42.

6. Jewell, R. A. Revised design charts for steep reinforced slopes. *Proc. Symp. Reinforced Embankments: Theory and Practice in the British Isles*, Cambridge, September. Thomas Telford, London, 1990, pp. 1–31.
7. Shercliff, D. A. (ed.), *Reinforced Embankments: Theory and Practice in the British Isles*. Symposium at Cambridge University, September 1989. Thomas Telford, London, 1990.
8. Bishop, A. W. & Morgenstern, N. Stability coefficients for earth slopes. *Geotechnique*, **10** (1960) 129–50.
9. Jewell, R. A. & Milligan, G. W. E. Deformation calculations for reinforced soil walls. *Proc. 12th Int. Conf. Soil Mechs And Fndn Engng*, Rio de Janeiro, Vol. 2, 1989, 1257–62.
10. Vaughan, P. R., Hight, D., Sodha, V. G. & Walbanke, H. J. Factors controlling the stability of clay fills in Britain. *Proc. Conf. on Clay Fills*, Institution of Civil Engineers, London, 1978.
11. Greenwood, J. H. & Jewell, R. A. Strength and safety: the use of mechanical property data. *Proc. Symp. Reinforced Embankments: Theory and Practice in the British Isles*, Cambridge, September. Thomas Telford, London, 1990, pp. 85–100.
12. Jewell, R. A. & Greenwood, J. H. Long term safety in steep soil slopes reinforced by polymer materials. *Geotextiles and Geomembranes*, **7**(1 & 2) (1988) 81–118.
13. Palmeira, E. M. & Milligan, G. W. E. Scale factors affecting the results of pull-out tests of grids buried in sand. *Geotechnique*, **39** (1989) 511–24.
14. Jewell, R. A., Milligan, G. W. E., Sarsby, R. W. & DuBois, D. D. Interactions between soils and grids. *Polymer grid reinforcement*, Thomas Telford, 1984, 18–30.
15. Ingold, T. S. The effects of compaction on retaining walls. *Geotechnique*, **29**(3) (1979) 265–83.

APPENDICES: STEEP REINFORCED SLOPE DESIGN CHARTS

Appendix 1

STEEP REINFORCED SLOPE DESIGN CHARTS
Jewell (1990)

CHART 1
$r_u = \frac{u}{\gamma z} = 0.00$

Minimum Required Force K_{Req}

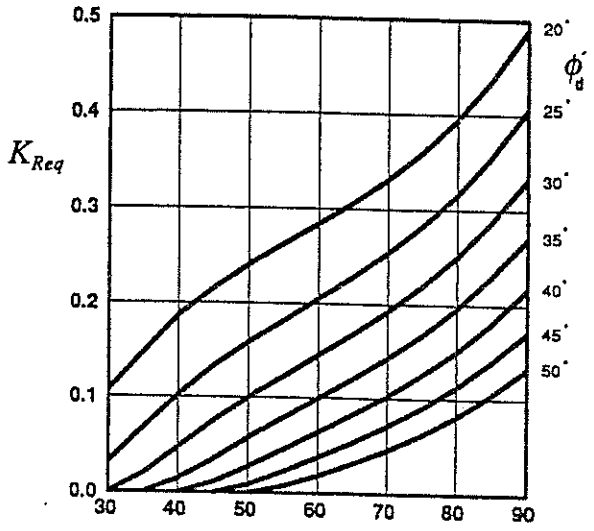

Minimum reinforcement length:

(1) The minimum length at the crest of the slope is that required for *overall stability.*

(2) The minimum length at the base of the slope is the greater of that required for *overall stability* and to prevent *direct sliding.*

(3) Where reinforcement of constant length is to be used select the greater length required to satisfy equilibrium at the base of the slope, (2) above.

(4) Where *direct sliding* governs the required reinforcement length at the base of the slope it is permissible to reduce the length uniformly from L_{ds} at the base of the slope to L_{ovrl} at the crest of the slope.

Minimum Required Length *Overall Stability* $(L_R/H)_{ovrl}$

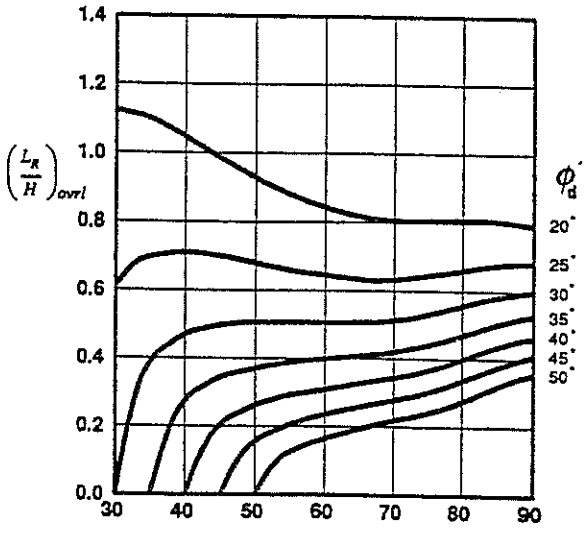

Minimum Required Length *Direct Sliding* $(L_R/H)_{ds}$

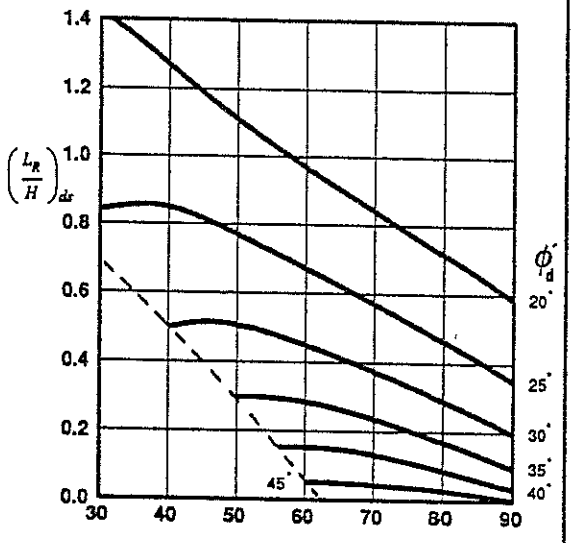

Appendix 2

STEEP REINFORCED SLOPE DESIGN CHARTS Jewell (1990)	CHART 2 $r_u = \frac{u}{\gamma z} = 0.25$

Minimum Required Force K_{Req}

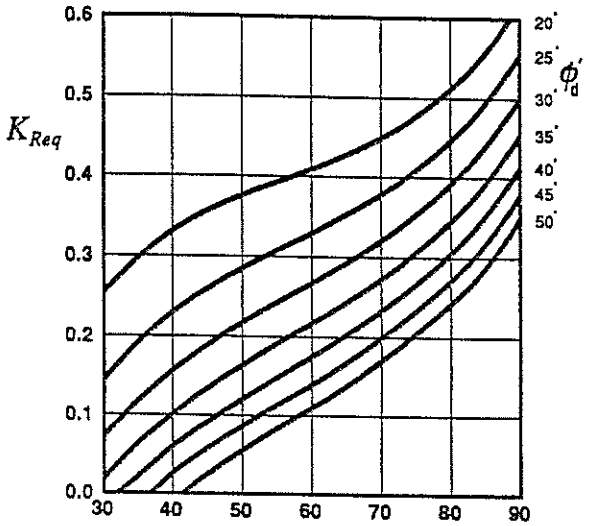

Minimum reinforcement length:

(1) The minimum length at the crest of the slope is that required for *overall stability*.

(2) The minimum length at the base of the slope is the greater of that required for *overall stability* and to prevent *direct sliding*.

(3) Where reinforcement of constant length is to be used select the greater length required to satisfy equilibrium at the base of the slope, (2) above.

(4) Where *direct sliding* governs the required reinforcement length at the base of the slope it is permissible to reduce the length uniformly from L_{ds} at the base of the slope to L_{ovrl} at the crest of the slope.

Minimum Required Length *Overall Stability* $(L_R/H)_{ovrl}$

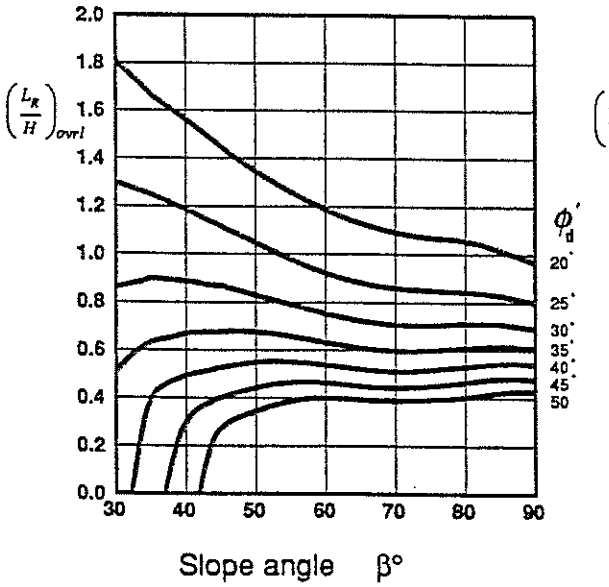

Minimum Required Length *Direct Sliding* $(L_R/H)_{ds}$

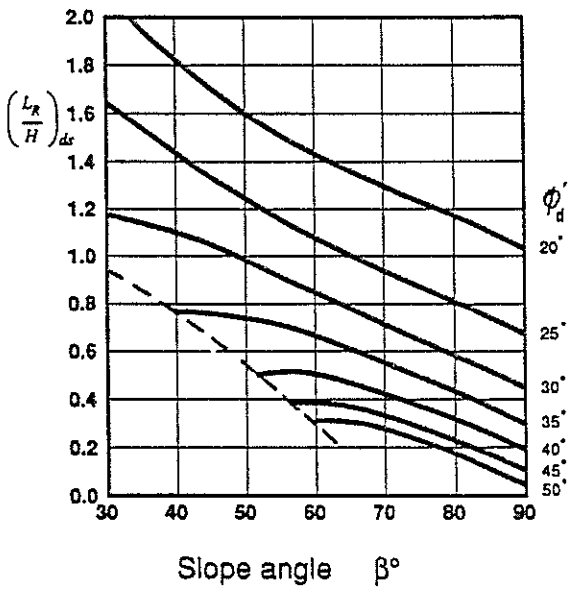

Appendix 3

STEEP REINFORCED SLOPE DESIGN CHARTS
Jewell (1990)

CHART 3
$r_u = \frac{u}{\gamma z} = 0.50$

Minimum Required Force K_{Req}

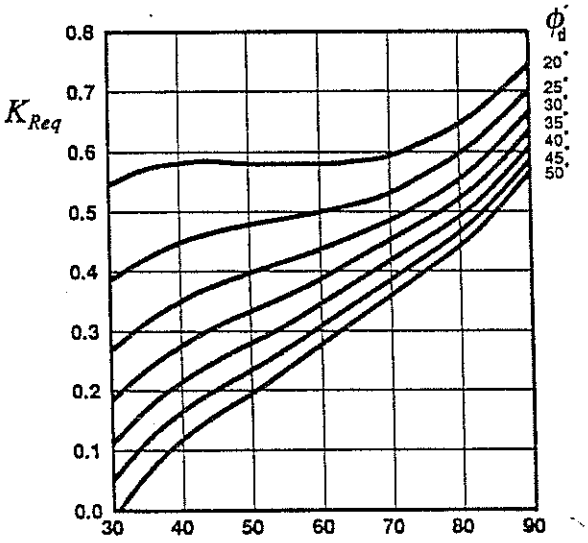

Minimum reinforcement length:

(1) The minimum length at the crest of the slope is that required for *overall stability*.

(2) The minimum length at the base of the slope is the greater of that required for *overall stability* and to prevent *direct sliding*.

(3) Where reinforcement of constant length is to be used select the greater length required to satisfy equilibrium at the base of the slope, (2) above.

(4) Where *direct sliding* governs the required reinforcement length at the base of the slope it is permissible to reduce the length uniformly from L_{ds} at the base of the slope to L_{ovrl} at the crest of the slope.

Minimum Required Length
Overall Stability $(L_R/H)_{ovrl}$

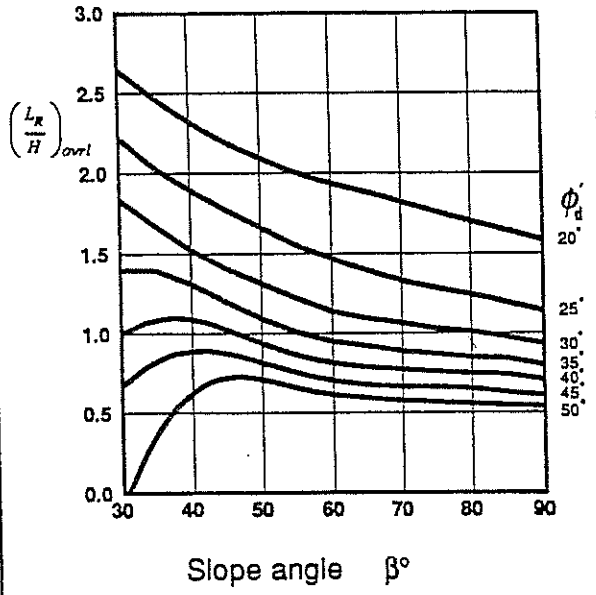

Minimum Required Length
Direct Sliding $(L_R/H)_{ds}$